# ATMOSPHERIC WATER VAPOR TRANSPORT AND THE HYDROLOGY OF NORTH AMERICA

by

Eugene M. Rasmusson

B. S., Kansas State University
(1950)

M. S., St. Louis University
(1963)



SUBMITTED IN PARTIAL FULFILLMENT
OF THE REQUIREMENTS FOR THE
DEGREE OF DOCTOR OF
PHILOSOPHY
at the

MASSACHUSETTS INSTITUTE of
TECHNOLOGY
May, 1966

Signature of Author.....
Department of Meteorology, 13 May 1966

Certified by.....
Thesis Supervisor

Accepted by.....
Chairman, Departmental Committee on Graduate Students

# ATMOSPHERIC WATER VAPOR TRANSPORT AND THE HYDROLOGY OF NORTH AMERICA

by

Eugene M. Rasmusson

Submitted to the Department of Meteorology on 13 May 1966
in partial fulfillment of the requirements for the degree of
Doctor of Philosophy.

## ABSTRACT

The atmospheric water vapor flux and certain aspects of the water balance over the North American Sector are investigated for the period May 1, 1961 - April 30, 1963.

The vertical variation of the flux, as well as the total vertically integrated flux, are investigated from mean monthly data. The flux exhibits important diurnal variations, particularly during the summer south of 50°N. These variations are primarily the result of diurnal variations in the mean wind, rather than in the moisture, and are particularly well organized over eastern North America, the Gulf of Mexico, and the Caribbean Sea.

Significant interannual changes in the flux are also observed. The relationship of these changes to the interannual changes in flux divergence and precipitation are discussed.

The mean vertical distribution of flux divergence is computed for the United States, for the months of January and July. Strong flux convergence in the lowest 100 mb, and divergence in the remainder of the troposphere, was found in July. Flux convergence was found throughout the troposphere in the east in January, with a maximum between 900 and 950 mb, while in the west convergence (with no particularly pronounced maximum) was found above 800 mb, with weak divergence below. Corresponding features of the profiles were found at higher elevations over the west, where the flux divergence above 500 mb is quite significant.

Particular emphasis is placed on computations of the vertically integrated vapor flux divergence, and its use in estimating $\overline{E-P}$, the mean difference between evaporation and precipitation. Water balance studies, using twice daily observations from the existing aerological network, indicate that reliable mean annual, seasonal, and monthly values of $\overline{E-P}$ can usually be obtained for areas of $20 \times 10^5$ km$^2$ or larger. The results usually deteriorate rapidly as the size of the area is reduced to less than $10 \times 10^5$ km$^2$. This deterioration is primarily the result of a systematic error pattern, which is tentatively ascribed to the effect of diurnal flux variations, small scale features in the mean flux field, and local station peculiarities.

The annual and seasonal values of $\overline{E-P}$ are computed for the Caribbean Sea and the Gulf of Mexico and are in excellent agreement with independent estimates.

Mean values of $\overline{E-P}$ are computed for North America north of the United States-Mexican border, and individually for the major watersheds of the continent. Latitudinally averaged values show a minimum between 55°N and 65°N.

More comprehensive balance studies were made over the United States and southern Canada. Of particular interest is the computation of mean monthly surface and subsurface storage changes directly from measured streamflow and vapor flux data. Consistent and reasonable storage changes are computed for the area as a whole, which indicate an average seasonal variation of around 8 cm. Little net storage change was computed during the two year period for the whole area, but substantial changes were indicated over the western part of the region during the first year, and over the eastern part during the second year. These changes appear to be in qualitative agreement with independent indicators.

Rough computations of mean monthly evapotranspiration are made for the United States and southern Canada, using precipitation and flux divergence data. Values exhibit the expected seasonal variations, with a maximum of around 8 cm/mo in summer and a minimum of 1-2 cm in winter. Computations for the larger subdivisions of this area give values which appear, for the most part, to be reasonable.

Thesis Supervisor: Victor P. Starr
Title: Professor of Meteorology

TABLE OF CONTENTS

LIST OF TABLES

LIST OF TABLES cont.

LIST OF FIGURES

LIST OF FIGURES - cont.

LIST OF FIGURES - cont.

LIST OF FIGURES - cont.

LIST OF FIGURES - cont.

LIST OF FIGURES - cont.

LIST OF FIGURES - cont.

LIST OF FIGURES - cont.

LIST OF FIGURES - cont.

LIST OF FIGURES - cont.

LIST OF FIGURES - cont..

LIST OF FIGURES - cont.

LIST OF FIGURES - cont.

# I. INTRODUCTION

Only a portion of the total water substance on this planet actively participates in the physical and biological processes occurring in the atmosphere and the surface layers of the earth. This is the water stored in the oceans, in the atmosphere, and over the land, as surface storage, soil moisture and shallow groundwater. The changes which take place in the total content of these reservoirs undoubtedly proceed at an exceedingly slow rate; consequently, this total water mass can, for most purposes, be considered constant. The principle of continuity, expressed in the form of a balance equation, then becomes the single most useful tool in the study of the processes by which water circulates between and within these reservoirs. In order to best utilize such an equation, one or more quantities in the equation must be accurately measured, and the remainder evaluated as a residual. It is, therefore, not surprising that the measurement of these quantities has been of primary concern to hydrologists, and indeed, the modern science of hydrology is often considered to have begun with the 17th century precipitation measurements in the basin of the Seine by the French physicists Perrault and Mariotte (Chow, 1964).

Even at the present time, progress in hydrology is seriously hindered by inadequate measurement of many of the processes involved

in these circulations. Among some of these measurement problems recently discussed by Ackerman (1965) are:

1. Inadequate knowledge of the physical-chemical characteristics of the different soil types (15,000 in the United States alone), which in turn leads to an inadequate knowledge of soil moisture characteristics.

2. Inadequate information on groundwater storage and movement.

3. Inadequate information on evapotranspiration under various conditions. Ackerman states: "Changes in regional or global supply of atmospheric moisture obtained from land and water surfaces by evapotranspiration processes are largely unknown.....Instruments are in use for measuring evapotranspiration for single site and environment. The effect of changes in environment can be quantified. New instruments or improved techniques for use with conventional instrumentation are needed, however, to quantify the exchange of moisture with the atmosphere over large areas for which water balance evaluations are required."

General use of the balance equation for the terrestrial branch of the hydrologic cycle has been seriously limited by the existence in the equation of two normally unmeasured quantities, evapotranspiration and change in surface and subsurface storage. Consequently, some additional relationship, involving no additional unknowns, is required in order to solve for these two quantities. The conventional approach

to this problem has centered on attempts to estimate actual evapotranspiration through the use of standard surface meteorological data. As noted by Thornthwaite and Hare (1965), all these systems contain the same essential elements: (1) a means of computing potential evapotranspiration, (2) a means of computing actual evapotranspiration and soil moisture, and (3) a system of budgeting soil moisture. Thus, evapotranspiration is assumed to be a function of potential evapotranspiration and available soil moisture. Since in these systems potential evapotranspiration itself is considered a function of meteorological factors, the computed evapotranspiration becomes a function of available soil moisture and meteorological conditions. In the view of many soil scientists, however, the ability of the soil to supply moisture to the surface becomes the dominant factor after the initial drying period. Gardner (1965) states that for much of the period between rains, evaporation from the soil is controlled, not by meteorology, but by the ability of soil to transmit moisture. In addition, the question of whether transpiration decreases as soil moisture decreases, or continues at a constant rate until the permanent wilting percentage is reached, is still considered by many an open question (Thornthwaite and Hare, 1965). The various techniques handle this problem differently.

Since evapotranspiration is assumed to be a function of available

soil moisture, an estimate must be made of this quantity. The estimated actual storage is kept track of by an accounting technique. Use of actual measurements of soil moisture are impracticable because of the great variability of such measurements over short distances (Thornthwaite and Hare, 1965). Furthermore, the rate of movement of water to the deeper layers and ultimately to the water table is difficult to evaluate. Recharge (rainfall minus runoff) is handled differently by the various methods; some assume no runoff until the soil moisture deficit is satisfied (Thornthwaite and Mather, 1955); others make the more realistic assumption that some runoff occurs before the deficiency is satisfied (Kohler and Richards, 1962). As in the case of soil moisture, the runoff used in the accounting procedures is usually computed rather than measured.

The actual value of soil moisture capacity can be measured at a particular site, but this quantity varies from point to point, and its mean value over any given region is essentially unknown. Furthermore, in order to apply these accounting techniques properly over a region, as opposed to a single point, it is not sufficient to know the mean soil moisture capacity; one must also know the distribution of this quantity over the region. Kohler and Richards (1962) attempted to handle this problem by assuming several values of moisture capacity for an area.

The weight which is applied to each value is then determined by correlation analysis. These weights depend on the purpose to be served and on the available data. In their case, the weights were determined to yield the best index of storm runoff. Presumably these weights might be different if used for other purposes. In any event, the computed soil moisture deficiencies served only as indices in an independent relationship for predicting direct runoff from individual storms.

There is a further problem involved in the use of the terrestrial water balance equation which is sometimes overlooked. This arises from the fact that errors in the measurement of precipitation are not random, but exhibit a negative bias (LaRue and Younkin, 1963). Consequently, precipitation measurements will, in most cases, underestimate the actual precipitation. This bias, which has been the subject of numerous investigations during the past 80 years, is thoroughly discussed in the comprehensive survey paper of Weiss and Wilson (1957). The error is mainly related to the speed of the wind and the character of the precipitation, and is most serious for the commonly used unshielded rain gage. Several comparisons have been made between an unshielded gage and a Koschmieder or pit gage, which Weiss and Wilson feel comes closest to giving a useful reference for "true" rain. In most of these tests the unshielded gage underestimated the actual rain-

fall by 5-15% at wind speeds of 4 meters $sec^{-1}$, 5-30% at 8 meters per second, and 5-50% at 12 meters per second.

Added problems arise in the measurement of snow, and several studies comparing ground measurements of snow with the catch in gages with flexible shields show an average underestimation ranging from 4 to 25% (Weiss and Wilson, 1957). The underestimation is much larger for unshielded gages and gages with rigid shields. General corrections cannot be made for these errors, since the bias is variable and primarily a function of local wind speed.

This bias is accentuated in mountainous areas, where reports are usually sparse and biased toward lower elevations. According to LaRue and Younkin (1963), the paucity of data in the mountainous regions of the United States probably leads to precipitation underestimates of a moderate degree. The lack of adequate precipitation data over large inland lakes, such as the Great Lakes, also creates difficulties.

The average amount by which precipitation is underestimated over North America is, of course, difficult to say, but in the light of the survey of Weiss and Wilson (1957), a figure of 5-10% would not seem unreasonable. This amounts to an average for the United States of about 3.5 to 7.5 cm/year, by no means a negligible figure when considering longer term storage changes. Although precipitation measurements will be used in the course of this investigation, in order to obtain estimates

of evapotranspiration, the shortcomings of these measurements must be kept in mind.

Until recent times, the hydrologist has been restricted to measurements involving only the terrestrial branch of the hydrologic cycle. Since the late 1930's, however, an improving network of radiosonde stations has allowed progressively more detailed measurements of atmospheric water vapor content and flux. These data have given rise to several important studies during the past 15 years, which have greatly increased our knowledge of the circulation and distribution of water vapor in the atmosphere.

Because of its high degree of mobility, the atmosphere transports huge quantities of water, even though its mean total water content only approximates that of the rivers of the earth. The continual operation of evaporation and precipitation processes, which are estimated by Budyko (1963) to proceed at an average rate of 100 cm/yr, causes a rapid turnover in the water content of the atmosphere, and limits the average residence time of atmospheric water to around 10 days.

Over any given region, one finds a source or sink of atmospheric water vapor, the strength of which depends upon the magnitude of the imbalance between evaporation and precipitation at the earth's surface. This must, in the long run, be compensated for by a divergence, either

positive or negative, of the atmospheric vapor flux over the region. Perhaps the most important single finding of the investigations of the past few years, from a hydrologic point of view, was the demonstration by authors such as Starr and Peixoto (1958), Benton and Estoque (1954), Hutchings (1957) and Starr, Peixoto and Crisi (1965) that the vapor flux divergence can be measured accurately enough to give useful estimates of the mean difference between evaporation and precipitation, provided the region considered is not too small and the time period not too short. In these cases, the problems involved in the estimation of evapotranspiration by empirical techniques can be avoided by using an atmospheric water vapor balance equation (Starr and Peixoto, 1958). Furthermore, for such problems as evaluating the heat balance of the earth-atmosphere, estimating the mean annual runoff from ungaged areas, computing surface and subsurface storage changes over land and, in addition, for many balance problems over ocean areas, it is sufficient to evaluate only the quantity $\overline{E-P}$ ; the mean difference between evaporation and precipitation. In these cases, the use of the atmospheric water vapor balance equation also avoids the problems arising from the bias in precipitation measurements. There are serious practical problems involved in the use of this approach over smaller regions, but when used over sufficiently large areas, where aerological data is adequate, there is ample reason

to believe that the problems involved are less formidable than those posed by the more conventional empirical techniques.

Extensive atmospheric water vapor flux data has recently become available for the first time. These data were processed as part of a large scale meteorological data processing program, supported by the National Science Foundation under grant Nos. GP-3657 and GP-820, and directed by Professor V. P. Starr at M. I. T. These data are, it seems, adequate for a rather detailed study of the water vapor flux and flux divergence over North America, provided certain care is used and certain precautions observed. It was felt that initial studies involving these data should pursue the following goals:

(1) A more detailed description of the atmospheric water vapor flux and flux divergence over the North American sector than has hitherto been possible.

(2) A thorough investigation of the advantages and limitations involved in the use of water vapor flux data in large scale water balance investigations.

(3) A contribution to a better understanding of the overall atmospheric and terrestrial water balance of North America.

A study of the water balance of the North American Continent and the neighboring Central American Sea (Caribbean Sea and Gulf of

Mexico), covering the period May 1, 1961 through April 30, 1963, has been made with these goals in mind. This report contains the more important results of that investigation.

## II. REVIEW OF PREVIOUS VAPOR FLUX INVESTIGATIONS

A considerable number of investigations of atmospheric water vapor flux and flux divergence, on scales ranging from less than $10^5$ $km^2$ to hemispheric, have been made during the past 15 years. Several of these which the author feels to be pertinent to the present investigation will be discussed in this section.

Observation of the atmospheric branch of the hydrologic cycle became possible as a result of the rapid expansion of the network of aerological stations just prior to and, in particular, during World War II. Meteorologists and hydrologists were slow in grasping this opportunity and very little use was made of these data until 1950 when Benton, Blackburn, and Snead (1950) used atmospheric flux data in a study of the water balance of the Mississippi Basin.

It had formerly been held by some hydrologists that a large part of the precipitation which fell over continental areas was derived from local sources of evaporation. This misconception arose, according to Gilman (1964), when the availability of runoff measurements showed that local evaporation amounted to a large percentage of the local precipitation. This knowledge, combined with an underestimation of the mobility of the atmosphere, led to a gross overemphasis of the direct effect of local evaporation on local precipitation. On the basis of these

conclusions, serious proposals were made to increase precipitation by locally increasing evaporation (Sellers, 1965). Holzman (1937) had previously recognized the importance of advected moisture to the local water balance and pointed out that most evaporation occurs into drier air masses, which generally produce little precipitation. The study of Benton, Blackburn and Snead further showed that most water evaporated over the Mississippi Basin is carried far outside the basin before falling again as precipitation.

This initial study was followed by a regional study over North America (Benton and Estoque, 1954), which is of considerable significance to the present investigation. Using twice daily data at 850, 700 and 500 mb from the rather sparse aerological network in existence over North America in 1949, and using the geostrophic approximation for the winds, Benton and Estoque made estimates of the flux across the continental boundaries, and described the broad scale features of the flux field during 1949. In addition, the computed flux divergence yielded reasonable estimates of average monthly and annual values of E-P for the continent as a whole. These estimates became less reliable as the size of the area was reduced (Benton, Estoque and Dominitz, 1953).

Hutchings (1957) made a careful study of the vapor flux across

a small quadrangular area of southern England ($9 \times 10^4$ km$^2$) delimited by aerological stations at the four vertices. The investigation included a statistical analysis of the probable errors in the flux measurements. This analysis is of interest since the vertical resolution in Hutchings' data was similar to that used in the present study, and will be discussed later with respect to data representativeness.

Hutchings (1961) also made a regional study of water vapor transfer over Australia during the year 1956. The network of Australian stations was roughly comparable to that available to Benton and Estoque over North America in 1949. Once daily data at the surface, 900, 850, 800, 700, 600, 500 and 400 mb levels were used. The study was complicated by the frequent occurrence above 850 mb of relative humidities too low to be measured. Nevertheless, the average annual flux divergence computed over eastern Australia, assuming the maximum possible mixing ratio in those cases where "motorboating" occurred, was in excellent agreement with independent estimates of $\overline{E-P}$. Mean monthly values were not in particularly good agreement. Lack of agreement during the winter months was probably due in part to errors in the independent estimate of evapotranspiration. These estimates were obtained by the Thornthwaite method (Thornthwaite and Mather, 1955) which has a tendency to underestimate evaporation during the winter months. One

might suspect that differences during the summer months were due, in part, to diurnal variations in the vapor flux. Such variations were found in the summertime flux over much of North America in the course of the present investigation, and render once daily observations unrepresentative of the mean daily flux.

In a recent study of evaporation over the Baltic Sea, Palmén (1963) found the average annual flux divergence to be in excellent agreement with independent estimates of $\overline{E-P}$. These results were based on data from Russian, Finnish, Swedish, Danish, and East German radiosondes.

The most extensive studies of the atmospheric branch of the hydrologic cycle, with the aim of finding its relationship to the general circulation of the atmosphere and to the large scale terrestrial water balance, have been conducted as part of the MIT Planetary Circulations Project, under the direction of Professor V. P. Starr. These studies were concerned with average annual or semi-annual conditions. White (1951), in an early study, estimated the water vapor transport across latitude circles from actual wind and humidity reports. This was followed by a series of investigations based on data from the year 1950. They included an initial study of the poleward flux of water vapor (Starr and White, 1955), followed by a more extensive investigation of the

meridional water vapor flux (Starr, Peixoto and Livadas, 1958). The first study, on a hemispheric basis, of the flux divergence and its relationship to the water balance of the earth was made by Starr and Peixoto (1958). These analyses were later discussed in great detail by Lufkin (1959). The techniques for obtaining the spatial distribution of flux divergence which are used in the current investigation, were discussed in some detail by Peixoto (1959).

The zonal water vapor flux (Starr and Peixoto, 1960) and the eddy flux (Starr and Peixoto, 1964) have also been studied. The final outcome of the 1950 investigations has been summarized in a monograph (Peixoto, 1958).

Similar studies of the hemispheric water balance (Starr, Peixoto and Crisi, 1965; Peixoto and Crisi, 1965) have recently been completed using the more extensive data available during the IGY year 1958. These data also made possible the first study of atmospheric humidity conditions over the entire African Continent (Peixoto and Obasi, 1965).

## III. FORMULATION OF THE BALANCE EQUATIONS

The following notation will be used:

$g$ = acceleration of gravity

$a$ = mean radius of the earth

$\lambda$ = longitude

$\phi$ = latitude

$p$ = pressure

$q$ = specific humidity

$p_o$ = pressure at the ground

$p_u$ = pressure at which the specific humidity becomes negligibly small

$u = a \cos\phi \frac{d\lambda}{dt}$ , zonal wind component

$v = a \frac{d\phi}{dt}$ , meridional wind component

$i_\lambda$, $i_\phi$ = eastward and northward pointing unit vectors, respectively

$G$ = total subsurface flow through a unit length of drainage basin boundary

$E$ = rate of evapotranspiration

$P$ = rate of precipitation

$RO$ = rate of stream flow from a drainage area

$S$ = total water storage on and below the surface of the earth per unit horizontal area.

$E$ = net sources of water vapor in a unit atmospheric column extending from $p_0$ to $p_H$

$t, \tau$ = time

$N$ = number of observations

$C$ = curve bounding a drainage area

$n_c$ = outward pointing unit normal on curve

$\overline{(\,)} = \frac{1}{\tau}\int_{\tau}(\,)\,dt$ = time mean

$(\,)' = (\,) - \overline{(\,)}$ = instantaneous departure from time mean

$\langle(\,)\rangle = \frac{1}{A}\int\int_{A}(\,)\,a^2\cos\phi\,d\lambda\,d\phi$ = spatial mean

The following vertical integrals will be referred to in the course of this report:

$\overline{W} = \frac{1}{g}\int_{p_H}^{p_0}\bar{q}\,dp$ mean precipitable water (gm cm$^{-2}$ or cm)

$\overline{Q_\lambda} = \frac{1}{g}\int_{p_H}^{p_0}\overline{qu}\,dp$ vertically integrated mean total zonal water vapor flux (gm (cm sec)$^{-1}$).

$\overline{Q_\phi} = \frac{1}{g}\int_{p_H}^{p_0}\overline{qv}\,dp$ vertically integrated mean total meridional water vapor flux (gm (cm sec)$^{-1}$).

$\overline{Q} = i_\lambda\overline{Q_\lambda} + i_\phi\overline{Q_\phi}$ vertically integrated mean total water vapor flux (gm (cm sec)$^{-1}$).

The form of the atmospheric water vapor balance equation is essentially that of Starr and Peixoto (1958), and Peixoto and Obasi (1965).

For a column of air, extending from the ground to a pressure $p_H$, one may write the atmospheric water vapor balance equation in the following form:

$$\frac{\partial W}{\partial t} + \nabla \cdot Q = E \qquad (1)$$

The atmosphere is assumed to be in hydrostatic equilibrium, and the flux through the upper boundary of the column is ignored, since $q$ is negligible at $p_H$.

Evapotranspiration from the earth's surface and precipitation falling from the air column constitute the major source and sink of water vapor. The formation (evaporation) of clouds within the column constitutes another possible sink (source), but the use of commonly accepted values for the water content of clouds (aufm Kampe and Weickmann, 1957; Atlas, 1965) indicates that the flux of water, in liquid and solid form, will rarely average 10 to 20 gm $(\text{cm sec})^{-1}$ for periods of a month or more. This, for example, represents around 1% of the total flux in the regions of persistent wintertime cloudiness along the west coast of North America. Since the flux divergence rather than the flux itself affects the accuracy of the water balance computation, it can be concluded that the transport of water in liquid or solid form may be of some significance in those rather localized regions of persistent formation or dissipation of clouds, or for occasional short

time periods, but can be safely ignored on a mean monthly basis for large scale water balance studies.

Thus

$$\mathcal{E} = E - P$$

When applied to mean conditions over a given region and time period, Eq. 1 becomes

$$\langle \nabla \cdot \bar{Q} \rangle = \langle E - P \rangle + \left\langle \frac{\overline{\partial w}}{\partial t} \right\rangle \tag{2}$$

For annual means, $\left\langle \frac{\overline{\partial w}}{\partial t} \right\rangle$ is usually negligible compared with the other terms. For monthly means, however, all terms are often of the same order of magnitude, particularly during the spring and fall.

The vapor flux divergence can be expressed in spherical coordinates:

$$\nabla \cdot \bar{Q} = \frac{1}{a \cos\phi} \left\{ \frac{\partial \bar{Q}_\lambda}{\partial \lambda} + \frac{\partial (\bar{Q}_\phi \cos\phi)}{\partial \phi} \right\} \tag{3}$$

This expression can be conveniently evaluated by finite difference methods to provide the mean divergence within each area defined by 4 grid points. However, when making detailed water balance studies which involve the use of stream flow data, it is usually more convenient to obtain the mean divergence over an irregularly shaped drainage basin. For this purpose, a useful expression for flux divergence may be obtained from Gauss's

Theorem:

$$\langle \nabla \cdot \bar{Q} \rangle = \frac{1}{A} \oint_c \bar{Q} \cdot m_c \, dC. \tag{4}$$

A second relationship is obtained as a balance equation for the ground branch of the hydrologic cycle. When applied to a particular drainage basin, this balance may be expressed, in its simplest form, as follows:

$$-\langle \overline{E-P} \rangle = \langle \overline{RO} \rangle + \left\langle \frac{\overline{\partial S}}{\partial t} \right\rangle + \frac{1}{A} \oint_c \bar{G} \cdot m_c \, dC. \tag{5}$$

$\langle \overline{RO} \rangle$ is the net stream outflow from the basin. $\left\langle \frac{\overline{\partial S}}{\partial t} \right\rangle$ is the mean rate of storage change (surface, soil moisture, and ground-water) over the basin. $\frac{1}{A} \oint_c \bar{G} \cdot m_c \, dC$ is the net underground flow through the vertical boundaries of the basin. This term will not include ground water flow which discharges into streams within the basin, and contributes only when ground water and surface divides do not coincide. The lack of coincidence of these divides in many limestone and lava regions is well known, and "lost rivers" are commonly encountered in such areas as the Columbia Plateau of the northwestern United States and in the karst areas of Kentucky and Central Europe (Maxey, 1964). Similarly, basins containing large outcrop areas of confined aquifers of broad regional extent may have abnormally low runoff due to precipi-

tation directly entering the aquifer within the basin, or infiltration from streams within the basin. This water is then discharged at downstream points. Typical of this phenomenon are the streams issuing from the mountains onto the alluvial fans of the basin and range province of the Western United States, and the eastward flowing streams of the Black Hills region of North Dakota (Maxey, 1964). These underground exchanges probably occur on a scale too small to be studied to advantage using the atmospheric water vapor balance equation. Little is known of the larger scale movement of groundwater, which would involve the major aquifer systems, and any interconnections between these systems. Although such exchanges appear to occur in some desert areas (Starr and Peixoto, 1958), they are probably quite small in most regions, and it was felt that attempts to evaluate this quantity over North America would be best deferred to a later time, when data will become available for a period of length sufficient to render surface and soil moisture storage changes unimportant. Lacking evidence to the contrary, such exchanges were assumed to be small over the large drainage areas investigated, when compared with the seasonal and interannual surface and subsurface storage changes.

Neglect of this term then leaves only two unknowns, $\langle \overline{E-P} \rangle$ and $\left\langle \frac{\overline{\partial S}}{\partial t} \right\rangle$, to be evaluated between Eqs. (2) and (5), since $\left\langle \frac{\overline{\partial w}}{\partial t} \right\rangle$

can be measured. Solving for surface and subsurface storage change gives:

$$\left\langle \overline{\frac{\partial S}{\partial t}} \right\rangle = \langle \nabla \cdot \overline{Q} \rangle + \left\langle \overline{\frac{\partial W}{\partial t}} \right\rangle - \langle \overline{RO} \rangle \tag{6}$$

Using precipitation measurements, one can also solve for $\langle \bar{E} \rangle$:

$$\langle \bar{E} \rangle = \langle \nabla \cdot \overline{Q} \rangle + \langle \bar{P} \rangle + \left\langle \overline{\frac{\partial W}{\partial t}} \right\rangle \tag{7}$$

These two simple relationships can then be used to evaluate the two unknowns of the terrestrial water balance equation, all other quantities in the equations being measured.

## IV. DATA AND PROCEDURES

The period studied extends from May 1, 1961 through April 30, 1963. 00 GMT meteorological data for the period May 1958 through April 1961 were also available, but were used only for special purposes. The basic meteorological data were obtained from the MIT GENERAL CIRCULATION LIBRARY and consisted of mean monthly values of the following quantities

$$\overline{q} = \frac{\Sigma q}{N} \qquad \overline{u} = \frac{\Sigma u}{N} \qquad \overline{v} = \frac{\Sigma v}{N}$$

$$\overline{qu} = \frac{\Sigma qu}{N} \qquad \overline{qv} = \frac{\Sigma qv}{N}$$

$$\overline{q'u'} = \overline{qu} - \overline{q}\,\overline{u} \qquad \overline{q'v'} = \overline{qv} - \overline{q}\,\overline{v}$$

Separate data were available for 00 GMT and 12 GMT at the surface, 1000 mb and at 50 mb intervals up to 200 mb for stations over North America and the surrounding area (see Fig. 1). Statistical estimates of $\overline{q}$, which are available when the humidity was so low that "motorboating" occurred, were treated as actual reports.

$\overline{w}$, $\overline{Q_\lambda}$ and $\overline{Q_\phi}$ were computed separately for 00 GMT and 12 GMT by applying the trapezoidal rule beginning with the first even 50 mb level above the surface and adding to this the additional contribution from the surface layer. The mean monthly surface pressure

was considered to be the pressure at the ground. Thus it was possible to have reports at pressures higher than that of the surface in those cases where the mean monthly surface pressure was only slightly below a standard reporting level; these reports were excluded from consideration. Monthly means at levels having less than 10 reports were not used. Instead the data were considered missing and the value was obtained by linear interpolation between the two nearest reporting levels. Stations were considered missing if data did not extend to 700 mb on at least 10 days of the month. Missing values at or above 500 mb were assumed to be zero if there were no data at higher levels. The total number of reports was tabulated for each station for each month in the course of the computations. Examination of these figures indicated that the percentage of missing reports generally ranged between 10% and 20%.

Separate monthly maps were plotted and analyzed for $\overline{Q}_\lambda$ and $\overline{Q}_\phi$ for each of the 24 months, at both 00 GMT and 12 GMT. In addition, a variety of auxiliary maps were plotted and analyzed in order to obtain additional information on precipitable water, diurnal flux variations, and mean seasonal patterns. Some of these special charts are included in this report.

Computations of flux divergence were made by applying finite

difference methods to Eq. 3 (Peixoto, 1959), using as data the values of $\overline{Q_\lambda}$ and $\overline{Q_\phi}$ on a 2.5° latitude by 2.5° longitude grid south of 57.5°N, and on a 5.0° longitude by 2.5° latitude grid north of this latitude. As before individual computations were made for each month, and separately for the 00 GMT and 12 GMT data.

In order to obtain accurate values of mean divergence for the various irregularly shaped regions considered in the water balance studies, the net flux across a convenient curve, closely approximating the actual boundary of the basin, was estimated directly from the flux component maps. It makes little difference for the larger regions whether one approximates a line integral around the basin or estimates the mean flux divergence directly from the grid point data. On the other hand, it is not always possible to satisfactorily approximate the flux through the boundaries of the smaller regions using only grid point data. Estimation of the mean flux divergence by planimetering a divergence analysis based on grid point data was not considered satisfactory, since the total divergence over an area, as represented by a summation of the flux through the boundary, may not be conserved in the isoline analysis.

Streamflow data were obtained from the Water Supply Papers of the U. S. Geological Survey and Water Resources Papers of the

Canadian Department of Northern Affairs, for an area of $85.7 \times 10^5$ km$^2$ covering almost all of the United States, and much of southern Canada. Immediate coastal regions were not included, partly because of the time involved in obtaining runoff from the great number of small coastal streams; and partly due to limitations imposed by the location of the last downstream streamgaging station, which is normally located some distance inland. This had the effect of keeping the boundary of the drainage area well within the outer ring of aerological stations. Streamgaging stations used in this study, the areas they gage, and additional regions of internal drainage are listed in Table 1.

Table 1. Streamgaging stations used in the investigation.

| River | Station | Drainage Area ($10^5$km$^2$) |
|---|---|---|
| Frazier | Hope, B. C. | 2.03 |
| Skagit | Mt. Vernon, Wn. | 0.08 |
| Cowlitz | Castle Rock, Wn. | 0.06 |
| Columbia | The Dalles, Ore. | 6.15 |
| Willamette | Wilsonville, Ore. | 0.22 |
| Umpqua | Elkton, Ore. | 0.10 |
| Rogue | Grants Pass, Ore. | 0.06 |
| Klamath | Klamath, Ore. | 0.31 |
| Eel | Scotia, Calif. | 0.08 |
| San Joaquim | Vernalis, Calif. | 0.73[1] |
| Cosumnes | McConnel, Calif. | 0.02 |

[1]Includes non-contributing Tulare Basin

Table 1 cont.

| River | Station | Drainage Area ($10^5 km^2$) |
|---|---|---|
| Mokelumne | Woodbridge, Calif. | 0.02 |
| Sacramento | Sacramento, Calif. | 0.67[2] |
| Colorado | Northern Int. Boundary U. S. - Mexico | 6.30[3] |
| Rio Grande | Caballo Dam, N. Mex. | 0.80 |
| Pecos | Girvin, Tex. | 0.77 |
| Colorado | Bay City, Tex. | 1.08 |
| Brazos | Juliff, Tex. | 1.14 |
| Trinity | Romayor, Tex. | 0.44 |
| Neches | Evadale, Tex. | 0.17 |
| Sabine | Ruliff, Tex. | 0.24 |
| Red | Alexandria, La. | 1.75 |
| Ouachita | Monroe, La. | 0.40 |
| Mississippi | Vicksburg, Miss. | 29.69 |
| Big Black | Bovina, Miss. | 0.07 |
| Pearl | Bogalusa, La. | 0.17 |
| Pascogoula | Merrill, Miss. | 0.17 |
| Tombigbee | Leroy, Ala. | 0.50[4] |
| Alabama | Clairborne, Ala. | 0.57 |
| Escambia | Century, Fla. | 0.10 |
| Choctawhatchee | Bruce, Fla. | 0.11 |
| Apalachicola | Chattahoochee, Fla. | 0.44 |
| Suwanee | Wilcox, Fla. | 0.25 |
| Santilla | Atkinson, Ga. | 0.07 |
| Altamaha | Doctortown, Ga. | 0.35 |
| Ogeechee | Eden, Ga. | 0.07 |
| Savannah | Clyo, Ga. | 0.26 |
| Edisto | Givhans, S. C. | 0.07 |
| Santee | Pineville, S. C. | 0.38[5] |

[2]Includes flow through Yolo Bypass
[3]Includes all closed basins entirely within the drainage area. All significant diversions from the basin above the gage are added to the gaged discharge; all diversions into the basin are subtracted.
[4]Flow estimated from upstream stations and gage height readings
[5]Includes diversion through Lk. Marion-Moultrie Canal

| River | Station | Drainage Area ($10^5 km^2$) |
|---|---|---|
| Peedee | Peedee, S. C. | 0.23 |
| Little Peedee | Galivants Ferry, S. C. | 0.07 |
| Cape Fear | Tarheel, N. C. | 0.12 |
| Neuse | Kingston, N. C. | 0.07 |
| Tar | Tarboro, N. C. | 0.06 |
| Roanoke | Randolph, Va. | 0.08 |
| James | Cartersville, Va. | 0.16 |
| Rappahannock | Fredricksburg, Va. | 0.04 |
| Potomac | Washington, D. C. | 0.30 |
| Susquehanna | Marietta, Pa. | 0.67 |
| Delaware | Trenton, N. J. | 0.18 |
| Hudson | Green Island, N. Y. | 0.21 |
| Conecticut | Thompsonville, Conn. | 0.25 |
| Merrimack | Lowell, Mass. | 0.11 |
| Androscoggin | Auburn, Me. | 0.08 |
| St. Francis | Hemming Falls, Que. | 0.10 |
| Richelieu | Fryer's Rapids, Que. | 0.22 |
| St. Laurence | Cornwall, Ont. | 7.68 |
| St. Maurice | Grand'mere, Que. | 0.42 |
| Ottawa | Grenville, Que. | 1.78[6] |
| Nelson | 54°47'N, 97°56'W | 10.09 |
| Burntwood | 55°44'N, 97°54'W | 0.16 |
| | Mississippi Basin | |
| Missouri | Sioux City, Ia. | 8.16 |
| Missouri | Hermann, Mo. | 13.70 |
| Mississippi | Alton, Ill. | 4.70 |
| Arkansas | Little Rock, Ark. | 4.10 |
| Ohio | Metropolis, Ill. | 5.27 |
| Estimated Additional Internal Drainage | | |
| Oregon | | 0.47 |
| Idaho-Wyoming | | 0.10 |
| Utah | | 1.12 |
| Nevada | | 2.52 |
| California | | 1.42 |
| New Mexico | | 0.39 |

[6]Estimated from upstream stations

Precipitation data used in this study was obtained from U. S. Weather Bureau Climatological Summaries, the Monthly Report of the Canadian Department of Transport, and a compilation by LaRue and Younkin (1963).

Information on the levels of the Great Lakes was furnished by the Lake Survey of the U. S. Army Corps of Engineers. Computations of evapotranspiration and soil moisture storage for the Ohio Basin, based upon the Thornthwaite method (Thornthwaite and Mather, 1955), were furnished by Mr. Wayne Palmer, of the Environmental Data Service, ESSA. Lake evaporation data (Kohler et al, 1955) was furnished by the Hydrologic Research and Development Laboratory of the U. S. Weather Bureau.

Several stations, mostly military operated, converted from the lithium chloride to the carbon humidity element during this two year period. No significant difference in the measurements obtained from these two elements could be detected in the monthly means; however, the dates of changeover of these stations are listed below.

Table 2. Dates of changeover from lithium chloride to carbon humidity elements. (Source: National Weather Records Center, Asheville, N. C.)

| Station | Date of Change | Remarks |
|---|---|---|
| Adak, Alaska | 9/29/61 | |
| Argentia, NFD | 1/30/61 | |
| Corpus Cristi, Tex. | 4/1/61 | |
| Key West, Fla. | 3/1/61 | Navy stations |
| Trinidad, BWI | 5/16/61 | |
| Pt. Arguello, Calif. | 1/15/62 | |
| Guantanamo, Cuba | 2/13/61 | |
| Kindley AFB, Bermuda | | Air Force stations- |
| Eglin AFB, Fla. | | date of changeover |
| Del Rio AFB, Tex. | | unknown but probably in mid 1961. Del Rio operated by Air Force until 3/3/63, then operated by the Weather Bureau, who used lithium chloride element. |
| Oakland, Calif. | 4/63 | |
| Midland, Tex. | 4/63 | U.S. Weather Bureau |
| Intl. Falls, Minn. | 4/63 | |
| Tatoosh, Wn. | 4/63 | |

## V. REPRESENTATIVENESS OF DATA AND ANALYSES

### A. Representativeness of the Water Vapor Flux Data

The extent to which the flux data represent the true conditions is determined by (1) how well the data taken at a particular hour, at a particular station, define the actual mean flux at that observing time, and (2) how well the mean of the 00 GMT and 12 GMT observations define the actual mean monthly flux.

The study of Hutchings (1957) previously cited throws some light on these problems, since the resolution of his data (surface and every 50 mb up to 750 mb, then every 100 mb to 350 mb) is similar to that used in the present study. Although not specifically stated, observations were apparently made with the Kew radiosonde. He obtained the following flux vector errors at various levels:

Table 3 . Water vapor flux vector errors (from Hutchings, 1957). Units: gm (cm mb sec)$^{-1}$

| Level | $\overline{gV}$ | Systematic error | Standard vector error | |
|---|---|---|---|---|
| | | | Total | Sampling |
| 950 mb | 4.5 | +.01 | .09 | .08 |
| 750 mb | 3.1 | +.07 | .07 | .06 |
| 550 mb | 1.5 | +.06 | .04 | .04 |
| 350 mb | 0.4 | +.03 | .01 | .01 |

$\overline{qv}$ is the mean water vapor flux at the 4 stations during the three month period June-August, 1954. The systematic error was due to humidity errors which were produced by instrumental lag. In this regard, it should be noted that Hutchings assumed no other systematic instrumental errors.

Lag errors in humidity measurements, wind errors, and sampling errors arising through the use of the arithmetic mean of two observations a day all contributed to the standard vector error. However, from Table 3 , it is apparent that sampling errors made the major contribution. It will be shown later that diurnal variations in the vapor flux will produce an additional systematic sampling error which often overshadows all others.

The following results were obtained for the vertically integrated transport:

Table 4 . Estimated vertically integrated water vapor flux vector errors (from Hutchings, 1957). Units: gm (cm sec)$^{-1}$.

| Systematic error | Standard vector error |
|---|---|
| +30 | 16 |

Sampling errors again make the major contribution to the standard vector error.

The following values were obtained for the flux divergence errors, assuming linear variations between stations:

Table 5 . Estimated vapor flux divergence errors (from Hutchings, 1957). Units: gm $(cm^2$ mb 3 months$)^{-1}$.

| Level | $\nabla \cdot \overline{q\mathbf{v}}$ | Systematic error | Standard error |
|---|---|---|---|
| 950 mb | -0.302 | 0 | 0.023 |
| 750 mb | +0.099 | 0 | 0.019 |
| 550 mb | +0.052 | 0 | 0.011 |
| 350 mb | +0.011 | 0 | 0.003 |

The errors at each level were not serious when compared with the computed values of divergence, even over the relatively small area being investigated. Errors produced by nonlinear flux variations between stations, which were not included in this estimate, may be more serious, however.

For standard errors of the vertically integrated divergence (including a contribution for nonlinear effects), Hutchings obtained an estimate of 4 g $cm^{-2}$ for the 3 month period. The magnitude of this error would, of course, decrease as the size of the area increased, provided the same spacing between stations was retained on the boundary.

The characteristics of the Kew radiosonde, as to lag and instrumental error, may not be the same as that of the American instru-

ment. Nevertheless, it seems probable that the overall error in the measurement of the mean monthly flux would be similar for the two instruments.

This study indicates that the mean monthly flux at a particular observation time is defined quite accurately if no observations are missing. The mean monthly data used in the present investigation were normally computed from something less than a complete set of monthly observations, but the number of missing observations was usually under 20%. This will undoubtedly increase the errors in the monthly means, but, barring a bias in the missing data, these errors will usually become quite small for seasonal and annual means.

There is a certain amount of variation in the response characteristics of different radiosonde humidity elements, and it is possible that the use of a large supply of instruments with abnormal characteristics will result in a bias in the monthly mean. Should this occur within the dense network of stations over the United States, and last for a period of months, it will be identifiable as a systematic, small scale feature in the analyses during that period. Such may have been the case in a few instances, although this is difficult to state with any degree of certainty. In any case, the analyst is well advised to smooth any small scale, transient irregularities, as they are difficult to define

properly, and at best add little to the large scale balance computations.

A few stations, most of them military, converted from a lithium chloride to a carbon humidity element during this two year period. Some information on the relative characteristics of these two elements can be found in a paper by Hodge and Harmantas (1965), but their relative behavior on a mean monthly basis is unknown. Therefore, a few simple checks of the data were made in an attempt to determine if any significant inconsistency was introduced into the flux measurements by this change.

A check of the observations at San Antonio and Del Rio, Texas was first made, since it is tempting to attribute the large differences often found in the measured 12 GMT flux at these two stations to the use of different elements. However, an inspection of the original data showed the difference to be due primarily to differences in the winds.

As a further check, mean monthly values of $W$ at Corpus Christi and Key West (carbon element) were compared with those at Brownsville and Miami (lithium chloride element). The most northerly station used the carbon element when Corpus Christi and Brownsville were compared, while the reverse was true in the case of Miami-Key West. Throughout most of the year, the stations exhibited the expected latitudinal effect, with values at the more northerly stations being lower in every case.

However, during the summer months, when the latitudinal effect is unimportant, the stations with the lithium chloride element recorded slightly higher values of $\overline{w}$ . The differences were not large, and may have been due to factors other than the humidity element.

Tinker AFB and Oklahoma City provided the best comparison of the two elements. Tinker AFB changed to the carbon element in November, 1961*, while Oklahoma City used the lithium chloride element throughout the two year period. The stations are only a few miles apart, and at practically the same elevation. Tinker AFB made observations at 06 and 18 GMT; Oklahoma City at 00 and 12 GMT. 12 months of data, four of which occurred before the change of elements at Tinker AFB, were available from which to make comparisons. Although the data did bring to light a systematic difference in wind observations between the stations, there was no indication of any important difference in humidity measurements, either before or after the change.

From these comparisons, it appears that differences in humidity measured by the carbon and lithium chloride elements create at most only small and, for our purposes, negligible differences in the mean monthly flux.

Hutchings (1957) study indicated a 50 mb resolution in the vertical

*Verbal communication from Mr. W. Tochiffely of the National Weather Records Center.

to be adequate for studies of this type. The results of this investigation support his conclusion, although the vertical profiles of flux divergence which were found during the summer, with their rapid changes in the lower levels, indicate that a 25 mb interval could be justified through the lowest 100 mb. An upper limit of 200 or 300 mb appears to be quite adequate for the vertical integration.

Perhaps the most serious problems of representativeness are concerned with approximating the mean daily flux from observations taken once or twice daily. Hutchings (1957) analyzed the magnitude of the random error which results from this approximation, and found it not serious. However, neither he, nor Benton, Estoque and Dominitz (1953) considered the possibility of systematic errors which can arise because of this approximation, if there exist large mean diurnal variations in the flux. Such variations were found in the course of this investigation, and will be discussed in detail later. These variations are large enough to produce unacceptable errors in the flux computations over much of the North American Sector when only once daily observations are used. The error is greatly reduced by using twice daily observations, but some error is, no doubt, still present, and its effect on the divergence computations has not as yet been adequately determined. This will require further investigation, using all available

6 hourly observations. Suffice to say that in many areas, particularly during the summer, the systematic error in the flux divergence, introduced by the use of twice daily observations to approximate the mean daily flux, is not negligible, but is an important factor in determining the smallest area to which the atmospheric water balance equation can be successfully applied.

B. Representativeness of Streamflow Data

The accuracy of streamflow data depends primarily on (1) the stability of the gage-discharge relation or, if the stream channel is unstable, the frequency of the discharge measurements, and (2) the accuracy of observations of stage, measurements of discharge, and interpretation of records (U. S. Geological Survey Water Supply Papers). The station description states the degree of accuracy of the records. The error in daily values is generally less than 10%; consequently the mean monthly and annual errors will, in general, be considerably less than this figure. No known systematic errors exist in these measurements.

C. Representativeness and uniqueness of the analyses

One can study the water vapor flux divergence by computing the

divergence within a polygon formed by aerological stations at the vertices, or by constructing maps of the flux components, from which data can, in turn, be obtained for divergence computations. The first method has the advantage of being completely objective, but the size and shape of the areas over which computations can be made is determined by the location of the aerological stations. Furthermore, it is difficult to assume anything but linear flux variations between stations. The second method is less restrictive, for one can use the analyses to compute a line integral around any desired region. Furthermore, it allows the introduction of nonlinearity in the analysis when indicated by the data. The introduction of these features, which depend to some extent on the judgement of the analyst, makes definitive statements on the representativeness and uniqueness of the analysis difficult. The use of objective analysis techniques can simplify this problem, and some promising progress along these lines has recently been made by personnel of the Travelers Research Center.

The question of uniqueness may be stated as follows. How much subjectivity does the station network reasonably allow in the determination of the mean divergence? A few simple tests were made in order to gain some insight into this problem. The first consisted of making two different analyses from the same data, the results of

which are illustrated in Figs. 6 and 7. The divergence field of Fig. 6 was obtained from analyses of mean 00 GMT data for the three month period June through August, 1958, while that of Fig. 7 was obtained by averaging the divergence computed from individual monthly analyses. The major features of the pattern are quite similar, as are many of the smaller scale features. Thus, differences in analysis would not be of much importance for averages over large portions of the continent. It is noteworthy that the smoother pattern is obtained when individual monthly analyses are averaged. This might be expected, since a part of the random analysis error is then removed. Consequently, this should also be the more representative of the two analyses, but since only 00 GMT data was used, neither analysis gives a good representation of the actual mean seasonal divergence.

Further checks on the uniqueness of the analyses were performed using line integrals around regions of varying size. Following the computation of the net flux into a given region, the flux field in the vicinity of the boundary was reanalyzed on acetate, making a conscious effort to maximize the net flux into the region, within the limits of a reasonable analysis. The changes which were produced in the mean divergence rarely exceeded 1/2 cm $mo^{-1}$ for areas larger than $15 \times 10^5$ $km^2$ (around 1/3 of the United States), and 1 cm $mo^{-1}$ for areas between

10 and 15 x $10^5$ $km^2$. However, for areas smaller than about 5 x $10^5$ km, changes of a few centimeters could sometimes be produced. Thus it appears that the judgement of the analyst becomes an important factor for areas smaller than 10 x $10^5$ $km^2$.

It should be remembered that these checks were made over a region of good data coverage. As the data become less dense, the judgement of the analyst becomes more important. Thus, only the broadscale pattern of flux divergence can be uniquely determined over such areas as the Gulf of Mexico and the Caribbean Sea, and little detail can be justified. In these regions the analyst should strive for a smooth field of the flux divergence as well as the flux components. A smooth analysis of the individual flux components will not necessarily produce a smooth divergence pattern. More likely a series of alternating convergence-divergence "couples" will result, merely because the data are not sufficient to define analyses which maintain the rather delicate balance between the flux components which is characteristic of a vector field whose divergent component is a small part of the total vector. The policy was adopted, for both areas of plentiful as well as sparse data, of striving for an analysis of the flux components, consistent with the data, which would produce the smoothest pattern of divergence. It was felt that no additional detail could be justified.

So far as representativeness of the analyses is concerned, it is quite clear from the previous discussion that a unique analysis, determined entirely by the data, may still not be representative of the mean monthly flux or flux divergence. Much of this report will be concerned with attempts to determine the minimum scale on which these analyses can be usefully applied. It appears that this is primarily determined by systematic errors of three general types; diurnal variations in the flux field, errors arising from local station peculiarities of the type observed at Oklahoma City and Tinker AFB, and the difficulty of separating small scale features from the large scale component of the flux. The latter is a particularly important problem in mountainous terrain, where the tendency to locate stations in valleys, or at lower elevations, creates a situation in which much of the integrated flux vector represents local low level circulations. The problem of systematic errors will be more thoroughly discussed in Chapter XI.

# VI. THE LARGE SCALE FEATURES OF THE NORTHERN HEMISPHERE VAPOR FLUX FIELD

The water balance of North America, or any other region, does not exist as an isolated phenomenon, but operates within the framework of the global hydrologic cycle. Even in a regional investigation, the results take on added meaning if veiwed in relation to the large scale hemispheric water balance. For this reason, it is desirable to discuss briefly the place of the North American sector in the large scale vapor flux field of the northern hemisphere. The discussion will be based primarily on conditions during the IGY year 1958, as illustrated by hemispheric maps (Figs. 2-4) and statistics from the study of Peixoto and Crisi (1965). More detailed mean monthly analyses were made for the North American sector in the course of the present investigation. Maps from this series, for January 1962 and 1963, and July, 1961 and 1962 are also included in this report (Figs. 8-19) for more detailed reference. Unless otherwise stated the discussion refers to the mean total vertically integrated flux.

Looking first at the statistics for the hemisphere, it is apparent that the primary source of atmospheric water vapor is found in the latitude belt extending from $15^{o}N$ - $35^{o}N$. The mean annual southward transport from these latitudes reaches a maximum around $10^{o}N$, then

decreases to practically zero at the equator. The northward transport into mid-latitudes reaches a maximum around 40°N. Conditions vary somewhat with the seasons, with northward transport across the equator in summer and southward transport across the equator in winter. Transient eddies transport water vapor northward at all latitudes, and are the dominant meridional transport mechanism north of 20°N. South of 20°N, the low level mean transport dominates.

The average hemispheric zonal transport broadly reflects the features of the low latitude easterlies and mid-latitude westerlies. The maximum mean annual eastward transport is located around 40°N, while the maximum westward transport occurs near 10°N. The change from eastward to westward transport is found between 20°N and 25°N. Transient eddies are a minor factor in the total zonal transport. The contribution from the higher levels represents a greater percentage of the total zonal transport than it does of the meridional transport, with sizable values observed even at 500 mb.

No westward transport is found at high latitudes in the hemispheric averages, but the total transport drops to almost zero at 75°N, and remains eastward only because of the contribution from the transient eddies.

Summer (April-September) and winter (October-March) hemi-

spheric statistics for the zonal flux reflect the seasonal shift of the westerlies. The latitude of maximum eastward flux moves from 40°N-45°N in summer, to 35°N in winter. Similarly, the latitude of change from eastward to westward transport shifts about 5° southward in winter. On the other hand, the latitude of maximum westward transport remains around 10°N during both seasons.

It becomes apparent, upon examination of Figs. 2-4, that significant large scale asymmetries exist in the hemispheric pattern of the flux components, which are necessarily averaged out in the mean hemispheric statistics. Furthermore, these asymmetries bear an unmistakable relationship to the distribution of the continents and oceans of the hemisphere.

The most intense mean annual meridional transport occurs over the oceans. The maximum southward transport at lower latitudes is found in the eastern Atlantic Ocean, over the Arabian Sea, and over broad areas of the Pacific Ocean. This corresponds to the eastern ends of the semipermanent Atlantic high and wintertime North African high, while the more uniform southward transport over the Pacific is probably due, in part, to the tendency for the Pacific high to split into two separate cells. Almost all of the mean annual northward outflow from low latitudes across 25°N occurs in three definite areas: the southwest

Pacific (south and east of Japan), the western Atlantic and Gulf of Mexico, and the Indian subcontinent and southeastern Asia. The last area is associated with the Asian Monsoon and is primarily a summertime phenomenon. The regions of northward flux in the western Pacific and western Atlantic-Gulf of Mexico mark the southwestern extremities of the major oceanic cyclone belts, and here moisture feeds northeastward from low latitudes into the developing cyclones. The maximum northward moisture flux, and the major oceanic cyclone belts, are found at progressively higher latitudes as one moves eastward across the oceans. Consequently, almost all of the mean annual northward transport across 50°N takes place in the Northeastern Pacific and the North Atlantic. Furthermore, since the mean annual northward transport associated with the Asian Monsoon becomes insignificant north of 35°N , it follows that the primary moisture transport to latitudes above 35°N is accomplished in the oceanic cyclone belts of the Atlantic and Pacific. It is therefore not surprising that this meridional transport is accomplished primarily by the transient eddies.

Important seasonal changes in this pattern are confined to the region of the Asian Monsoon, where the northward transport covers a broader area, is more intense, and extends further north in summer. Even so, the northward flux extends only to 30°N over eastern India, and to 40°N over eastern China, so that the transport to higher latitudes is

still accomplished primarily in the Atlantic and eastern Pacific.

The mean annual zonal flux clearly shows a three wave pattern. At low latitudes, maximum westward transport is found in the central Pacific, over the Caribbean Sea and over the western Arabian Sea and the Horn of Africa. These centers are almost equally spaced around the hemisphere. Three centers of eastward transport are also found, and, as in the case of the meridional transport, are located over the major ocean areas, and associated with the Atlantic and Pacific cyclone belts, and the Asian Monsoon. The maxima over the Atlantic and Pacific are found at progressively higher latitudes as one moves eastward across the oceans, as was the case for the meridional transport. The three maxima are again roughly $120^{o}$ apart but because of the difference in latitude of the ocean areas (the Indian Ocean being at much lower latitudes than the Atlantic or Pacific), they are not symmetric about the pole.

Seasonal changes consist mainly of the southward migration of the major maxima of eastward transport over the Atlantic and Pacific in winter, and the westward extension of the Pacific subtropical westward transport across the Indian subcontinent. This results in a pattern in winter which is more symmetric about the pole; the eastward maximum over southern Asia having shifted northward to around $25^{o}$N.

The major features of the flux fields over North America can now be considered within the framework of the hemispheric circulation pattern.

Two main currents are observed on mean maps. One crosses the Pacific Coast, generally between 40°N-55°N, usually weakens rapidly, and finally merges with the second, more intense current east of the Continental Divide. It has the appearence of a rather diffuse, high level current on mean monthly and seasonal charts. The tendency for a relatively large part of this influx to take place above 850 mb is apparently the result of the high terrain of the Pacific coastal regions, since the eastern Atlantic counterpart of this current shows a strong low level influx well into central Europe.

The second major inflow area is associated with the western Atlantic-Gulf of Mexico region of northward transport previously discussed. The mean westward transport in the western Atlantic becomes more southerly east of the Greater Antilles and off the southeast coast of the United States. South of 25°N the flux remains westward into the Central American Sea. Here the mean current splits into two branches; one moving southwestward across central America; the remainder turning northward and entering the continent in northeastern Mexico and along the western gulf coast of the United States.

The inflow to the southeastern United States moves into the southwestern extension of the Atlantic cyclone belt, while the influx across the Pacific coast is associated with the northeastern extremity

of the Pacific cyclone belt. The history of these two influx currents prior to entering the continent is therefore quite different. In the case of the Pacific coast inflow, the air is relatively cold, and has been moving across the cool waters of the central and north Pacific, through a region of strong flux convergence. The moisture entering the southeastern United States arrives from warm regions of strong vapor flux divergence.

From the previous discussion, it is apparent that the flux pattern over the North American sector is strongly dependent on longitude. For example, the mean annual northward flux maximum occurs around $45^{o}N$-$50^{o}N$ on the Pacific coast, while in the western Atlantic and eastern North America the maximum is found around $25^{o}N$-$30^{o}N$. No low latitude mean southward flux is apparent through the Western Atlantic and eastern Caribbean Sea, but mean southward transport is found as far north as $35^{o}N$ along the west coast of North America. Similar asymmetries are found in the mean annual eastward flux; the maximum is located between $45^{o}N$-$50^{o}N$ over the western portions of the continent, and between $35^{o}N$-$30^{o}N$ east of the Continental Divide. This has the effect of creating a region of light mean annual transport over the southwestern portions of the United States.

We have described, in this section, only the broadscale features of the water vapor flux field over North America. The temporal and

spatial variations of the vapor flux will be described in more detail in the final sections of this report, when the atmospheric water balance of the Central American Sea, and the atmospheric and terrestrial water balance of various regions of the North American Continent will be considered.

# VII. THE VERTICAL DISTRIBUTION OF FLUX DIVERGENCE OVER THE UNITED STATES

A general investigation of the moisture flux on various pressure surfaces was not attempted in this study. However, the series of vertical cross-sections (Figs. 27-39) may be used to define the flux through the boundaries of two areas: ($30^{o}$-$47.5^{o}$N; $80^{o}$-$100^{o}$W) and ($100^{o}$W to the Pacific coast; $30^{o}$ or $32.5^{o}$-$47.5^{o}$N). Except for that portion of the boundary between $30^{o}$ and $32.5^{o}$ N at $105^{o}$W, the flux through the boundaries is completely depicted on the cross-sections.

Values of the boundary flux were tabulated at 50 mb intervals from 1000 mb to 400 mb from data on the cross-sections. Data for El Paso was used as an estimate of the zonal flux through the gap at $105^{o}$W. Additional values were interpolated from the cross-sections at 975 mb and 925 mb when needed to properly define the vertical profiles. The ground profile along the boundaries was estimated as accurately as possible, and outflow was computed only when the pressure surface was above ground level.

The total outflow at each pressure surface was divided by the enclosed area (eastern region $33.6 \times 10^{5}$ km$^{2}$; western region $32.6 \times 10^{5}$ km$^{2}$) in order to obtain a value of outflow per unit area. This figure is eqivalent to the areal mean flux divergence at levels above the

highest terrain. At lower levels, the mean flux divergence over that portion of the area where the pressure surface is actually above ground level will obviously be greater than the total areal average by the ratio of the two areas.

January and July profiles for the two regions are shown in Fig. 96. The January profile for the eastern area shows negative flux divergence at all levels. The maximum near 925 mb coincides with the level of maximum inflow from the south. It is interesting to note that no strong increase in divergence is found at the level of maximum outflow on the east coast (750-800 mb), as this outflow is more than offset by mean inflow through the three remaining boundaries.

The January profile for the western area differs from that in the east in some important respects. With the exception of the 1000 mb level, the region below 850 mb is found to be divergent. Examination of the flux along the boundary reveals outflow in the lower levels east of the Continental Divide and also into the Gulf of California which more than offsets the inflow across the Pacific Coast. Since both the Colorado River Basin and the area east of the Continental Divide are isolated from the remainder of the region by mountains which rise above the 850 mb level, the outflow must have originated within the individual areas, through evaporation or decreased atmospheric storage, or have been supplied from higher elevations by a downward flux

or by evaporation from falling precipitation. The mean flux divergence becomes negative at 850 mb, and maintains a rather constant negative value to 400 mb. The flux convergence above 650 mb is significantly greater than that found over the eastern area.

The July profiles are similar in both east and west, but differ markedly from those found during January. Strong net inflow in the lower elevations is capped by divergence at higher levels. In the east, the maximum inflow occurs between 950 and 1000 mb, and again coincides closely with the level of maximum inflow from the Gulf of Mexico. In addition, the level of maximum net outflow, (between 800 and 900 mb) now coincides with the level of maximum transport across the east coast.

Low level convergence is found throughout a deeper layer over the western area. This is to be expected because of the extensive areas of high terrain, and the variable elevation of the ground. The computed magnitude of this convergence may be somewhat excessive between 850 and 950 because of a probable excess of low level inflow across $100^{o}W$ associated with systematic divergence errors east of the Rocky Mountains. (See Chapter XII of this report). Similarly, the low level convergence of the eastern region may extend through a somewhat deeper layer than indicated by the computation. The high level flux divergence is located at considerably higher elevations over the west, in a manner similar to

the high level convergence pattern in winter.

The contribution to the total integrated flux divergence from each 50 mb layer is given in Table 6. Values above 400 mb were obtained by assuming a linear decrease of divergence to zero at 250 mb. Contributions from the layer below 1000 mb are small, and are not included.

Table 6. Vapor flux divergence. Units: gm $(cm^2\ mo)^{-1}$

| Pressure (mb) | West | | East | | Total | |
|---|---|---|---|---|---|---|
| | Jan | Jul | Jan | Jul | Jan | Jul |
| 1000-950 | +0.02 | -0.87 | -0.43 | -1.02 | -.21 | -0.95 |
| 950-900 | +0.14 | -1.45 | -0.69 | +0.03 | -.28 | -0.70 |
| 900-850 | +0.18 | -1.15 | -0.59 | +0.60 | -.21 | -0.25 |
| 850-800 | +0.03 | -0.32 | -0.49 | +0.66 | -.23 | +0.18 |
| 800-750 | +0.16 | +0.10 | -0.44 | +0.51 | -.30 | +0.31 |
| 750-700 | -0.26 | +0.37 | -0.35 | +0.33 | -.31 | +0.35 |
| 700-650 | -0.29 | +0.47 | -0.29 | +0.28 | -.29 | +0.37 |
| 650-600 | -0.33 | +0.53 | -0.22 | +0.24 | -.28 | +0.38 |
| 600-550 | -0.31 | +0.59 | -0.14 | +0.12 | -.22 | +0.35 |
| 550-500 | -0.27 | +0.50 | -0.13 | +0.11 | -.20 | +0.30 |
| 500-450 | -0.25 | +0.35 | -0.12 | +0.10 | -.18 | +0.22 |
| 450-400 | -0.21 | +0.21 | -0.08 | +0.09 | -.15 | +0.15 |
| (400-250) | (-0.26) | (+0.25) | (-0.08) | (+0.12) | (-.17) | (+0.18) |
| $\langle \nabla \cdot \bar{Q} \rangle$ | -1.97 | -0.42 | -4.05 | +2.17 | -3.03 | +0.89 |
| $\langle \Delta w \rangle$ gm $cm^{-2}$ | +0.5 | +0.3 | +0.2 | +0.3 | +0.3 | +0.3 |
| contribution above 500 mb | -0.72 | +0.81 | -0.28 | +0.31 | -0.50 | +0.55 |

The July profiles may be compared with the June-August, 1954 results of Hutchings (1957) for southern England. He found strong convergence below 850 mb, and divergence at all higher levels up to 350 mb. The values were, however, much larger than the July values over North America, with peak values of $10 \times 10^{-2}$ gm $(cm^2$ mb $mo)^{-1}$ for the low level convergence and $3.3 \times 10^{-2}$ gm $(cm^2$ mb $mo)^{-1}$ for high level divergence.

The contribution to the total vertically integrated divergence from the layers above 500 mb is surprisingly large over the higher terrain of the western region, and it is quite apparent that significant systematic errors will arise in the computed mean monthly divergence if these layers are not included in the vertical integration. On the other hand, the error apparently reverses sign with the season; a consequence of the fact that the higher layers are convergent in winter and divergent in summer. Consequently such errors will have the effect of damping the actual seasonal variations of flux divergence. Since these seasonal errors will tend to cancel, the average annual error will not be large. The contribution from the layers above 500 mb follows a similar pattern in the east, but here amounts to only 7-15% of the total integrated flux divergence.

Given these data, together with an estimate of the rate of evaporation from the surface of the earth, one can estimate the vertical vapor

flux through the lower atmospheric layers in those cases where condensation is not a significant factor. Condensation can probably be safely neglected below 500-800 meters in summer, but such an assumption is less acceptable in winter. Computations of the vertical flux were made for the eastern region at a few of the lower levels, assuming no condensation losses and no changes in atmospheric storage in the layers. Estimates of evaporation from the earth's surface were based on the water balance computations to be discussed in Chapter X, and are listed in the following table as the flux from the surface.

Table 7. Eastern Area - Computed vertical water vapor flux (assuming no condensation or atmospheric storage changes) Units: gm/cm$^2$ mo.

| | January | July |
|---|---|---|
| surface | 2.5 | 9 |
| 950 mb | 3.0 | 10 |
| 925 mb | 3.5 | 10 |
| 900 mb | | 10 |

It is interesting to note that even with the strong low level convergence observed in July, the vertical vapor flux in the lower layers is still primarily the same as the evaporation rate up to 900 mb. Hutchings (1957) computed a vertical transport of around 13 1/2 gm/cm$^2$ mo through the 950 mb level. Of this amount, he estimated 6 gm/cm$^2$ mo was

transported by the large scale vertical motions, and the remainder by convection and small scale turbulence. Evaporation was estimated at around 8 gm/mo. Rainfall during the three month period which he investigated was abnormally high (140% of normal). It seems probable that large scale vertical motion plays a more important role in the summertime vertical vapor flux over England (particularly during the excessively wet summer of 1954) than it does over the United States south of 47.5°N.

The values of the low level vertical flux shown for January are around one-third of those found in July. Because of the neglect of condensation, these values are probably slight overestimates of the actual vertical flux.

# VIII. DIURNAL VARIATIONS OF THE WATER VAPOR FLUX

The random errors which arise when estimating the vapor flux from observations taken once or twice daily have been discussed by Benton, Estoque, and Dominitz (1953) and Hutchings (1957), and estimates of their magnitude have been made. On the other hand, little or no attention has been given the possibility of systematic errors arising from diurnal flux variations. Such errors can be produced by diurnal variations in either the wind or specific humidity or through a correlation of variations in both quantities. Since systematic errors cannot be reduced by increasing the length of the averaging period, they create problems which are, in many respects, more serious than those arising from random errors.

Relatively little information is available on the mean monthly diurnal variations of wind and humidity in the troposphere, as most previous studies have been limited to a few individual stations, or to scattered data from rather restricted areas. However, the existence of diurnal wind variations, under certain conditions and over certain regions, is well known. The complex local land-sea breeze systems have been widely studied. The existence of mountain-valley wind systems (Defant, 1951) has a pronounced effect at some stations in the mountainous regions of North America. Low level nocturnal wind

maxima have been investigated by Gehardt (1962), Hoecker (1963, 1965) Izumi and Barad (1963), Izumi (1964), Kaimal and Izumi (1965) and others, and theories on their existence and behavior have been proposed by Blackadar (1957) and Wexler (1961). Curtis and Panofsky (1958) found important diurnal variations in the mean large scale vertical motion field over the midwestern United States during a 10 day period in July. These appeared to be related to the nocturnal thunderstorm maximum of the Great Plains. Bleeker and Andre (1951) found significant diurnal changes in the mean divergence field in the same general area during August. These two investigations suggest the possibility of significant diurnal variations in the vapor flux divergence as well as in the vapor flux itself. Harris (1959) evaluated the first two harmonics of the tropospheric diurnal wind variations during three summer months at Washington, D. C., and found first harmonic components which exceeded 1 m $sec^{-1}$, and second harmonic components which exceeded 0.4 m $sec^{-1}$. Hering and Borden (1962), in an investigation which clearly indicates the necessity for dealing with this problem, found prominent diurnal variations in the mean monthly summer wind field over the central United States.

Preliminary investigation of the summertime vapor flux did indeed show the presence of significant differences between the mean

00 GMT and 12 GMT flux, and a more detailed investigation was then undertaken. Since the available data consisted almost entirely of observations at 00 GMT and 12 GMT, the investigation was necessarily centered on differences between these two observation times. A limited amount of data taken 4 times daily was available from Ft. Worth and the Tinker AFB-Oklahoma City combination, and this allowed a somewhat more detailed study of these two points. The month of July was chosen for the most detailed investigation, since the oscillations have their greatest amplitude during summer.

The total mean water vapor flux at a particular level may be written:

$$\overline{\rho V} = \overline{\rho}\,\overline{V} + \overline{\rho' V'} \tag{8}$$

$\overline{\rho V}$ is evaluated from data obtained once or twice daily; the implication being that these data give an unbiased estimate of $\overline{\rho}$, $\overline{V}$, and $\overline{\rho' V'}$. Let us, for the purpose of this discussion, define the following quantities:

$$( \;) = \{\overline{(\;)}_h\} + \overline{(\;)}_h^{*} + (\;)'$$

where $\overline{(\;)}_h = \dfrac{\Sigma(\;)_h}{N}$, the mean "h" hour value

$\{(\;)\} = \dfrac{\Sigma(\;)}{H}$, the mean daily value

$(\;) - \{(\;)\} = (\;)^{*}$ = departure from the daily mean

$(\;) - \overline{(\;)} = (\;)'$ = departure from the "h" hour mean

$N$ = number of monthly observations at "h" hour

$H$ = total number of observations each day

The mean monthly vapor flux may then be written:

$$\{\overline{(q v)_h}\} = \{\bar{q}_h\}\{\bar{v}_h\} + \{\bar{q}_h^* \bar{v}_h^*\} + \{\overline{(q' v')_h}\} \qquad (9)$$

The bar operator, as stated above, refers to the mean of the observations taken at "h" hour only. If no systematic diurnal variations exist, the bracket operator becomes superfluous, and the equation is identical with Eq. (8).

Only small diurnal variations of $\bar{q}$ were found in the July data, while large diurnal variations were found in the wind. Considering $\bar{q}$ as constant throughout the day leads to the following approximation of Eq. (9):

$$\{\overline{(q v)_h}\} \approx \bar{q}\{\bar{v}_h\} + \{\overline{q' v'}_h\} \qquad (10)$$

Furthermore, where diurnal variations were important, the diurnal variation in the eddy transport was found to be small compared with the total flux variation. Consequently, the most prominent diurnal variations are due to diurnal variations in the first term on the right side of the equation, i. e., they are the result of diurnal variations in $\bar{v}_h$ .

Some idea of the extent and magnitude of the summertime oscillations can be obtained from Figs. 20 and 21, which show the difference between the 12 GMT and 00 GMT values of $\overline{Q_\lambda}$ and $\overline{Q_\phi}$ during June, July and August of 1961 and 1962. The details of the oscillation cannot, of course, be determined from twice daily observations. However, data from Ft. Worth and Oklahoma City, and the results of Hering and Borden, indicate the oscillations to be approximately elliptic, with axes of the same order of magnitude. Thus the vector defined by the component maps can be used as a rough estimate of the amplitude of the oscillation. These vectors are shown in Fig. 22. The magnitude of the variations may be compared with the mean July flux shown in Figs. 8 through 15.

There can be little doubt of the reality of the major features of Figs. 20 and 21, as the pattern obtained from the data is quite coherent, even over those areas where values are small. Only station 72836 (Moosinee) was ignored in the analysis; this because of apparently unrepresentative data for 00 GMT, August 1961. In addition, data from three other stations were smoothed on one or more individual monthly analyses. The 12-00/2 difference vector computed from the smoothed analysis is also shown at the appropriate stations on Fig. 22. These adjustments produce changes in detail only.

Analyses of individual monthly maps (not shown here) indicate the same general pattern south of 45°N, but further north, where the magnitude of the oscillations are small, the pattern is more variable from month to month, particularly in the meridional component.

The maps bring out several significant facts. First of all, the oscillations are by no means limited to the continent proper, but occur throughout the Caribbean and Gulf of Mexico as well. Except for the western Caribbean, the characteristic feature over these ocean regions is a clockwise turning of the integrated flux vector, and consequent increase in northward flux, between 00 and 12 GMT. The diurnal change is particularly pronounced around the western Gulf of Mexico, where Merida, on the Yucatan Peninsula, consistently shows the greatest diurnal changes on the map.

The northward flux of moisture across the Gulf coast increases substantially between 00 and 12 GMT primarily because of these diurnal changes in the western Gulf of Mexico. This region of increased northward flux extends into the Ohio Valley and lower Great Lakes, but extends only to 35°N over the western plains.

The diurnal variations of the zonal flux form an interesting pattern over the United States and southern Canada (Fig. 20). Over extreme western Canada and the western United States, the eastward

flux decreases between 00 and 12 GMT, thus giving a relative offshore flow along the west coast at 12 GMT. The eastern boundary of this regime coincides roughly with the Continental Divide. The 12 GMT transport is relatively eastward between the Rocky Mountains and the east coast south of 42.5°N, and over a rather narrow region extending northwestward just to the east of the Canadian Rockies. The oscillations over this region are most pronounced between the Rocky Mountains and Appalachians, and along the southeast coast. The third major region is one of increased westward flow at 12 GMT, and extends westward from Newfoundland through the Great Lakes, Hudson Bay and northwestward to the vicinity of the Great Slave Lake.

Since we see that

$$\nabla\cdot\overline{Q}_{12\,GMT} - \nabla\cdot\overline{Q}_{00\,GMT} = \nabla\cdot(Q_{12\,GMT} - Q_{00\,GMT})$$

we are able to evaluate the difference between the mean flux divergence computed at the two observation times by taking the divergence of the vector field defined by Figs. 20 and 21. It is apparent from an inspection of these figures that such differences do exist. A particularly prominent example can be found in the southern Rocky Mountain region. West of the Continental Divide, the 12 GMT flux is relatively westward. East of the divide, the relative transport is eastward. The meridional

flux exhibits no significant gradients in this region. Thus the flux divergence computed from the 00 GMT data will be much larger negative than that computed from the 12 GMT data; consequently the flux divergence computed from 00 GMT (or 12 GMT) data alone will give highly unsatisfactory results.

The difference between the 12 GMT and 00 GMT mean flux for the three winter months (December, January, February) is shown in Figs. 23 and 24. The patterns are much weaker than those found during summer, but the main features of the summer zonal oscillations are still identifiable. The meridional component is similar only south of $30^{\circ}$N.

The characteristics of the diurnal variations of $\overline{\rho v}$ and $\overline{v}$ at various heights was investigated. Hodographs were plotted for July, 1961 and 1962, for 77 stations located in southern Canada, the United States, and in the Gulf of Mexico-Caribbean Sea region.

The important characteristics of the July oscillations can be described by dividing the area into several regions, in each of which the hodographs exhibit broadly similar characteristics. These regions are illustrated on Fig. 22.

Region A includes most of the Caribbean and eastern Gulf of Mexico. Typical hodographs for this area are shown in Fig. 40. The hodograph for Key West represents conditions in the eastern Gulf of

Mexico, while the hodographs for 78866 (St. Maarten) and 78897 (Guadeloupe) are typical of most of the Caribbean stations within this region. The Caribbean hodographs differ mainly in the lowest few hundred feet, where the flux at Guadeloupe is strongly retarded, while at St. Maarten the maximum flux is found at the surface. St. Maarten is a very small island with little relief, so that of the two hodographs it is probably the more typical of conditions over the open water. On the larger island of Guadeloupe, under normal conditions of westward flow, the air will have passed over land for more than 20 kilometers before reaching the observation point at Pointe a Pitre. There is, in addition, a range of mountains not far to the east and southeast of the station which rise to elevations of over 1000 meters, and which may also affect the low level flow.

A comparison of the $\overline{V}$ and $\overline{\rho V}$ hodographs for Guadeloupe and St. Maarten clearly show the dominant effect of the wind in producing the diurnal flux variations. Furthermore, these variations in the wind are by no means small when compared with mean monthly values, nor are they limited to the lower levels, but often extend undiminished into the upper troposphere. On the other hand, the $\overline{\rho V}$ oscillation decreases with height in response to the decrease in $\overline{\rho}$. Thus the vapor flux oscillations above 850 mb are less important than those in

the lower layers, but are by no means negligible. The veering of $\overline{gV}$ between 00 and 12 GMT, and the accompanying increase in southerly flow, which is typical of this region, is quite apparent at all three stations.

It is of interest to note the relative magnitude of the 00 and 12 GMT surface flux. At St. Maarten the flux was greatest at 12 GMT, while at Key West, the magnitude was about the same at both observation times. At Guadeloupe the surface flux was strongest at 00 GMT. 12 GMT corresponds to approximately 0630 local time at Key West, and to about 0800 local time at the other two stations. As in the case of the mean flux itself, the low level flux oscillation at St. Maarten may be most typical of conditions over the surrounding sea. Riehl (1954) has noted a nocturnal increase in the winds in the lower layers upstream from Hawaii, with an accompanying lowering of the trade inversion. Thus the low level diurnal wind changes over the tropical oceans may often be opposite to those observed over land, where the surface wind speed decreases at night in response to the decrease in the downward momentum flux.

Over ocean areas, where data is sparse, it is important that available observations be representative of conditions over a broad surrounding area. Data from small and low isolated islands should

closely reflect the transport over the open sea. Island stations located some distance above sea level, or strongly affected by local terrain, will usually be highly unrepresentative. Caribbean hodographs also suggest that small errors are introduced because of the retardation of the flow in the lowest levels. The most serious problem in the Caribbean area arose in connection with the station at Kingston, Jamaica. These observations are strongly affected by the nearby mountains, particularly under conditions of northeasterly flow. The scale of the disturbance is too small to be properly defined by the existing network of stations; consequently the difficulty in interpreting the data in terms of the large scale flux pattern makes this station of little value during the winter months, when the prevailing flow is from the northeast.

Region B consists of an area of northeasterly flow in the western Caribbean, which is illustrated by the San Andres hodograph (Fig. 41). The backing of the flux vector from 00 GMT to 12 GMT, at levels below 700 mb, constitutes the main difference between this hodograph, and the hodographs of region A, and leads to an increase in the southward flux at 12 GMT. Comparison of the $\overline{gV}$ and $\overline{V}$ hodographs again verifies the importance of the wind variation in producing the vapor flux oscillation. Note the shift from a backing to a veering wind change above 650 mb. Changes of this type, characterized by an opposite diurnal

turning of the mean flux and wind vectors in the lower and middle troposphere, are also typical of region C. As in the case of St. Maarten, the surface flux across this small island is stronger in the morning than in the evening.

Region C includes eastern Mexico, the western Gulf of Mexico, and most of the United States east of the Continental Divide and south of 42.5°N. Hodographs from that part of the area in which the oscillation is most strongly developed (denoted as sub area $C_1$) are illustrated by Merida, Fig. 41, and the Brownsville, San Antonio and Oklahoma City hodographs of Figs. 42 and 43. The diurnal changes which are exhibited by these hodographs are quite remarkable, and have two distinct characteristics; (1) a region in the lower troposphere in which $\overline{\rho V}$ and $\overline{V}$ turn anticyclonically between 00 and 12 GMT, surmounted by a region in which the vectors turn cyclonically during the same period, (2) the appearance of a mean low level jet in the vertical profiles, 50 to 100 mb above the surface, at 12 GMT. It should be emphasized that the low level jet of this discussion refers to a maximum in the vertical profiles and not in the horizontal plane. The region of anticyclonic turning does not always extend to the surface, probably because of the dominance of local effects in the very lowest levels. The mean low level jet appears to be most strongly developed in the region extending from the lower Rio Grande

Valley northward through northeastern Texas and Arkansas. The details of the oscillation and low level jet cannot be determined south of the Rio Grande. It is unfortunate that data over Mexico and Central America is not sufficient to better define the characteristics and areal extent of the oscillations in this region; however the very large diurnal variations at Merida indicate that they extend at least as far south as the Yucatan Peninsula.

Observations taken four times daily by the Oklahoma City (00-12 GMT)-Tinker AFB (06-18 GMT) combination allow one to obtain a better picture of the behavior of the oscillation in that particular area. These stations are only a few miles apart, and at practically the same elevation (approximately 970 mb). Data were available from Tinker for June and July, 1961, and hodographs for this period, for the four observation times, are shown in Fig. 43. Also sketched on the figure are the oscillations at the 950, 850 and 800 mb levels. No reasonable curve could be constructed from the surface observations, possibly because of local differences between the two stations. Analysis of several months of winter data indicated the presence, in addition to the diurnal oscillations, of a systematic difference between the mean monthly winds at the two stations, which in turn masks the weaker diurnal oscillations above 800 mb. The flux appears to reach a minimum around 18 GMT (12 LST) or possibly

a few hours later, and a maximum a little before 06 GMT. The 06 and 18 GMT flux vectors differ primarily in magnitude, while differences between 00 and 12 GMT are primarily in direction. The difference in the estimate of $|\overline{Q}|$ using all 4 observations, and using 00 and 12 GMT data only, amounts to 130 gm (cm sec)$^{-1}$. However, this results from the systematic wind difference between the stations, as well as from the lack of symmetry of the oscillation.

Perhaps a more reliable estimate of this difference can be made for Ft. Worth. Wind data for this station for July 1956 and 1957 have been supplied by the Atmospheric Analysis Branch of ESSA. Winds for July 1958 have been estimated from Figs. 1 and 2 of Hering and Borden (1962). Since the eddy term contributes little to the diurnal variation of $\overline{Q}$ at this time of year in this area, we may approximate the variations by evaluating only the mean term, $\overline{\rho}\,\overline{V_h}$. This term was approximated by using the observed values of $\overline{V_h}$, and the 5 year mean July value of $\overline{\rho}$ for the years 1958-1963. The results, shown in Fig. 45 indicate considerable difference in the oscillation from year to year, in agreement with the findings of Hering and Borden. Mean values of $\overline{Q}$, computed from 00 and 12 GMT observations only, and those computed from all four observations, differed in magnitude by about 100 gm (cm sec)$^{-1}$ in both 1957 and 1958. Errors of this magnitude are sufficient

to account for much of the error observed in the flux divergence field over the Great Plains.

It is apparent from the $\overline{\rho V}$ hodographs of region $C_1$ that the mid-troposphere is of relatively minor importance so far as the vapor flux oscillation is concerned. However, it represents a region in which the diurnal wind variations are comparable to those in the lower troposphere. The $\overline{V}$ hodographs can therefore be related to the findings of Hering and Borden; the low level 12-00 GMT anticyclonic change corresponding to their low level oscillation, and the upper region of cyclonic turning corresponding to the mid-tropospheric oscillation.

These same characteristics are found over all of region C, although the boundary between the cyclonic and anticyclonic changes is not always as clear cut as in $C_1$, and the low level jet is not so well developed. Hodographs from the remainder of region C (Pittsburgh, North Platte, Charleston, and Nashville) are shown in Fig. 44.

Region D includes those stations which exhibit a mixture of the characteristics of regions A and C. Examples (Jackson, Tampa, Montgomery and Burrwood) are shown in Fig. 44. A mean 12 GMT low level jet is found at the northerly stations, but unlike region C this development is accompanied by a cyclonic turning of the flux vector. The southerly stations exhibit the increased 12 GMT southerly flow typical

of region A, but the hodographs are quite dissimilar in other respects.

Region E includes the area west of the Continental Divide, exclusive of the Pacific coast. The hodographs are strongly influenced by local conditions, which make it difficult to isolate the significant large scale features. Salt Lake City, Grand Junction, and Tucson, three of the more extreme examples, are illustrated in Fig. 44.

Stations on the Pacific Coast (region F) exhibit a great deal of diurnal variability in the lower levels. This is not surprising since the 00 GMT observation coincides closely with the time of maximum sea breeze development. The strong sea breeze regimes of San Francisco Bay and the Los Angeles Basin show up strongly on the Los Angeles and Oakland hodographs (Fig. 42). Data from Oakland, and to a lesser extent from Los Angeles, are not always representative of the general conditions along the California coast during the summer, for as one might surmise, they often give overestimates of the onshore flow.

It was difficult to find any definite pattern in the diurnal variations of the hodographs over Canada and the northern United States, since in this region, even in July, the oscillations are quite small. This, together with the more variable summer conditions, makes it desirable to analyze more than two years of data at these northerly latitudes in order to obtain meaningful results.

The patterns exhibited by the hodographs of regions A and C indicate the existence of a strong and well organized diurnal circulation system, which is by no means limited to the central United States, but includes most of the area east of the Rockies and south of 42°N, the Gulf of Mexico, and possibly the Caribbean. Some idea of the broad scale characteristics of this system can be obtained from Figs. 25 and 26. Fig. 25 shows the mean low level departure vector field during July. The vector is derived from an average of the 900 and 950 mb winds where the surface pressure is greater than 950 mb; otherwise from the average of the winds at the first two standard 50 mb levels above the surface. Fig. 26 shows the mean mid-tropospheric departure vector field derived from an average of the winds at 500 and 550 mb. The heavy dashed line on each chart indicates the position of a prominent low level mean streamline around the subtropical high, obtained by averaging the 00 and 12 GMT observations. These maps have counterparts in Figs. 6 and 7 of Hering and Borden (1962). Their data is for July, 1958 and is somewhat scanty, and limited to the United States. However, where comparisons can be made, the vectors are usually in excellent agreement.

The characteristic features of the hodographs can now be explained in terms of the large scale diurnal circulation. The veering of the low level wind between 00 and 12 GMT in region C is the manifestation of an

oscillation occurring in the regions bordering the western extension of the subtropical high. The oscillation results in a pronounced convergence of the low level flow into the region of high pressure at 12 GMT. The limited data of Hering and Borden indicate the 18-06 GMT departure vectors to be roughly orthogonal to those of 12-00 GMT. Thus the mean inflow will apparently cease around noon or shortly thereafter, and by evening the pattern will have reversed, with strong low level divergence from the high, and convergence in the vicinity of the Rocky Mountains. By midnight the convergence will have shifted to the plains, in agreement with the findings of Curtis and Panofsky (1958). The mid-tropospheric oscillation is seen to correspond to a compensating flow above a level of non-divergence. Thus, at 12 GMT we find marked convergence in the lower troposphere, and marked divergence in the upper troposphere above the western end of the high. One might also note that region D, in which the hodographs exhibit mixed characteristics, lies approximately over the mean position of the axis, or possibly center, of the high.

In summary, the observed diurnal oscillations of the wind, and, as a consequence, the mean monthly diurnal oscillations of the water vapor transport over North America and the Central American Sea, appear to be produced by a combination of local and large scale effects. At points such as Grand Junction, or Los Angeles, the diurnal changes are mostly

local in nature, although there is some indication of a weak large scale oscillation (relatively westward at 12Z) over the western United States. East of the Continental Divide, and south of $42^{o}$N, the local oscillations fit into a beautifully organized large scale diurnal circulation pattern.

Wexler (1961) concluded that the behavior of the low level nocturnal jet could not be explained solely in terms of local conditions. This conclusion seems equally valid in regard to the large scale diurnal circulation patterns. Furthermore, the appearence of related diurnal oscillations throughout much of the troposphere shows them to be more than low level boundary layer phenomena. Because of the apparent relationship of these oscillations to the large scale flow pattern over eastern North America, one would expect changes in the details of the diurnal circulation from year to year. The data for Ft. Worth, and the results of flux divergence computations over eastern North America (See Fig. 91) indicate this to be true.

The complications which these diurnal variations introduce into any study of the atmospheric vapor flux, or for that matter, in any study which depends upon the accurate evaluation of atmospheric transport processes, is quite apparent. The results of this study have implications for other types of investigations as well. Some investigators have, in the past, evaluated the atmospheric tidal motions at a single station, or at

best, at a very few stations, and have then attempted to generalize these results to world-wide conditions. Such generalization is apparently not warranted for the troposphere, since even as far south as $12^{o}$N, the oscillations have markedly different regional characteristics. These oscillations may also have an important influence on any estimates of kinetic energy generation, which depend upon an accurate evaluation of the term $\overline{V}\cdot\nabla\overline{P}$ . Over many areas, this term will change sign in the lower and middle troposphere during the day because of the highly ageostrophic character of the oscillations. As previously noted, these effects are strongest south of $50^{o}$N in summer and are much less of a problem in winter.

One might speculate concerning the relationship of these oscillations to the summertime diurnal variations in precipitation over eastern North America and the Gulf of Mexico. Suffice to say that the results of this investigation suggest that these oscillations may be related to the summertime precipitation climatology of a more extensive region than has previously been suspected. Such relationships certainly deserve further study.

# IX. THE ATMOSPHERIC WATER BALANCE OF THE CENTRAL AMERICAN SEA

The ocean areas comprising the Gulf of Mexico and Caribbean Sea, referred to by Wüst (1964) as the Central American Sea, play a key role in the water balance and overall climate of much of southern and eastern North America. This region, together with the western Atlantic, comprises one of the three northern hemisphere regions of major northward moisture flux across $20^{o}$N and $30^{o}$N. The entire area lies between $10^{o}$N and $30^{o}$N, and thus straddles the latitudes from which huge amounts of latent heat energy are exported. The western portions of the Central American Sea act as a distribution zone for the moisture entering from the Atlantic and added by excess evaporation within the region. Part of this moisture flows northward into eastern North America, but most of the outflow is southwestward across Central America toward the equatorial trough region. Lesser amounts of moisture cross the mountains of Mexico and the South American coasts in a direction which varies with the season. The seasonal and inter-annual variations in the partitioning of this flux, and their relationship to the water balance of the surrounding area, is not without interest.

The network of aerological stations in the environs of the Central American Sea consists primarily of a series of mainland and island

stations on the periphery of the basins. This network is inadequate if one wishes to define the details of the flux pattern, but is well suited for a computation of $\langle \overline{E-P} \rangle$ for the entire area, or independently over the Gulf of Mexico and Caribbean Sea.

The southern portion of this network has been used by Colón (1960) in a study of the energy budget of the Caribbean Sea and the overlying troposphere. As a part of this study, he obtained estimates of mean monthly precipitation from independent water balance and heat balance computations, for December 1956 and January 1957, which agreed within a factor of 2. The results led Colón to speculate that atmospheric water balance computations might well furnish the most reliable approach to estimates of oceanic precipitation.

The ring of aerological stations is not without its weaknesses, but some of these are not so serious as they at first appear. The great distance between stations on the South American coast is not critical if one uses a latitude circle as the boundary of the basin. The flow will then be essentially parallel to the boundary, and one need evaluate only a small normal meridional component. The northern boundary of the region is well defined; the eastern and northeastern boundaries are adequately defined during most months, while the western boundaries give rise to most of the major difficulties. It was necessary to exclude

the extreme western portion of the Caribbean Sea from consideration, since it lies outside the ring of aerological stations. The southwestern and western boundary of the Gulf of Mexico was particularly difficult to handle because of a maximum in the meridional flux component which often occurred between Vera Cruz and Merida. In such a region, one must figuratively "lift oneself up by his bootstraps" by subjectively extending the analysis of $\overline{Q}_\lambda$ and $\overline{Q}_\phi$ from better defined regions in a way which produces reasonable values and changes in both the divergence and curl of the flux vector, as well as in the magnitude of the components themselves. Nonlinear variations in the flux components will then often be required for a consistent analysis. In this way, one is able to put a small and more acceptable error in place of one which may be large and possibly ruinous. The divergence estimate will be of little value locally, but one can be fairly confident that the estimate of the mean divergence over the much larger region under investigation will not suffer from a large boundary error in the flux. Adoption of this technique introduces a surprisingly strong constraint on the analyses, and may well spell the difference between satisfactory and mediocre results in areas of sparse data.

The boundaries for the computation, shown in Fig. 77, were chosen so as to lie near or just within the surrounding ring of stations.

In addition, they were chosen so that grid point values, previously tabulated for use in constructing maps of divergence, could be used for these computations as well. Estimation of the boundary flux from a $2.5^{o}$ grid was deemed adequate in the light of the other uncertainties involved in the computation. No corrections were applied for the land areas within the boundary, as it was felt that the station data itself was not sufficiently dense to allow such a distinction to be made. This may not be entirely true near the northern boundary of the Gulf of Mexico.

Computations of the flux across the various boundaries, and the residual mean flux divergence of the area, were made on a mean monthly basis. No effort was made to compute actual month to month changes in atmospheric storage. However, some correction for storage change must be made in order to avoid biased values of $\langle \overline{E-P} \rangle$ arising because of normal seasonal changes in $\langle W \rangle$ in spring and fall. For this purpose, mean monthly storage changes were estimated from the two years of data, and these were used to approximate the normal seasonal changes. This approximation may introduce small errors of around 1/2 - 1 cm for individual monthly estimates of $\langle \overline{E-P} \rangle$, particularly during spring and fall, but the error introduced in annual or semiannual means is insignificant.

Average annual and semiannual values of $\langle \overline{E-P} \rangle$, computed

for the Caribbean Sea, are shown in Table 8, together with two independent estimates of this quantity. Following Wüst (1963) the year is divided into a wet summer season (June-November) and a dry winter season (December-May).

Table 8. Mean annual water balance - Caribbean Sea

| | Summer Jun-Nov cm/6 mo $\langle\overline{E-P}\rangle$ | Winter Dec-May cm/6 mo $\langle\overline{E-P}\rangle$ | Annual cm/yr $\langle\overline{E}\rangle$ | $\langle\overline{P}\rangle$ | $\langle\overline{E-P}\rangle$ |
|---|---|---|---|---|---|
| Water vapor balance equation | 25 | 66 | | | 91 |
| Colón-Möller (Wüst, 1964) | 26 | 63 | 161 | 72 | 89 |
| Budyko-Drozdov (Budyko, 1963) | | | 177[1] | 85[1] | 92[1] |

[1]Estimated from isoline analyses of mean annual precipitation and mean monthly evaporation.

Wüst considered the Colón-Möller estimate to be the best available at the time of his publication. It is derived from mean monthly estimates of evaporation by Colón (1963) and precipitation charts from Möller's "Vierteljahrskarten des Niederschlags fur die ganze Erde", and applies to an elliptic area covering most of the Caribbean, and corresponding roughly to the area used for the atmospheric water balance computation. The evaporation figures were obtained from a computation

of the heat balance of the Caribbean Sea, in which the heat flux to the atmosphere was computed as a residual, and the flux of sensible and latent heat separated by assuming a Bowen ratio of .10. In his estimates of precipitation, Möller reduced the values at coastal stations by around 20% when extrapolating to conditions over the open sea.

The Budyko-Drozdov estimate is based on charts from Budyko's recently revised "Atlas of the Heat Balance of the Earth" (Budyko, 1963). Precise values cannot be determined since they must be estimated by interpolation from isolines. Budyko estimates evaporation through the use of a diffusion equation and, contrary to Möller, Drozdov considered coastal precipitation reports to be typical of conditions over the open sea. It should be emphasized that this evaporation estimate is obtained from Budyko's revised atlas, and is around 30 to 40 cm/year higher than the value given in the previous edition. It is the older estimate which is quoted by Malkus (1962), Colón (1963), and Wüst (1964). It is interesting to note that the Colón-Möller and Budyko-Drozdov estimates of $\langle \overline{E-P} \rangle$ are in better agreement than the individual estimates of $\langle \overline{E} \rangle$ and $\langle \overline{P} \rangle$ ; the higher estimates of precipitation by Drozdov being offset by Budyko's higher estimates of evaporation.

The extremely close agreement between annual values computed from the atmospheric water balance equation, and the independent esti-

mates, must be considered to some extent fortuitous, since we are comparing estimates of long term mean conditions with values obtained during a two year period. Large differences in $\langle\overline{E-P}\rangle$ were often computed for comparable months of this two year period, and even the annual mean values differed by 11 cm. Conditions over the Gulf of Mexico were even more variable.

The seasonal values of $\langle\overline{E-P}\rangle$ estimated by Colón-Möller and computed by the vapor balance equation were also in excellent agreement, and suggest a comparison of mean monthly values as well. Fig. 84 shows the mean monthly values of $\langle\overline{E-P}\rangle$ obtained from the vapor balance equation, together with estimates of mean monthly evaporation by Colón and Budyko. Also shown is the difference between the evaporation estimates and $\langle\overline{E-P}\rangle$ . Again, one must be rather cautious in interpreting the last quantity, since the averaging of only 2 years of data falls short of providing long term monthly means. Nevertheless, there are indications that the curves bring out the important seasonal variations of precipitation. First of all, they exhibit the well known double maxima of precipitation often found in tropical regions. Secondly, they appear to be consistent with the results of a study by Portig (1965) in which he investigated the rainfall frequencies from ship observations over an ocean area which included both the Caribbean Sea and Gulf of

Mexico. Portig found October to be the month of maximum precipitation frequency in the western and northern portions of the Caribbean Sea, while the southeastern sections showed frequency maxima in November and December. A secondary maximum was observed in June over most of the area. March was the month of lowest frequency, although April was also very low. The tendency for a secondary minimum in August was observed over the western and northern portions of the area. Thus, if one assumes a relationship between precipitation frequency and total amount (which need not always be the case) the results of the two studies are in broad agreement.

Certain details of the derived precipitation curves, such as the negative values in February, March and August, are obviously not representative of actual mean conditions. This may be due to errors in $\langle \overline{E-P} \rangle$ or $\langle \overline{E} \rangle$, or to abnormal conditions during this two year period.

The results of the water balance computation for the Gulf of Mexico, together with mean monthly evaporation estimates of Budyko (1963) are shown in Fig. 85. Mean annual values are given below.

Table 9. Mean annual water balance - Gulf of Mexico. Units: cm/yr

| | $\langle\overline{E}\rangle$ | $\langle\overline{P}\rangle$ | $\langle\overline{E-P}\rangle$ |
|---|---|---|---|
| Budyko-Drozdov | 176[1] | 92[1] | 84[1] |
| water vapor balance equation | | | 82 |

[1]Estimated from isoline analysis of mean annual precipitation and mean monthly evaporation.

In contrast to the Caribbean, $\langle\overline{E-P}\rangle$ shows essentially a single maximum and minimum, although there is some indication of a minor maximum in May. The major winter maximum is rather flat, with values from October through March differing by less than 4 cm. The strong increase in $\langle\overline{E-P}\rangle$ from the minimum in September to the high value of October coincided with a change in the mean monthly meridional flux component from strong southerly to northerly. Investigation of data from September and October of 1958, 1959, and 1960 indicated that such pronounced changes do not always occur. Consequently the October values of $\langle\overline{E-P}\rangle$ during this two year period may be somewhat above normal.

The derived precipitation curve shows two main features: a decided minimum in May, and a strong maximum in September. This, again, is in agreement with Portig's rainfall frequency study.

Fig. 85 also shows estimates for the total Central American Sea,

again using Budyko's evaporation estimate. The pattern is not so clear cut when both basins are combined. Spring appears to be the season of minimum precipitation, while the maximum occurs in fall.

The mean monthly moisture flux across the eastern and western boundaries of the Central American Sea are shown in Fig. 79, while Fig. 80 illustrates the flux across the northern and southern boundaries. The general characteristics of the vertical distribution of the influx from the Atlantic can be obtained from the cross sections along 80°W (Figs. 33 and 35). The bulk of the transport into the Caribbean Sea takes place below 800 mb with a maximum around 950 mb during both summer and winter. At 80°W, the boundary between easterly and westerly flow at the surface is found just south of 30°N in both January and July. However, this boundary shifts southward during the winter in the Gulf of Mexico, with the displacement increasing as one progresses westward. This accounts for the seasonal change in sign of the average flux across the meridional boundaries of the Gulf of Mexico. Even in winter, however, the vertically integrated flux in the southern portion of the basin is directed westward.

The Caribbean Sea shows a strong inflow from the east during the entire year. This flow exhibits a double maximum; the more intense one occurring in July and a much weaker maximum occuring in

December or January. The July maximum coincides with the occurrence of high values of $\overline{q}$, and is associated with a northward flux component. The winter maximum coincides with near minimum values of $\overline{q}$, high values of evaporation, and a southward flux component. Figs. 33 and 35 indicate no essential difference in the vertical flux distribution at the time of the two maxima, and one must conclude that the winter maximum is primarily the result of an increase in the mean winds. The outflow across the western boundary shows essentially the same pattern and magnitude as the eastern inflow.

The flux across the zonal boundaries has some interesting features. Looking first at the southern boundary of the Caribbean, one notes a seasonal shift in direction; northward from May through October, and southward during the remainder of the year. The peak northward flux, which closely coincides with the two computed Caribbean precipitation maxima, occurs in June and September. Since the flux along this boundary is quasi-zonal, the moisture crossing from the south must normally be of recent Atlantic origin, having had only a short trajectory across the extreme northern portions of Venezuela. In winter, the west-southwestward flux across the Venezuelan Coast is ultimately blocked by the Cordillera de Merida east and southeast of the Maracaibo Basin. This inflow thus represents a moisture source for the wintertime precipitation on the

eastern slopes of these mountains.

A strong seasonal change is also noted in the magnitude of the northward flux across the southern boundary of the Gulf of Mexico. With the exception of October, the flux is always from the south, but as previously noted, October 1961 and 1962 may not be representative of normal conditions. There is still some indication of the twin maxima found on the South American coast, although the June maximum is dominant. Two years of data are probably not sufficient to establish the reality of the weaker maximum.

The transport across the northern boundary of the Gulf of Mexico shows the least seasonal variation, although a maximum northward flux appears in spring, and a minimum in late summer or fall. The values for September may be affected by the occurrence of hurricane Carla, which struck the Texas coast in September 1961. A sharp minimum of northward flux is again observed in October. One should not equate the flux across this boundary, which extends only to 97.5°W, with the flux from the Gulf of Mexico into the United States, as during summer a large part of the moisture crossing the western boundary of the Gulf of Mexico ultimately enters the United States between 97.5°W and the Rocky Mountains. This is quite apparent from Fig. 27.

Since there are no stations over Central America north of the

Canal Zone, nor are there any stations in the eastern Pacific, one cannot directly measure the moisture transported from the Caribbean Sea to the Pacific. It is possible, however, through continuity considerations, to make a good estimate of this quantity.

The total annual outflow of moisture across the western boundary of the Caribbean between $10^{o}$N and $20^{o}$N is approximately $8.2 \times 10^{15}$ kg. Adding to this the outflow across the eastern part of the Isthmus of Panama ($1.5 \times 10^{15}$ kg), which is included as part of the southern boundary, gives a total outflow of $9.7 \times 10^{15}$ kg. Most of the inflow to the Gulf of Mexico west of $85^{o}$W ($1.1 \times 10^{15}$ kg) is derived from this Caribbean outflow, and, together with the losses over Central America and the western Caribbean, must be subtracted from the above figure. The losses over Central America are, of course, unknown, but a reasonable estimate will be satisfactory. Budyko (1963) indicates a value for $\langle \overline{E-P} \rangle$ for this region of -100 to -150 cm $yr^{-1}$. This amounts to a loss of $1 - 2 \times 10^{15}$ kg/yr over the area. Thus the net annual moisture flow from the Caribbean to the Pacific must be around $6.5 - 7.5 \times 10^{15}$ kg, approximately equal to the inflow to the Caribbean from the Atlantic.

The variability in the monthly and annual values of the flux and flux divergence has previously been noted. The values of the total annual flux divergence for the two years investigated is shown below.

Table 10. Annual water vapor flux divergence. Units: cm/yr.

| | May '61-April '62 | May '62-April '63 |
|---|---|---|
| Gulf of Mexico | +66 | +99 |
| Caribbean Sea | +85 | +96 |

The variability in the mean annual flux is illustrated in Table 11, which shows the average 00 GMT mean annual flux for 10 stations in the Caribbean Sea and southern Gulf of Mexico during a 5 year period.

Table 11. Mean annual vertically integrated water vapor flux.[1] Units: gm (cm sec)$^{-1}$

| Year (May - April) | | | | | |
|---|---|---|---|---|---|
| 1958-59 | 1959-60 | 1960-61 | 1961-62 | 1962-63 | 5 yr mean |
| -2355 | -2073 | -2053 | -2101 | -1844 | -2085 |
| 145 | 131 | 212 | 69 | -289 | 54 |

[1]Average for the following stations: 76644, 78383, 78397, (78467-78486), 78501, 78526, 78866, 78897, 78988, 80001.

Apparently the interannual variability of these tropospheric circulation statistics is quite significant in the tropics, even when averaged over regions as large as the Central American Sea.

# X. THE WATER BALANCE OVER NORTH AMERICA

## A. Introduction

Adequate aerological data are available for an investigation of the large scale atmospheric water balance of the contiguous United States, Alaska and Canada. In addition, the streamflow data which are available for the United States, a large part of southern Canada, and portions of Alaska, allow a computation of surface and subsurface storage changes in this area.

The first section of this chapter will be devoted to a brief description of some of the features of the continental water balance. This will be followed by a discussion of the water balance of the northern portion of the continent. The major part of the chapter will then be devoted to a more comprehensive discussion of the atmospheric and terrestrial water balance of the United States and southern Canada, and the various subdivisions of this area shown in Fig. 77. The nomenclature of Fig. 77 will be used throughout this chapter.

## B. North American Water Balance

Mean monthly values of $\langle \overline{P-E} \rangle$ , computed from the water vapor balance equation for an area of $170 \times 10^5$ km$^2$ north of the United States - Mexican border (see Fig. 77) are shown in Fig 86. We have

reversed the order of E and P in this expression from that previously used in order to obtain a normally positive quantity over land. The corrections of $\langle \nabla \cdot \overline{Q} \rangle$ for atmospheric storage changes were computed from aerological data over the United States, and estimated over Canada and Alaska.

With the possible exception of midsummer, this portion of the continent acts as a sink for atmospheric water vapor. The sink is, however, much weaker than the source over the Central American Sea, where mean monthly values of $\langle \overline{E-P} \rangle$ exceeding 10 cm were often computed, and where mean annual values had magnitudes almost 4 times those found over the continent.

The mean annual values of $\langle \overline{P-E} \rangle$ differed by only 1.1 centimeters (+23.1 and +24.2 cm) during these two years. Previous computations for approximately the same area have indicated values of +19 cm for 1950 (Lufkin 1957) and +18 cm for 1949 (Benton and Estoque, 1954). The earlier computations are probably somewhat less reliable because of lack of data, but the agreement between the four values is still quite good.

The total vapor flux divergence over the large watershed regions of the continent is of some interest. Annual values of these quantities have been estimated from the grid point values of divergence shown in

Fig. 74 and are given in the following table.

Table 12. Total annual flux divergence over the major watershed areas of North America. May 1961-April 1963. Units: $10^{13}$ kg $yr^{-1}$.

| Area | |
|---|---|
| Arctic Ocean and Bering Sea Drainage | 120 |
| Hudson Bay Drainage | 75 |
| Hudson Bay Drainage and Hudson Bay | 105 |
| Atlantic Drainage (30.0°N-62.5°N) | 85 |
| Pacific Drainage (North of 32.5°N) | 130 |
| Gulf of Mexico Drainage (North of Rio Grande) | 75 |

The above values include the divergence computed over those peripheral continental areas outside the basic area previously discussed. The computed divergence over these peripheral areas is not as well defined by the data, and is therefore more subject to error than values over the remainder of the continent.

It is doubtful whether the network of stations surrounding Hudson Bay is sufficient to sharply define any gradients between the bay and the surrounding land areas. Furthermore, there are indications of a summertime diurnal variation in the flux divergence over the bay which may not be adequately described by twice daily observations. For these reasons, the total convergence over Hudson Bay may be somewhat too large, and that over the Hudson Bay Drainage Area somewhat too small.

Streamflow from all but the coastal regions of the Gulf of Mexico Drainage Area averaged 70 x $10^{13}$ kg $yr^{-1}$ during this two year period, a value close to the computed water vapor convergence into the area. One might compare this figure with the average annual value of $\langle \overline{E-P} \rangle$ computed over the Gulf (133 x $10^{13}$ kg $yr^{-1}$). Apparently well over half of the water lost from the Gulf of Mexico by excess evaporation is returned again by surface streamflow.

The following latitudionally averaged values of water vapor inflow were obtained for the continent.

Table 13. Total annual inflow of water vapor to North America (north of United States-Mexican Border). Units: $10^{13}$ kg $yr^{-1}$.

| Latitude (°N) | mass ($10^{13}$ kg $yr^{-1}$) | average depth (cm) |
|---|---|---|
| 65-70 | 35.6 | 22 |
| 60-65 | 111.4 | 45 |
| 55-60 | 87.4 | 35 |
| 50-55 | 74.4 | 28 |
| 45-50 | 59.7 | 23 |
| 40-45 | 48.9 | 20 |
| 35-40 | 16.6 | 7 |
| 30-35 | 46.3 | 23 |

The large values of convergence computed in the 55-65°N latitude band account for the relatively high values of convergence computed over

The Bering Sea, Hudson Bay, and Arctic Drainage Areas. Individual values between 30°N-50°N may be slightly in error; the result of systematic errors in the divergence computations. These errors will be discussed in Chapter XIII.

C. Northern North America

1. Water balance

The water balance of the area extending from the Arctic coast southward to around 55°N in western Canada and 50°N in eastern Canada, and including Hudson Bay, will now be considered.

The monthly march of $\langle \overline{P-E} \rangle$ is shown in Fig. 86. These values were obtained by adjusting $\langle \nabla \cdot \overline{Q} \rangle$ for average monthly changes in $\langle \overline{w} \rangle$. It is unlikely that monthly errors exceeding 0.5 cm will arise because of this approximation.

The water balance computations result in mean annual values of $\langle \overline{P-E} \rangle$ of +27.8 and +32.8 cm. Scattered streamflow data from the area indicate that runoff during the second year was probably above normal; consequently $\langle \overline{P-E} \rangle$ may also have been above normal during that period. The value of $\langle \overline{P-E} \rangle$ is noticably affected by the location of the western boundary of the area, since the Pacific coastal areas make a large contribution to the total divergence.

The seasonal variation of $\langle \overline{P-E} \rangle$ has the same general features during each of the two years: a major maximum in late summer or early fall; a minimum during spring and early summer, and a possible minor maximum in March. The basic difference between this northern land area and the tropical ocean areas previously discussed are apparent. Mean monthly evapotranspiration never exceeded precipitation over the land area, while the reverse was true over the Central American Sea.

The small amount of streamflow data available to the author, all from the western third of the area, lends support to the computed increase in $\langle \overline{P-E} \rangle$ during the second year. Annual runoff from the Yukon Basin above Kaltag, Alaska, averaged 24.5 cm the first year; 32.7 the second. Runoff over much of the Alaska panhandle during the winter of 1962-63 was excessive. Streamflow figures available for the MacKenzie River at Norman Wells, N. W. T. for the months of October through March of 1961-62 and 1962-63 showed a mean increase in flow of 40% during the second year. In addition, the occurrence of record flows in July 1963 suggests that spring storage in the basin was above normal. Runoff from the Churchill River was also higher during the second year. These basins comprise about one-third of the total area under consideration.

2. Vapor flux

The mean monthly moisture flux across the boundaries of the

region is illustrated in Fig. 81. Mean annual values are shown in Fig. 78. The mean annual flux across the northern boundary was directed into the Arctic Ocean, but was quite small. It is, of course, of local importance, but was of significance to the large scale water balance of the area only during July and possibly in August. The mean flux across the west coast of Alaska was also of minor importance to the annual balance of the total area, amounting to only 10% of $\langle \overline{P-E} \rangle$ . However, it was of some importance on a mean monthly basis during the summer months.

Taken together, the flux across the Arctic and western Alaskan boundaries was of even less importance to the computation. This is due to the fact that much of the summertime flow which crosses the western Alaskan Coast from the southwest leaves the area again through the Arctic boundary. Thus, the mean water balance of this area was essentially determined by the flux across the Pacific, southern and Atlantic boundaries.

Some idea of the vertical distribution of the Pacific inflow can be obtained from Figs. 36 and 38. The pattern is rather flat in both winter and summer, usually with a diffuse maximum between 700 and 850 mb. The relation of this maximum to the Pacific cyclone belt has been discussed previously.

The mean monthly Pacific inflow reaches a maximum in August,

one month after the maximum on the western Alaskan coast. This flux maximum apparently continues to migrate southward during the winter. The maxima along the California coast occurred in February, 1962 and April, 1963, which coincided with the two months of heaviest precipitation in that area. Thus, the movement of the local flux maximum down the entire western Alaskan and Pacific coasts appears to coincide with the seasonal southward shift of the local precipitation maximum, and, like the local precipitation maximum, does not appear to return northward in spring. One must be cautious in relating these changes in precipitation directly to the changes in vapor flux; for it may be argued that both are the result of the southward shift of cyclonic activity.

The vertical structure of the Atlantic outflow can be implied from Figs. 33 and 35. This region lies north of the main belt of eastward transport during the entire year. A westward transport into the continent is found north of $60^{o}$N during the winter, possibly the result of westward flow on the northern side of the intense oceanic low pressure areas. The maximum eastward flux is again found in August.

The inflow across the southern boundary followed a seasonal pattern similar to that of the Atlantic outflow. The northward low level eddy flux from the Gulf of Mexico, which is strongest during summer, accounts for a significant portion of the mean annual inflow through this

boundary.

D. United States and Southern Canada

1. Introduction

An accurate evaluation of surface and subsurface storage changes over the northern sections of the continent is precluded by inadequate streamflow data. However, over the United States and portions of southern Canada data are sufficient for a more comprehensive investigation of the atmospheric and terrestrial water balances.

The region chosen for study, shown in Fig. 77, comprises an area of $86.5 \times 10^5$ km $^2$ from which all streamflow is measured. The average characteristics of the entire area were first investigated. This was followed by studies of progressively smaller subdivisions. The investigations were primarily concerned with the evaluation of surface and subsurface storage changes; however, precipitation was estimated for the entire area, and individually for the eastern and western portions of the area, in order to obtain estimates of evapotranspiration.

2. Vapor flux

The characteristics of the flux over this area, and across its boundaries, are illustrated by the maps and cross sections appearing in Figs. 8 through 38. We shall briefly note the more important features

of the flux field.

Most of the inflow from the Pacific Ocean crosses the west coast north of 40°N in winter and 50°N in summer, and enters the area from the west and northwest. As previously noted, this appears as a diffuse, high level inflow on mean monthly charts, particularly in the region east of the Continental Divide.

Charts from Peixoto and Crisi (1965), and additional cross sections (not shown here) show that the mean total flux through the northern boundary, between the Appalachian and Rocky Mountains, is usually the difference between a southward mean flux and a northward eddy flux.

The inflow through the southern boundary is illustrated by tne cross sections along 30.0-32.5°N (Figs. 38-40). The difference between the January and July inflow, as well as the summertime diurnal variations, is quite pronounced. Additional cross sections (not shown here) and previous studies have established the January inflow to be primarily an eddy transport, while the July inflow is due primarily to transport by the mean monthly wind. The strong and persistent northward flux in summer around the western end of the subtropical high results in a concentrated region of intense inflow over Texas. The strong influence of this low level moisture influx on the water balance of eastern North America is well known.

A rather surprising secondary maximum in the summertime northward moisture transport is found at the northern end of the Gulf of California. In the lower levels, this moisture almost certainly moves northward from the Gulf of California. Even at levels above the height of the Rocky Mountains and the Sierra Madre Occidental, hodographs show the mean summertime inflow to be from the southeast to south-southeast, i.e., the inflow appears to be primarily up the Gulf of California. The high salinity of the warm waters of the Gulf of California (Sverdrup, Johnson and Fleming, 1942) suggests that this body of water, although small, may contribute significantly to the inflow. For example, the average July northward flux at the northern end of the Gulf of California, below 800 mb, was around $10^7$ kg $sec^{-1}$. This would be equivalent to the water vapor supplied to the atmosphere from the Gulf of California if, on the average, mean monthly evaporation exceeded precipitation by 15 cm. Actual summertime values of $\langle \overline{E-P} \rangle$ over the Gulf of California may well reach a sizable fraction of this amount.

The southeastward inflow through the northern and western boundaries, and the northward inflow from the Gulf of Mexico, which appear as two distinct currents on the mean monthly cross sections at 100°W (Fig. 39), merge into a single maximum at 80°W (Figs. 33 and 35). The core of this current is at a significantly higher elevation than that of the inflow

from the Gulf of Mexico; in part a consequence of lifting as this moisture moves northeastward.

The total vertically integrated mean monthly flux across various portions of the boundary is illustrated in Figs. 82 and 83. Separate values for 00 GMT and 12 GMT have been shown in order to illustrate the effects of the diurnal flux variation. Mean annual values are shown in Fig. 78.

The most pronounced differences between 00 GMT and 12 GMT are found in summer along the eastern, western and Gulf coast boundaries. No significant systematic differences are apparent in the average for the northern boundary. Estimates of the flow across the Continental Divide indicate the eastward flux to be slightly stronger at 00 GMT.

The mean flux divergence over the area also shows a marked diurnal variation, produced primarily by a lack of balance between increased 12 GMT Gulf Coast inflow, increased 12 GMT east coast outflow, and decreased 12 GMT west coast inflow. The magnitude, and the sign of this imbalance changed throughout the year, resulting in lower values of divergence at 12 GMT from January through June, much higher values from June through September, and little difference from October through December. Variations during comparable months of the two year period differed considerably, sometimes even in sign. Thus, this pattern may not be representative of long term mean conditions.

It has previously been noted that diurnal variations in $\overline{q}$ are usually quite small. This is illustrated by the fact that the summertime (June-August) values of $\overline{W}$ over this area showed an average increase from 00 GMT to 12 GMT of only .02 cm. However, the spatial distribution of the changes was fairly coherent. Increases were limited to the region of strong inflow over the southern plains, the southern Rockies, and scattered stations in the southwest and along the Pacific coast. Small decreases, generally less than .10 cm, were observed at almost all other stations.

These changes are the net result of diurnal variations in vapor flux, precipitation, and evapotranspiration. Diurnal flux variations produce a diurnal variation in $\overline{W}$ which is difficult to estimate from only twice daily observations. However, the 12-00 GMT difference in the flux divergence suggests that the variation in $\overline{W}$ due to this effect alone is probably less than .05 cm, although it may rise to higher values locally over the mid-continent. Diurnal changes in evapotranspiration will contribute toward higher values of $\overline{W}$ at 00 GMT. Because of differences in local time, the changes between 00 GMT and 12 GMT will be most pronounced in the eastern portion of the area. Assuming a mean summertime evapotranspiration rate of around 7 cm/mo for the total area (a value consistent with results discussed later in this

chapter), and assuming that 5 to 6 cm of this amount is lost between 12 and 00 GMT, gives a diurnal change in $\overline{W}$ of between .10 and .17 cm from this effect alone. Summertime precipitation decreases at night over the area as a whole (although there are notable local exceptions). This partially offsets the effect of the decreased nocturnal evapotranspiration. Thus, of these three factors, it appears that diurnal changes in evapotranspiration will be most effective in producing diurnal variation in $\overline{W}$ .

The irregular variation of the mean monthly flux through the boundaries indicates that a longer period of record is needed in order to firmly establish the important features of the seasonal pattern. For example, it would be of interest to establish whether the sharp drop in transport across the Gulf coast in August, which occurred during each of the two years studied, is typical for this month.

The total annual flux across the boundaries and the average flux divergence over the entire area are shown in the following table:

Table 14. Total annual mean flux and flux divergence for the United States and southern Canada. Units: $10^{13}$ kg/yr.

| | Time (GMT) | 1961-62 | | 1962-63 | |
|---|---|---|---|---|---|
| West Coast inflow | 00 | 471 | 432 | 482 | 448 |
| | 12 | 392 | | 415 | |
| Southwest inflow | 00 | 70 | 67 | 74 | 73 |
| | 12 | 64 | | 72 | |
| Gulf of Mexico inflow | 00 | 418 | 458 | 329 | 379 |
| | 12 | 498 | | 429 | |
| Atlantic outflow | 00 | 604 | 648 | 616 | 626 |
| | 12 | 692 | | 636 | |
| Northern outflow | 00 | 140 | 146 | 149 | 138 |
| | 12 | 151 | | 128 | |
| $-\langle \nabla \cdot \bar{Q} \rangle$ | 00 | 215 | 163 | 120 | 136 |
| | 12 | 111 | | 152 | |

Year to year variations in the predominantly zonal inflow and outflow were small during this two year period, but changes in the flux divergence, and in the meridional flux from the Gulf of Mexico were significant.

3. Water balance

Neglecting groundwater outflow in comparison with surface outflow and storage changes leaves only storage terms as unknown in the balance equation. The change in atmospheric storage from the beginning

to the end of each month can be obtained, leaving only the surface and subsurface storage changes to be evaluated.

Mean monthly values $\langle \overline{P-E} \rangle$, $\langle \overline{RO} \rangle$, and $\langle S \rangle$ are shown in Fig. 87. Annual values are given below.

Table 15. United States and southern Canada. Area = 86.5 x $10^5$ $km^2$. Units: cm $yr^{-1}$.

| | May '61-April '62 | May '62-April '63 |
|---|---|---|
| $\langle \overline{P-E} \rangle$ | 18.8 | 16.0 |
| $\langle \overline{RO} \rangle$ | 20.6 | 15.7 |
| $\langle \Delta S \rangle$ | -1.8 | +0.3 |

These values represent an average for an area over which mean annual precipitation varies from less than 15 cm to over 250 cm, and mean annual runoff varies from zero to over 100 cm (Miller, Geraghty, and Collins, 1963). The seasons of highest and lowest flow differ locally, but for the area as a whole the maximum outflow occurred in spring and the minimum in the fall. Mean monthly runoff ranged from 0.8 to 2.6 cm during the two years investigated.

The pattern of wintertime streamflow was considerably different in each of the two years. Marked increases over the fall minimum were observed during the first year, while little or no recovery took place during the second year. The relatively low flow during the second winter

was primarily the result of unusually cold and dry conditions over the eastern part of the continent.

$\langle\overline{E-P}\rangle$ shows a more irregular pattern, and greater seasonal changes, than does the streamflow. Maximum values occur during the winter, minimum values during the summer. In contrast to the northern sections of the continent, where precipitation exceeded evapotranspiration throughout the year, one finds an excess of evapotranspiration during the three summer months.

Since the difference between $\langle\overline{P-E}\rangle$ and $\langle\overline{RO}\rangle$ changes sign from winter to summer, there must be an accumulation of water over the continent during the late fall, winter, and early spring, which is lost again during the warmer months of the year. The computed seasonal change in storage is also shown in Fig. 87. Storage was arbitrarily assumed zero on May 1, 1961, so values indicate the total storage change from that date. This, to the author's knowledge, is the first attempt to compute storage changes directly from actual measurements of the remaining terms of the balance equation.

The characteristics of the computed seasonal storage change agree well with what is know of this quantity. Soil moisture, as well as the water table, reach their highest values over most of the area in spring, and surface storage in the form of snow reaches a maximum in late winter

and early spring. Late spring and summer mark a period of high evapotranspiration and decrease in storage. The lowest values of soil moisture, water table, and streamflow most often occur in the early fall, and for this reason hydrologists have found it convenient to begin the so-called water year on October 1.

Surface and subsurface hydrologic data alone are not adequate to determine the amplitude of these seasonal changes, but Van Hylckama (1956) has estimated the storage over the continents using the empirical techniques of Thornthwaite. Mean monthly values were computed for the land area within each $10^{o}$ x $10^{o}$ region of the earth. The average monthly storage changes for a combination of areas which approximates the United States and southern Canada (30 - $50^{o}$N, 70 - $130^{o}$W plus 50 - $60^{o}$N, 100 -$100^{o}$W) was computed from his data, and is shown along with the results of this investigation, in Fig. 88. Van Hylckama's estimates were taken to represent storage on the 15th of each month.

The two curves are nearly in phase, although the maximum and minimum values computed by the water vapor balance equation appear to lag those of Van Hylckama by about half a month. However, the amplitude of the annual variations differs by more than a factor of two. A systematic underestimation of the moisture flux, and consequent underestimation of flux divergence might be suggested as a possible reason for this

difference, but since the mean annual flux divergence over the area is negative, this would lead to a sizable systematic overestimation of the storage loss. Such does not appear to be the case, since only a small net storage change was computed during the two year period. A flux error which varies systematically throughout the year could also produce erroneous values of seasonal storage change, and still give correct year to year changes. As was shown in Chapter VI, this type of error can arise if the vertically integrated flux does not include the contribution from the layers above 500 mb. This, however, is not a factor in the present investigation, since all available data up to 200 mb was used.

Since the amplitude of the annual storage curve was not very different during each of the two years, it seems probable that these results are a reasonable estimate of the long term mean seasonal storage changes. The excessive amplitude obtained by Van Hylckama may be due, at least in part, to the tendency for the Thornthwaite method to undercompute wintertime evapotranspiration and runoff, which in turn, requires the excess storage to be disposed of in summer. This appears to be accomplished by an overcomputation of summertime evapotranspiration.

Because of the difference in the land area of the Northern and Southern Hemisphere, these seasonal changes in storage represent a substantial seasonal shift of water from the oceans to the continents. Conse-

quently, the total water content of the oceans is lowest in March and highest in October (Donn, Patullo, Shaw, 1964). The difference represents only a small change in mean sea level and is thus difficult to estimate. Van Hylckama (1956) cites a calculation by Munk, using tidal gage data, which showed an oceanic storage change from March to October of $.50 \times 10^{19}$ gm (1.4 cm). Van Hylckama, himself, computes a change of $.75 \times 10^{19}$ gm (2.10 cm). However, on the basis of the comparison of his computed storage changes with the results from the vapor balance equation, one would expect his figure to be too high. The percentage overestimation at low latitudes is likely to be less than that indicated over the United States and southern Canada, since wintertime undercomputation of $\overline{E}$ would probably be less of a factor. Thus the percentage overcomputation for the total land area of the earth may not be as great as it appears to be over the United States and southern Canada. In any case, the estimate of Munk appears to be the better one.

No attempt was made to compute the average monthly measured precipitation over the area directly from precipitation reports, primarily because of the time required to tabulate these data for such a large area (even using climatological zonal averages). However, there is available a tabulation of the total areas bounded by certain isohyets during each month of the years 1961-62, for the United States and Canada south of $49^{o}$N and west of the northern tip of Maine (LaRue and Younkin, 1963).

These data can be used to obtain an estimate of the total precipitation volume. LaRue and Younkin computed the monthly precipitation volumes during 1961, but computed only the annual volume for 1962. In order to compute monthly precipitation volume during the second year, the following assumptions were made: (1) except for a minor amount of smoothing, the weight assigned to each isohyetal interval, when converting interval area to precipitation volume, was the same as that for the corresponding month of 1961. (2) Since no value was given for the .01 - .50 inch isohyetal interval, its monthly volume contribution was determined in the same way that LaRue and Younkin determined the annual contribution; by assuming the same ratio between the .01 - .50 and .50 - 1.00 intervals as was measured during the comparable month of 1961.

The area over which $\langle \overline{P-E} \rangle$ has been computed includes portions of Canada not included in the tabulation of LaRue and Younkin, and does not include the immediate coastal region of the United States. In order to compare regions which more nearly coincide, the Nelson River Basin was excluded from the divergence computation.

The estimates of $\langle \overline{P} \rangle$ are shown in Fig. 89, together with values of $\langle \overline{E} \rangle$ obtained by subtracting $\langle \overline{P-E} \rangle$. The approximations involved in the estimation of $\langle \overline{P} \rangle$, and the lack of coincidence of the two areas undoubtedly leads to some errors; however, only the

value of $\langle\overline{E}\rangle$ for February, 1962 appears to be considerably out of line. Careful checking indicated no errors in the computations and analyses for that month. Therefore, it is believed unlikely that there was any major error in the evaluation of the flux divergence.

In order to more clearly determine the reason for the unusual value of $\langle\overline{E}\rangle$, the average precipitation over the actual area used for the divergence computation was estimated, for this month only, from isohyetal analyses in the state climatological summaries. This computation gave a value of 5.8 cm for $\langle\overline{P}\rangle$, a little more than a cm higher than the estimate obtained from the data of LaRue and Younkin. Computations for subdivisions of the area indicated quite reasonable values of $\langle\overline{E}\rangle$ over the eastern two-thirds of the area, but practically no evapotranspiration was computed for the area west of the Continental Divide. The heaviest monthly precipitation in the Western Region during this period occurred in February, 1962. Snow was particularly heavy. Since it is under these conditions, and in this type of terrain, that precipitation will most likely be seriously underestimated, it may be that actual precipitation during this month was considerably more than measured, which in turn would lead to higher computed values of $\langle\overline{E}\rangle$.

The highest values of evapotranspiration, around 8 cm/mo, are computed in June during both years. Wintertime values appear to range

around 1 - 2 cm/mo. The particularly sharp drop from September to October, observed during both years, may be due to the decrease in transpiration at the end of the growing season.

The relative loss of water by evapotranspiration and runoff is of some interest. We may define a runoff coefficient:

$$C_R = \frac{\langle \overline{RO} \rangle}{\langle \overline{RO} \rangle + \langle \overline{E} \rangle}$$

which expresses the percent of the total loss due to runoff. Monthly values of $C_R$ were computed for the 20 month period for which rainfall estimates are available, and are shown in Fig. 89. Runoff represented more than 50% of the total loss only during February and March, but this value fell to less than 20% during the summer and early fall. Values of $C_R$ for the period May-December were consistently lower during the second year; the result of both lower streamflow and higher computed evapotranspiration.

E. Central Plains and Eastern Region - Water Balance

A water balance computation was made for that portion of the United States and southern Canada east of the Continental Divide. Results are shown in Fig. 91, and annual values are given below:

Table 16. Central Plains and Eastern Region. Area = 64 x $10^5$ $km^2$. Units: cm $yr^{-1}$.

| | May 1961-April 1962 | May 1962-April 1963 |
|---|---|---|
| $\langle\overline{P-E}\rangle$ | 16.4 | 15.0 |
| $\langle\overline{RO}\rangle$ | 22.4 | 15.4 |
| $\langle\Delta S\rangle$ | -6.0 | -0.4 |

Computed storage losses over this area occurred primarily during the first year. Further subdivision of the area indicated that most of first year losses occurred in the western two-thirds of the area. During the second year, computed increases in storage in the western half of the area compensated for heavy losses in the east.

Since a well organized pattern of diurnal wind variations exists over eastern North America, it is of interest to examine the diurnal variations in the flux divergence over this region. Mean monthly values of flux divergence for 00 and 12 GMT, for each of the 24 months, are shown in the lower portion of Fig. 91. Differences between 00 and 12 GMT showed no particular pattern during most of the period; however during the summer and early fall of 1962 the 00 GMT divergence greatly exceeded that at 12 GMT. The marked difference between this period, and the comparable period in 1961, again shows that substantial year to year variations can be expected in the patterns of diurnal variation. These results, and the annual results previously given for the United States

and southern Canada, well illustrate the difficulty of estimating the flux divergence from single daily observations.

F. Western Region - Water Balance

This region consists of that portion of the United States and southern Canada west of the Continental Divide.

Monthly values of $\langle\overline{P-E}\rangle$, $\langle\overline{RO}\rangle$ and $\langle S\rangle$ are shown in Fig. 90. Mean annual values are given in the following table.

Table 17. Western Region. Area = $22.4 \times 10^5$ km$^2$. Units: cm yr$^{-1}$.

| | May 1961-April 1962 | May 1962-April 1963 |
|---|---|---|
| $\langle\overline{P-E}\rangle$ | 25.2 | 18.2 |
| $\langle\overline{RO}\rangle$ | 15.2 | 16.3 |
| $\langle\Delta S\rangle$ | +10.0 | +1.9 |

The computed storage changes shown in Fig. 90 exhibit the expected seasonal variations. A rather sharp minimum is reached at the end of September, while the maximum occurs sometime between early April and late May. The amplitude of the seasonal variation is difficult to determine because of the substantial net storage change computed during the first year, but may be estimated at about 12 cm.

Although larger average year to year storage changes can be

expected when smaller areas are investigated, the computed change over this region during the first year is so large that one might question its reality. A check of the climatological records for the area for the periods January-April 1961 and January-April 1962 indicates the period preceeding May 1, 1961 to have been abnormally dry, while precipitation during the period prior to May 1, 1962 was well above normal. This is well illustrated by the following remarks from the Climatological Data-National Summary.

January, 1961 --- "Snowpack in the western mountains remained below normal ... in the far west temperatures generally averaged well above normal ... warmest January on record at San Diego and Los Angeles ... second warmest in Seattle .... in most of the area between the Cascade and Sierra Nevada Mountains and the Appalachians, precipitation was less than 50% of normal".

February, 1961 --- "Mild and dry in western half of the nation .. precipitation less than 50% of normal in north central Montana, and the far southwest ... Phoenix and Prescott, Arizona driest February since 1924 ... San Francisco driest February in 38 years ... Santa Maria, Calif. driest since 1900 ... Grand Junction, Colorado 11th consecutive month with below normal precipitation ... precipitation 200% of normal over Washington and portions of

extreme northern Idaho and Oregon .... snowfall unusually light in far west ... in much of far west the mountain snowpack at the end of the month was less than 50% of normal".

March, 1961 --- "precipitation above normal in Washington and Oregon ... in much of California, Nevada and Utah, where winter precipitation was less than 50% of normal, the irrigation water outlook for the coming season was very unfavorable ... in the far west heavy snowfall substantially increased the mountain snowpack in Utah, Colorado and New Mexico, but it still remained below normal, except near normal in New Mexico ... pack about normal in Washington but below normal in other western states ... in California the pack is only 30% of normal in the extreme southern Sierras, 50% of normal in the Central Sierras, and about normal or above in some northern areas".

April, 1961 --- "drought conditions continued in the Great Basin and far southwest ... precipitation in Las Vegas, Nevada for January-April only 47% of normal ... April snowfall in west was not heavy enough to raise the mountain snowpack to average levels, and the water content of the pack remained below normal in most areas. The pack was average or above mainly in the northern areas."

In contrast, the following are comments from the records for February through April, 1962.

February, 1962 --- "snowfall was unusually heavy in the far west ... heavy precipitation included most of California, Nevada, Utah and western Colorado ... one of the wettest Februarys in California since 1850 ... Reno, Nevada had 4th greatest total for February since 1870 ... heavy precipitation ended a three year drought in California ... boosted water supply outlook to normal or above in all areas of the state, and greatly improved outlook in remainder of far west, except in Washington and Oregon".

March, 1962 --- " above normal precipitation in most of the far west further improved the irrigation water outlook there ... Far west mountain snowpack was generally much above normal at the end of the month ... Winslow, Arizona reported record snowfall for the month; Pocatello heaviest since 1916. Ely, Nevada had 15.0 inches for the month, unusually heavy for that location. Salt Lake City had more than 3 times the usual amount ... Spokane, Washington had greatest March total since 1897."

April, 1962 --- "Moderate to heavy precipitation in the Pacific Northwest and northern Rockies ... dry conditions over the far southwest ... snowfall totals were generally below normal in the far west ... however, the snowpack at higher elevations is still generally near normal in the Pacific Northwest, except in portions of Washington

and Oregon, and above normal in the middle and southern Rockies, and in the far southwest. At low and intermediate elevations, however, snow cover was generally depleted by above normal warmth, resulting in wet mountain soils, and generally high rivers."

From these comments it appears that a significant increase in storage may well have taken place between May 1, 1961 and May 1, 1962.

G. Central Plains Region - Water Balance

This region consists of the Mississippi Basin exclusive of the Ohio Basin, the Nelson Basin, and the Gulf Coast drainage between the Mississippi River at Vicksburg, Mississippi and the San Antonio Basin. Monthly values of $\langle \overline{P-E} \rangle$, $\langle \overline{RO} \rangle$, and $\langle S \rangle$ are shown in Fig. 92. Annual values are given below.

Table 18. Central Plains Region - Area: $41.9 \times 10^5$ km$^2$. Units: cm yr$^{-1}$.

| | May 1961-April 1962 | May 1962-April 1963 |
|---|---|---|
| $\langle \overline{P-E} \rangle$ | 5.3 | 11.3 |
| $\langle \overline{RO} \rangle$ | 11.4 | 7.0 |
| $\langle \Delta S \rangle$ | -6.1 | +4.3 |

The seasonal storage reaches a peak in spring, and during these

two years exhibited maxima around April 1 and June 1. The minimum is again found in September. The amplitude of the storage change appears to be around 8 cm, somewhat less than that estimated for the Western Region. Because of seasonal differences in precipitation, with a wintertime maximum over much of the west, and a summertime maximum over the Central Plains, this difference seems reasonable. Summertime losses over the west will largely derive from precipitation which fell during the previous winter, while much more of the summer loss over the plains is supplied by summertime convective precipitation.

Computed storage losses during the first year were approximately balanced by gains during the second. Computations for various subdivisions of the area indicated losses during the first year over all but the Upper Mississippi Basin. Computed decreases in storage during the second year were most pronounced over the Upper Mississippi Basin, while the major increases were indicated over the Nelson and Upper Missouri Basins.

H. Eastern Region - Water Balance

This region, consisting of the Ohio Basin, the St. Lawrence Basin above Cornwall, Ontario, the Ottawa Basin, and the eastern Gulf coast and east coast drainage ($22.2 \times 10^5$ km$^2$), was singled out for the most intensive study. Mean monthly precipitation, streamflow, and moisture

flux data were tabulated for the region.

The two years covered by this investigation coincided with a period of sharp falls in the levels of the Great Lakes and a definite turn toward drier conditions over large portions of the area. The period marked the early stages of the severe drought of the early and mid 1960's which occurred over portions of southeastern Canada and the northeastern United States.

Mean monthly values of the principal components of the water balance are shown in Fig. 93. Annual values are given below.

Table 19. Eastern Region - Area = 22.2 x $10^5$ $km^2$. Units: cm $yr^{-1}$.

| | May 61-April 62 | May 62-April 63 |
|---|---|---|
| $\langle\overline{P-E}\rangle$ | 37.9 | 20.3 |
| $\langle\overline{RO}\rangle$ | 44.5 | 31.7 |
| $\langle\Delta S\rangle$ | -6.6 | -11.4 |
| $\langle\bar{P}\rangle$ | 101.3 | 87.4 |
| $\langle\bar{E}\rangle$ (computed) | 63.4 | 67.1 |

The computed value of $\langle\overline{P-E}\rangle$ for August, 1961 looks suspicious, and may be somewhat too large. The Climatological Data - National Summary shows a band of heavy rainfall during the month which was centered approximately on the southeastern boundary of the area. It may be that the aerological network was not sufficient to adequately define

the divergence pattern along this boundary, under these conditions.

The marked storage losses computed during the two year period make it difficult to accurately define the mean seasonal change; however, an estimate of 12-16 cm change in storage from spring to fall appears to be reasonable. In Fig. 88, the changes during the first year, and the average for the two years, are compared with the mean changes computed by Van Hylckama (1956) for the area between 30°N and 50°N and 70°W and 90°W. The values of Van Hylckama again appear to significantly overestimate the actual storage changes.

The storage changes in the Great Lakes follow a pattern which is almost out of phase with the remainder of the region; lake storage is highest in mid summer and lowest in late winter. This amounted to a 2-3 cm damping of the seasonal storage changes of the remainder of the area, i.e., the average seasonal storage changes for the portion of the area exclusive of the Great Lakes appear to be around 14 to 19 cm.

Mean monthly values of precipitation were computed for the land areas within the United States from state climatological zonal averages. Values over southern Canada were estimated from the isohyetal maps of the Canadian Monthly Record. Values over the Great Lakes were estimated from the available data, with no corrections attempted for possible differences between precipitation over land and water. Mean

monthly values of evapotranspiration were then computed using these data. Results are shown in Fig. 93. Subtracting the volume of evapotranspiration computed over eastern North America from that computed earlier for all of the United States and southern Canada (except the Nelson Basin) provides the estimate for the Western and Central Plains subdivisions shown in Fig. 89. The approximations involved in obtaining these values require one to treat them as rather rough estimates. Nevertheless, they appear, for the most part, to be quite reasonable. The questionable value of $\langle \overline{P-E} \rangle$ for August 1961 has already been mentioned, and may have led to the low value of $\langle \overline{E} \rangle$ computed for the eastern area during that month.

The mean annual march of evapotranspiration computed for the Eastern Region differs in some important respects from that found over the West and Central Plains. Maximum evapotranspiration is shown in June for the West and Central Plains, while in the Eastern Region it continues to rise to a maximum in July. An earlier summer maximum in the west and midwest seems reasonable, since soil moisture deficiences which develop over the more arid regions will usually keep summer evapotranspiration well below the potential rate. Larger soil moisture reserves in the east probably allow heavy evapotranspiration to continue into midsummer. Generally lower evapotranspiration rates

are computed for the west and midwest throughout the year, but particularly during winter.

Values of $C_R$ for Eastern North America are shown in Fig. 92. Runoff accounted for around 50-60% of the total loss from December through March, but this percentage dropped rapidly to 15-35% from May through October. The value of $C_R$ from the Eastern Region, for the entire first year, was 41% as compared with 25% for the remainder of the United States and southern Canada. Thus the percentage loss due to runoff was considerably higher over the east, as would be expected. A drop in $C_R$ is again observed during the second year, primarily the result of a sharp decrease in runoff.

Perhaps the most interesting single result of these computations is the sharp drop in surface and subsurface storage computed during the two year period. As previously mentioned, this is in qualitative agreement with independent indicators. The levels of the Great Lakes dropped sharply and losses in lake storage alone amounted to 3 cm when averaged over the entire area. Perhaps of more importance is the suggestion from the falling lake levels of possible heavy soil moisture and ground water losses in the surrounding areas as well. Palmer (1965) has developed an index of meteorological drought which is dependent on the duration and magnitude of abnormal moisture deficiency and is normalized in such a

way that it permits time and space comparisons of drought severity. The index is designed to reflect the disruption of the local economy produced by a departure from normal of the moisture aspect of the local weather. Mr. Palmer has kindly prepared maps for the area for which values of the index are available. This includes an area of the United States north of about 35°N which extends from the east coast to about 105°W. Maps were prepared for conditions as of April 30, 1961, and at 6 month intervals through April 30, 1963.

Conditions on April 30, 1961 were classed as normal to moderately wet over most of the analyzed area included in the Eastern Region. Only over lower Michigan was there any appreciable below normal area; this region being classed as having mild drought.

By April 30, 1962 considerably drier conditions were indicated. The area from Virginia and North Carolina westward through Kentucky and Tennessee was still classed as moderately wet to very wet, but most of the remainder of the area within the Eastern Region had markedly lower indices than 12 months previous, being generally classed as incipient drought to mild drought.

By April 30, 1963 droughty conditions had noticably worsened. Only a small area in eastern Kentucky and Tennessee and in Central Indiana was still classed as slightly to moderately wet. The remainder

of the area generally ranged from incipient drought to severe drought, and areas of southeastern Wisconsin and southern Michigan were classified as having an extreme drought.

The trend toward drier conditions over that portion of the Eastern Region which was included on Palmer's maps was apparently quite pronounced during the two year period. The trend toward drier conditions over the remainder of the Eastern Region is also quite apparent from stream flow records, which indicate decreased flows during comparable seasons of the second year. Typical examples are shown below:

Table 20. Average outflow ($10^3$ $ft^3$ $sec^{-1}$)

| | May 61-Oct 61 | Oct 61-Apr 62 | May 62-Oct 62 | Oct 62-Apr 63 |
|---|---|---|---|---|
| Alabama River at Clairborne, Ala. | 21 | 70 | 14 | 37 |
| Altamaha River at Doctortown, Ga. | 11 | 23 | 6 | 16 |
| Ottawa River at Grenville, Que. (estimated) | 65 | 67 | 54 | 47 |

I. Great Lakes and Ohio Drainage - Water Balance

The problems which arose in the balance computations for the Ohio Basin and Great Lakes are typical of those encountered as the size

of the area was further decreased.

The results for these combined basins are shown in Fig. 94. Annual values for $\langle \overline{P-E} \rangle$, $\langle \overline{RO} \rangle$ and $\langle \Delta S \rangle$ are given below.

Table 21. Ohio Basin -Great Lakes Drainage. Area = $13.0 \times 10^5$ km$^2$. Units: cm yr$^{-1}$.

| | May 61-April 62 | May 62-April 63 |
|---|---|---|
| $\langle \overline{P-E} \rangle$ | 42.9 | 15.5 |
| $\langle \overline{RO} \rangle$ | 40.9 | 29.6 |
| $\langle \Delta S \rangle$ | +2.0 | -14.1 |

Records of the elevation of the surfaces of the Great Lakes, provided by the Lake Survey, were used to estimate the actual storage changes of the lakes. It was then possible to compute a storage change for that portion of the area exclusive of the Great Lakes. These values, as well as the values computed for the entire area, are shown in Fig. 94.

The overall relationship of $\langle \overline{RO} \rangle$ and $\langle \overline{P-E} \rangle$ is, for the most part, still quite reasonable, with losses in storage shown during the spring and summer, and increases during the fall, and during the first winter. A net storage loss was computed during the two year period, with the average loss over the portion of the area exclusive of the Great Lakes being less than one-third the average loss of the lakes themselves.

The storage loss during the second year is not very different from that computed for the entire Eastern Region. However, an actual increase in storage is computed during the first year, the result of computed storage increases over the area draining into the Great Lakes which are greater than the computed losses from the lakes themselves and the Ohio Basin. Since this does not appear to agree with the results of Palmer, and the implications of the falling lake levels, one must suspect that the water vapor convergence was overcomputed, at least during the first year.

If one examines only the Great Lakes drainage (Fig. 95), it becomes rather apparent that a general overcomputation of $\langle \overline{P-E} \rangle$ is occurring. A mean annual increase in storage is computed for the total area, even in the face of average annual losses of around 3.5 cm from the lakes alone. Computed increases over the area exclusive of the lakes amounts to around 12 cm/year.

Acknowledging these deficiencies in the computed values, they are still sufficient to allow an estimate of the amplitude of the annual storage change which is probably at least as good as that given by Van Hylckama (1956). Fig. 95 shows a comparison of these results with the storage changes computed for the area $40^{o}$-$50^{o}$N and $80^{o}$-$90^{o}$W from Van Hylckama's data.

The results of Van Hylckama were presented as being for the land areas of the world, but since he used these results to compute seasonal changes in sea level, it appears that they should also reflect the storage changes of the lakes and landlocked seas. If such changes were indeed taken into consideration, his values grossly overestimate the seasonal storage changes in this region, which are probably no more than 8-10 cm. On the other hand, it appears that he may have neglected the changes in lake storage, and in this case his results can be compared with those obtained from the water balance computation for the land area only. Adjusting for the 12 cm annual storage change, computed during this period, one might estimate from the water balance computation a seasonal change in storage of 20 to 25 cm, as compared with around 31 cm computed by Van Hylckama. These results are in fair agreement, but still indicate the possibility of an overcomputation by Van Hylckama.

Mean monthly results for the Ohio Basin are also shown in Fig. 95. Although a decrease in storage is computed during the two year period, the magnitude of the decrease appears to be excessive. This, as well as computed evapotranspiration, indicate an overcomputation of the flux divergence. For example, the computed evapotranspiration during the second year was 93 cm, a figure which is comparable to, or possibly a little larger than the mean annual lake evaporation for the area as computed by Kohler, Nordenson, and Baker (1959).

The separate results for the Ohio Basin and Great Lakes area suggest the possibility that part of the error is due to an improper determination of the flux across their common boundary, so that the inflow to the Great Lakes and the accompanying outflow from the Ohio Basin is often overestimated. This could occur as a rather systematic error, or as a large occassional or seasonal error, or possibly as a combination of the two. Comparison of the mean monthly values of $\langle\overline{P-E}\rangle$ for the two basins indicates the probability of large errors of this type in October, December, and possibly in July. In June, however, there seems to be an error in the opposite direction, with apparent overcomputation of convergence in the Ohio Basin at the expense of the Great Lakes drainage. In any event, the compensating errors in $\langle\overline{P-E}\rangle$ which apparently occur between these two basins well illustrate why the results obtained for their combined areas are superior to those for the individual basins.

One should not be overly pessimistic concerning these results, or what they imply concerning the possibility of obtaining useful results over areas of this size. While it is true that one cannot rely on the individual monthly values of $\langle\overline{P-E}\rangle$ or on computed interannual storage changes, it is also true that the mean monthly values were of the correct order of magnitude, and did indeed produce, for the Great Lakes Basin, an annual storage curve which apparently reflects the correct order of magnitude of the seasonal changes. It may well be that further investigation will lead

to an improvement in the results for areas of this size.

One should also not overlook the possibility that, on this scale, significant errors may on occasion occur in measured precipitation and possibly even in runoff. For example, the mean precipitation computed from climatological zonal averages, for the Ohio Basin, was less than the reported runoff during each of the two months, March and April, 1962. The probability that actual precipitation exceeds the measurements has been discussed previously. Another unusual situation occurred during March-April 1963, when comparison of the total flow from the Ohio at Metropolis, Ill., with that of the Mississippi at Vicksburg, Miss., indicated questionably large losses between these two points. Without a more thorough investigation, one cannot say which, if any, of these data were seriously in error, but they do suggest that substantial errors may not always be safely attributed to incorrect evaluation of the vapor flux.

# XI. INTERANNUAL FLUX VARIATIONS

Little information is available on seasonal and interannual vapor flux variations, since almost all previous investigations have been limited to a period of one year or less. One exception, however, is a study of the seasonal variations of vapor flux at Oklahoma City covering a period of almost 12 years (Benton, 1960). These results indicated that the total movement of water in the atmosphere over Oklahoma City did not vary greatly from year to year. In addition, correlations between the anomolies in vapor flux magnitude, and precipitation, were low.

Five years of mean annual values of the 00 GMT flux components, averaged for several stations in the neighborhood of the Central American Sea, were presented in Chapter IX. These data showed a variation in the magnitude of the mean annual flux of more than 650 gm (cm sec)$^{-1}$ during the period; more than 30% of the five year mean value. Interannual differences of as much as 950 gm (cm sec)$^{-1}$ were observed at an individual station (Willemstad).

Some of the annual values of boundary flux shown on Fig. 78 also exhibit marked differences between individual years.

A detailed investigation of interannual changes in the vapor flux will be left to future studies. However, it appears worthwhile to briefly review the overall characteristics of the year to year changes which

occurred during the two years covered by this investigation. It is of particular interest to note the relationship of these changes to changes in $\langle\overline{E-P}\rangle$, and, where possible to changes in precipitation.

A clear picture of the year to year changes in the flux can be obtained from Figs. 106 and 107, which show the interannual difference in the mean annual values of the individual flux components. Figs. 104 and 105, which present the mean annual values for the two year period, are included for comparison.

Considering first the Central American Sea, we note the following changes from the first to the second year: (1) a decrease in the mean northward flux, (2) a decrease in the mean westward flux, and (3) an increase in $\langle\overline{E-P}\rangle$ .

The decrease in the westward flux was observed over the entire Caribbean Sea, and over all but the western and extreme northern Gulf of Mexico. Interannual differences in the central Caribbean amounted to more than 400 gm $(\text{cm sec})^{-1}$, and as much as 30% of the two year mean annual flux at some points.

Decreased northward flux was indicated over all but the southwestern Caribbean and extreme western Gulf of Mexico. Changes in the meridional flux were particularly pronounced in the northcentral Gulf.

Comparison of the year to year changes in the flux components

with the mean annual values indicates a decrease, during the second year, in the magnitude of the flux over almost the entire Central American Sea. Only in the extreme western Gulf of Mexico did the flux increase in magnitude.

Because of the dominance of the zonal flux component, and the relatively small zonal eddy flux, (Peixoto and Crisi, 1965), the mean annual flux over the Caribbean Sea is primarily the result of transport by the mean annual wind. Consequently, interannual flux differences of the magnitude found over much of that area are most likely due to the vertically integrated changes in the mean annual wind and specific humidity. The degree to which each of these factors contributed to the change cannot, of course, be determined without an analysis of the data at each level. These data were not immediately available to the author. A check of mean annual values of total water content, $\overline{w}$ , at stations in the area was rather inconclusive, with about as many stations showing increases as decreases during the second year. The largest change, a decrease of .32 gm $cm^{-2}$ at Grand Cayman, represented 8% of the two year mean value at that station, while the change in the magnitude of the flux at the station amounted to about 20% of the mean value. Thus, the data suggest that the interannual flux changes over the Caribbean were primarily the result of a decrease in the strength of the mean easterlies.

It is interesting to note the changes in the configuration of the vector field which are associated with the interannual change in the flux divergence. Over the Caribbean Sea, where the annual divergence change amounted to only +11 cm, there is no clear cut pattern of change in the individual component's contribution to the divergence. Over the Gulf of Mexico, however, where the computed divergence change was +33 cm, the pattern is more clear cut. Here the two components contribute oppositely to a divergence change, with the net divergence change being of the same sign as the change in the divergence of the zonal component. It is apparent that the change in the deformation component of the vector field is usually much larger than the change in the divergent component. This is also true of the mean components themselves on individual maps. Thus, for interannual changes in the flux vector field, as well as for the mean field itself, the non-divergent component is normally much larger than the divergent component.

Interannual changes over the North American Continent are probably best discussed in terms of the regions previously used for water balance computations.

Over Northern North America, changes from the first to the second year consisted of: (1) a general decrease in eastward flux, (2) minor changes in the meridional flux, and (3) a slight decrease in $\langle \overline{E-P} \rangle$.

The decrease in eastward flux amounts to a sizeable percentage of the two year mean value over most of northern and eastern Canada. It is this decrease in flux through the eastern boundary which primarily accounted for the decrease in the computed value of $\langle\overline{E-P}\rangle$ during the second year.

Flux changes over the Western and Central Plains Region were, in general, rather small, and, except for a few small scale features, showed little organization.

The most interesting interannual changes are found over the Eastern Region. Changes in this area consisted of: (1) a decrease in the eastward flux, (2) a decrease in the northward flux, (3) an increase in computed $\langle\overline{E-P}\rangle$ (18 cm), (4) a decrease in $\langle\overline{P}\rangle$ (14 cm), and (5) a decrease in $\langle\overline{W}\rangle$ . As in the case of the Central American Sea, the increase in $\langle\overline{E-P}\rangle$ was accompanied by a decrease in the magnitude of the flux. Compensating changes in the individual component's contribution to the flux divergence was again observed, but contrary to the situation over the Gulf of Mexico, the change in the divergence was of the same sign as the change in the contribution from the meridional component.

Values of $\overline{W}$ were lower during the second year at almost all stations in the Eastern Region, with the largest decreases (generally

. 10 - . 20 gm $cm^{-2}$) over the northeastern United States and southeastern Canada.

The flux changes in the Eastern Region, and over the Gulf of Mexico, represent changes in the western portions of the flux maxima associated with the Atlantic cyclone belt (see Figs. 2 - 3). Thus, it may be that the general decrease of the flux over that area is associated with weaker cyclonic activity, or perhaps the result of a southeastern shift of the western end of the cyclone belt. The apparent westward shift and overall weakening of the meridional flux pattern in the Gulf of Mexico during the second year, which appears as a decrease in northward flux in the northcentral Gulf, and an accompanying increase in northward and westward flux over the western Gulf, northeastern Mexico, and Texas may be one of the more significant features of the pattern.

Two years of data are, of course, not sufficient to establish relationships between seasonal or annual changes in the configuration of the vapor flux field, and changes in precipitation or flux divergence. The analyses do show that large scale, well organized interannual changes do occur, and that these changes can be of appreciable magnitude. The analyses also suggest that interannual changes in $\overline{E-P}$ , or $\overline{P}$ , in addition to being directly related to changes in the divergence of the vapor flux, may, in some areas, be correlated with changes in other

differential properties of the vapor flux vector field and possibly with changes in the magnitude of one or both of the components as well.

# XII. FLUX DIVERGENCE MAPS AND AN ANALYSIS OF SYSTEMATIC FLUX ERRORS

The regional water balance computations discussed in Chapters IX and X yield a great deal of information concerning the accuracy of the computed mean flux divergence over a particular region. However, they give little information on the type of errors which lead to the deterioration of the results as the size of the area is decreased. Further information concerning this important question can be obtained if the flux divergence is computed with a higher degree of resolution. Such computations were made, as previously noted, using a $2.5^{o}$ x $2.5^{o}$ grid south of $57.5^{o}$N and a $2.5^{o}$ latitude x $5.0^{o}$ longitude grid north of $57.5^{o}$N. Individual computations were made for each of the 24 months, at both 00 and 12 GMT. These results were in turn combined into mean monthly, mean seasonal, and mean annual maps. Mean seasonal maps of the flux divergence difference, 12-00/2, were also computed in order to more clearly ascertain the effect of diurnal variations on the computations. Computer printout of mean monthly, seasonal, and annual values, together with a printout of summer and winter values of diurnal flux differences, are shown in Figs. 46-76. Computations were performed over Continental North America north of the United States-Mexican border, over the Central American Sea, and in the area west of the

Bahama Islands. Other regions, in which no computations were made, were assigned grid point values of zero. Rather than referring to the basic computer printout, it will be convenient, during much of this discussion, to refer to Figs. 97-103, which present analyses constructed from the seasonal and annual grid point values of flux divergence.

We shall not attempt to compare the values of $\nabla\cdot\overline{Q}$ on individual monthly maps with the distribution of precipitation during that month, but will merely record a few general observations. It is hard to estimate the relationship to be expected during summer between a divergence map, and a precipitation map such as that presented in the Climatological Data-National Summary, without additional information. Antecedent conditions, and the timing of precipitation during the month are important factors in this relationship. Furthermore, the erratic patterns of convective precipitation often create difficulties in the construction of a meaningful summertime precipitation map. Nevertheless, there can be little doubt that the summertime flux divergence maps are overlaid with a substantial amount of error, which in many areas strongly distorts, or completely masks the true pattern of divergence.

During winter, when evapotranspiration over the land is low, leading to patterns of $\overline{P-E}$ and $\overline{P}$ which are often similar, the mean monthly divergence patterns show a great improvement. Large scale areas of heavy precipitation are usually accompanied by corresponding

minima of computed divergence in the same general area. Areas with spuriously large values of either convergence or divergence are also much less in evidence during winter.

The extent to which the error pattern obscures the true pattern is probably best illustrated by the mean annual divergence map (Fig. 97). As one would expect from the regional water balance computations, the map captures the broad scale features of the divergence pattern. The Central American Sea is shown as being primarily divergent. Convergence is the rule over the continent, with the expected large values on the north Pacific Coast, and in the southeastern United States. However, the gradients in many areas, and the magnitude of many of the major features on this map cannot be supported by independent hydrologic data, and in some cases are undoubtedly in error.

Problems in the divergence distribution over the Central American Sea were anticipated, even though efforts were made to produce a smooth field. The non-representativeness of the data from Kingston, Jamaica has already been discussed, and the very strong gradient between convergence in the northeastern Caribbean and divergence to the west may be due, in part, to improper interpretation of these data. It should be emphasized that it is primarily the distribution of the divergence within the basin, and not its average value, which is in question, since it was

shown in Chapter IX that the average value is in excellent agreement with independent estimates of $\langle \overline{E-P} \rangle$.

Data from the missle range stations in the Bahamas were not available with sufficient regularity to be of use during this two year period, nor were any data available from Havana. Consequently, the distribution of divergence over Cuba and the Florida straits, and in the area to the east of the Greater Antilles is unreliable. Furthermore, data over Florida, and computations on a $2.5^{o}$ grid, are not sufficient to adequately resolve differences between values of divergence over the peninsula and over the surrounding waters of the Gulf and the Atlantic.

Some of the features along the edges of the continent are due to uncertainties of analysis, but most of the large scale pattern over North America is well established by the data. Questionable features over the continent include:

(1) The intense area of divergence over the northwestern United States, and the excessive convergence to the south of this area.

(2) The elongated area of divergence parallel to and just to the east of the Continental Divide, extending from the Yukon Territory almost to the Gulf Coast.

(3) The strong convergent area over southern Texas

(4) The strong convergence over and just to the east of the

Continental Divide.

(5) The area of convergence extending from south of Lake Michigan, northward, then eastward through Ontario. It is the intensity of the convergence in this area which is in question.

(6) The divergent area extending from Lake Erie to Hatteras

(7) The divergent area over northeastern Quebec and northern Labrador.

(8) The convergence maximum over Hudson Bay

(9) The maxima over Labrador and Newfoundland. Again in (8) and (9), it is the magnitude of the values which is in question.

Examination of the seasonal analyses (Figs. 98-101) and the annual mean maps for the two individual years (not shown here) reveals the following facts.

(1) All of the previously described features appear on each annual mean map in approximately the same geographical location, but vary somewhat in intensity.

(2) The strong convergence over Hudson Bay does not appear in winter and spring, and the divergence over northeastern Quebec and northern Labrador does not appear in winter. All other features are recognizable on each seasonal map.

(3) The seasonal variation in the intensity of these features is

not uniform. Some are most intense in summer. Examples are the divergent area over the northwestern United States, the divergent area east of the Continental Divide, the convergence over and just to the east of the Southern Rockies, and the features over Hudson Bay, Quebec, and Labrador. The convergence north of the Great Lakes was strongest in fall, while convergence over and just to the east of the Central Rockies was strongest in fall and winter. The area of convergence south of Lake Michigan, and the divergence over the Upper Ohio Valley do not appear to follow any particular seasonal pattern.

The conclusion is therefore inescapable that insofar as these features represent errors in the divergence field, they are of a systematic rather than a random nature, appearing each year, and, for the most part, in all seasons (except north of $50^{o}$). In this regard it should be noted that several of the major features appearing on these maps are also apparent in the less detailed analysis of 1958 data by Peixoto and Crisi (1965); notably the convergent area over south Texas and the southern Rockies, the belt of divergence east of the Continental Divide, and the excessive convergence over the Canadian Rockies.

The reasons for the systematic errors are by no means clear. However, there are some possible sources of error which it seems safe to discount. It has previously been pointed out that the transport of

liquid or solid water is a minor factor; a conclusion which is borne out by the excellent balance between runoff and computed mean flux divergence over the larger regions.

The 50 mb vertical resolution in the data may produce some systematic sampling errors in the lowest levels, but because of the varying wind regimes, and station elevations, these errors should be rather random and local in nature.

It also seems unlikely that large errors will be produced by the neglect of the flux above 200 mb, although there could be some systematic error at the higher reporting levels produced by the use of statistical estimates of humidity, and the increased number of missing reports. In particular, this could be a factor within and along the boundaries of mountainous regions. However, it is exceedingly doubtful if such errors could be of the magnitude necessary to produce the features found in the northwestern United States and just east of the Continental Divide.

The more important errors can, it appears, be most logically attributed to a combination of the following factors: (1) the improper definition of the diurnal flux variations by two daily observations, (2) the inability to separate smaller scale features of the flux field from the broad scale pattern, and (3) local station peculiarities.

The errors produced by the inability of two daily observations to

define the mean daily flux are undoubtedly of importance in some areas, particularly during summer. The characteristics of these oscillations have been discussed in Chapter VIII. Some idea of the magnitude of the diurnal change in the flux divergence produced by these oscillations can be gained from an examination of Figs. 102 and 103, which show the difference between the 12 GMT and 00 GMT divergence fields for summer and winter.

The summertime pattern of diurnal change is dominated by the effects of the large scale oscillation over eastern North America and the Gulf of Mexico. Changes in the divergence pattern between 12 GMT and 00 GMT in this area are quite remarkable. The decrease in convergence over the Rockies and high plains, and the increase in convergence over the Mississippi Valley between 00 and 12 GMT is consistent in most respects with the vertical motion field found by Curtis and Panofsky (1958) and the low level convergence patterns found by Bleeker and Andre (1951). The greatest changes in convergence are found over the Gulf of Mexico, where differences between 00 and 12 GMT flux convergence of as much as 50 gm $(cm^2\ mo)^{-1}$ were computed.

It is also interesting to note the small maximum in the (12-00)/2 difference which is located over Hudson Bay, indicating relatively more convergence over the bay in the morning than in the evening.

Wintertime differences between the 12 GMT and 00 GMT flux divergence are much reduced, but many of the features of the summer pattern can still be recognized. The changes over the Gulf of Mexico are still quite pronounced, but the pattern over the plains, although still identifiable, is quite weak. The pattern of variations north of 52.5°N has almost completely disappeared, except in the area over Alaska and the Yukon, and here the summertime pattern is reversed.

Although the mean monthly flux vector may be defined with fair accuracy by two daily observations, the error in the computed flux divergence may still be large if the systematic flux errors form a highly divergent vector field. The difference during July at Ft. Worth (Fig. 45), between the average of the 00 and 12 GMT flux, and the average of the four daily observations, is probably a fair estimate of the flux error. Errors of this magnitude could easily account for much of the noise found in the summer divergence patterns.

Where errors due to diurnal flux variations are dominant, one would expect the maximum error in summer when the oscillations are most strongly developed and the minimum error in winter. As previously noted, major features on the map which exhibit such a seasonal variation are the divergent area over the northwestern United States and the accompanying area of excessive convergence further south, the

divergent area east of the Continental Divide, the convergent area over and just to the east of the southern Rockies, and the features over Hudson Bay, Quebec and Labrador. Added evidence that these particular features may be caused primarily by improper evaluation of the diurnal flux variations is found in the fact that each of the above areas is closely associated with a maximum difference between the 00 GMT and 12 GMT divergence, thus suggesting that the areas may be regions of local maximum diurnal variability of the flux divergence.

Localized smaller scale effects are, beyond doubt, important sources of error in western North America, and perhaps in the vicinity of the Appalachian Mountains and the east coast as well. It is also tempting to attribute the strong divergence found over the Ozark plateau partly to such effects. The Ozark region presents the first topographic barrier of any consequence to the strong low level influx from the Gulf of Mexico. Analysis of individual monthly maps suggests a tendency for the stronger flux to pass on one side or the other of the plateau. Thus it may be that Columbia, Missouri on the north, and Little Rock, Arkansas on the south will show systematically higher values of flux than the area between. Excessive divergence will then result if the area between is analysed linearly.

In the case of the Appalachian Mountains, there is, in addition to

other possible smaller scale effects, an apparent decrease in the flux across the ridges which is not well defined by the data.

On the basis of the comparison of 12 non-consecutive months of wind and flux data from Tinker AFB, and Oklahoma City, it is suggested that local station pecularities may also be the source of some of the remaining error. The mean vector flux difference between these stations during the period analyzed was 192 gm $(\text{cm sec})^{-1}$, with Tinker consistently showing the stronger mean monthly flux. This difference was primarily the result of a systematic difference in the winds. Furthermore, the differences were by no means limited to the lower levels, but extended throughout at least the lower half of the troposphere. They were observed throughout the year (although most of the period investigated consisted of winter months), and were almost certainly not primarily the result of systematic diurnal variations.

The explanation for this systematic difference can only be guessed at . One possibility which suggests itself is improper calibration of the ground equipment. In any event, errors of this magnitude are again large enough to account for much of the observed error pattern.

In the light of the previous discussion, it is a fair question to ask how, with the apparent presence of a substantial amount of systematic error, it was possible to evaluate $\langle \nabla \cdot \bar{Q} \rangle$ rather accurately over the

larger areas studied. The reason apparently lies in the fact that the average flux divergence over an area is a function only of the flux on the boundary. Thus, a boundary error will tend to produce compensating divergence errors in the two regions sharing the common boundary. Consequently, there is a tendency for one to obtain satisfactory results if the area considered is large enough to include the larger scale adjacent regions of compensating error. Such compensation becomes less likely as the size of the area decreases, and the typical scale of the error pattern probably accounts for the particularly rapid deterioration in the results as the area is decreased to less than $10 - 15 \times 10^5$ $km^2$. However, it is apparent that even for rather large areas, the results will, to some extent, depend upon the area chosen. For example, one would not obtain satisfactory results if an area corresponding to the belt of divergence east of the Continental Divide were chosen for study. Until further investigation and added data lead to methods for correcting these errors, one can use these or similar divergence maps as a rough guide for choosing the size and shape of areas over which satisfactory results can be expected.

In the previous discussion, it was pointed out that the true divergence is apparently superimposed on a more or less systematic error field. If this error field were precisely the same from year to year, one

might be able to compute the year to year difference in the divergence with a greater accuracy than is possible for the annual divergence itself. Comparison of the annual results for the two years studied indicates that this may, to some extent, be the case. However, water balance computations for the Central Plains and Eastern Region (Fig. 91) indicated substantial year to year differences in the relationship of the mean monthly 00 and 12 GMT flux convergence, which in turn implies the probability of some differences in the error field as well. Further investigation is necessary in order to determine if useful computations of the year to year difference in $\langle \nabla \cdot \bar{Q} \rangle$ can be made over areas appreciably smaller than those for which reasonable annual values of $\langle \nabla \cdot \bar{Q} \rangle$ itself can be computed.

# XIII. CONCLUSIONS AND SUGGESTIONS FOR FURTHER RESEARCH

## A. Conclusions

### 1. Evaluation of the flux divergence

The results of this investigation establish the following facts concerning the accuracy of vapor flux divergence computations.

(a) The aerological data over North America are sufficiently dense and sufficiently accurate to be used to advantage in large scale regional water balance studies. When used on the proper time and space scale, vapor flux data provide estimates of $\langle \overline{E-P} \rangle$ not easily or accurately obtained from the more conventional methods of evaluating evaporation and precipitation.

(b) The minimum spatial scale on which the atmospheric water balance equation can be used to advantage over the North American sector is, at present, primarily determined by the systematic errors in the computed flux divergence. These errors are tentatively ascribed to: (1) errors produced by diurnal variations in the vapor flux, (2) difficulties in separating smaller scale features of the flux field from the broadscale pattern, and (3) local station pecularities.

(c) Results over North America indicate that when twice daily observations are used, and some judgement is exercised in the choice of the area to be studied, fairly accurate estimates of $\langle \overline{E-P} \rangle$ can

usually be obtained from the vapor balance relation, on a mean monthly basis, for areas of approximately 20 x $10^5$ $km^2$ or larger. In addition, much useful information can often be obtained for areas of 10 - 20 x $10^5$ $km^2$. As the areas decrease to less than 10 x $10^5$ $km^2$, results normally deteriorate rapidly.

Data surrounding the Gulf of Mexico and Caribbean Sea are apparently sufficient to obtain satisfactory mean seasonal, and possibly even mean monthly values of $\langle\overline{E-P}\rangle$ for these basins.

(d) The vertical distribution of flux divergence can be satisfactorily defined on at least as small a scale as the vertically integrated divergence. This is particularly true over the United States in summer, when the vertically integrated flux divergence results from the small difference between a strong convergence in the lower layers, and divergence above.

(e) These results could, of course, be improved by decreasing the sampling interval, in time and space. Over the Central American Sea, and north of 50°N, it is hard to say whether a greater improvement would be realized by shortening the sampling interval in time, or space. Over the United States, however, it is the view of the author that the greater overall improvement would be attained by shortening the sampling interval in time, even though a few additional stations at crucial locations

would certainly be highly desirable. In other words, the results over the United States would probably benefit more by having observations four times daily from the present station network, than by doubling the number of stations. The more frequent observations would allow a better evaluation of the diurnal flux variations, and, in addition, reduce the random sampling error, which becomes important for shorter time periods.

2. Vapor flux and flux divergence over the North American Sector

We shall not repeat the details of the results which were presented throughout this report; but will merely list a few general findings.

(a) The vapor flux and flux divergence exhibit diurnal variations which are particularly pronounced south of $50^{o}$N during the summer. Of particular interest is the well organized pattern of diurnal change over eastern North America and the Central American Sea.

The more significant variations are usually the result of diurnal variations in the wind, rather than in the specific humidity.

(b) Large scale, well orgainized interannual changes in the vapor flux, of appreciable magnitude, were observed over much of the area during the two year period studied. However, when viewed in relation to the large scale flux field, these were usually changes in detail only. Consequently, Figs. 106 and 107 are believed to exhibit the main features

of the mean annual flux field fairly accurately.

(c) During July, the atmosphere over the United States showed pronounced vapor flux convergence in the lower 100 mb, and flux divergence above. Flux convergence was observed at all levels in January. As a general rule, corresponding features of the profiles were found at higher elevations over the western half of the United States. Furthermore, the contribution to the total integrated flux divergence from the layers above 500 mb was quite significant over the west, the apparent result of the higher terrain of that region.

3. The water balance of North America and the Central American Sea

The more general results of the water balance computations of Chapters IX and X are listed below.

(a) Over the Gulf of Mexico and Caribbean Sea, the mean annual and seasonal values of $\langle\overline{E-P}\rangle$ computed from the water balance equation were in excellent agreement with independent estimates. Furthermore, use of computed mean monthly values of $\langle\overline{E-P}\rangle$ and estimates of evaporation led to mean monthly values of precipitation, and seasonal variations in precipitation, which appear, for the most part, to be reasonable.

(b) For North America, north of the United States-Mexican border, latitudinally averaged values of divergence showed a minimum between

55°N and 65°N. The total area acted as a sink of water vapor, with mean monthly convergence during 23 of the 24 months studied.

(c) For the United States and southern Canada, evaporation exceeded precipitation only during the three summer months. Little net surface and subsurface storage change was computed during the two year period for the area as a whole. However, systematic seasonal storage changes were computed. The average decrease in storage from spring to fall was around 8 cm.

Estimates of mean evaporation for the area indicated a maximum of around 8 cm in June, and a minimum of 1-2 cm during winter.

(d) Although little net storage change was computed for the area as a whole, appreciable increases were computed for the Western Region during the first year, and large decreases were computed for the Eastern Region, particularly during the second year. These changes appear to agree qualitatively with independent data.

Although further investigation is necessary in order to evaluate possible systematic errors in these computations, the results strongly indicate that the imbalance between the computed atmospheric vapor influx, and the measured streamflow, can be evaluated accurately enough to detect significant interannual and seasonal storage changes over the larger regions investigated.

B. Suggestions for further research

The author feels that the results of this study, insofar as they have established somewhat more clearly the practical limitations, and the advantages in the use of vapor flux data, can serve as a guide in determining the most productive approach to future research along these lines.

Much of this investigation can be considered in the realm of pilot studies, undertaken partially for the purpose of determining the quality of results which could be obtained. Those studies which were shown to be feasible should now be extended, and further feasibility studies suggested by this investigation should be performed. The following are the authors specific suggestions.

1. Continue the studies begun in this investigation by the analysis of a longer period of data. Since, over a long enough period, surface and subsurface storage changes can be ignored, this will provide a basis for a more accurate determination of the magnitude and distribution of the systematic errors which are now present in the flux divergence computations.

A longer period of data would also provide a more stable climatology of atmospheric humidity statistics, which would certainly be of value. Furthermore, it would provide a clearer picture of the patterns

of year to year and seasonal variations, and the relationship of these changes to changes in other circulation statistics.

2. Investigate more extensively the errors which now limit the usefulness of the vapor balance equation. It would perhaps be most productive to first investigate more thoroughly the characteristics of the diurnal wind and flux variations during the summer months. All available wind and humidity data should be used, including a careful use of pibal data. Since interest in diurnal wind variation extends beyond the area of humidity studies, it might be worth considering the possibility of initiating a program of four daily observations for part of the existing North American rawinsonde network for a limited period, perhaps for three summer months. This would provide the data from which to make a more definitive study of these phenomena.

3. Investigate more thoroughly the three dimensional structure of the flux and flux divergence.

4. Carry out more detailed regional water balance studies. Such studies should, at present, be limited to regions large enough to provide reliable results.

5. It would be of value to study periods shorter than one month; perhaps even as short as a single day. One might then be able to better estimate the standard error in mean monthly computations on various

scales.

It is probable that much can be learned by choosing homogeneous periods for study: for example, dry periods following a period of heavy precipitation, and periods of heavy precipitation.

6. Atmospheric humidity studies which must rely on hand analyses are seriously limited by the great amount of time required for plotting, analyzing, and grid point reading. The use of objective analysis techniques for the determination of the flux divergence should therefore be investigated. This problem is now being investigated by personnel of Travelers Research Center. Preliminary results appear promising, particularly when applied over areas the size of the United States.

ACKNOWLEDGEMENTS

The author is deeply indebted to Professor Victor P. Starr for his suggestion of the problem, and for his constant interest, guidance, and encouragement during the course of the investigation.

The helpful suggestions of Dr. Jose Peixoto and Dr. Paul Bock during the initial stages of the investigation were very much appreciated.

The massive amount of data processing required for this investigation was accomplished through the efforts of a number of people: Mr. Howard Frazier and Mr. Raymond Ellis of Travelers Research Center, Mr. Salmon P. Seroussi of Mitre Corp, and Mrs. Judy Copeland and Miss Judy Roxborough of M. I. T. Calculations were performed at the Geophysical Fluid Dynamics Laboratory, Mitre Corp. and the M. I. T. Computation Center.

Mr. William Schallert of the Environmental Data Service, ESSA, is to be thanked for providing a certain amount of additional flux data.

Credit for the cross sections in Figs. 27 through 38 goes to Maj. Merwin Richards, Capt. David Feruzza, and Mr. Throop Berg, and the author is grateful for their use.

Miss Isabelle Kole drafted the figures and Miss Ruth Benjamin typed the manuscript. Additional help was received from Mrs. Barbara Goodwin, Mrs. Nita Waters, Miss Mary Bagarella, and Mrs. Susan Nemeti. For this the author is very grateful.

The author's wife, Georgene, was a source of encouragement and constant help during this effort, particularly in the tedious job of reading and recording the tens of thousands of grid point values.

The author wishes to express his appreciation to the Environmental Science Services Administration, and particularly to Dr. Joseph Smagorinsky for the opportunity to perform this investigation.

The research was made possible through the support of the National Science Foundation under grant numbers GP-820 and GP-3657. Thanks are also due to the Environmental Science Services Administration, the U.S. Air Force and Mitre Corp. for additional assistance.

# BIBLIOGRAPHY

Ackermann, William C., 1965: Committee on status and needs in hydrology: a look at data and instrumentation. Trans. AGU, 46, 700-715.

Atlas, David, 1965: Model atmospheres for precipitation. Handbook of Geophysics and Space Environments (Shea L. Valley, Ed.). Chapt. 5, 6-11. AFCRL, Bedford, Mass.

aufm Kampe, H. J., and H. K. Weickmann, 1957: Physics of clouds. Meteor. Monographs, Vol. 3, 183-225, Am. Meteor. Soc., Boston, Mass.

Baujitti, K., and A. K. Blackadar, 1957: Theoretical studies of diurnal wind-structure variations in the planetary boundary layer. Quart. J. R. Meteor. Soc., 83, 486-500.

Benton, G. S., 1960: Quantitative relationships between atmospheric vapor flux and precipitation. Int. Assn. Sci. Hydrology, Pub. No. 51, 60-70.

Benton, G. S., R. T. Blackburn, and V. O. Snead, 1950: The role of the atmosphere in the hydrologic cycle. Trans. AGU, 31, 61-73.

Benton, G. S., M. A. Estoque, and J. Dominitz, 1953: An evaluation of the water vapor balance of the North American continent. Sci. Rept. No. 1, Contract No. AF19-122-365, Johns Hopkins University. Baltimore, Md.

Benton G. S., and M. A. Estoque, 1954: Water vapor transfer over the North American continent. J. Meteor., 11, 462-477.

Blackadar, A. K., 1957: Boundary layer wind maxima and their significance for the growth of nocturnal inversions. Bull. AMS., 38, 283-290.

Bleeker, W., and M. J. Andre, 1951: On the diurnal variation of precipitation, particularly over the Central USA. Quart. J. R. Meteor. Soc., 77, 260-271.

Budyko, M.I., 1956: The heat balance of the earth's surface. Gidrometeorologicheskoe izdatel'stvo, Leningrad, 255 pp. (Translated by Nina A. Stepanova; translation distributed by USWB, Washington, D.C., 1958).

Budyko, M.I., 1963: Atlas teplovogo balansa Zemnogo Shara. USSR Glavnaia geofizicheskaia observatoriia. 69 pp. (Text translated by Irene A. Donchoo as Guide to the Atlas of the heat balance of the earth; distributed by USWB, Washington, D.C.).

Byers, H.R., 1943: Characteristic weather phenomena of California. MIT Meteor. Papers, Vol. I., No. 2, 54 pp.

Chow, Ven Te, 1964: Hydrology and its development. Handbook of Appl. Hydrology, Sec. I, McGraw-Hill Inc., New York, N.Y.

Colón, J., 1960: On the heat balance of the troposphere and water body of the Caribbean Sea. National Hurricane Res. Proj., Rept. No. 41, U.S. Dept. of Commerce, USWB, Washington, D.C., 65 pp.

Colón, J., 1963: Seasonal variations of heat flux from the sea surface to the atmosphere over the Caribbean Sea. J. Geophys. Res., 68, 1421-1430.

Curtis, R.C., and H.A. Panofsky, 1958: The relation between large-scale vertical motion and weather in summer. Bull. AMS, 39, 521-531.

Defant, Friedrich, 1951: Local winds. Compendium of Meteorology, Am. Meteor. Soc., Boston, 655-672.

Department of Transport, Meteorological Branch: Monthly Record, Meteorological observations in Canada, May 1961-April 1963.

Donn, William L., J. Pattullo, and D.M. Shaw, 1964: Sea level fluctuations and long waves. Research in Geophysics, Vol. II, 243-269, MIT Press, Cambridge, Mass

Department of Northern Affairs and National Resources, (Ottawa, Canada): Water resources paper, Surface Water data 1961-1963.

Fujita, T., K. A. Styber, and R. A. Brown, 1962: On the mesometeorological field studies near Flagstaff, Arizona. J. Appl. Meteor., 1, 26-42.

Gardner, W. R., et al, 1965: Water transfer from soil to the atmosphere as related to soil properties, plant characteristics, and weather. Annual Report, U. S. Salinity Lab., U. S. Dept. of Agriculture, Riverside, Calif.

Gardner, W. R., 1965: Rainfall, runoff and return. Meteor. Monographs, Vol. 6, No. 28, 138-147. Am. Meteor. Soc., Boston, Mass.

Gerhardt, J. R., 1962: An example of a nocturnal low-level jet stream. J. Atmos. Sci., 19, 116-118.

Gilman, Charles S., 1964: Rainfall. Handbook of Appl. Hydrology, Sec. 9, McGraw-Hill Inc., New York, N. Y.

Harris, Miles F., 1959: Diurnal and semidiurnal variations of wind, pressure and temperature in the troposphere at Washington, D. C. J. Geophys. Res., 64, 983-995.

Harris, Miles F., F. G. Finger, and S. Teweles, 1962: Diurnal variation of wind, pressure, and temperature in the troposphere and stratosphere over the Azores. J. Atmos. Sci., 19, 136-149.

Hering, W. S. and T. R. Borden, Jr., 1962: Diurnal variations in the summer wind field over the central U. S. J. Atmos. Sci., 19, 81-86.

Hodge, M. W., and C. Harmantas, 1965: Compatibility of U. S. radiosondes. Mon. Wea. Rev., 93, 253-266.

Hoecker, Walter H. Jr., 1963: Three southerly low-level jet systems delineated by the Weather Bureau special pibal network of 1961. Mon. Wea. Rev., 91, 573-582.

Hoecker, Walter H. Jr., 1965: Comparative physical behavior of southerly boundary-layer wind jets. Mon. Wea. Rev., 93, 133-144.

Holzman, B., 1937: Sources for moisture for precipitation in the United States. Tech. Bull., 589, Dept. of Agriculture, Washington, D. C.

Hutchings, J. W., 1957: Water vapor flux and flux divergence over southern England: summer 1954. Quart. J. R. Meteor. Soc., 84, 30-48.

Hutchings, J. W., 1961: Water-vapor transfer over the Australian Continent. J. Meteor., 18, 615-634.

Izumi, Y., and Morton L. Barad, 1963: Wind and temperature variations during development of a low-level jet. J. Appl. Meteor., 2, 668-673.

Izumi, Y., 1964: The evaluation of temperature and velocity profiles during the breakdown of a nocturnal inversion and a low level jet. J. Appl. Meteor., 3, 70-82.

Kaimal, J. C. and Y. Izumi, 1965: Vertical velocity fluctuations in a nocturnal low-level jet. J. Appl. Meteor., 4, 576-584.

Kohler, M. A., T. J. Nordensen, and W. E. Fox, 1955: Evaporation from pans and lakes. Res. Paper No. 38, 21 pp. USWB, Washington, D. C.

Kohler, M. A., T. J. Nordensen and D. R. Baker, 1959: Evaporation maps for the United States. Tech. Paper No. 37, 13 pp. USWB, Washington, D. C.

Kohler, M. A., and M. M. Richards, 1962: Multicapacity basin accounting for predicting runoff from storm precipitation. J. Geophys. Res., 67, 5187-5197.

Langbein, W. B., 1949: Annual runoff in the United States. Circular No. 44, U. S. Geological Survey, Washington, D. C.

LaRue, J. A. and R. J. Younkin, 1963: Large-scale precipitation volumes, gradients, and distribution. Mon. Wea. Rev., 91, 393-401.

Linsley, Ray K. Jr., Max. A. Kohler, and Joseph L. H. Paulhus, 1949: Applied Hydrology, 1st Ed. McGraw-Hill Inc., New York, N. Y. 689 pp.

Lufkin, D. H., 1959: Atmospheric water vapor divergence and the water balance at the earth's surface. Sci. Rept. No. 4, General Circulations Project, MIT, 44 pp.

Malkus, Joanne S., 1962: Large Scale Interactions, The Sea, Vol. 1, 88-285. Interscience Publishers, New York, N. Y.

Mather, John R., 1961: The climatic water balance. Pubs. in Climatology, 14, 251-264. Laboratory for Climatology, Centerton, N. J.

Maxey, George B., 1964: Hydrogeology. Handbook of Applied Hydrology, Sec. 4-I, (Ven Te Chow, Ed). McGraw-Hill Inc., New York, N. Y.

McGuinnes, C. L., 1964: Generalized map showing annual runoff and productive aquifers in the conterminous United States. Hydrologic Investigations Atlas HA-194, U. S. Geological Survey, Washington, D. C.

Miller, David W., James J. Geraghty, and Robert S. Collins, 1963: Water atlas of the United States. Water Information Center Inc., Port Washington, N. Y.

Palmén, E., 1963: Computation of the evaporation over the Baltic Sea from the flux of water vapor in the atmosphere. Int. Assn. Sci. Hydrology, Pub. No. 62, 244-252.

Palmer, Wayne C., 1965: Meteorological drought. Res. Paper No. 45, 58 pp. USWB, Washington, D. C.

Peixoto, J. P., 1959: O campo da divergencia do transporte do vapor de aquo na atmosfera. Separata da revista da faculdade de crencias de Lisboa, Serie B, 7, 25-56.

Peixoto, J. P., 1958: Hemispheric humidity conditions during the year 1950. Sci. Rept. No. 3, General Circulations Project, MIT, 142 pp.

Peixoto, J. P., and G. O. P. Obasi, 1965: Humidity Conditions over Africa during the IGY. Sci. Rept. No. 7, Planetary Circulations Project, MIT, Cambridge, Mass.

Portig, W. H., 1966: Rainfall frequencies from ship observations for the area $0^{o}$-$30^{o}$N, $50^{o}$-$100^{o}$W. Paper presented at the 4th Technical Conference on Hurricanes and Tropical Meteorology, Am. Meteor. Soc.

Riehl, H., 1954: Tropical Meteorology, 99-119. McGraw-Hill Inc., New York, N. Y.

Sellers, William D., 1965: Physical Climatology, 100-127. University of Chicago Press, Chicago, Ill.

Starr, V. P. and R. M. White, 1955: Direct measurement of the hemispheric poleward flux of water vapor. J. Mar. Res., 14, 217-225.

Starr, V. P., J. P. Peixoto, and G. Livadas, 1958: On the meridional flux of water vapor in the northern hemisphere. Geof. Pura e Appl., 39, 174-185.

Starr, V. P. and J. P. Peixoto, 1958: On the global balance of water vapor and the hydrology of deserts. Tellus, 10, 189-194.

Starr, V. P. and J. P. Peixoto, 1960: On the zonal flux of water vapor in the northern hemisphere. Geof. Pura e Appl., 47, 199-203.

Starr, V. P. and J. P. Peixoto, 1964: The hemispheric eddy flux of water vapor and its implications for the mechanics of the general circulation. Arch. Meteor. Geoph. Biokl. A., Bd. 14, H. 2, 111-130.

Sverdrup, H. V., M. W. Johnson, and R. H. Fleming, 1942: The Oceans. New York, Prentice Hall, Inc., 1087 pp.

Thornthwaite, C. W., 1948: An approach toward a rational classification of climate. Geogr. Rev., 38, 55-94.

Thornthwaite, C. W. and F. Kenneth Hare, 1965: The loss of water to the air. Meteor. Monographs, Vol. 6, No. 28, 163-180. Am. Meteor. Soc., Boston, Mass.

Thornthwaite, C. W. and J. R. Mather, 1955: The water balance. Publ. in Climatology. Drexel Inst. of Tech. Lab. of Climatology, 8, 1-86.

U. S. Dept. of Commerce - Weather Bureau: Climatological Data- National Summary, April 1961-May 1963.

U. S. Dept. of Commerce - Weather Bureau: Climatological Data- State Annual Summaries, 1961-1963.

U.S. Geological Survey: Surface Water Records 1961-1963.

Van Hylckama, T.E.A., 1956: The water balance of the earth. Publ. in Climatology. Drexel Inst. of Tech. Lab. of Climatology, 9, 57-105.

Weiss, L.L., and W.T. Wilson, 1958: Precipitation gage shields. Transactions, Int. Assn. Sci. Hydrology, Toronto, 1957, Vol. 1, 462-484.

Wexler, H., 1961: A boundary layer interpretation of the low level jet. Tellus, 13, 368-378.

White, R.M., 1951: The meridional eddy flux of energy. Quart. J.R. Meteor. Soc., 77, 188-199.

Wisler, C.O. and E.F. Brater, 1959: Hydrology, 2nd Ed., 408 pp. J. Wiley, New York, N.Y.

Wüst, George, 1964: Stratification and circulation in the Antillean-Caribbean Basins. Columbia University Press, New York, N.Y. 201 pp.

## BIOGRAPHICAL NOTE

Eugene Martin Rasmusson was born at Lindsborg, Kansas on February 27, 1929, and attended the public schools of McPherson County, Kansas. He received a Bachelors Degree in Civil Engineering from Kansas State University in 1950.

Following a brief period of employment with the Kansas State Highway Commission, the author entered the Air Force. During his four year period of service he completed the basic meteorology course for Air Force officers at the University of Washington.

Upon release from the service in 1955, the author accepted a position with the U. S. Weather Bureau as a meteorologist and hydrologist in St. Louis, Missouri. Part-time academic work at St. Louis University during the next several years led to a Masters Degree in Engineering Mechanics in June, 1963.

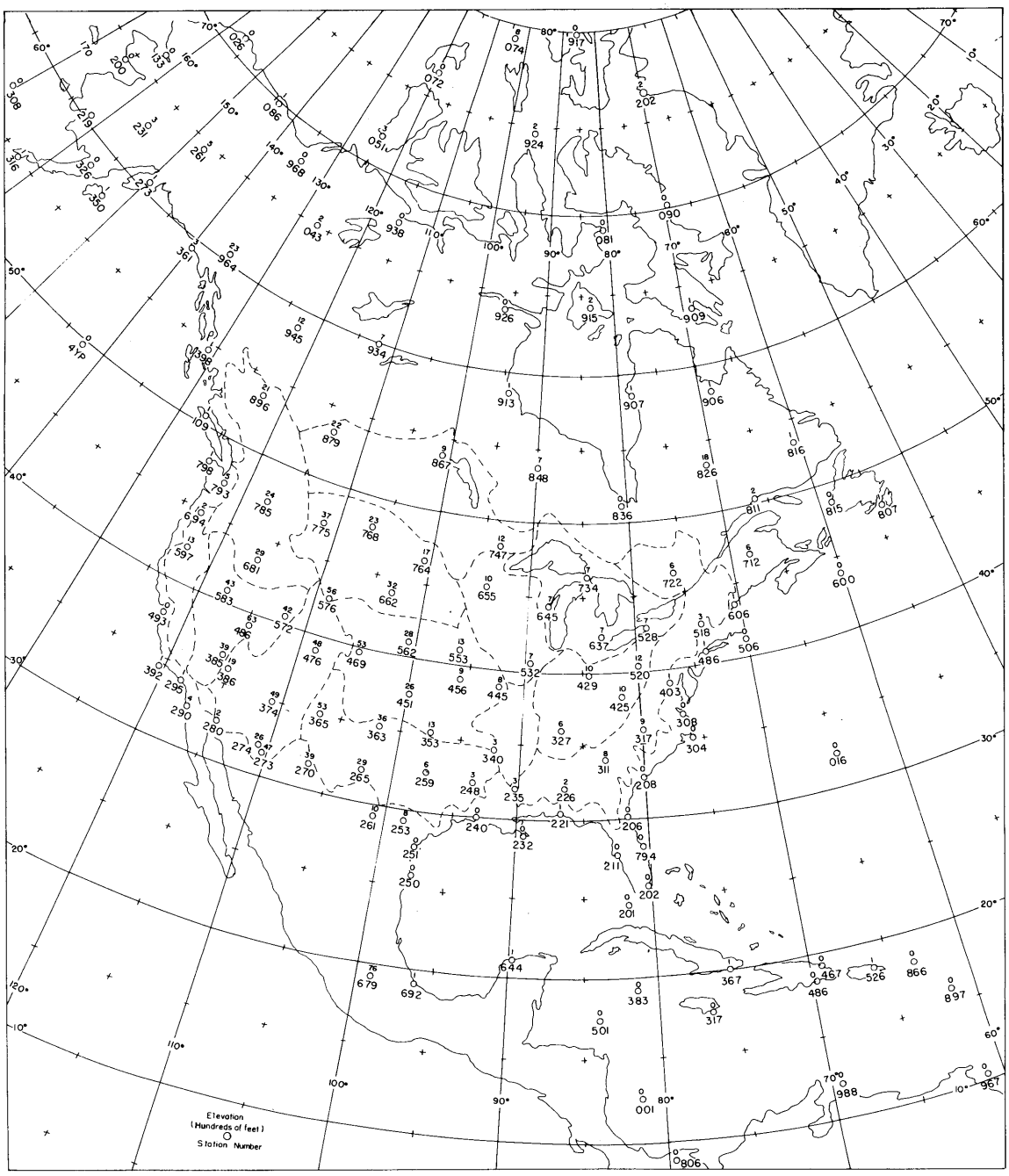


Figure 1. Distribution of aerological stations used in the investigation.

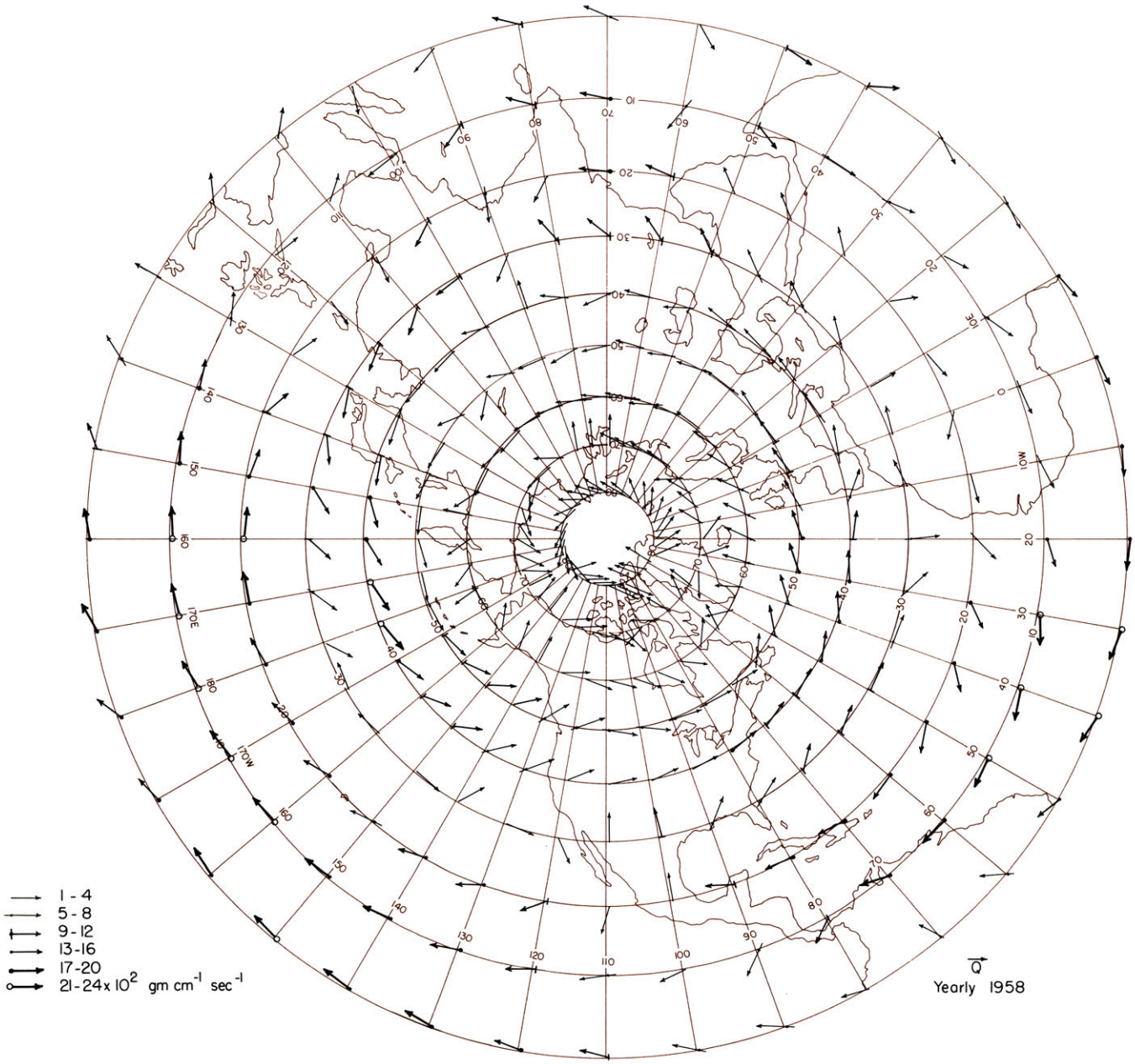


Figure 2. Vertically integrated mean total water vapor flux vector field, $\overrightarrow{Q}$ , 1958. (From Peixoto and Crisi, 1965).

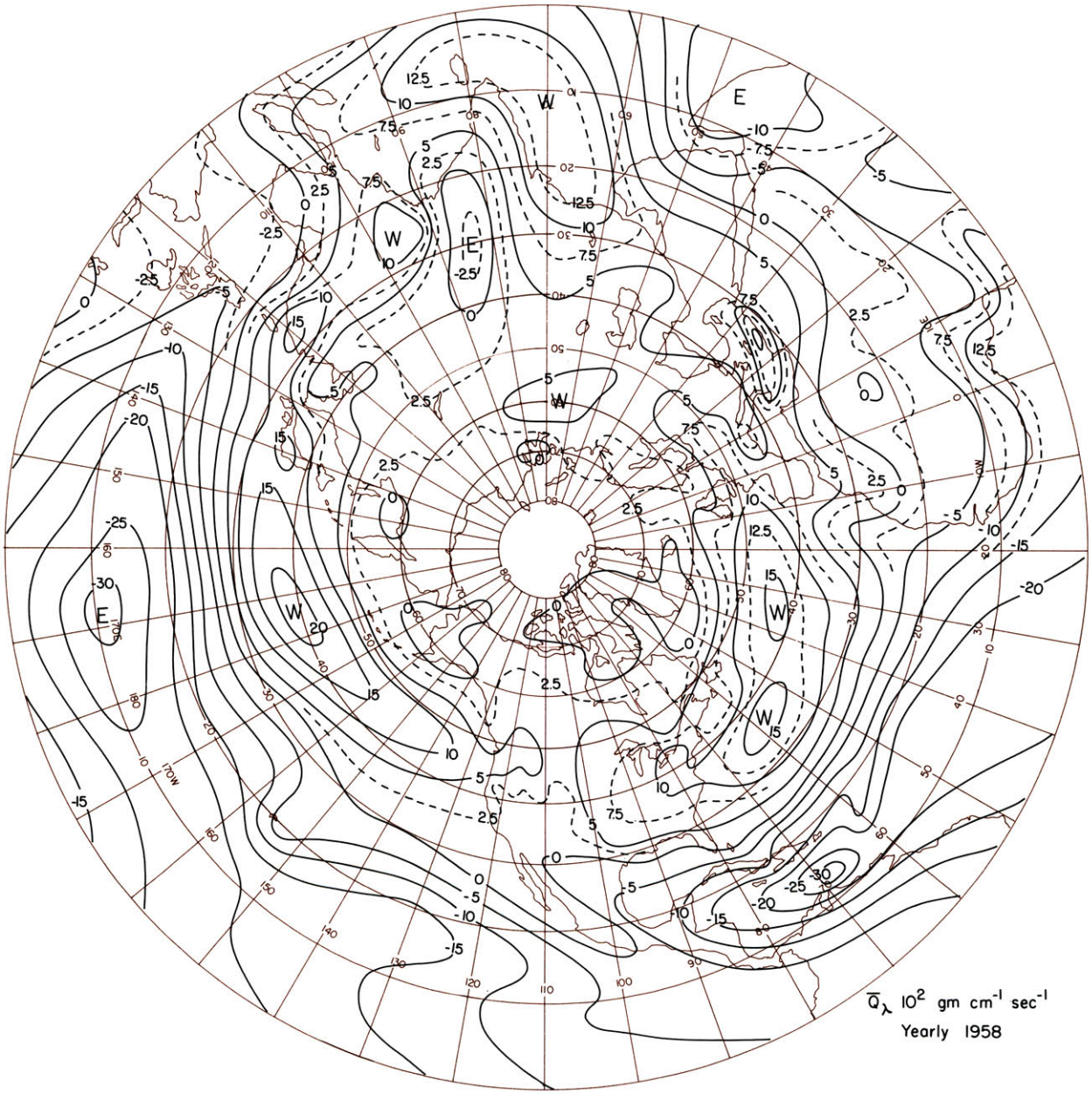


Figure 3. Vertically integrated mean total zonal water vapor flux, $\overline{Q}_\lambda$, 1958. Units: $10^2$ gm (cm sec)$^{-1}$. (From Peixoto and Crisi, 1965).

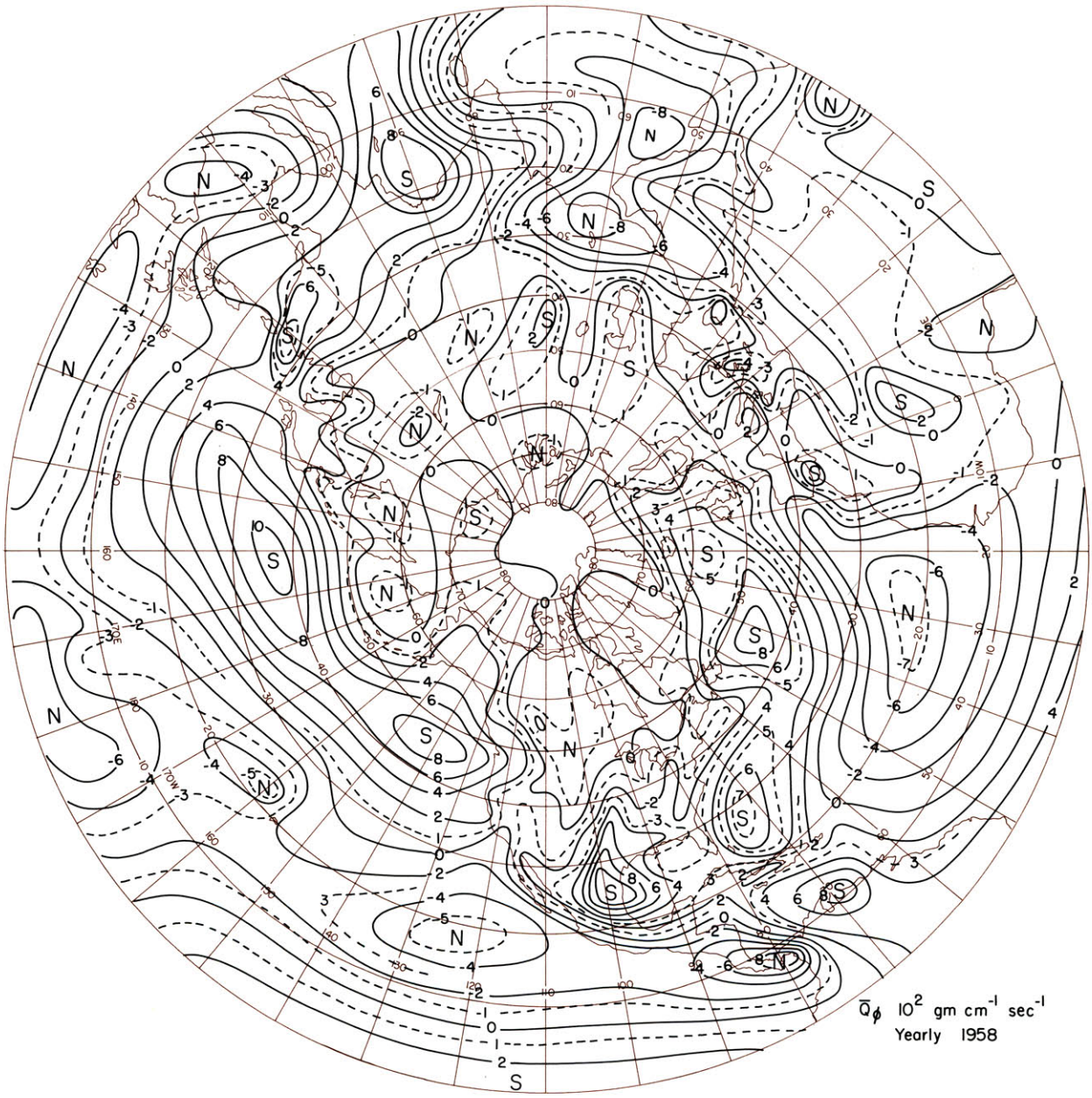


Figure 4. Vertically integrated mean total meridional water vapor flux, $\overline{Q}_\phi$, 1958. Units: $10^2$ gm (cm sec)$^{-1}$. (From Peixoto and Crisi, 1965).

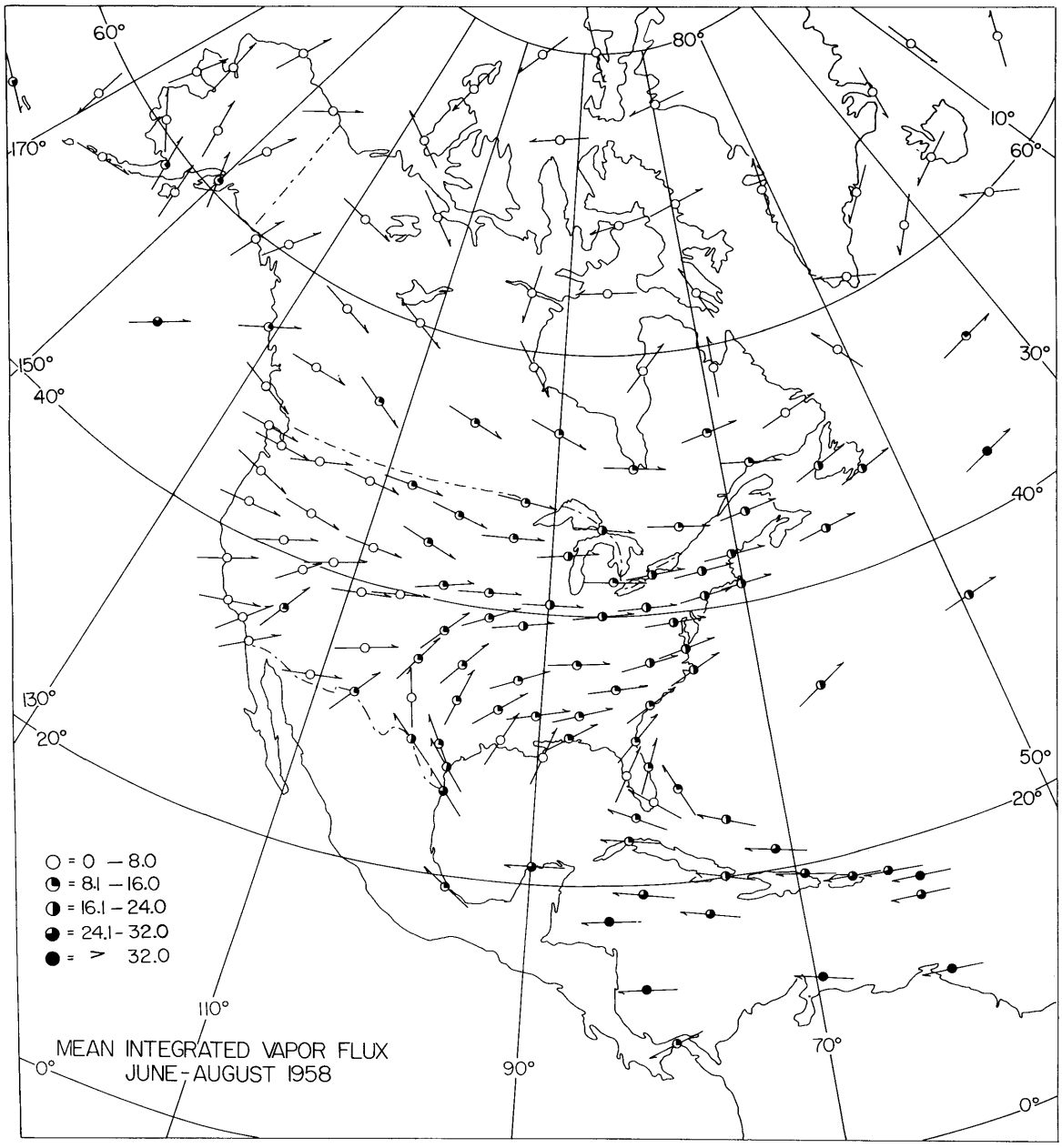


Figure 5. Vertically integrated mean total water vapor flux vector field, $\overline{\mathbf{Q}}$, 00 GMT, June-August, 1958. Units: $10^2$ gm (cm sec)$^{-1}$.

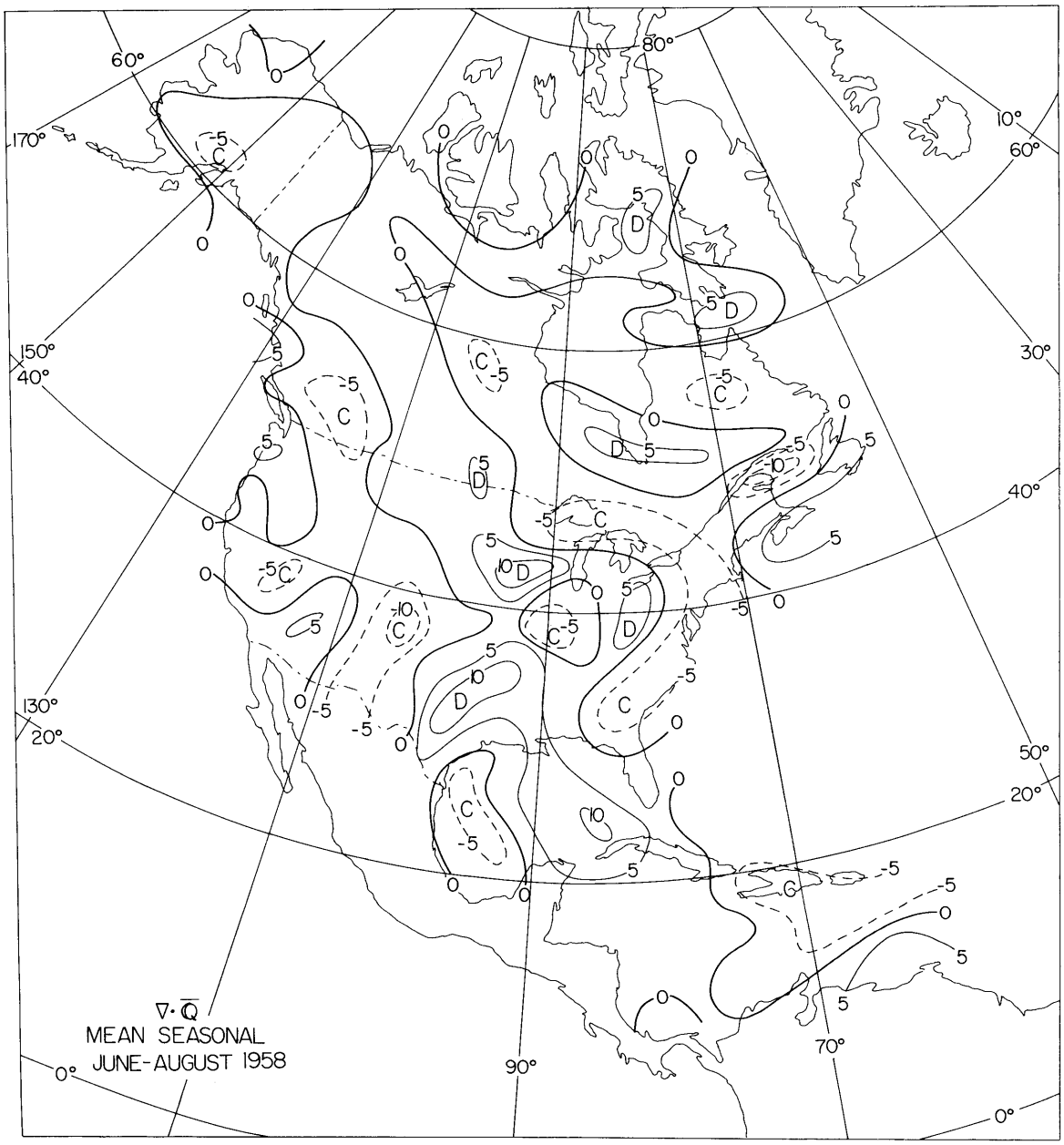


Figure 6. Divergence of the vertically integrated mean total water vapor flux, $\nabla \cdot \overline{Q}$, 00 GMT, June-August, 1958; computed from mean seasonal flux maps. Units: gm ( 3 months)$^{-1}$.

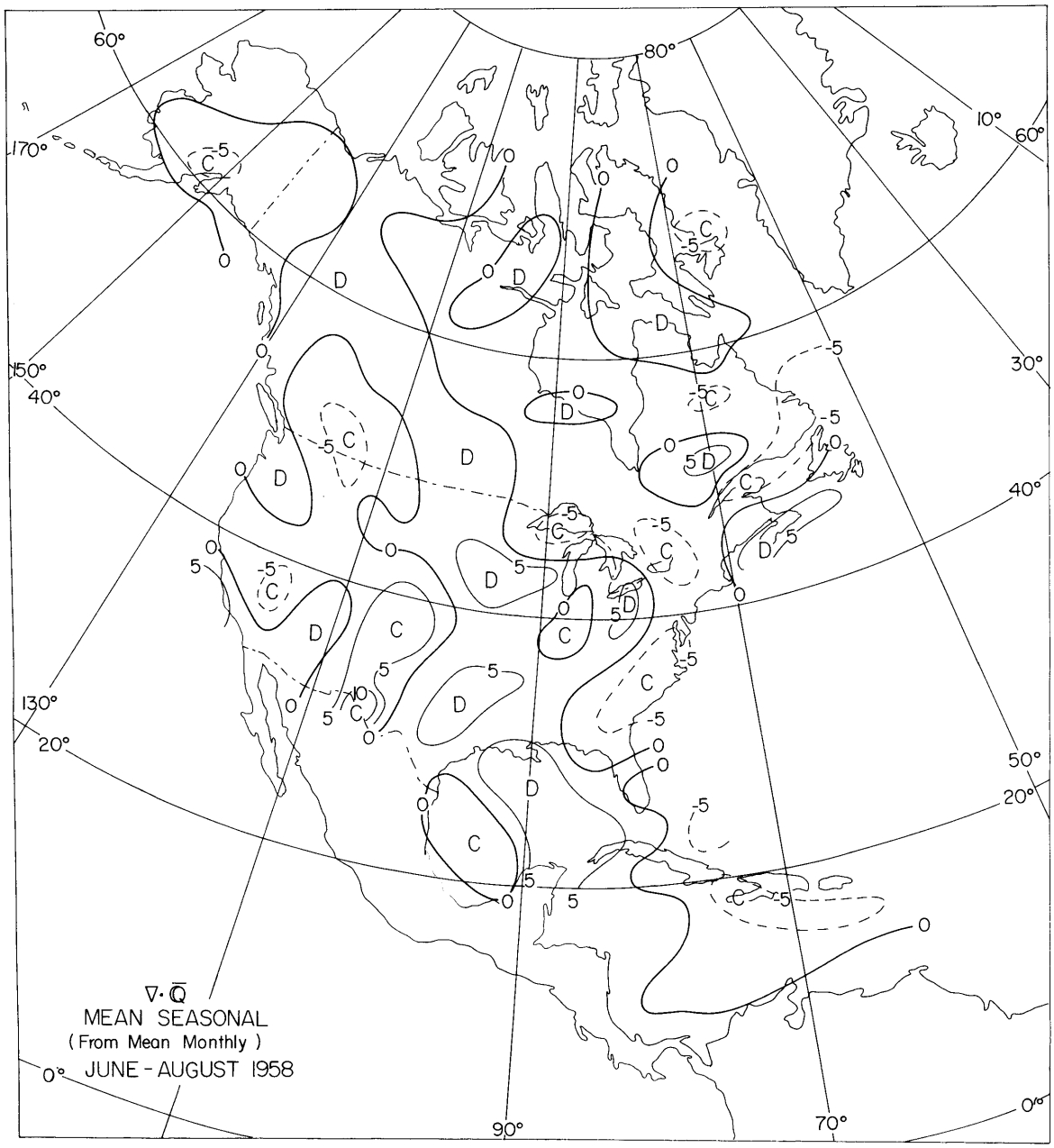


Figure 7. Divergence of the vertically integrated mean total water vapor flux, $\nabla \cdot \bar{Q}$ , 00 GMT, June-August, 1958, obtained by averaging mean monthly values.
Units: gm (3 months)$^{-1}$

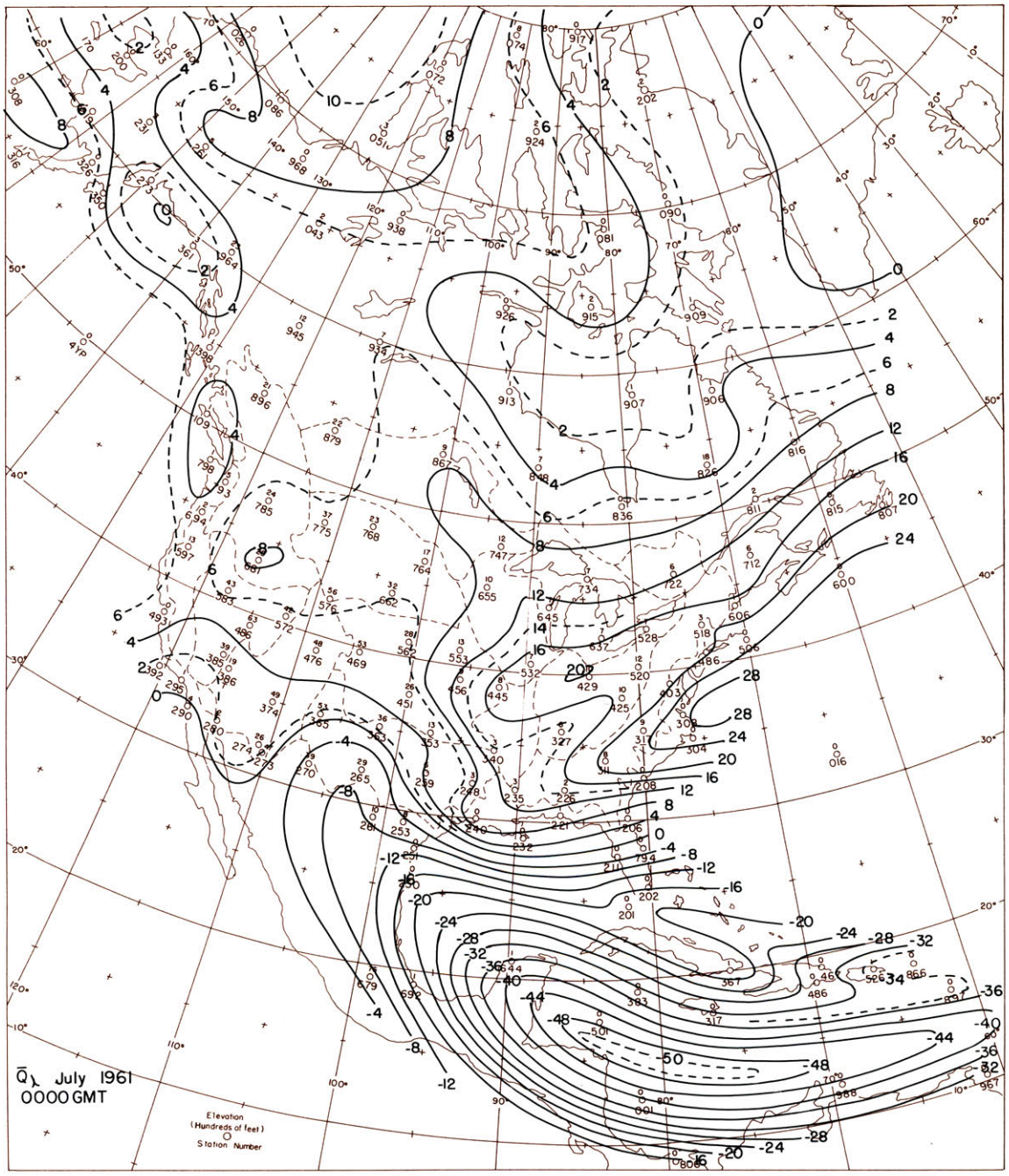


Figure 8. Vertically integrated mean total zonal water vapor flux, $\overline{Q_\lambda}$, 00 GMT; July, 1961. Units: $10^2$ gm (cm sec)$^{-1}$.

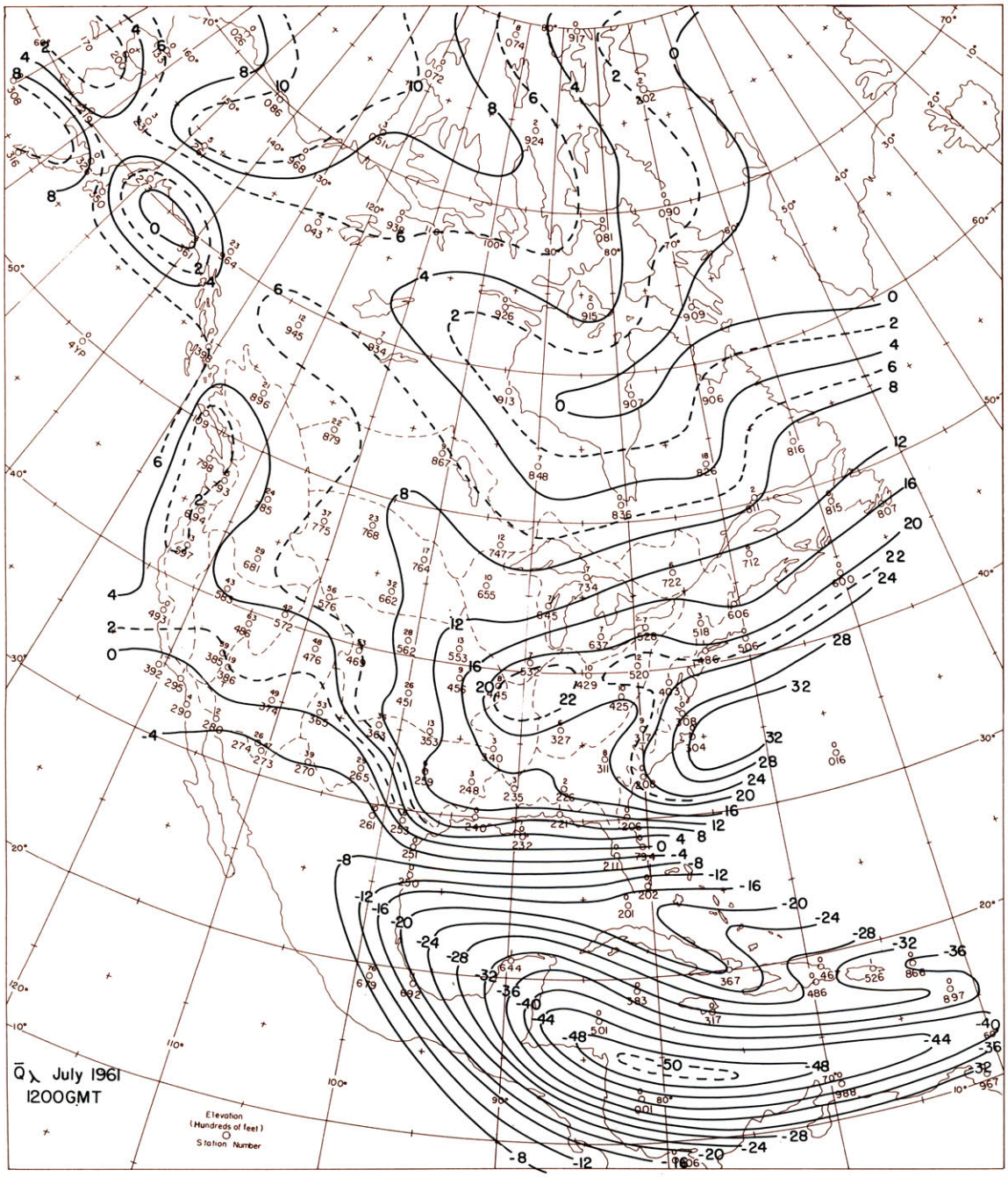


Figure 9. Vertically integrated mean total zonal water vapor flux, $\overline{Q}_\lambda$ , 12 GMT; July, 1961. Units: $10^2$ gm (cm sec)$^{-1}$.

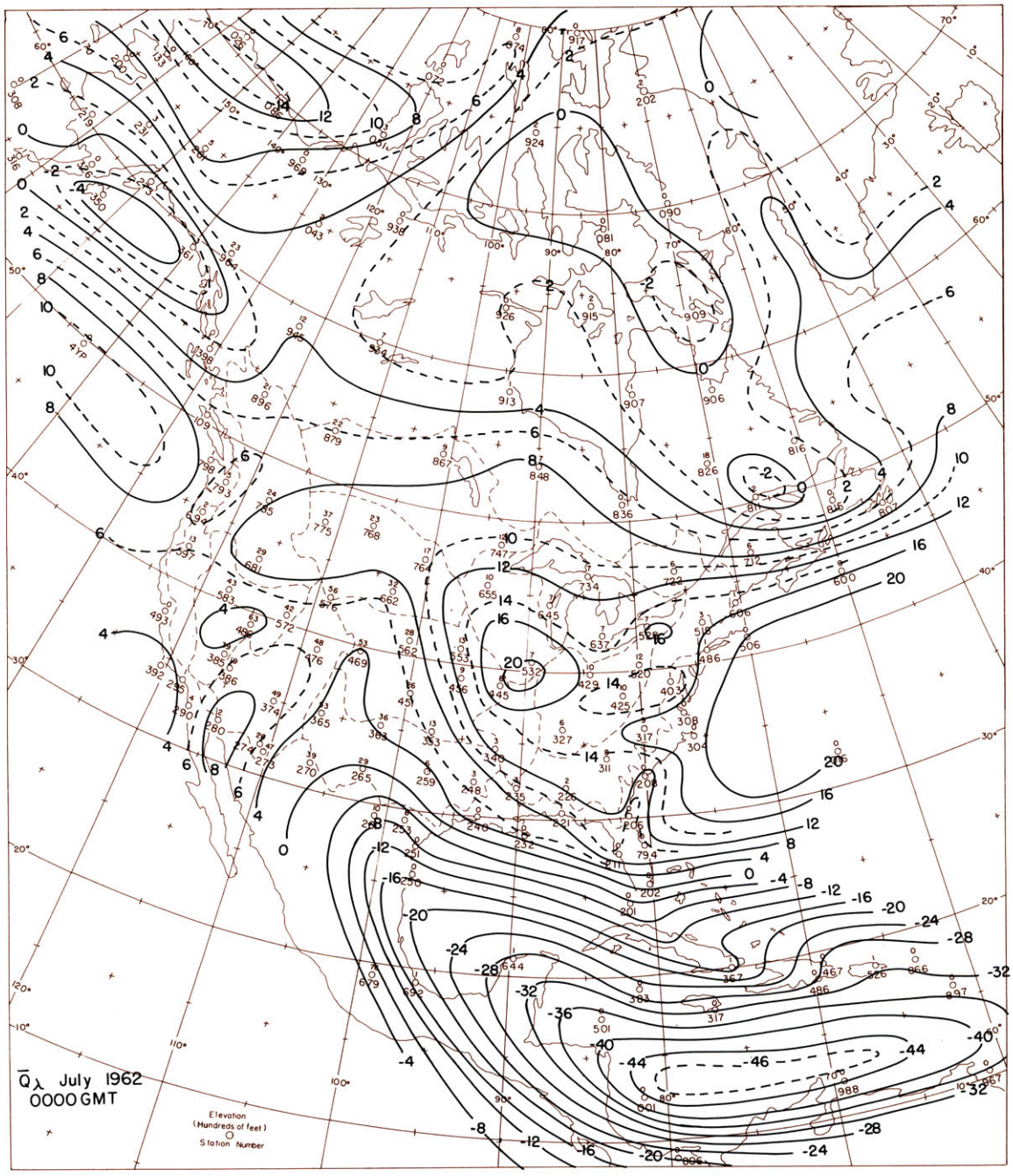


Figure 10. Vertically integrated mean total zonal water vapor flux, $\bar{Q}_\lambda$, 00 GMT; July, 1962. Units: $10^2$ gm (cm sec)$^{-1}$.

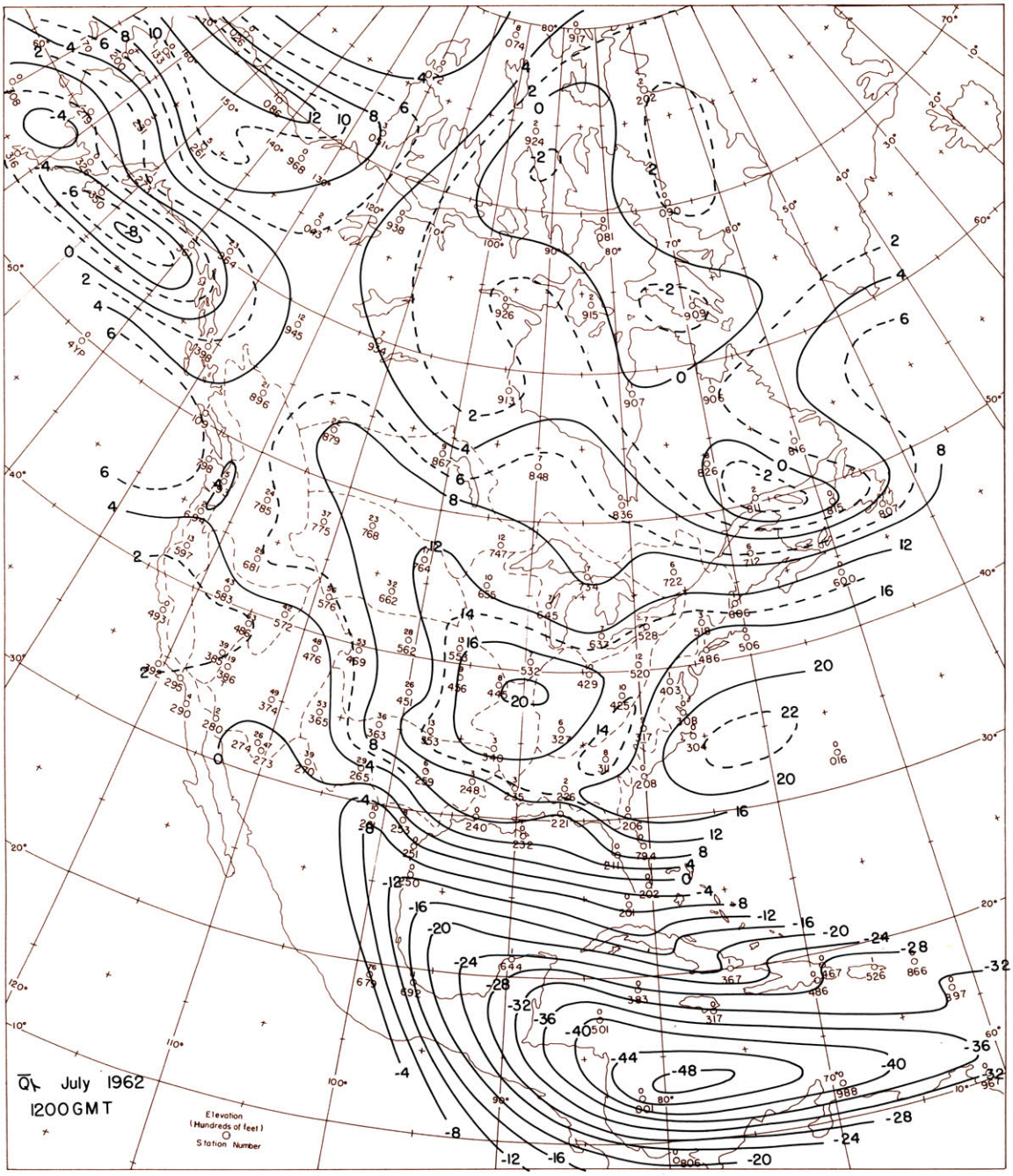


Figure 11. Vertically integrated mean total zonal water vapor flux, $\overline{Q}_\lambda$, 12 GMT; July 1962. Units: $10^2$ gm (cm sec)$^{-1}$.

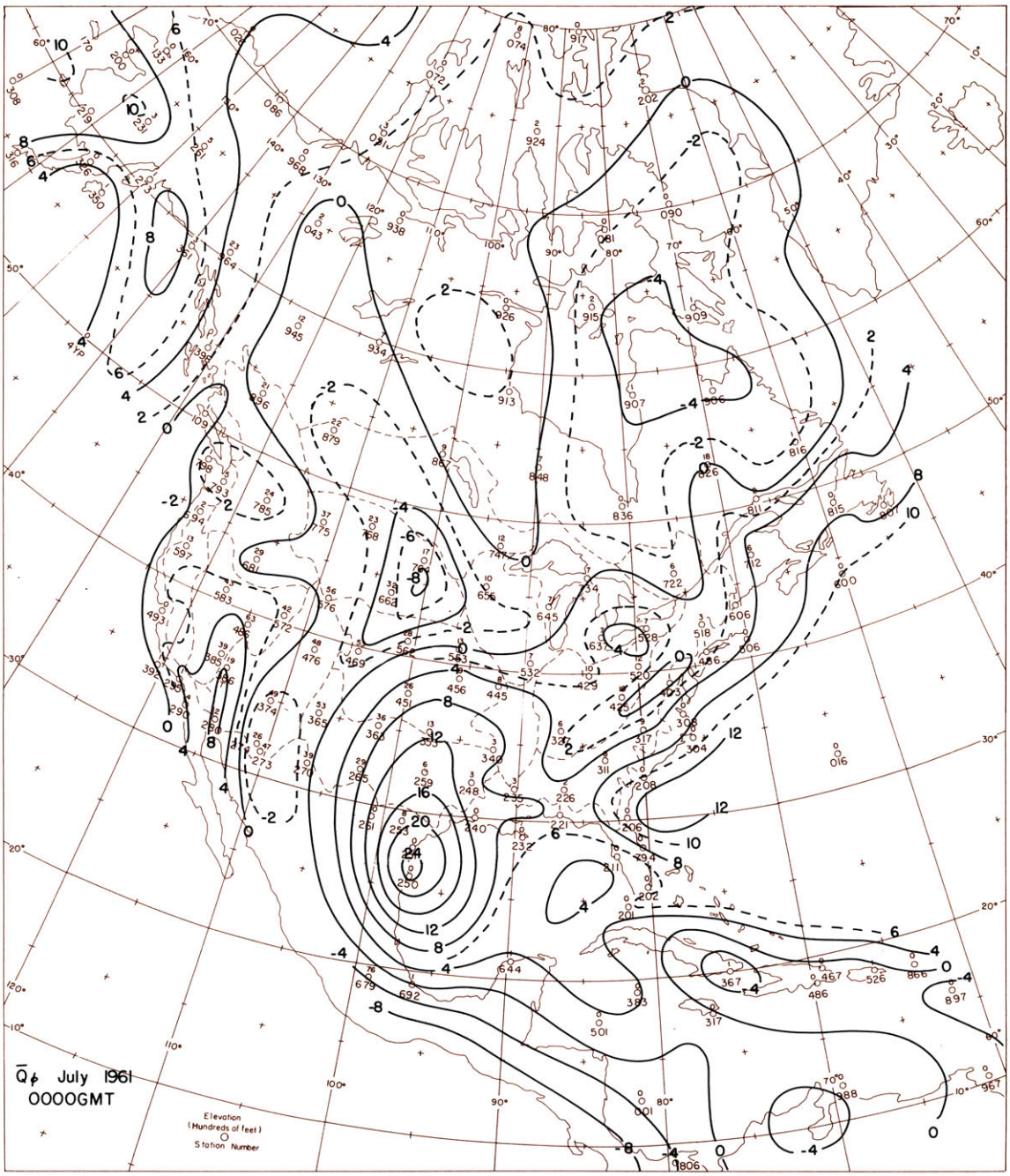


Figure 12. Vertically integrated mean total meridional water vapor flux, $\bar{Q}_\phi$ , 00 GMT; July, 1961. Units: $10^2$ gm (cm sec)$^{-1}$.

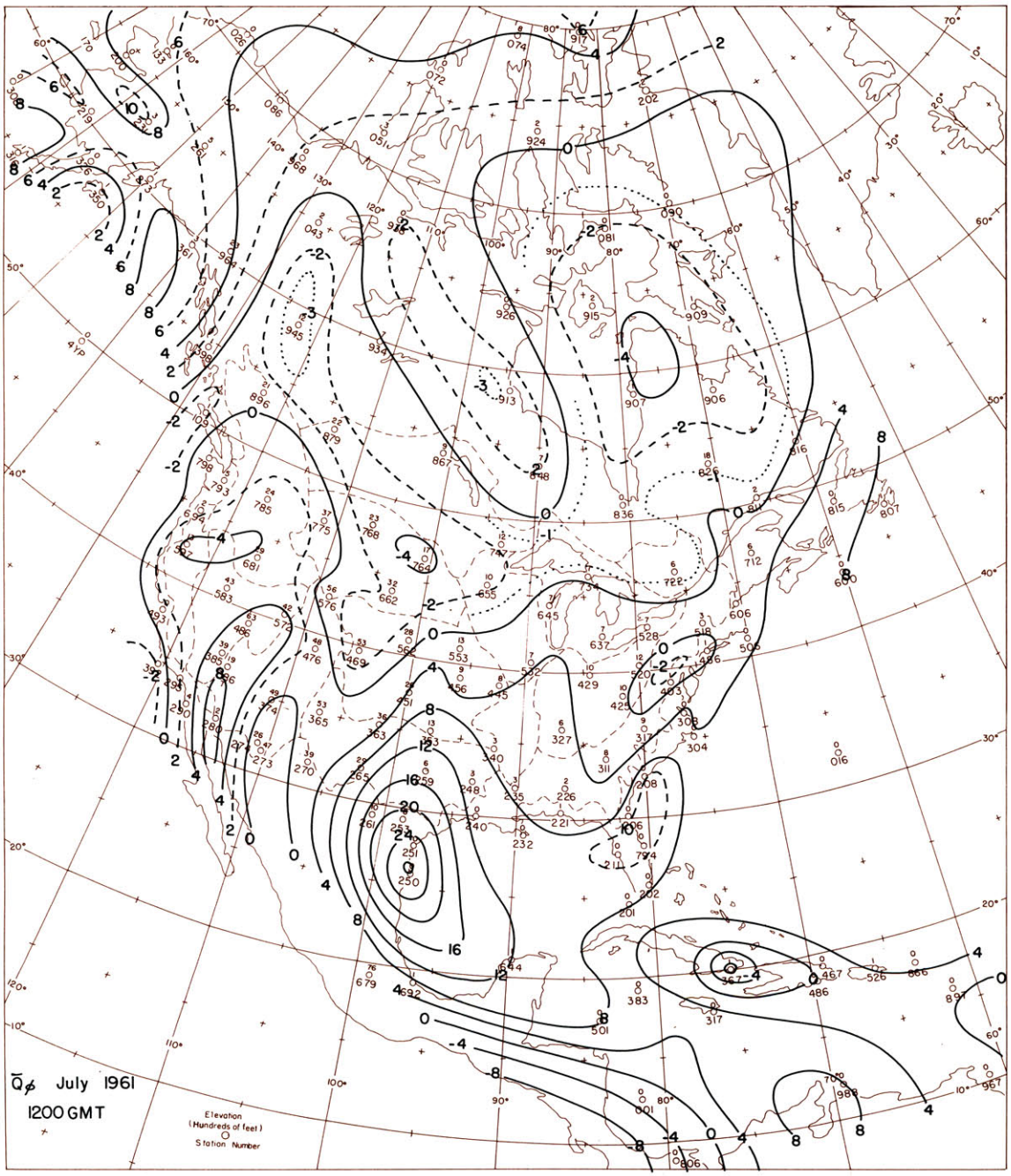


Figure 13. Vertically integrated mean total meridional water vapor flux, $\bar{Q}_\phi$ , 12 GMT; July, 1961. Units: $10^2$ gm (cm sec)$^{-1}$.

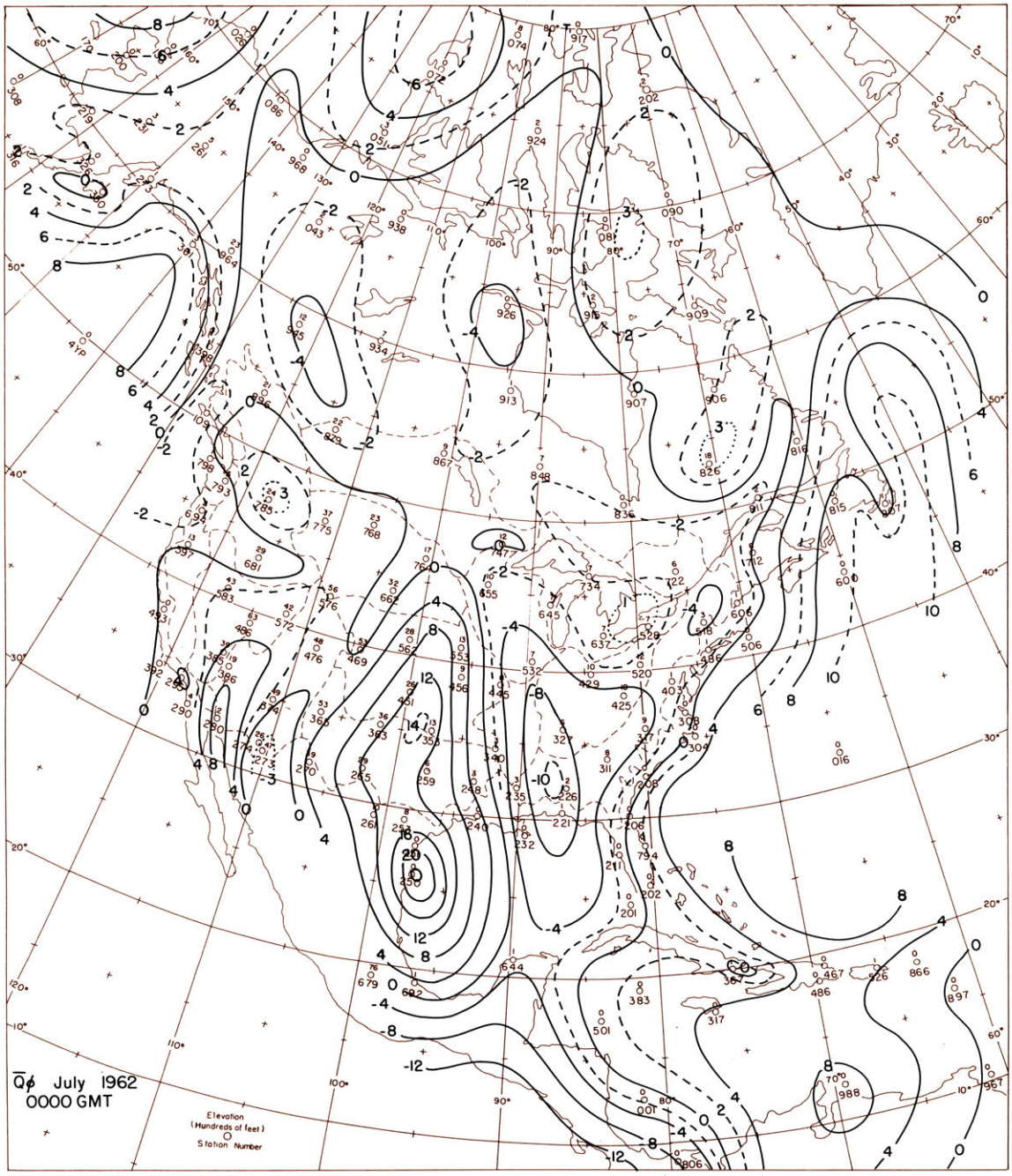


Figure 14. Vertically integrated mean total meridional water vapor flux, $\overline{Q\phi}$, 00 GMT; July, 1962. Units: $10^2$ gm (cm sec)$^{-1}$.

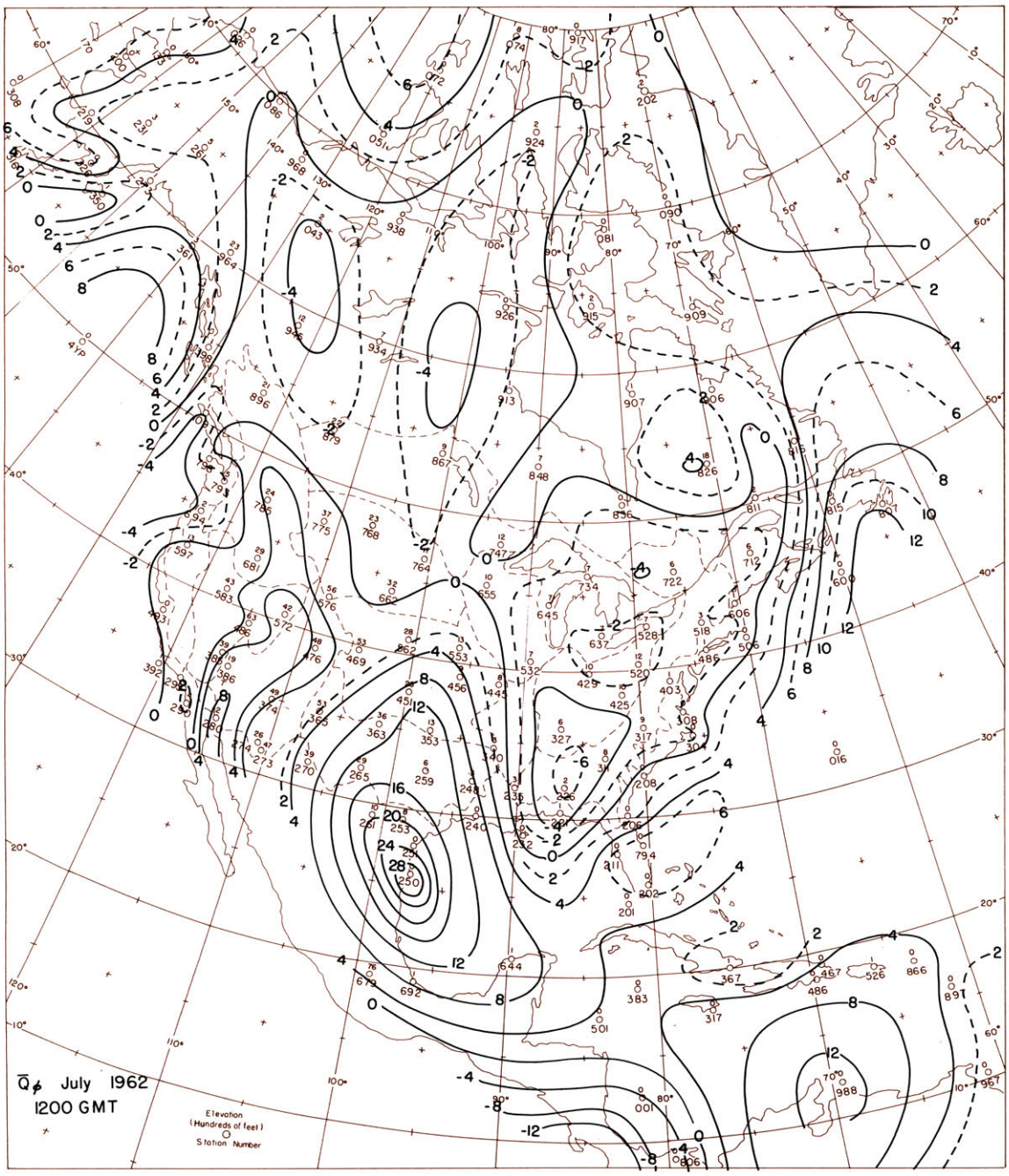


Figure 15. Vertically integrated mean total meridional water vapor flux, $\overline{Q_\phi}$, 12 GMT; July, 1962. Units: $10^2$ gm (cm sec)$^{-1}$.

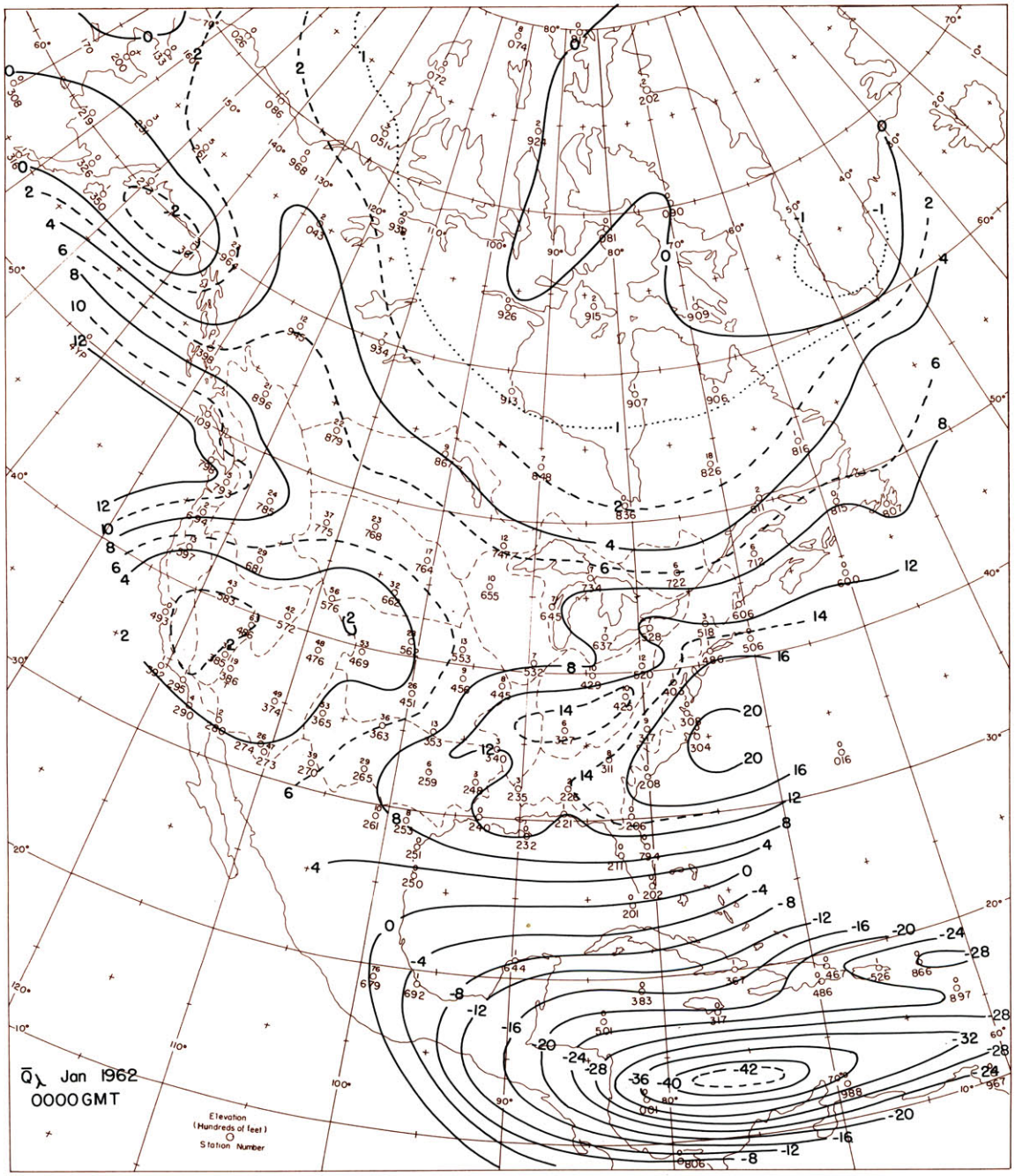


Figure 16. Vertically integrated mean total zonal water vapor flux, $\bar{Q}_\lambda$, 00 GMT; January, 1962. Units: $10^2$ gm (cm sec)$^{-1}$.

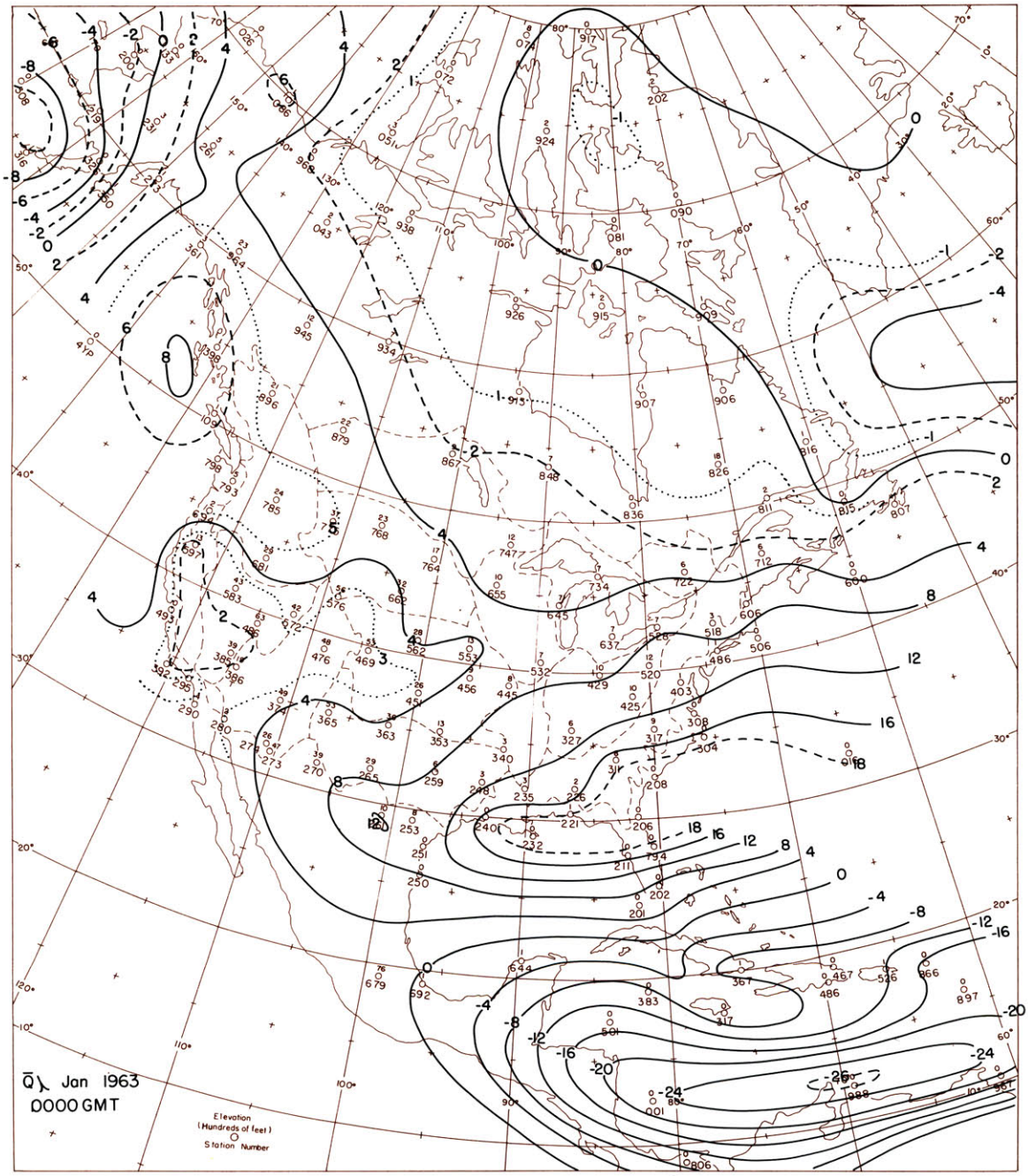


Figure 17. Vertically integrated mean total zonal water vapor flux, $\bar{Q}_\lambda$, 00 GMT; January, 1963. Units: $10^2$ gm (cm sec)$^{-1}$.

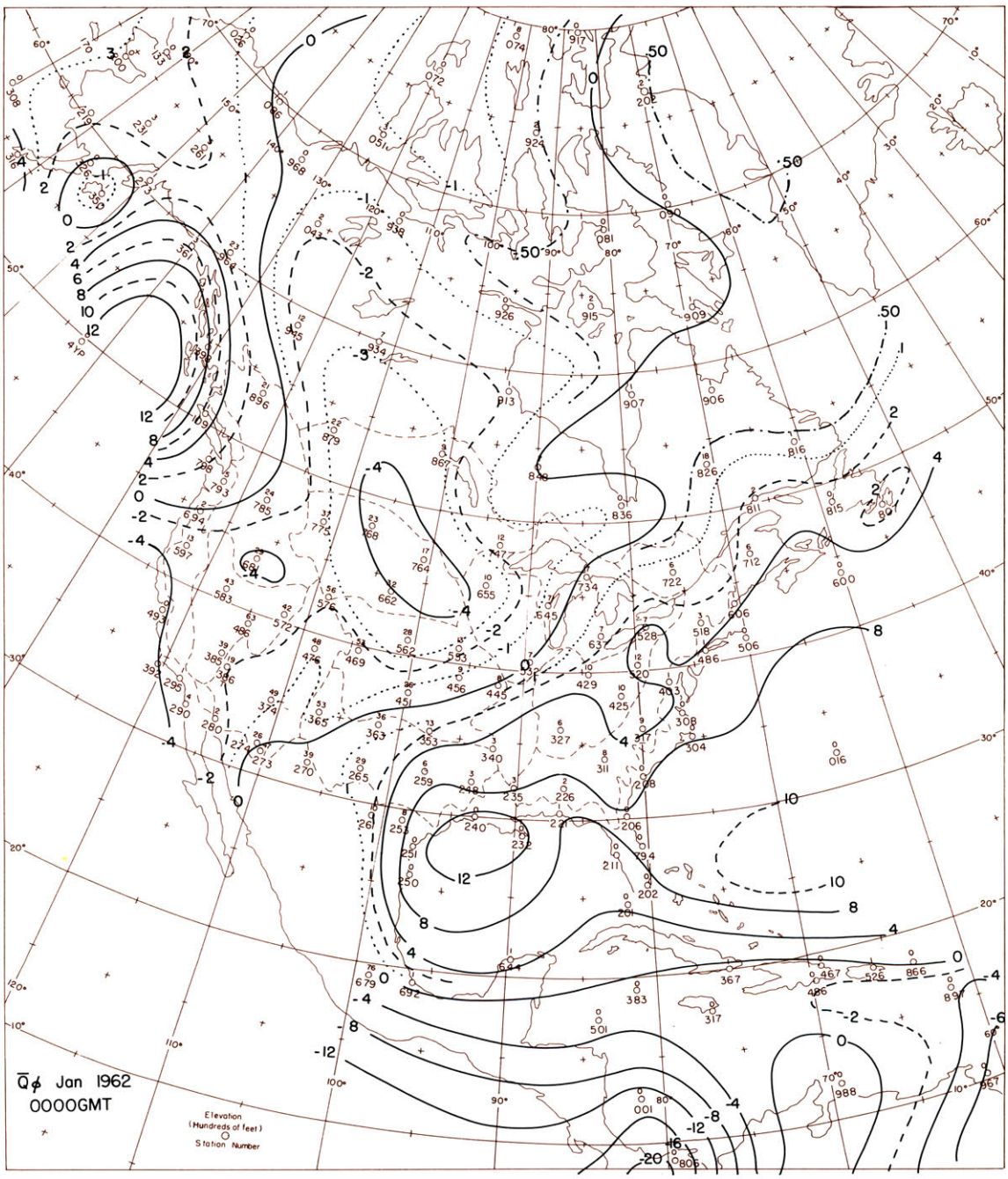


Figure 18. Vertically integrated mean total meridional water vapor flux, $\overline{Q\phi}$, 00 GMT; January, 1962. Units: $10^2$ gm (cm sec)$^{-1}$.

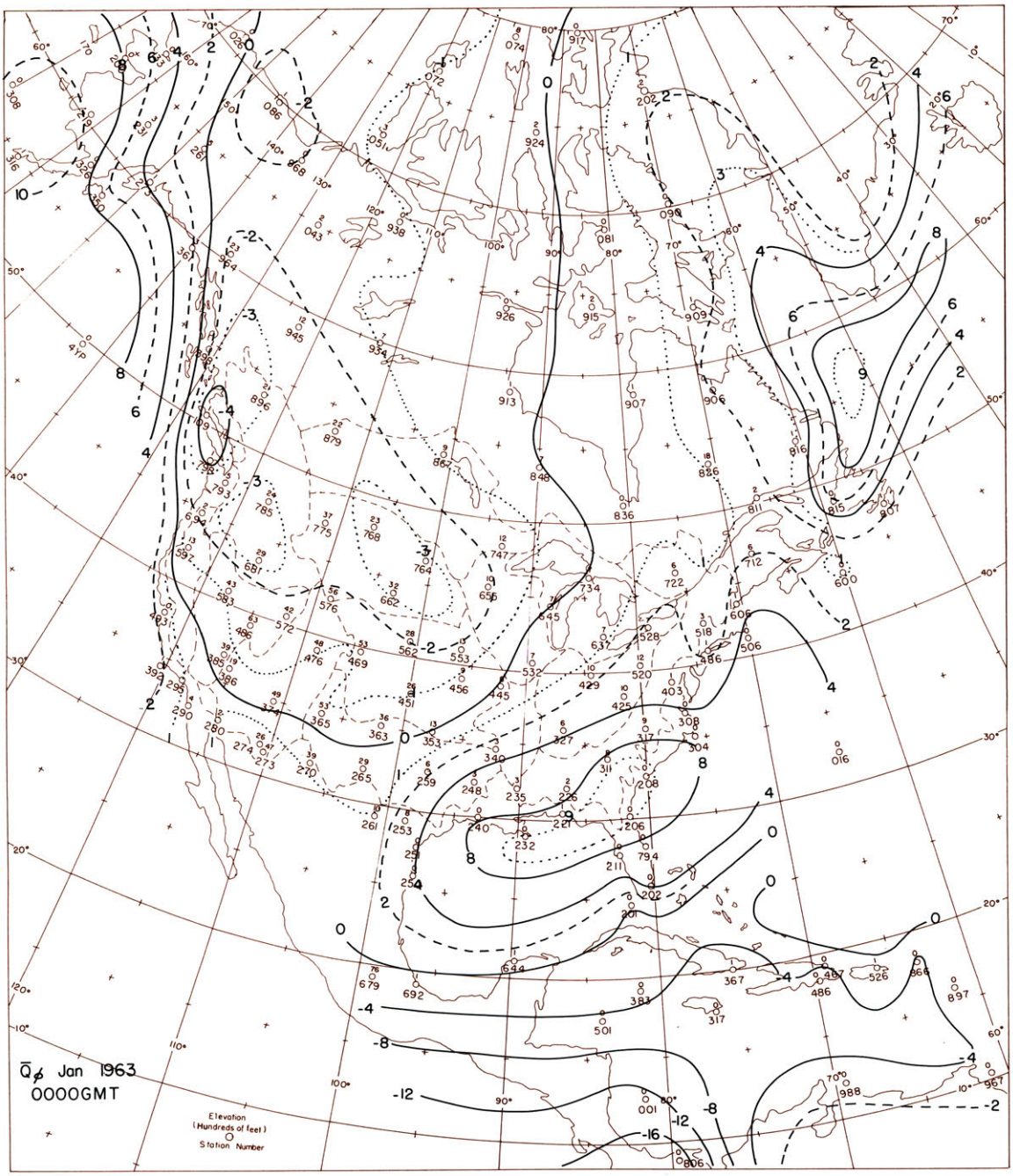


Figure 19. Vertically integrated mean total meridional water vapor flux, $\bar{Q}_\phi$, 00 GMT; January, 1963
Units: $10^2$ gm (cm sec)$^{-1}$

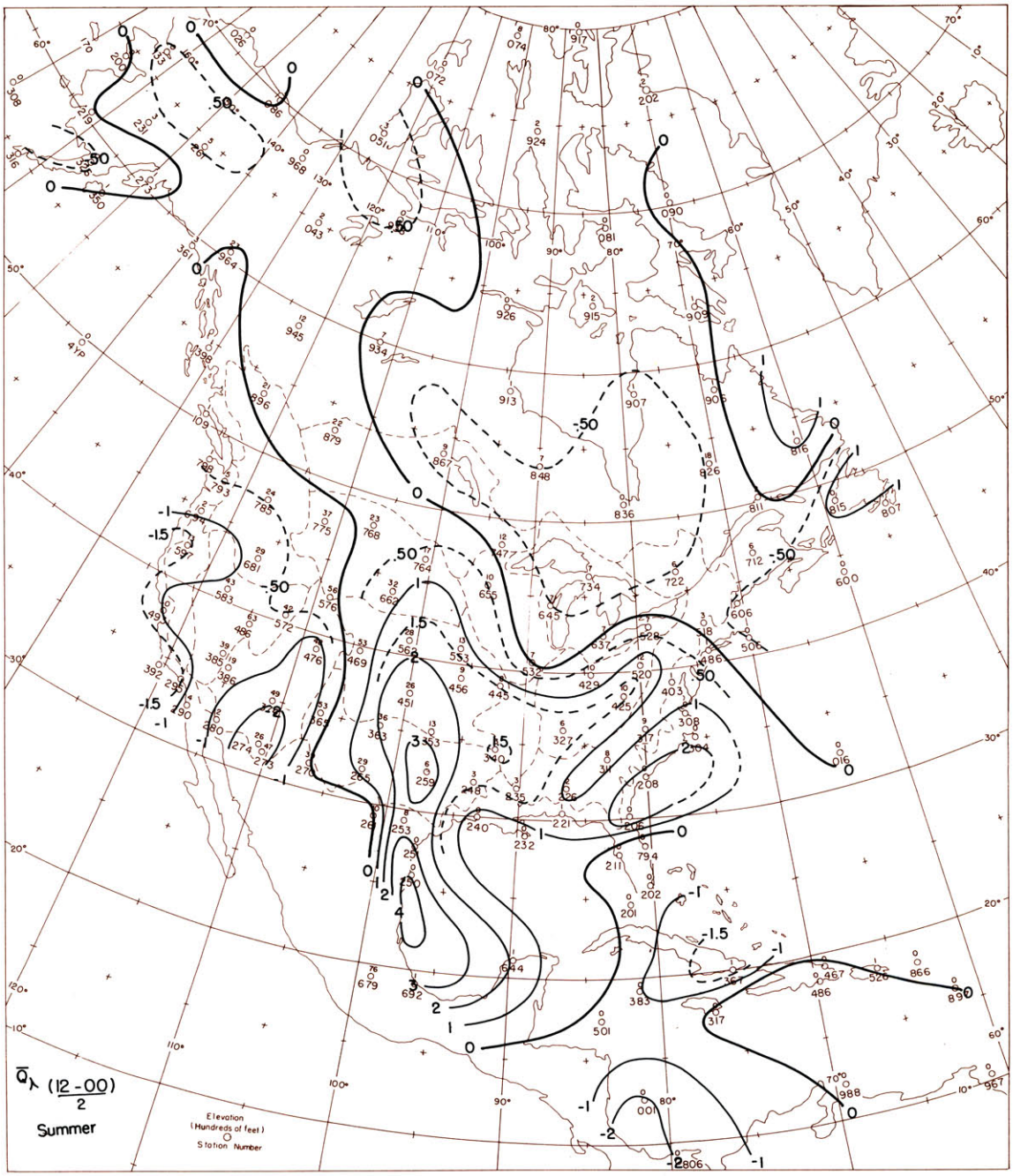


Figure 20. Difference, (12 GMT-00 GMT)/2, of the vertically integrated mean total zonal water vapor flux; June-August, 1961 and 1962. Units: $10^2$ gm (cm sec)$^{-1}$.

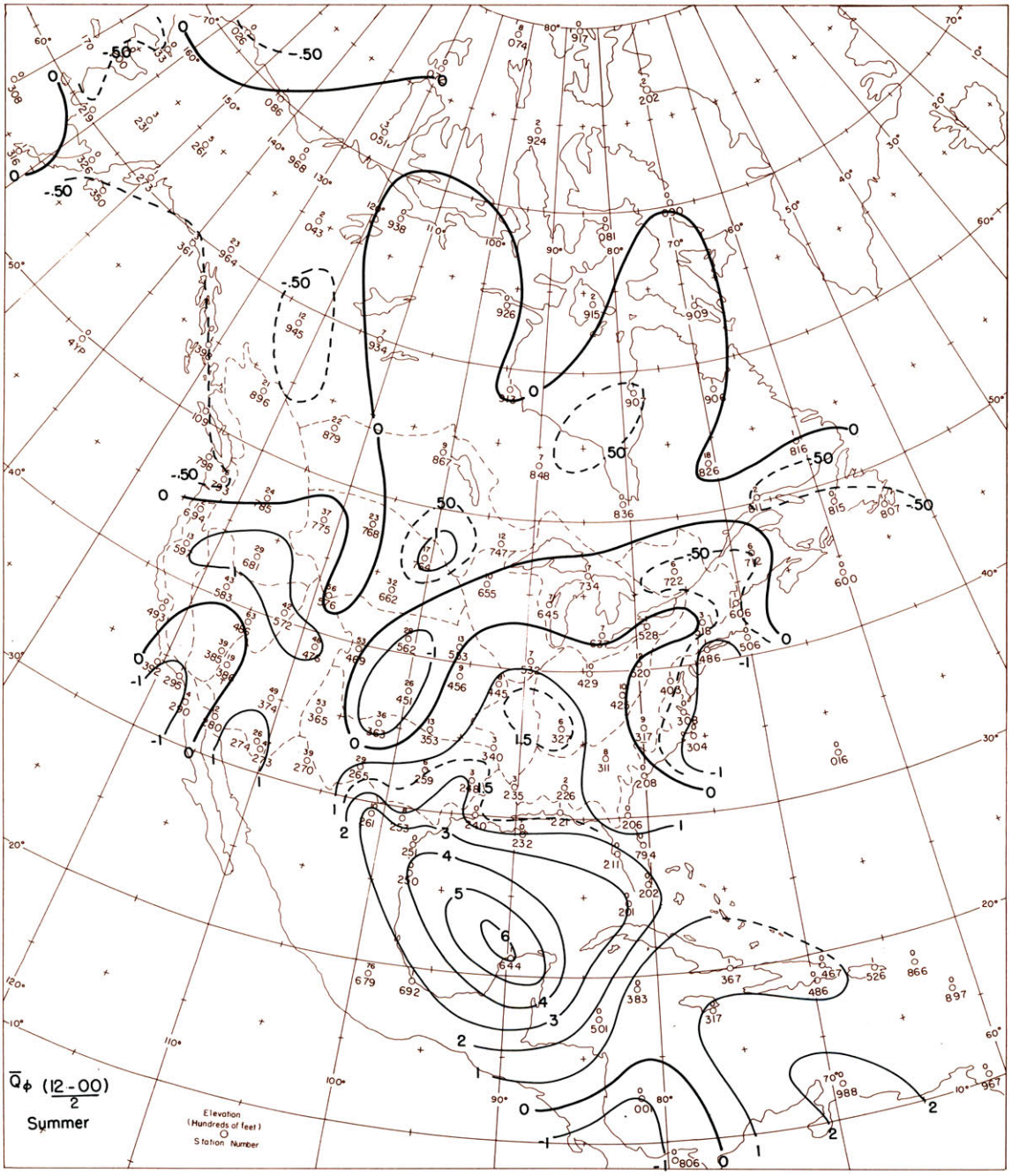


Figure 21. Difference, (12 GMT-00 GMT)/2, of the vertically integrated mean total meridional water vapor flux; June-August, 1961 and 1962. Units: $10^2$ gm (cm sec)$^{-1}$.

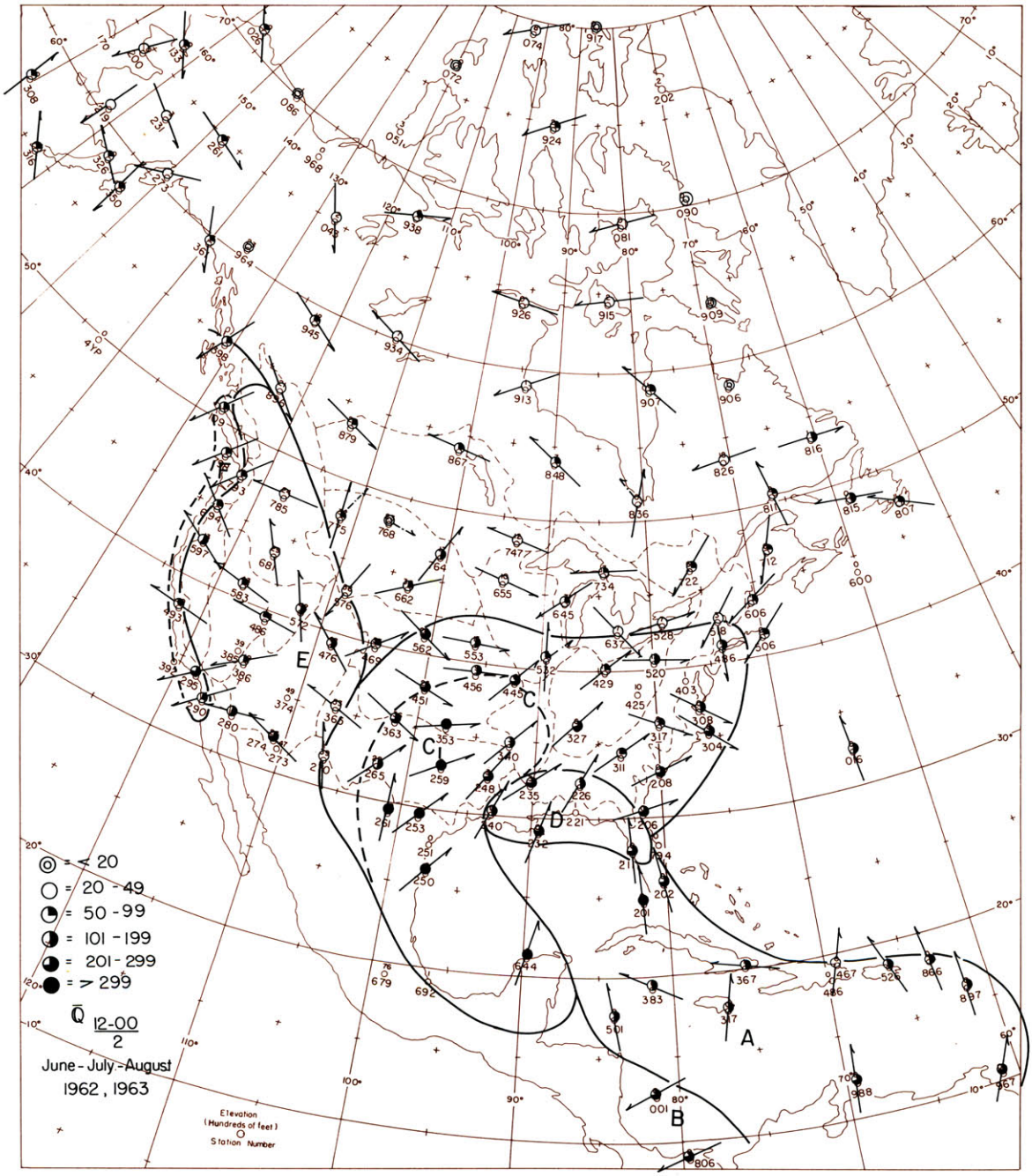


Figure 22. Difference, (12 GMT-00 GMT)/2, of the vertically integrated mean total water vapor flux vector; June-August, 1961 and 1962. Units: gm (cm sec)$^{-1}$. Designated regions are those in which flux variations exhibit similar characteristics.

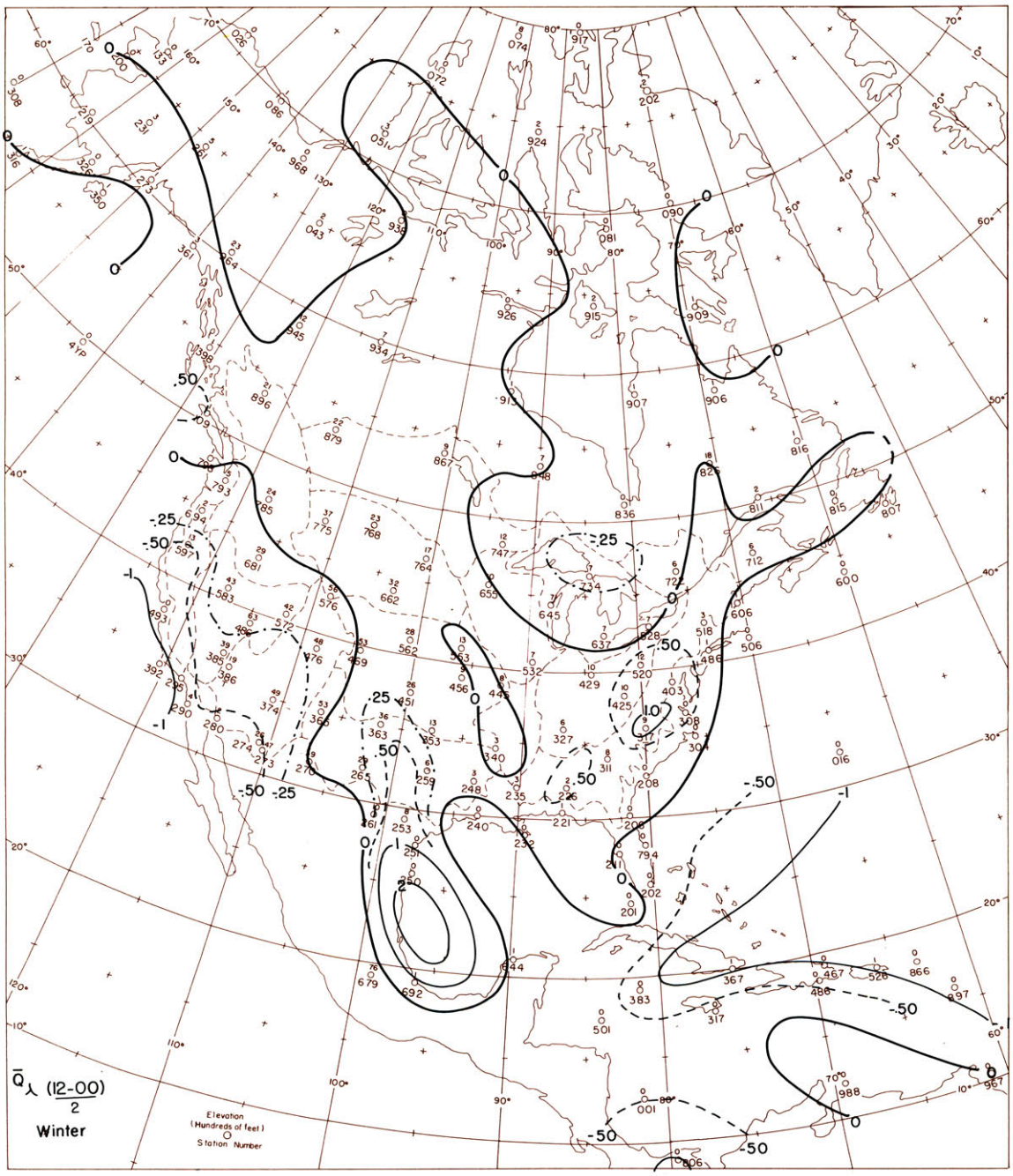


Figure 23. Difference, (12 GMT-00 GMT)/2, of the vertically integrated mean total zonal water vapor flux; December-February, 1961-62 and 1962-63.
Units: $10^2$ gm (cm sec)$^{-1}$.

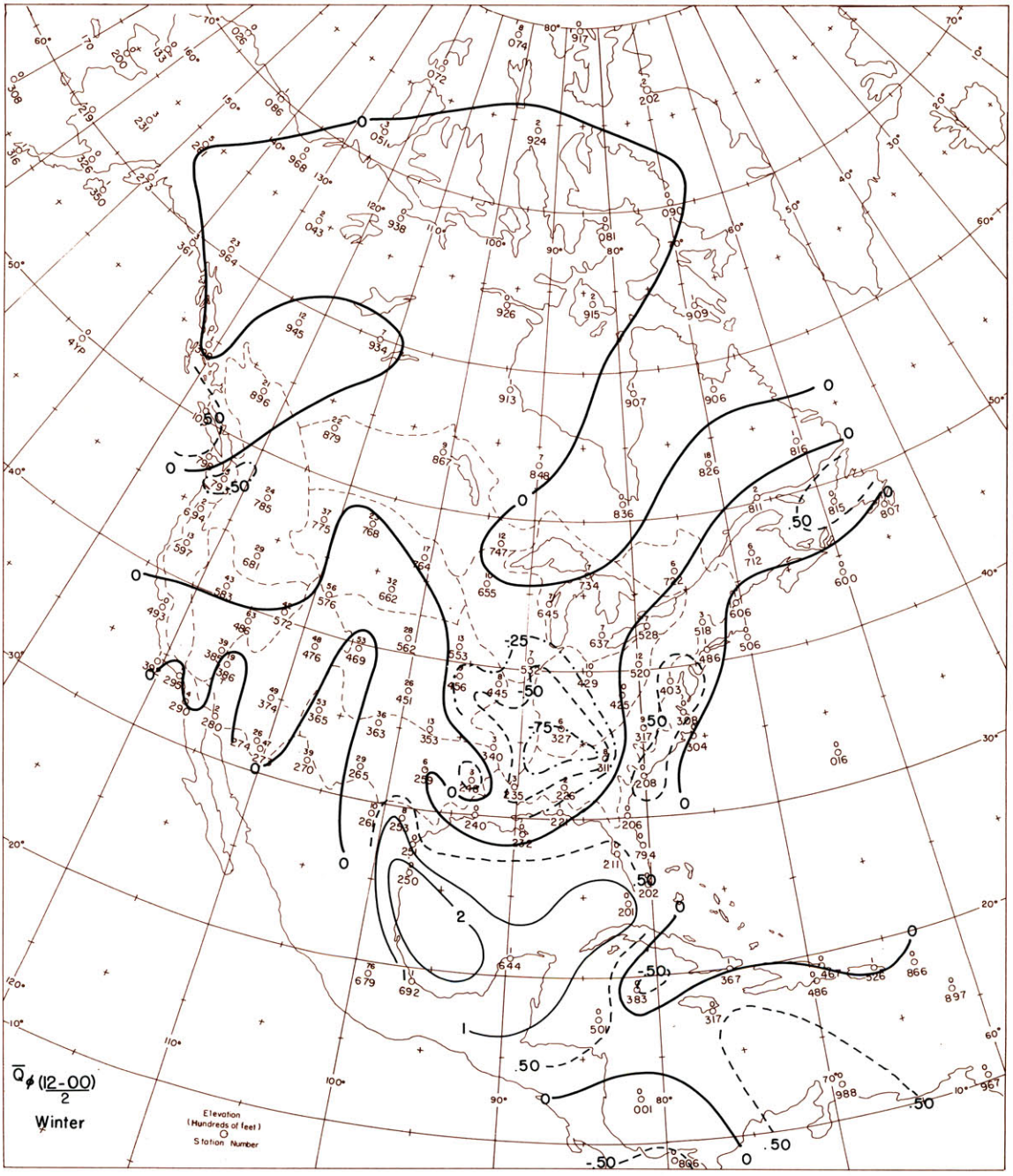


Figure 24. Difference, (12 GMT-00 GMT)/2, of the vertically integrated mean total meridional water vapor flux; December-February, 1961-62 and 1962-63. Units: $10^2$ gm (cm sec)$^{-1}$.

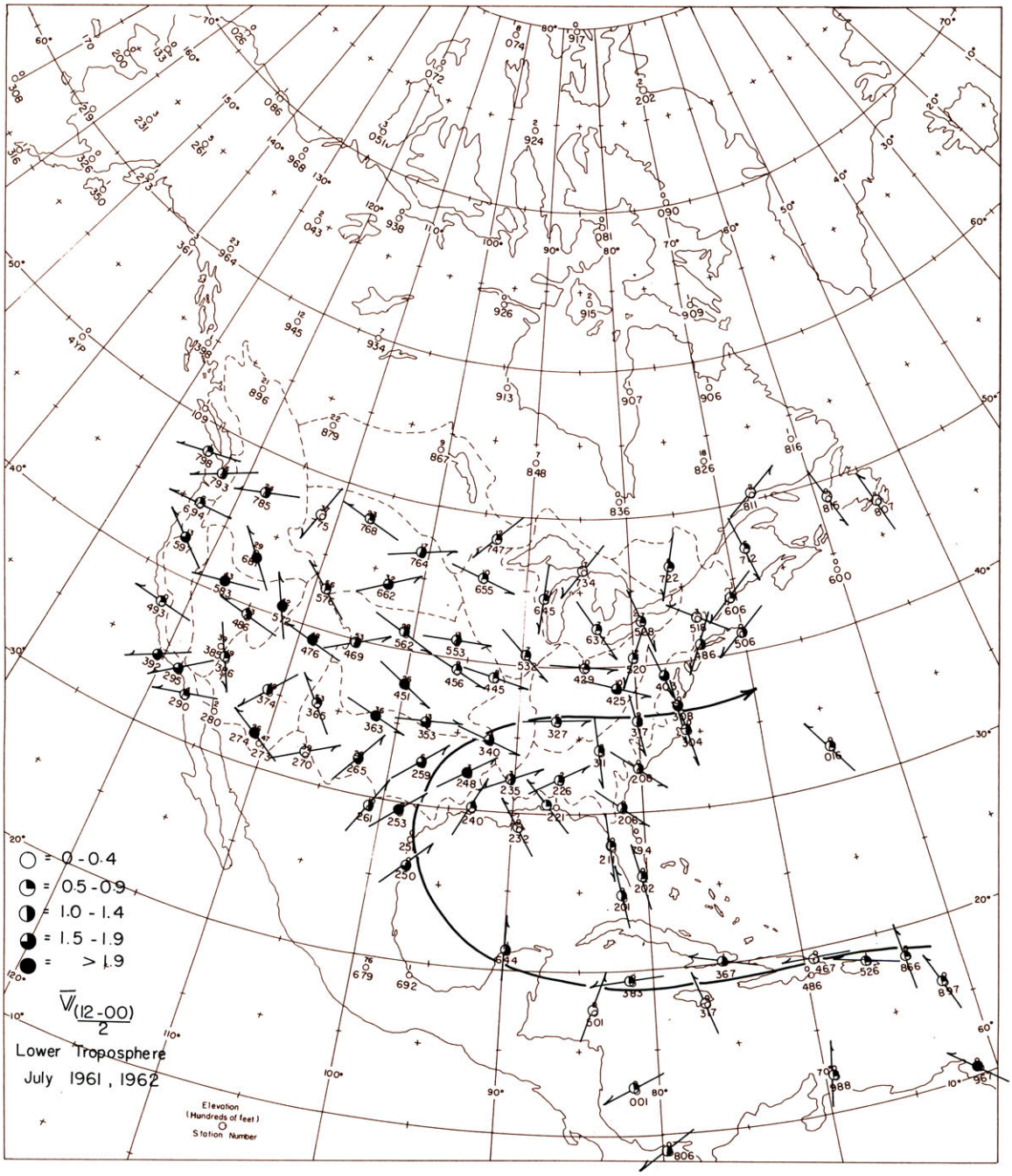


Figure 25. Difference, (12 GMT-00 GMT)/2, of the average of the wind at the first two standard levels (50 mb intervals) above the ground for July 1961 and 1962. Units: meters $sec^{-1}$.

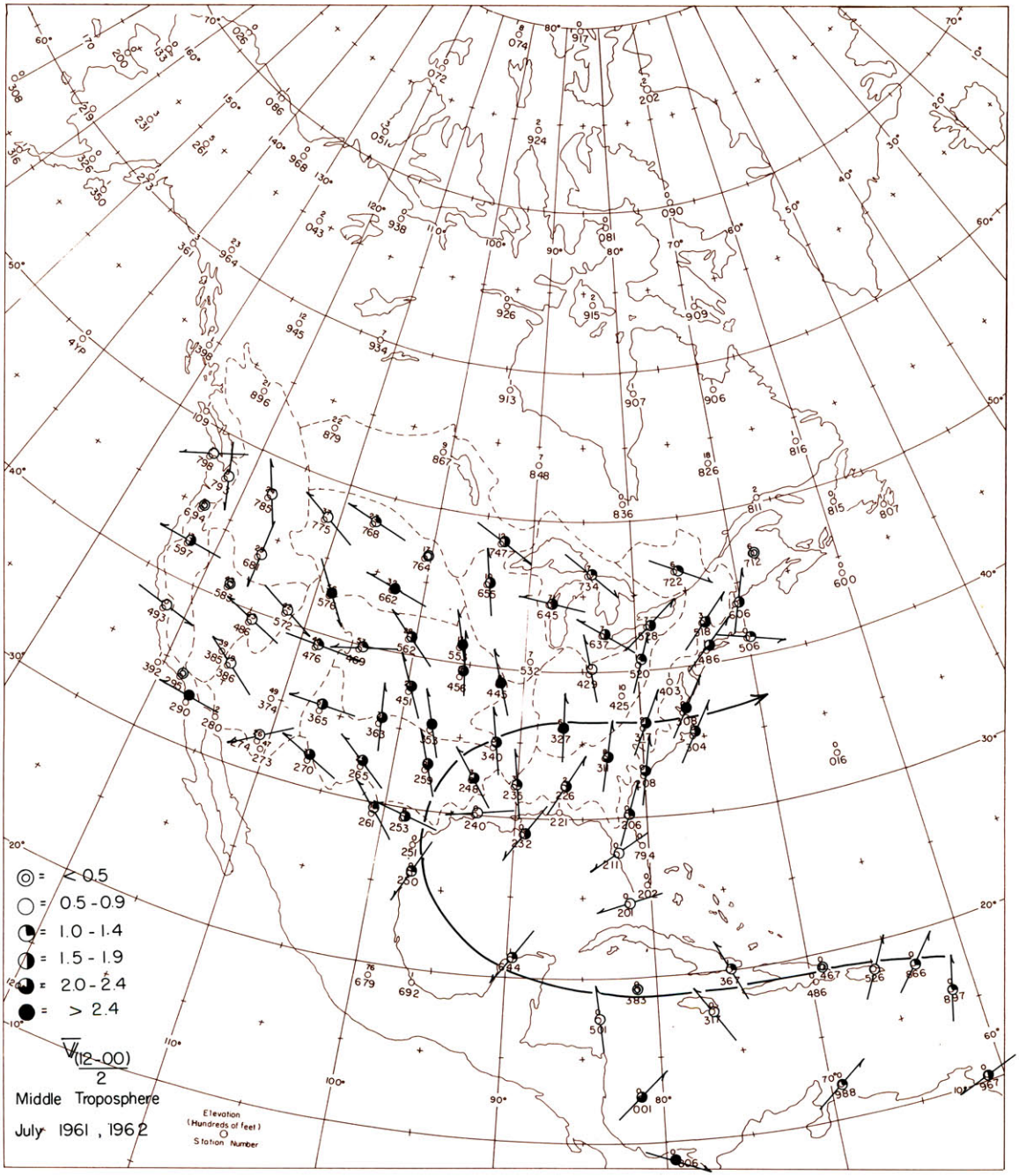


Figure 26. Difference, (12 GMT-00 GMT)/2, of the average of the wind at 500 and 550 mb for July, 1961 and 1962. Units: meters $sec^{-1}$.

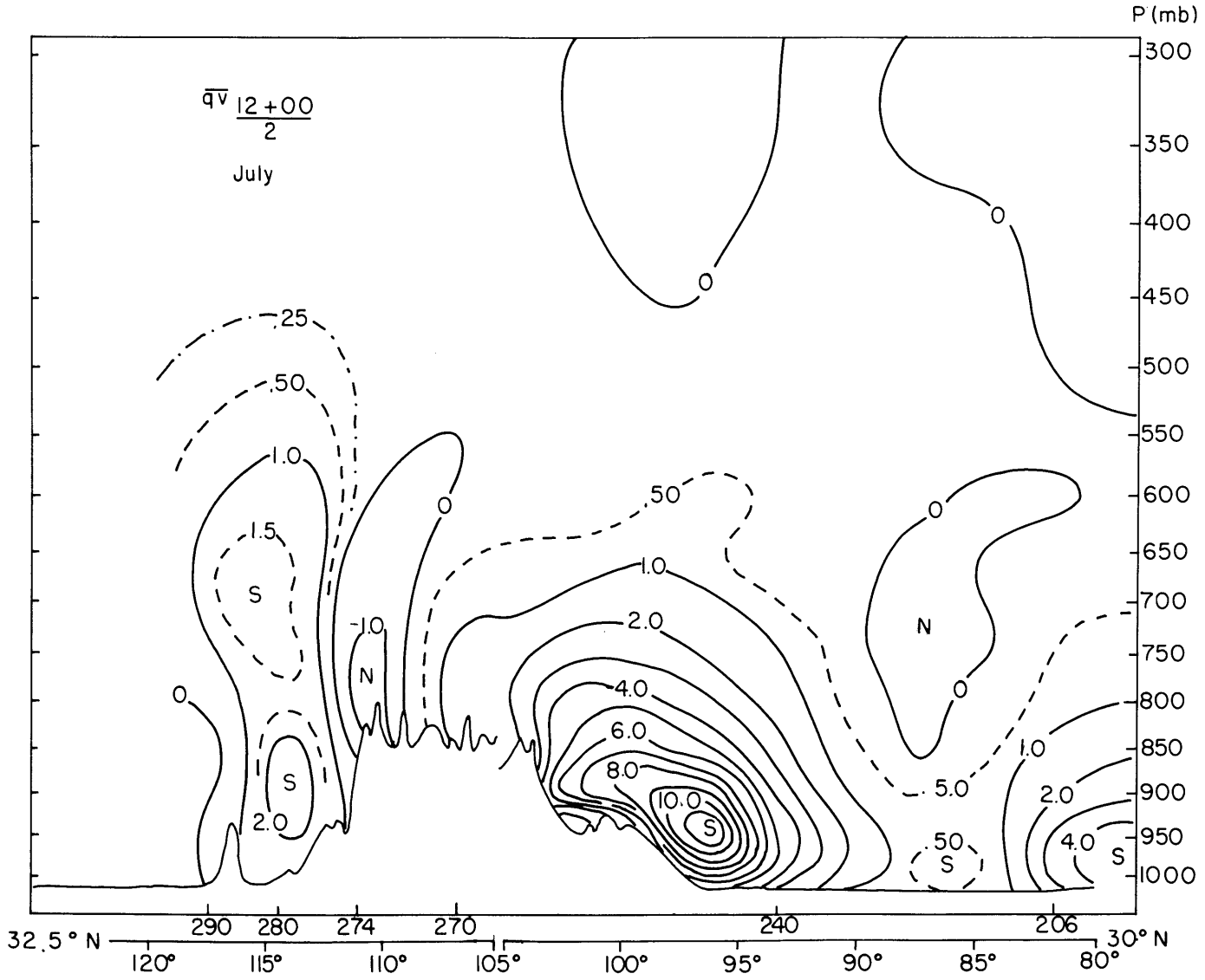


Figure 27. Mean total meridional water vapor flux. 30°N; 80°W-105°W. 32.5°N; 105°W-117.5°W. July, 1961 and 1962. Units: gm (cm mb sec)$^{-1}$.

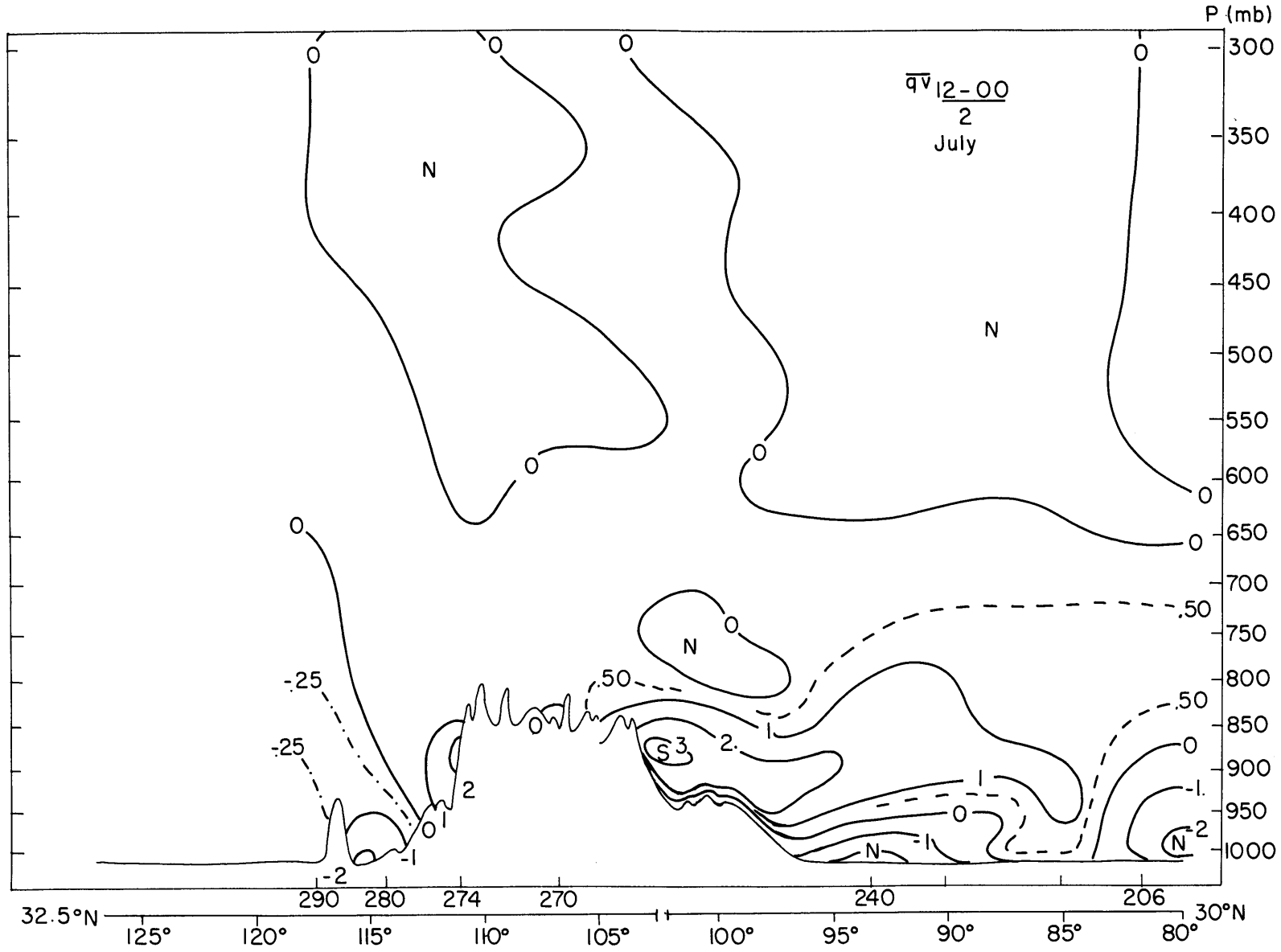


Figure 28. Difference, (12 GMT-00 GMT)/2, of mean total meridional water vapor flux. 30°N; 80°W-105°W. 32.5°N; 105°W-117.5°W. July, 1961 and 1962. Units: gm (cm mb sec)$^{-1}$.

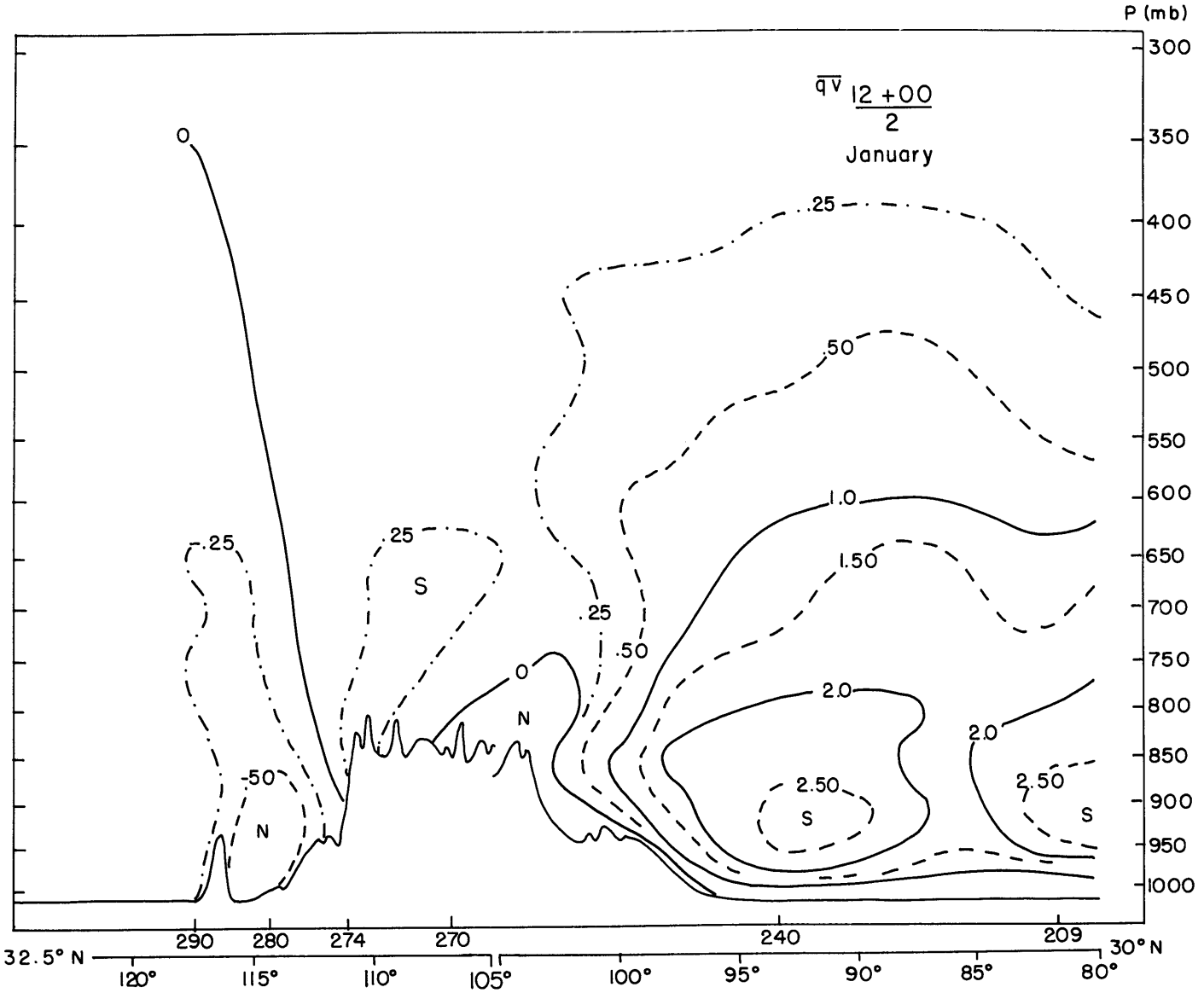


Figure 29. Mean total meridional water vapor flux. 30°N; 80°W-105°W. 32.5°N; 105°W-117.5°W. January, 1962 and 1963. Units: gm (cm mb sec)$^{-1}$.

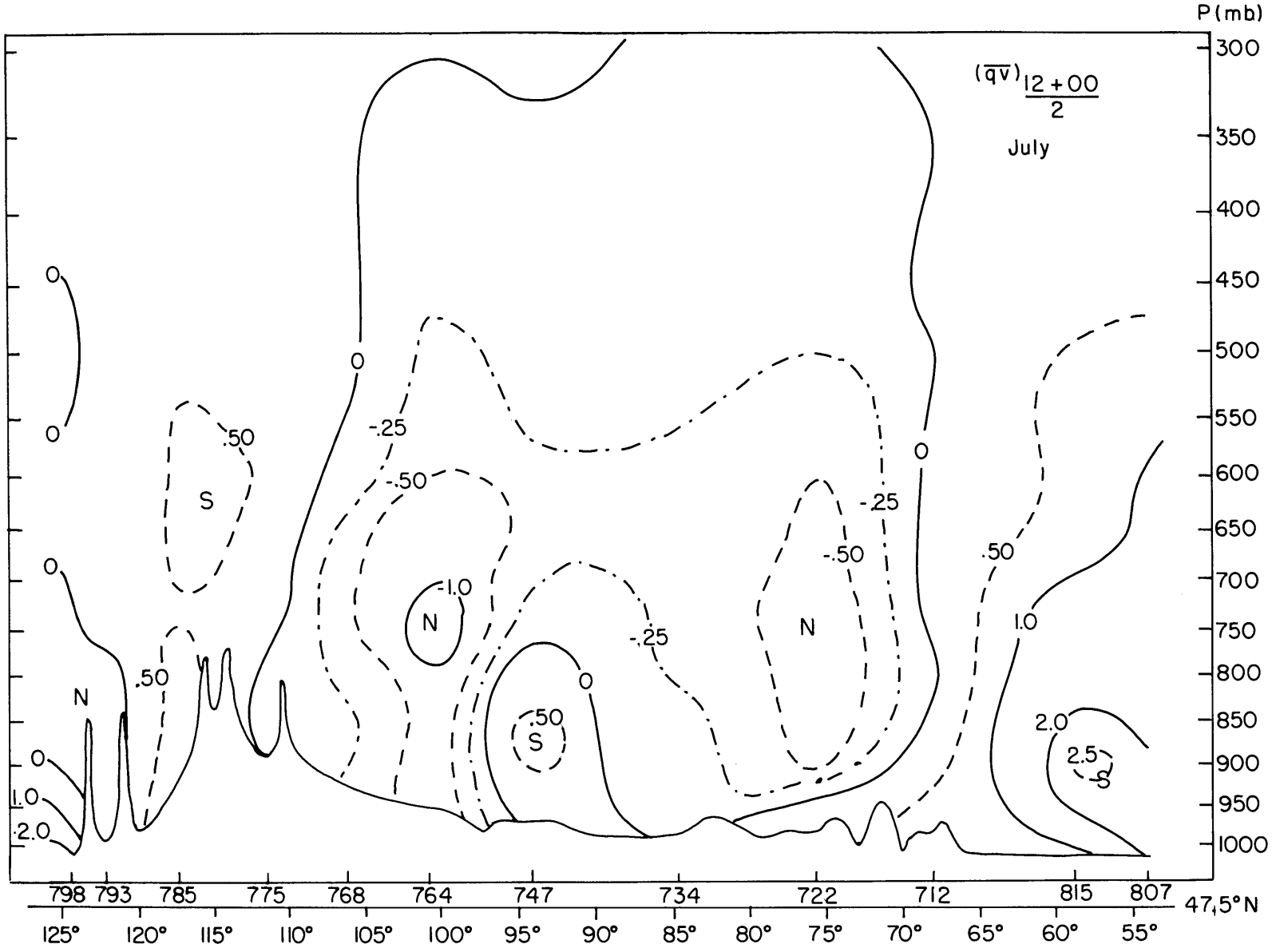


Figure 30. Mean total meridional water vapor flux. 47.5°N; 55°W-125°W. July, 1961 and 1962. Units: gm (cm mb sec)$^{-1}$.

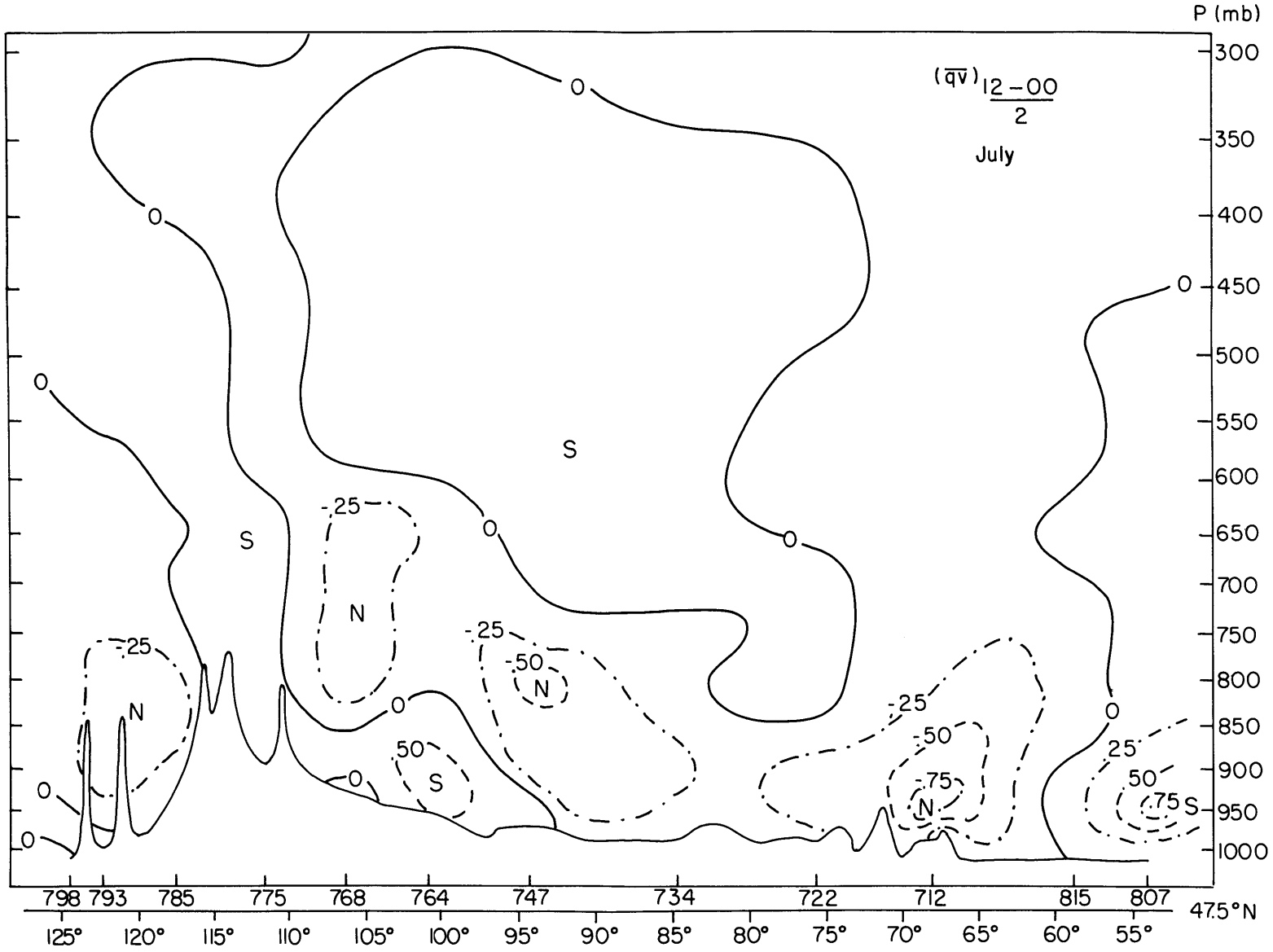


Figure 31. Difference, (12 GMT-00 GMT)/2, of mean total meridional water vapor flux. 47.5°N; 55°W-125°W. July, 1961 and 1962. Units: gm (cm mb sec)$^{-1}$.

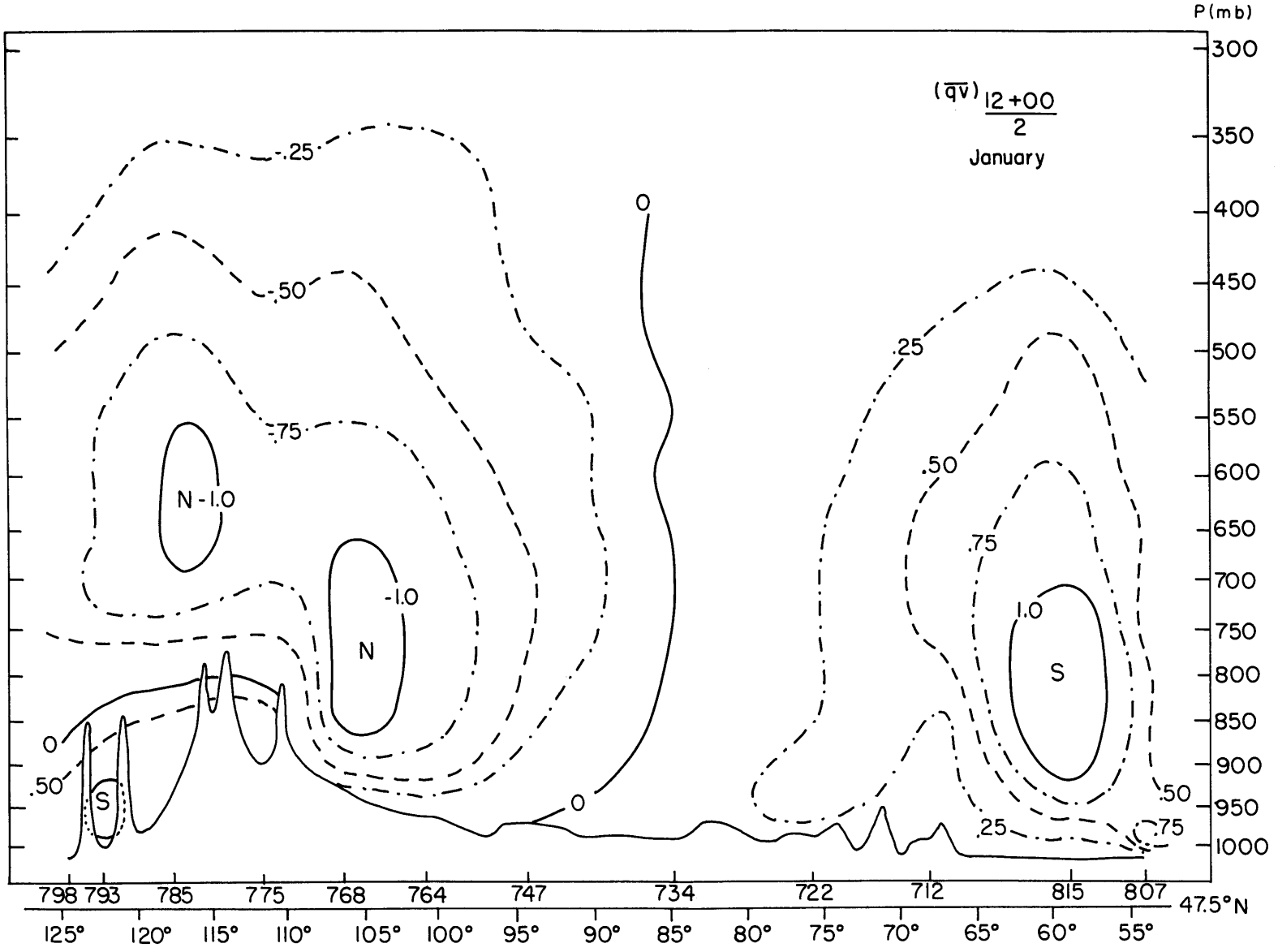


Figure 32. Mean total meridional water vapor flux. 47.5°N; 55°W-125°W. January, 1962 and 1963. Units: gm (cm mb sec)$^{-1}$.

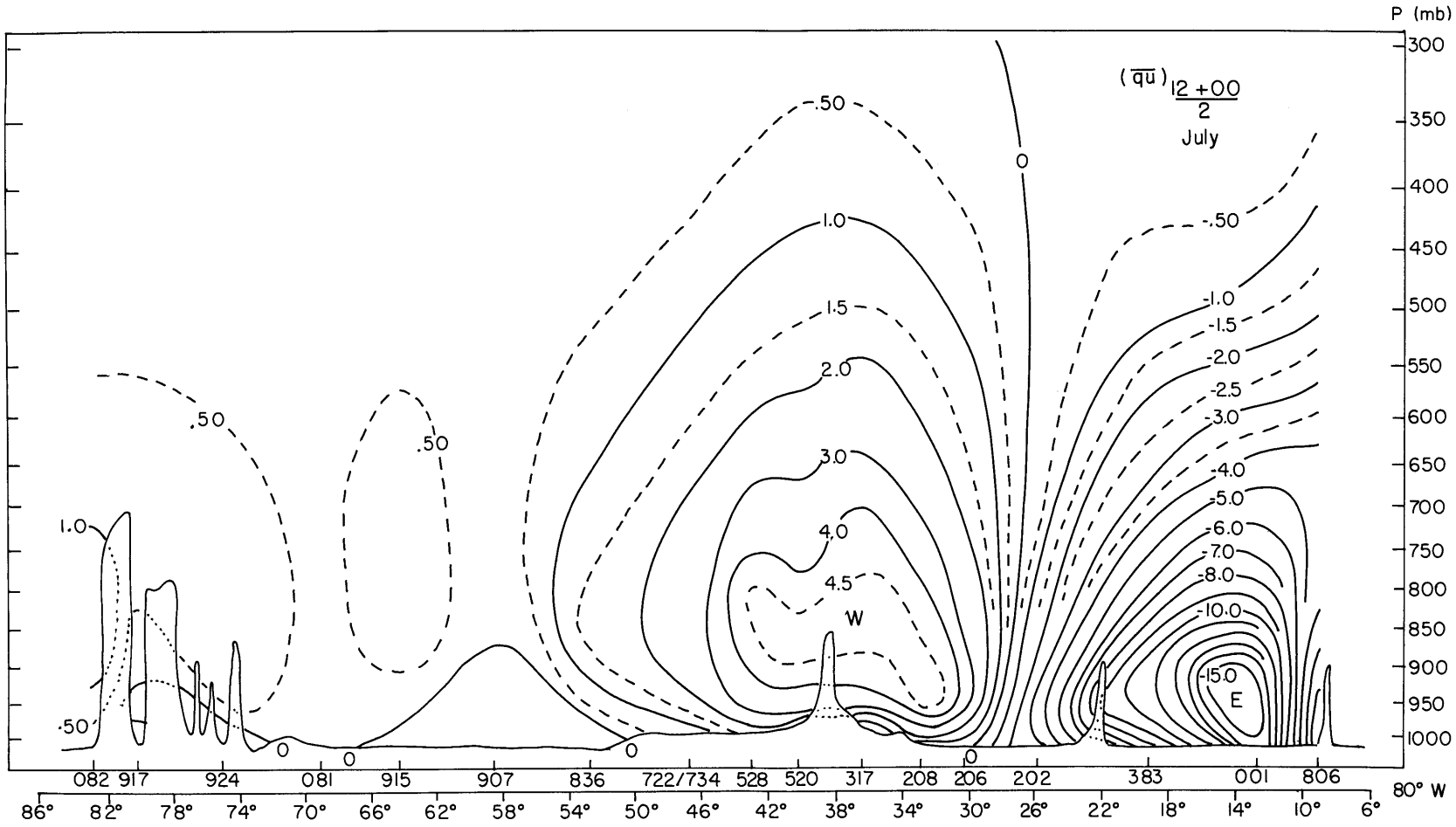


Figure 33. Mean total zonal water vapor flux. 10°N-83°N; 80°W. July, 1961 and 1962. Units: gm (cm mb sec)$^{-1}$.

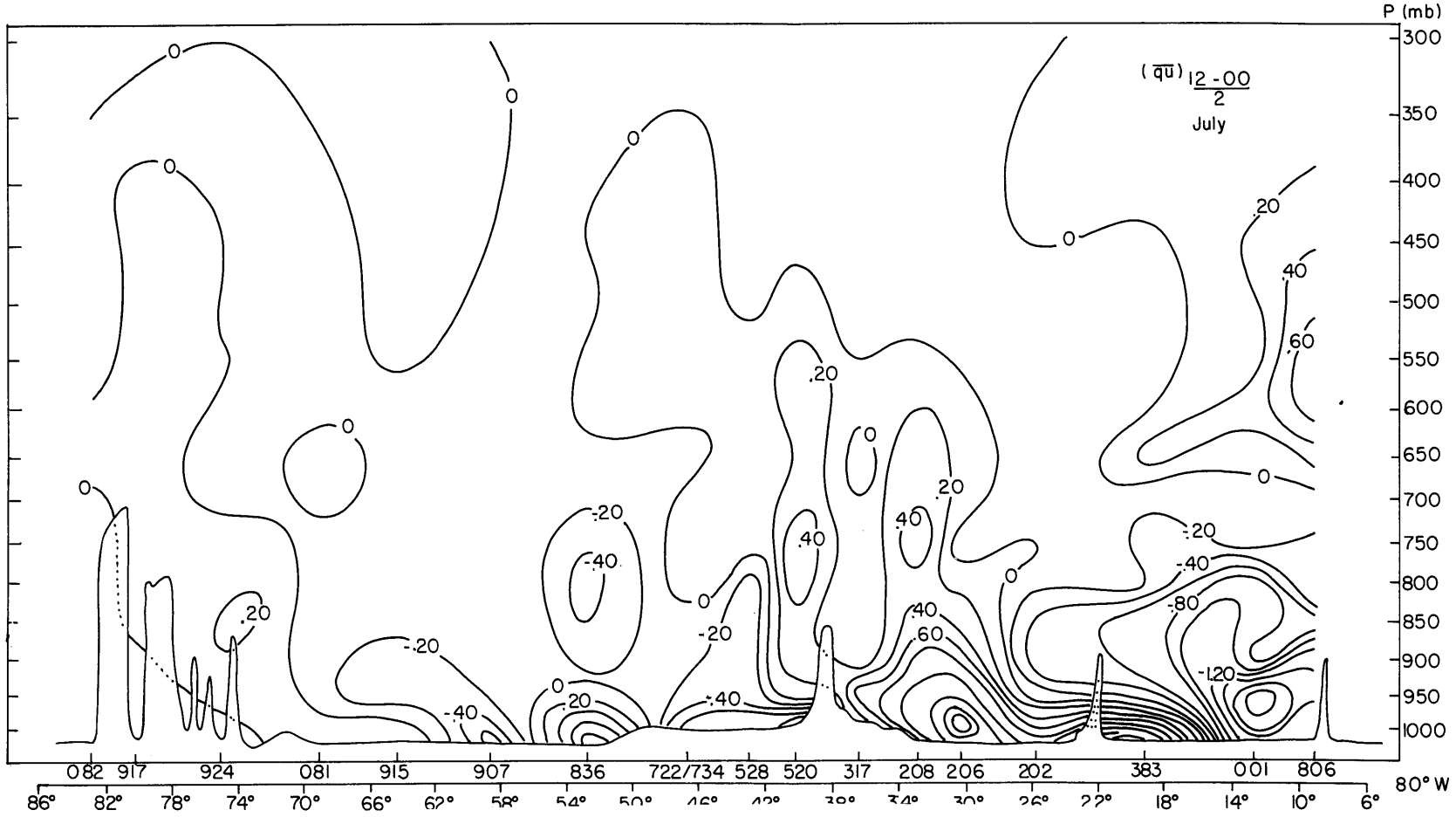


Figure 34. Difference, (12 GMT-00 GMT)/2, of mean total zonal water vapor flux. 10°N-83°N; 80°W. July, 1961 and 1962. Units: gm (cm mb sec)$^{-1}$.

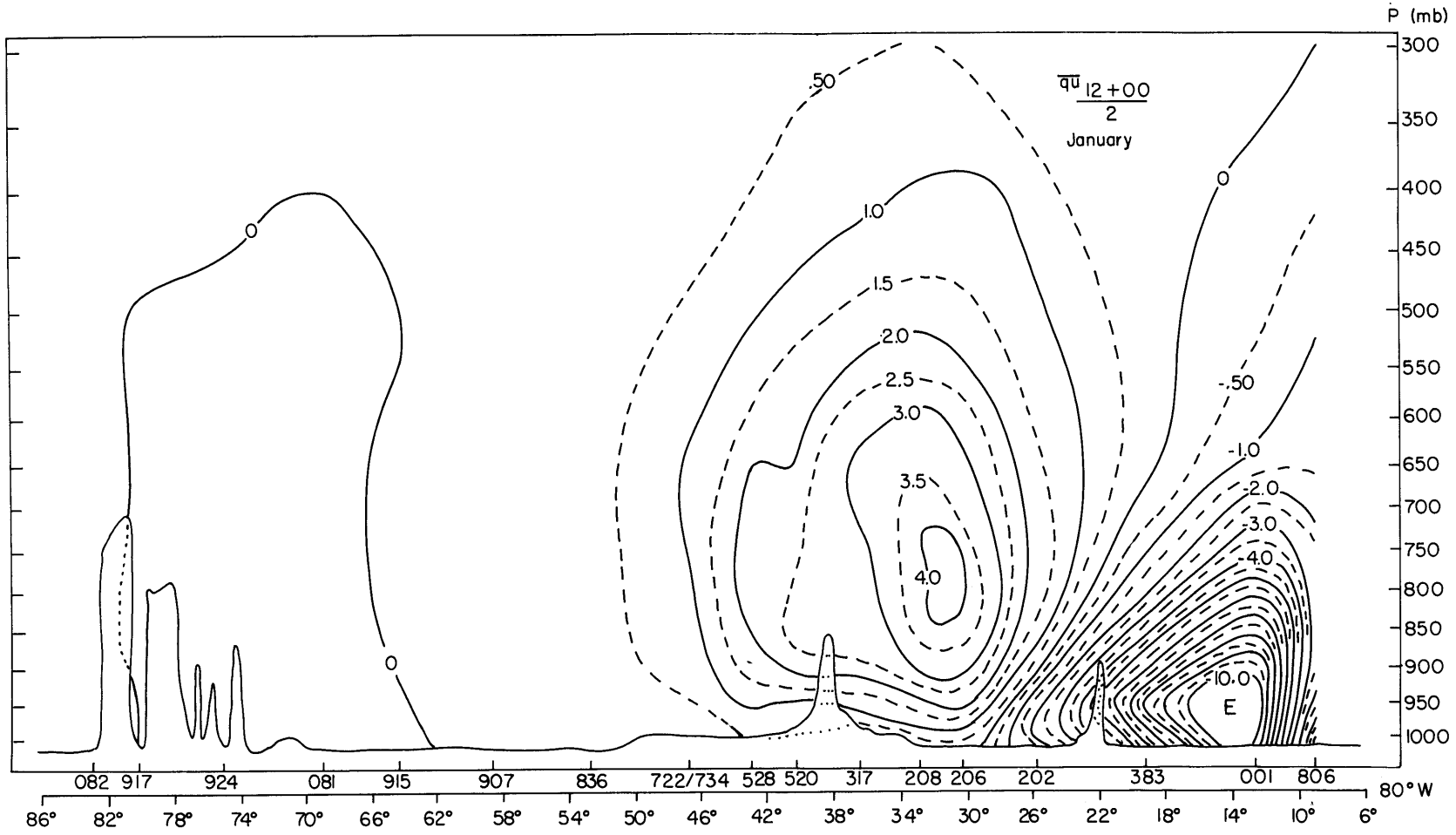


Figure 35. Mean total zonal water vapor flux. 10°N-83°N; 80°W. January, 1962 and 1963. Units: gm (cm mb sec)$^{-1}$.

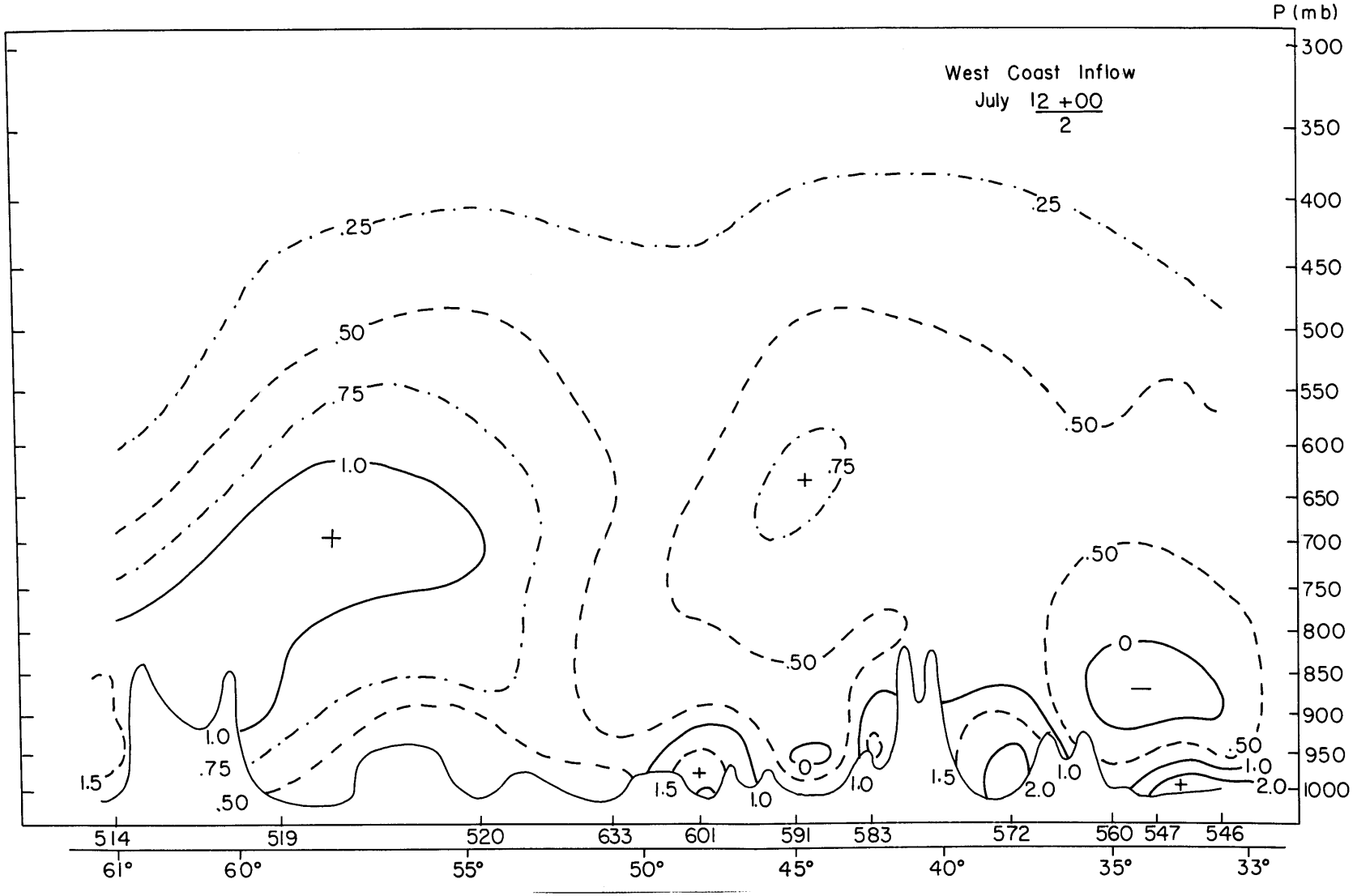


Figure 36. Mean total water vapor influx-west coast. 32.5°N-61°N. July, 1961 and 1962. Units: gm (cm mb sec)$^{-1}$.

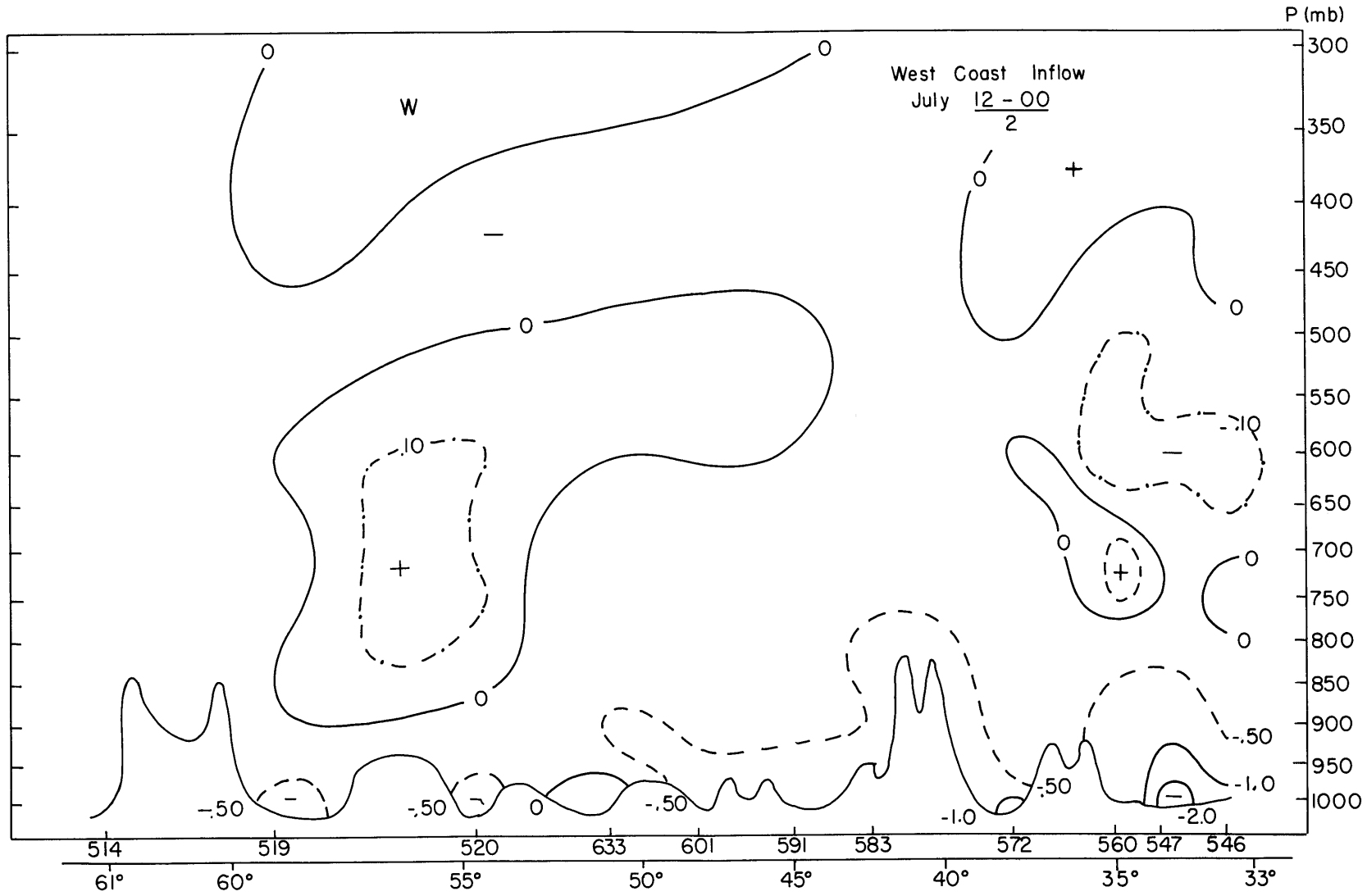


Figure 37. Difference, (12 GMT-00 GMT)/2, of mean total water vapor influx-west coast. 32.5°N-61°N. July, 1961 and 1962. Units: gm (cm mb sec)$^{-1}$.

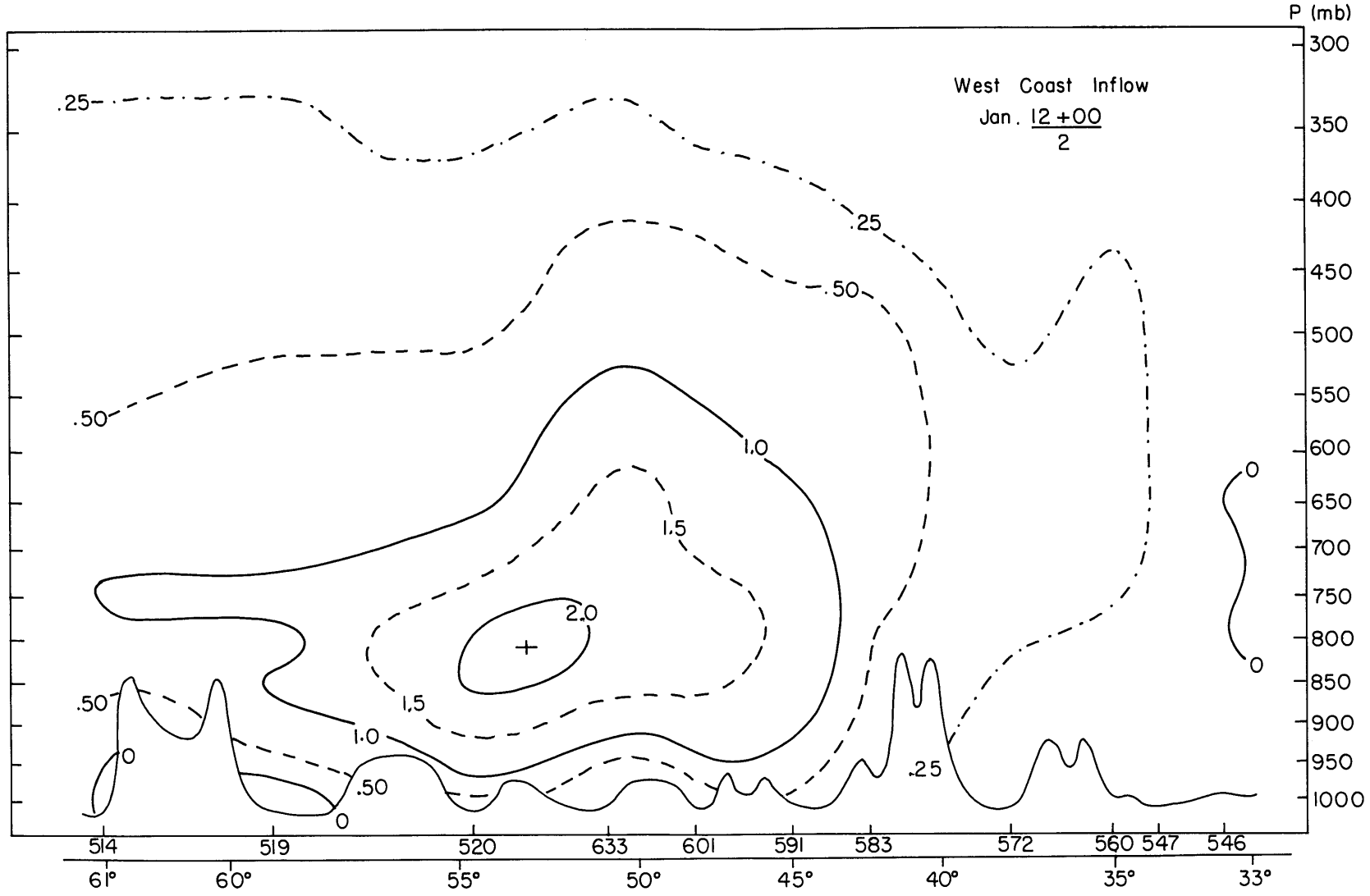


Figure 38. Mean total water vapor influx-west coast. 32.5°N-61°N. January, 1962 and 1963. Units: gm (cm mb sec)$^{-1}$.

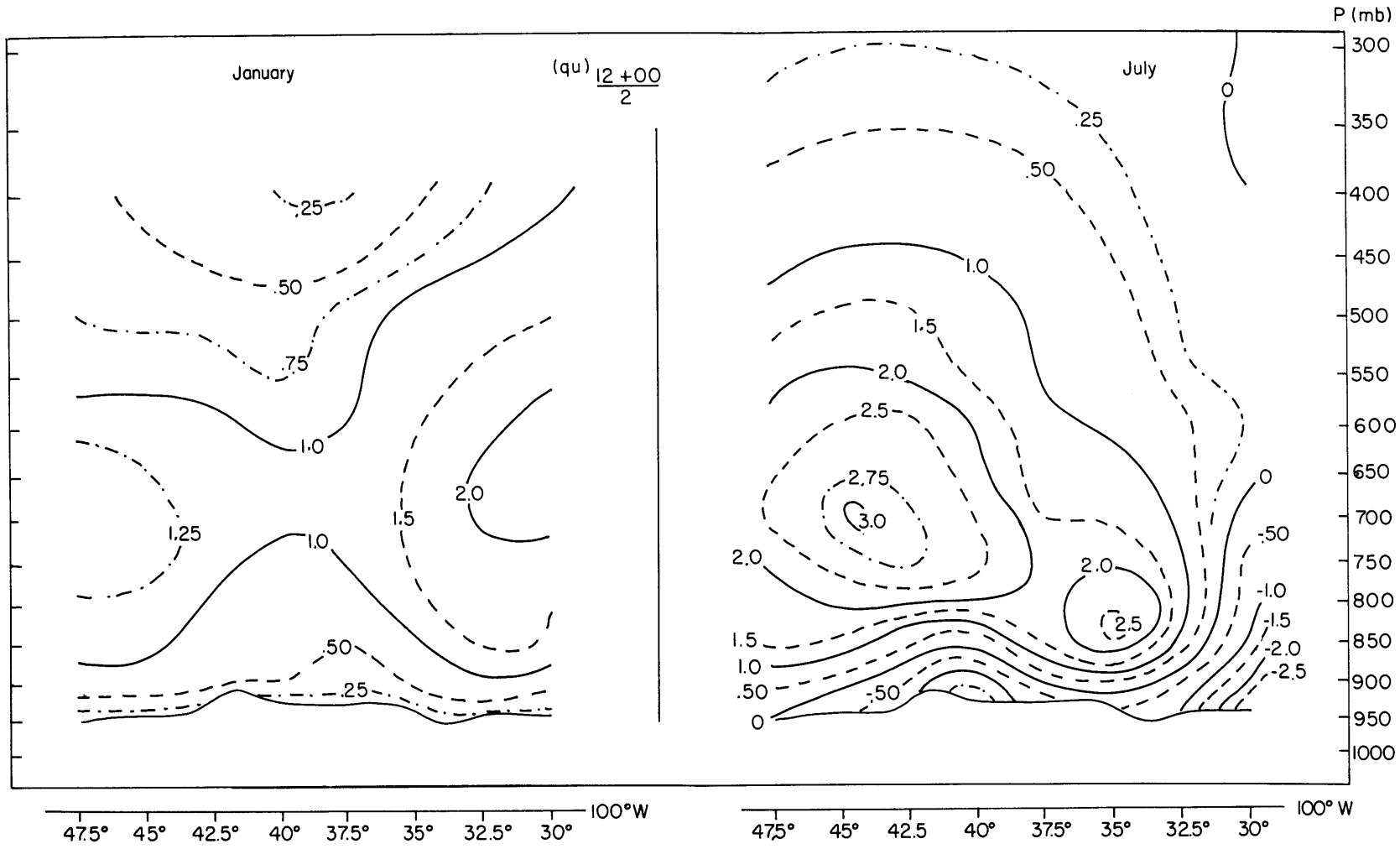


Figure 39. Mean total zonal water vapor flux. 30°N-47.5°N; 100°W. January, 1962 and 1963. July, 1961 and 1962. Units: gm (cm mb sec)$^{-1}$.

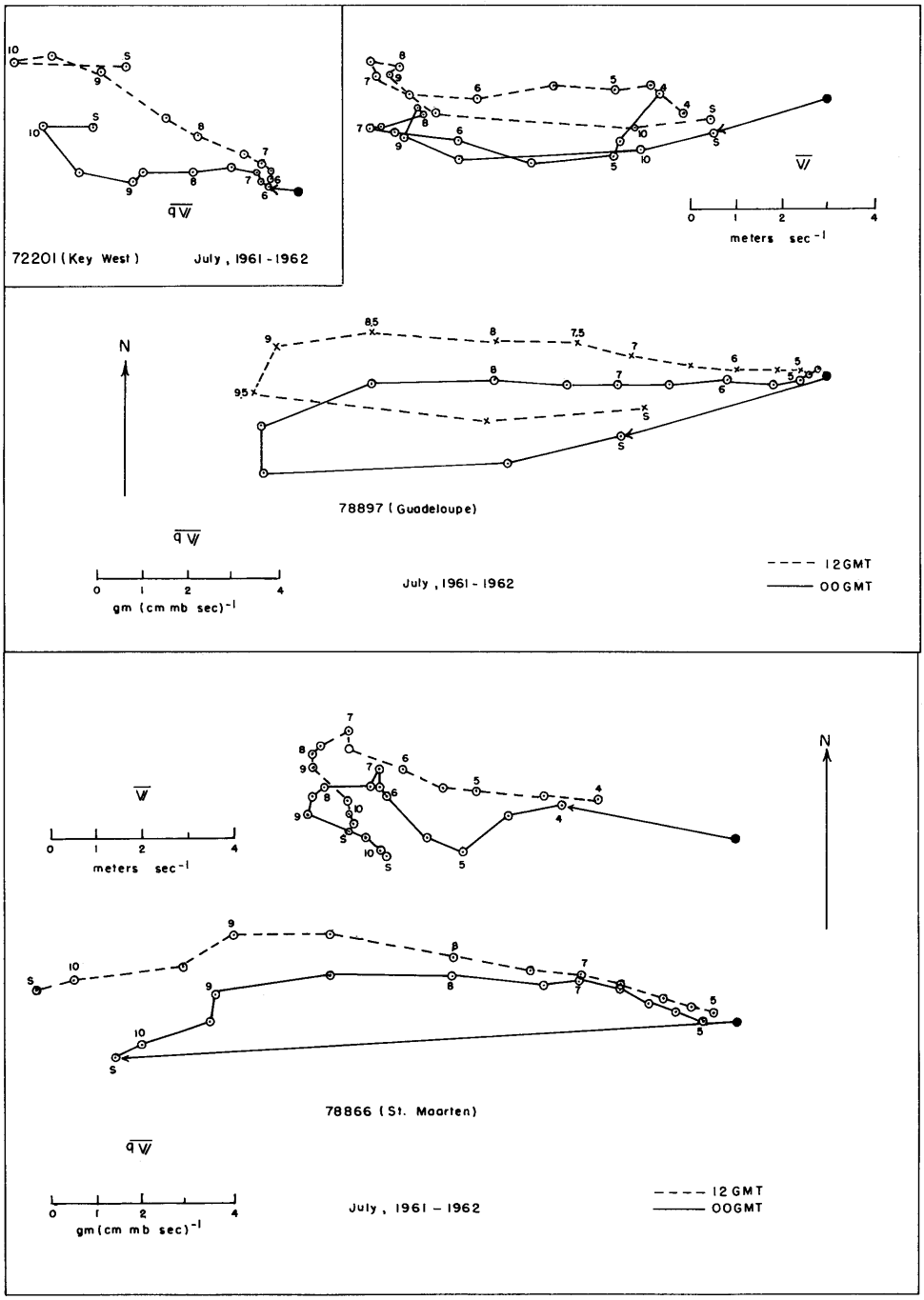


Figure 40. Hodographs: $\overline{qv}$ and $\overline{v}$. July, 1961-62. Origin denoted by solid circle. Pressure given in hundreds of millibars. "S" denotes surface value.

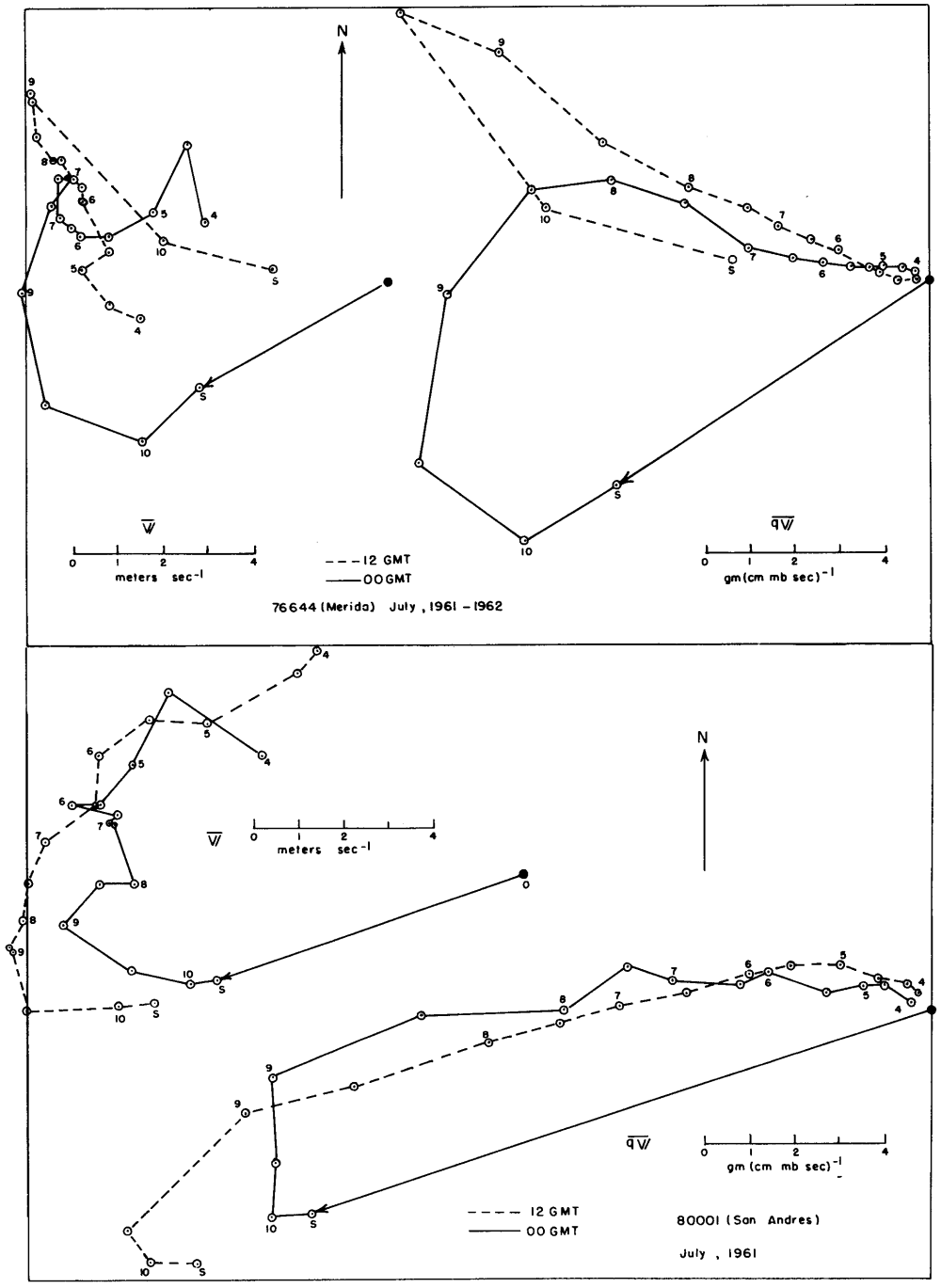


Figure 41. Hodographs: $\overline{qv}$ and $\overline{V}$. Origin denoted by solid circle. Pressure given in hundreds of millibars. "S" denotes surface value.

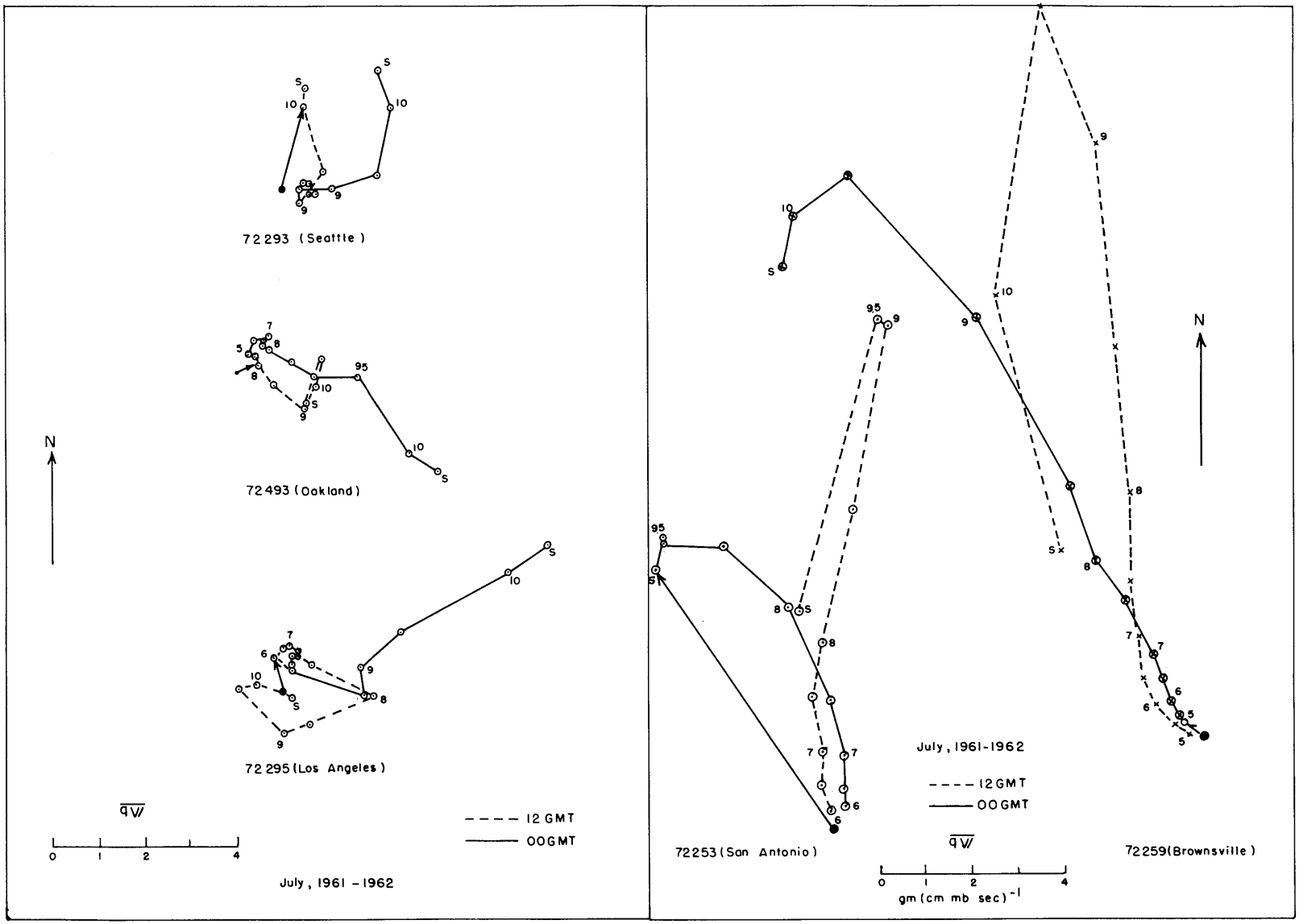


Figure 42. Hodographs: $\overline{qv}$ July, 1961-62. Origin denoted by solid circle. Pressure given in hundreds of millibars. "S" denotes surface value.

Figure 43. Hodographs: $\overline{\rho V}$ and $\overline{V}$ . Oklahoma City-Tinker AFB. Upper left: diurnal variations at the surface, 950, 900, 850 and 800 mb. GMT observation times given . 00 and 12 GMT observations taken at Oklahoma City; 06 and 18 GMT observations taken at Tinker AFB. Data for June-July 1961. Upper right: $\overline{\rho V}$ , Oklahoma City and Tinker AFB. Lower: $\overline{\rho V}$ and $\overline{V}$ for Oklahoma City for the period July 1961-1962. The origin is denoted by a solid circle. Pressure is given in hundreds of millibars. "S" denotes surface value.

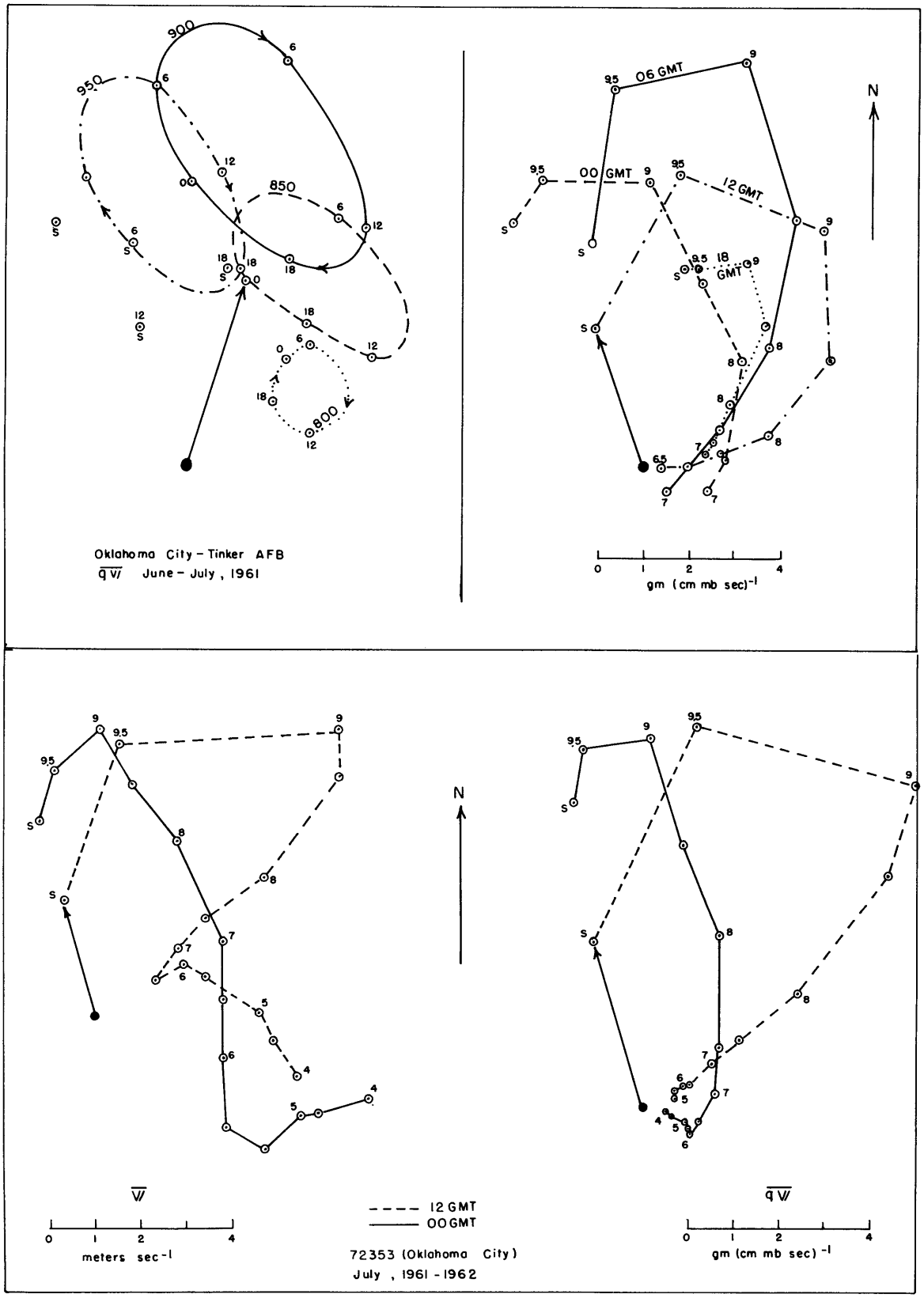
900
950
850
800
Oklahoma City - Tinker AFB
$\overline{qv}$ June - July, 1961
06 GMT
00 GMT
12 GMT
18 GMT
N
0 1 2 4
gm (cm mb sec)$^{-1}$
$\overline{v}$
meters sec$^{-1}$
12 GMT
00 GMT
72353 (Oklahoma City)
July, 1961 - 1962
$\overline{qv}$
gm (cm mb sec)$^{-1}$

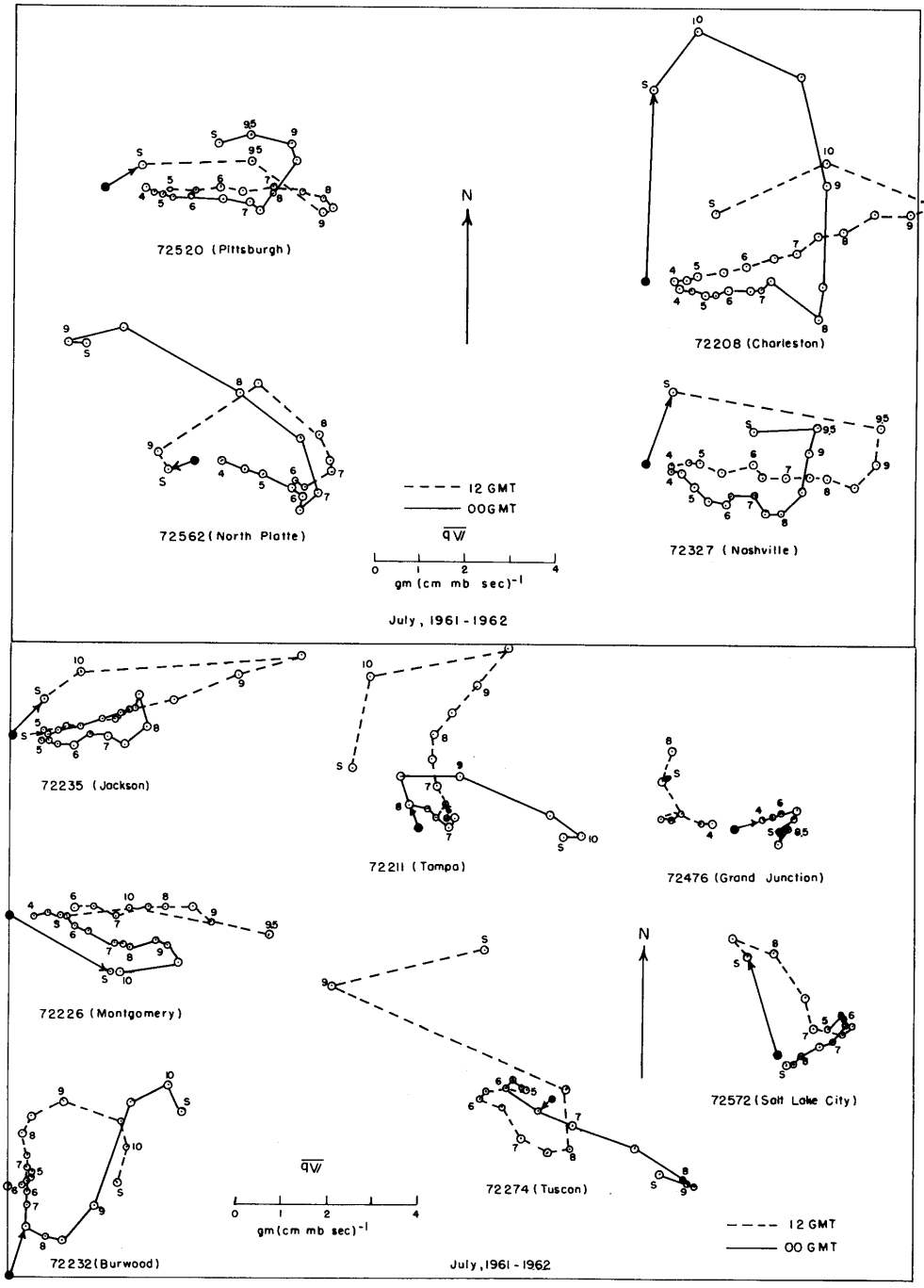


Figure 44. Hodographs: $\overline{qv}$ , July, 1961 and 1962. Origin denoted by solid circle. Pressure given in hundreds of millibars. "S" denotes value at the surface.

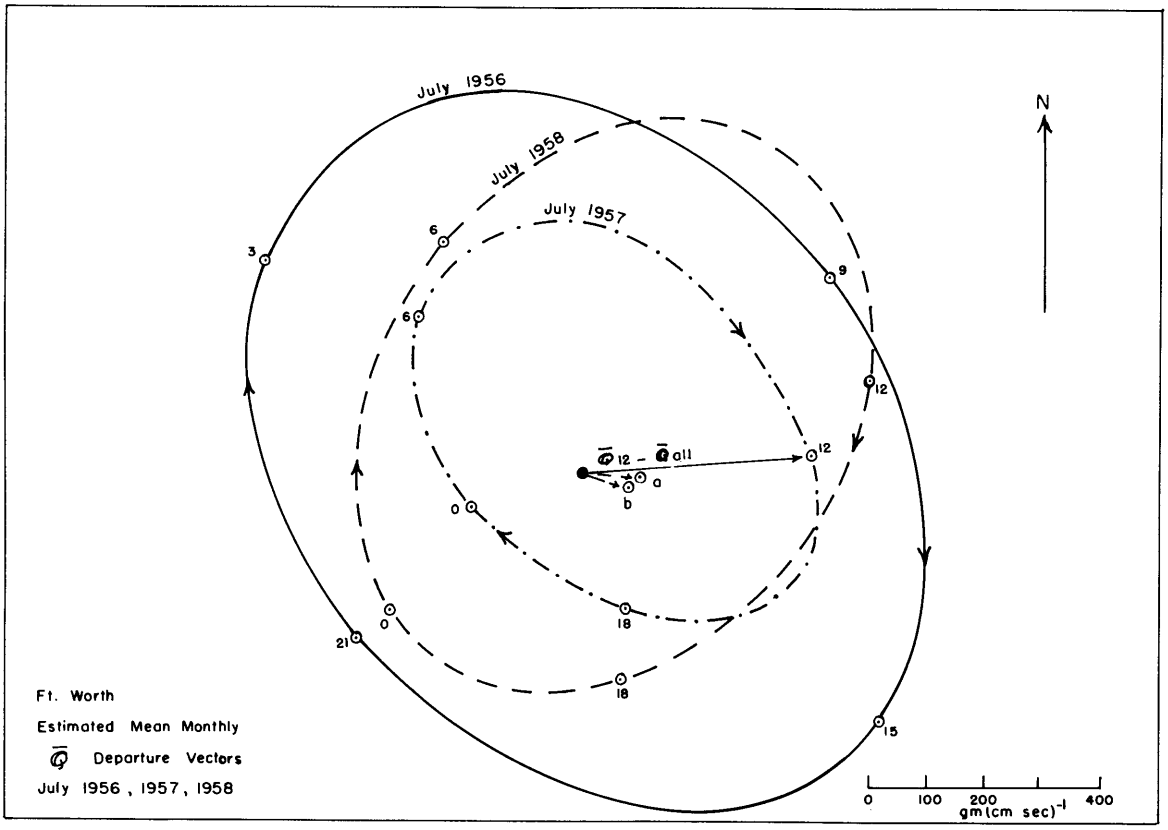


Figure 45. Estimated vertically integrated mean total flux departure vector, Ft. Worth, July 1956, 1957, 1958. GMT observation times are shown. Origin (vector mean of the 4 daily observations) denoted by solid circle. Also shown are the differences between the mean of the 12 GMT and 00 GMT observations, and the mean of all observations for July, 1957 (o-a) and July 1958 (o-b).

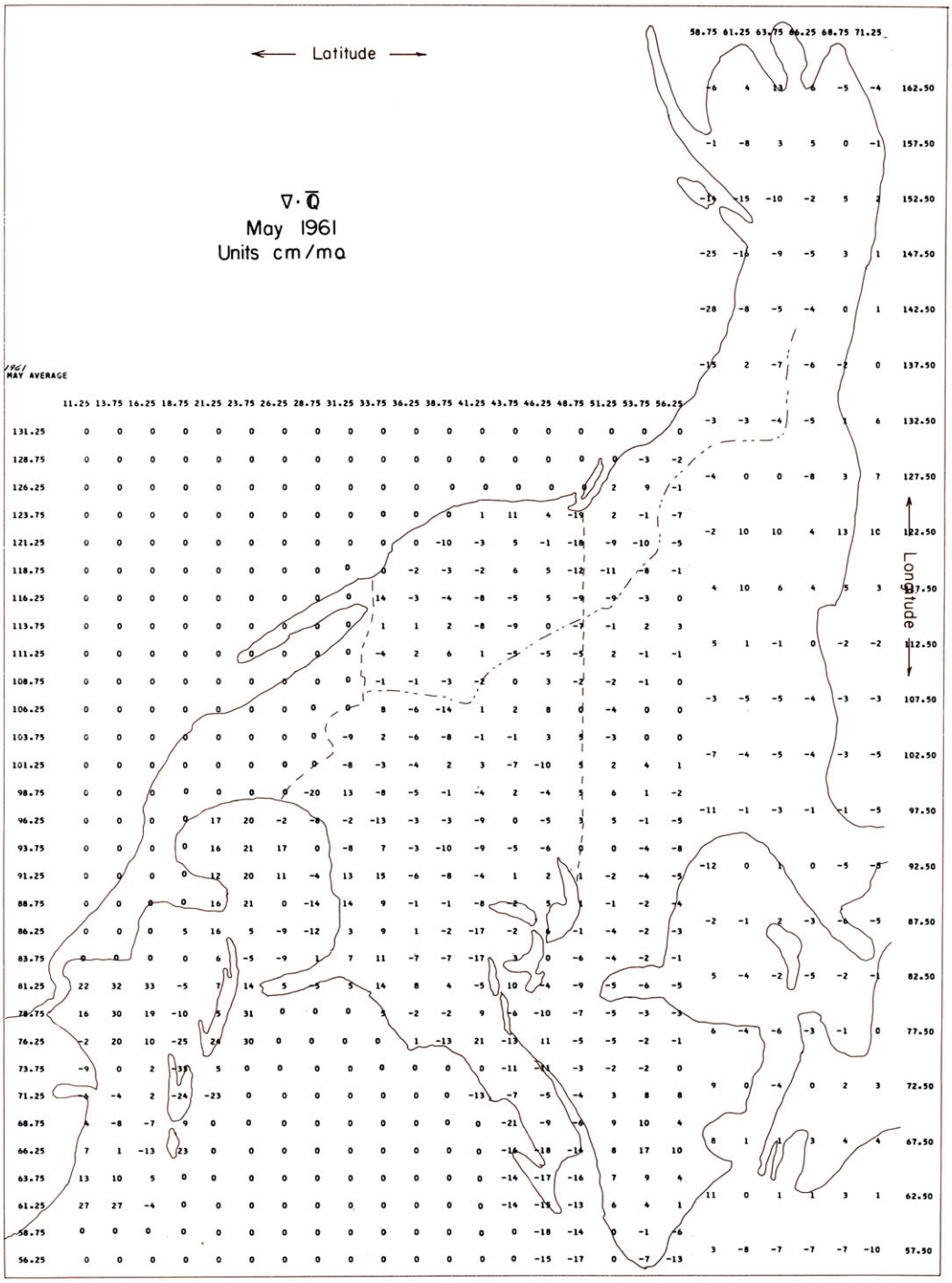


Figure 46. Mean monthly divergence of the vertically integrated water vapor flux. May, 1961. Units: gm $(cm^2\ mo)^{-1}$.

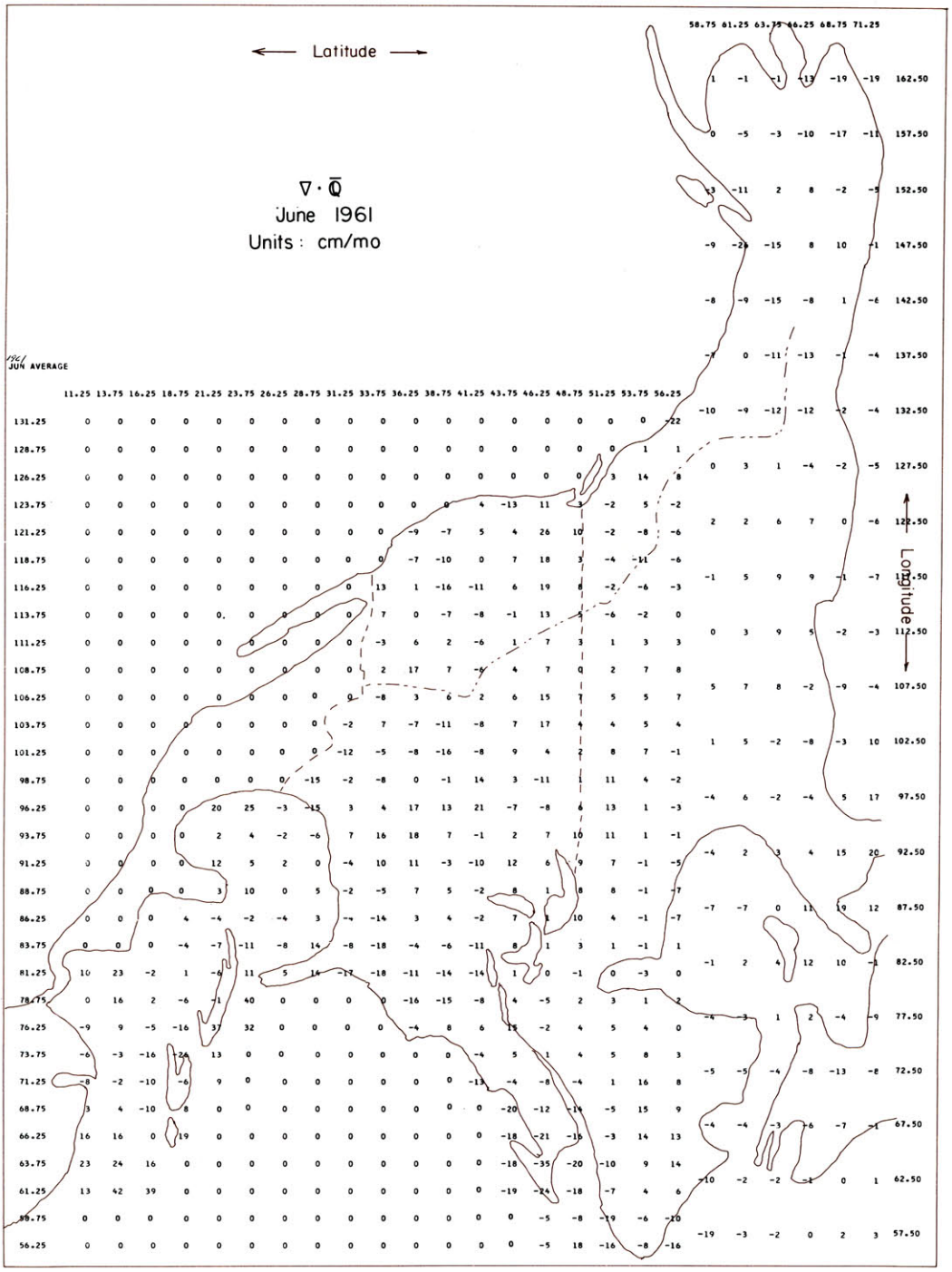


Figure 47. Mean monthly divergence of the vertically integrated water vapor flux. June, 1961. Units: gm $(cm^2\ mo)^{-1}$.

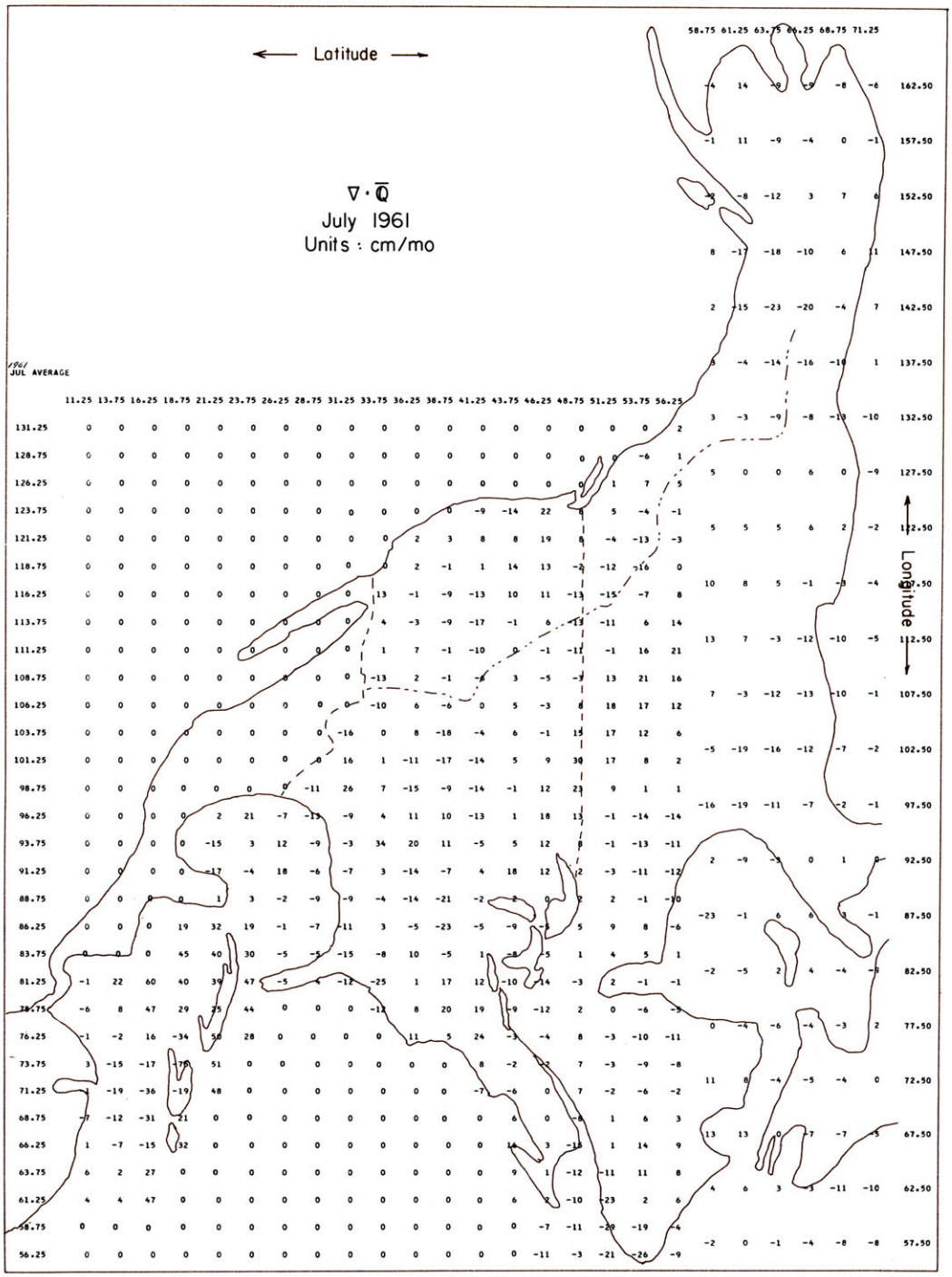


Figure 48. Mean monthly divergence of the vertically integrated water vapor flux. July, 1961. Units: gm $(cm^2\ mo)^{-1}$.

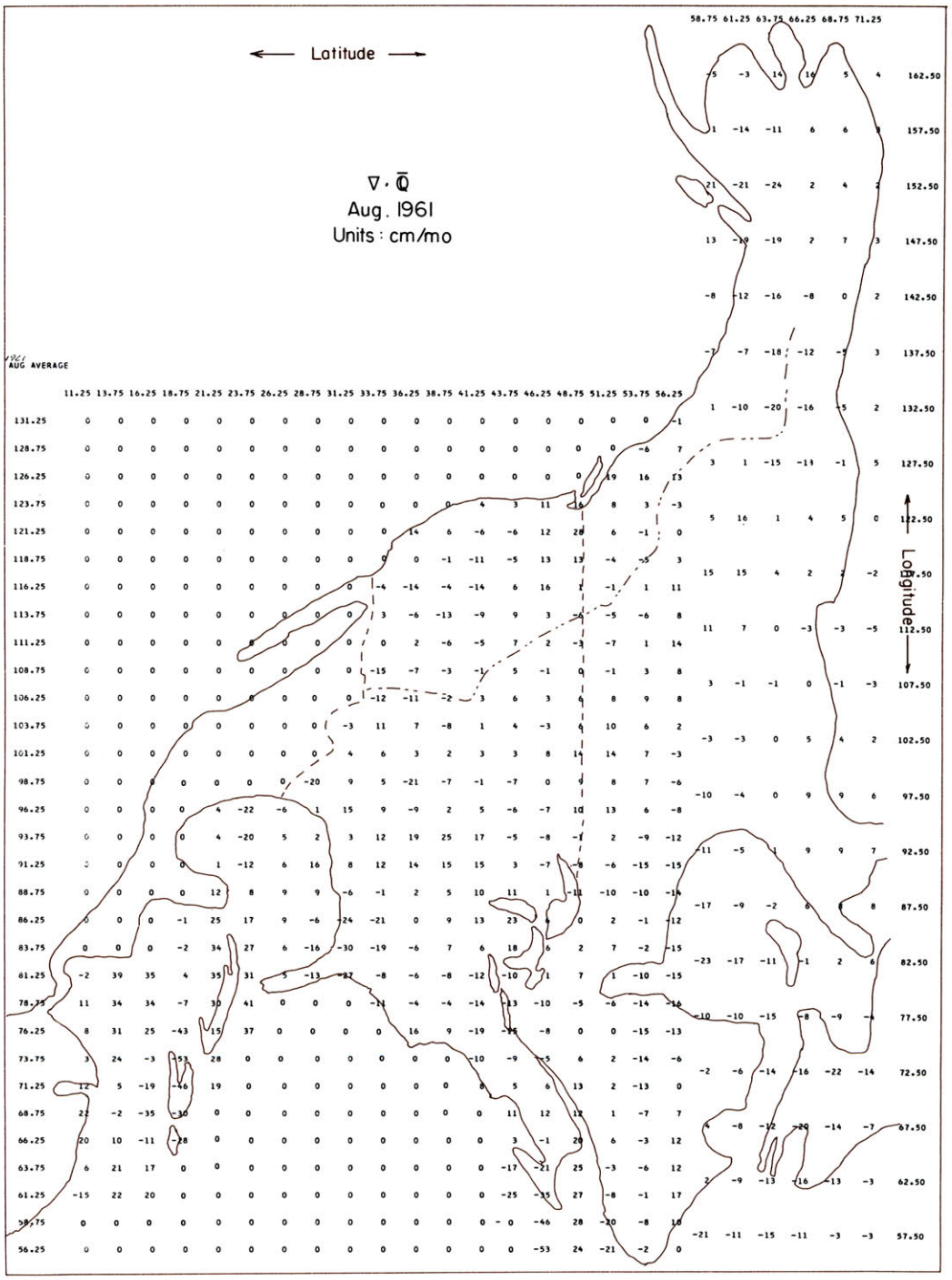


Figure 49. Mean monthly divergence of the vertically integrated water vapor flux. August, 1961. Units: gm $(cm^2\ mo)^{-1}$.

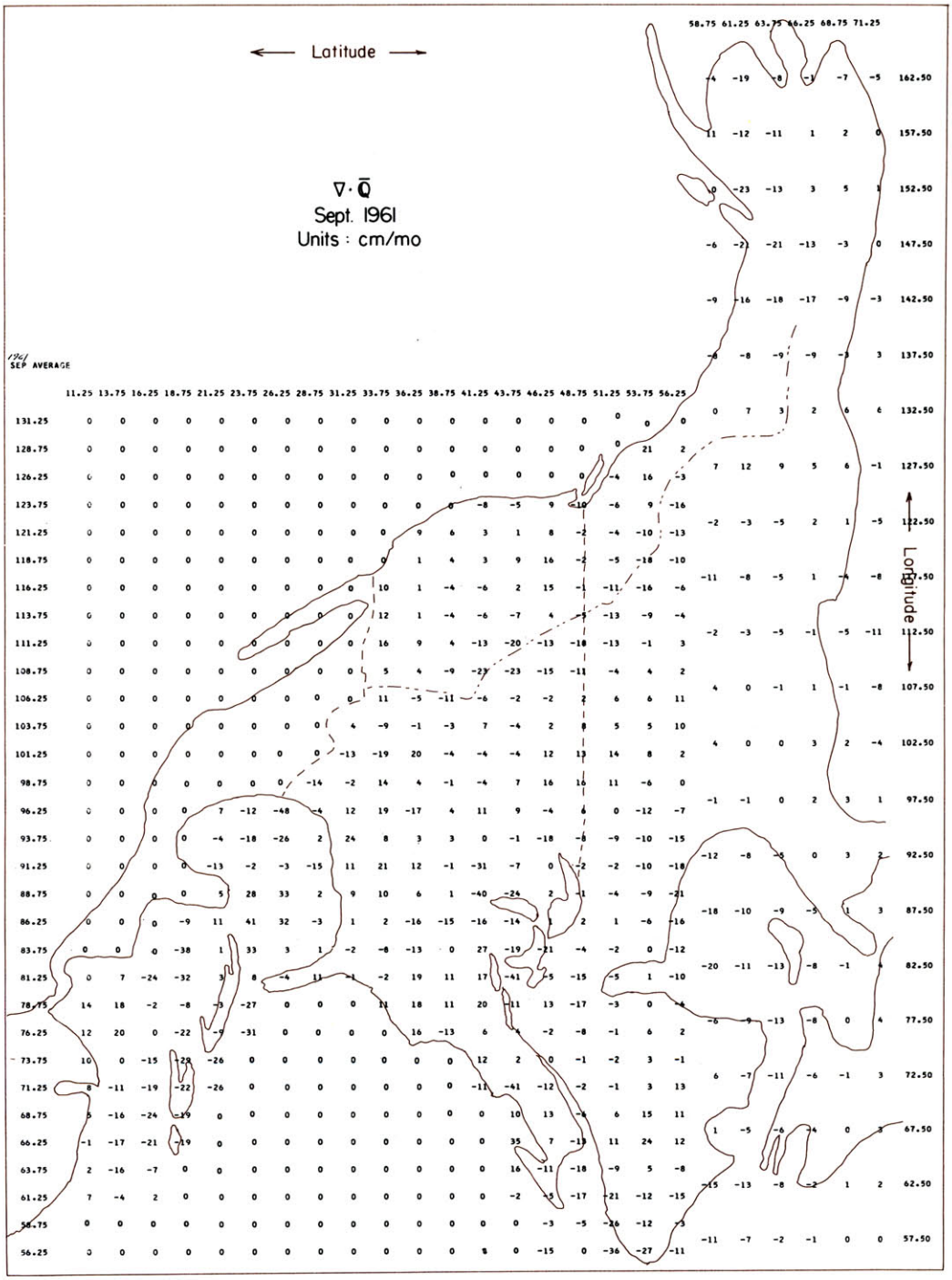


Figure 50. Mean monthly divergence of the vertically integrated water vapor flux. September, 1961. Units: gm $(cm^2\ mo)^{-1}$.

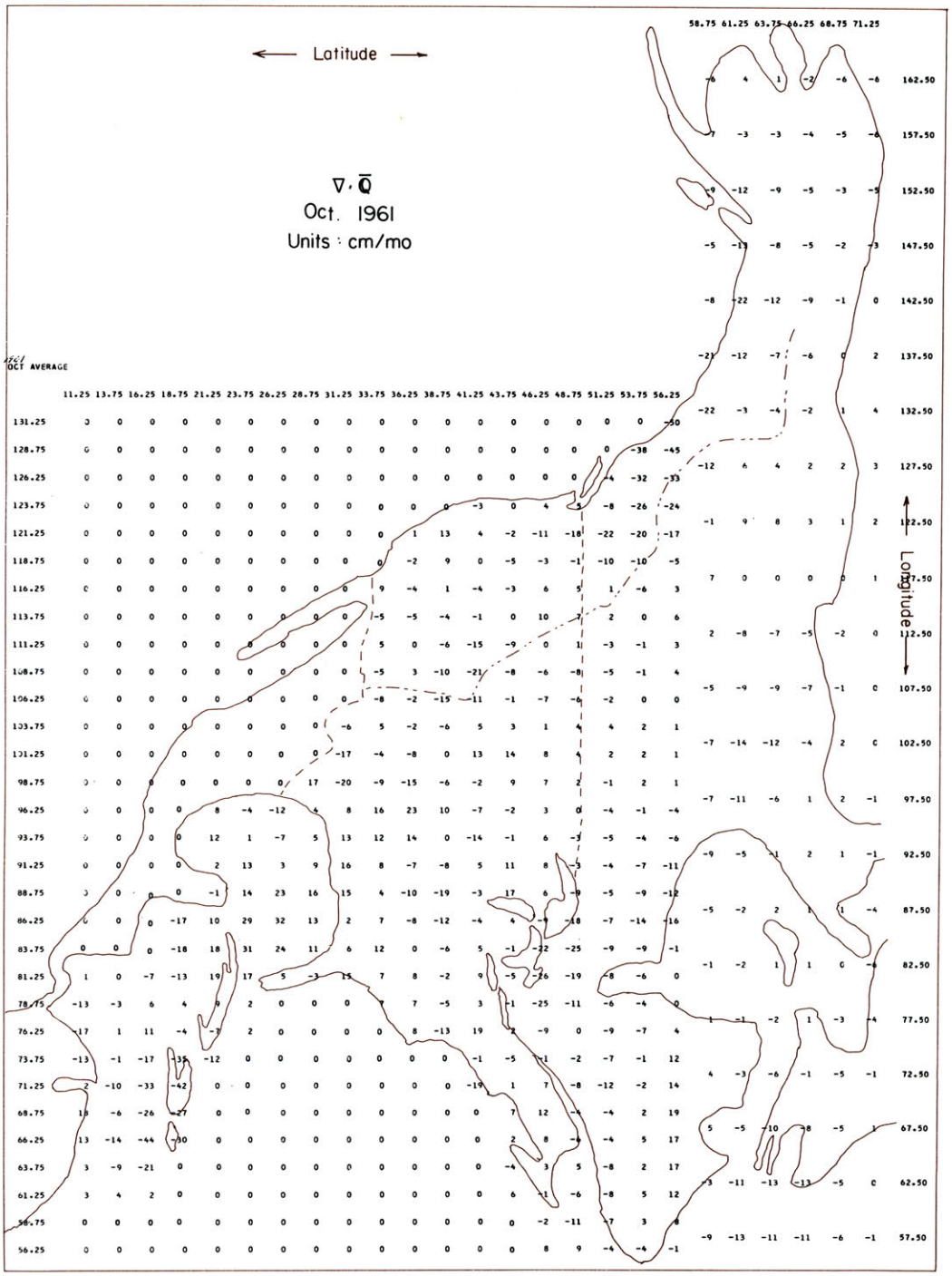


Figure 51. Mean monthly divergence of the vertically integrated water vapor flux. October, 1961. Units: gm $(cm^2\ mo)^{-1}$.

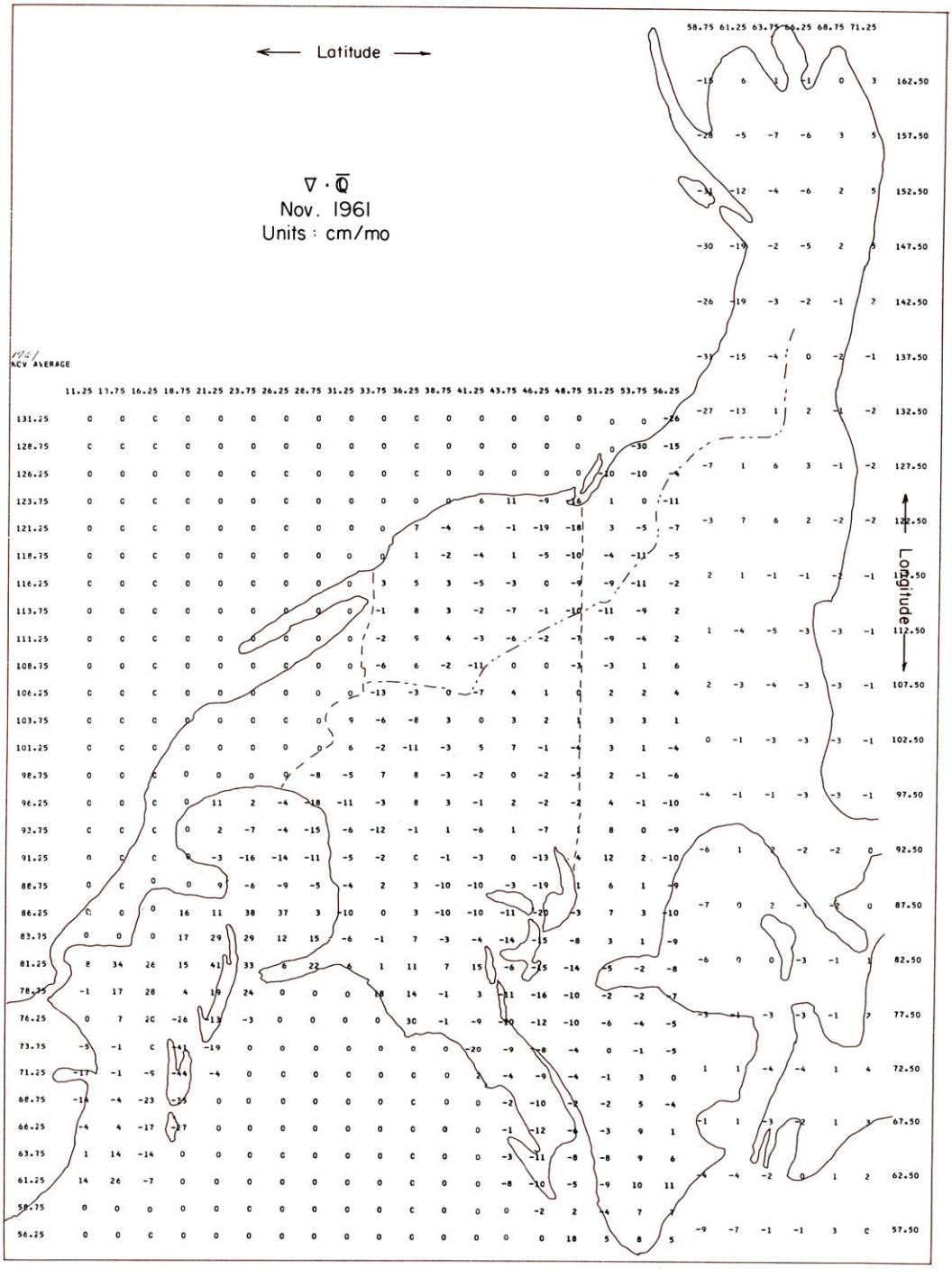


Figure 52. Mean monthly divergence of the vertically integrated water vapor flux. November, 1961. Units: gm $(cm^2\ mo)^{-1}$.

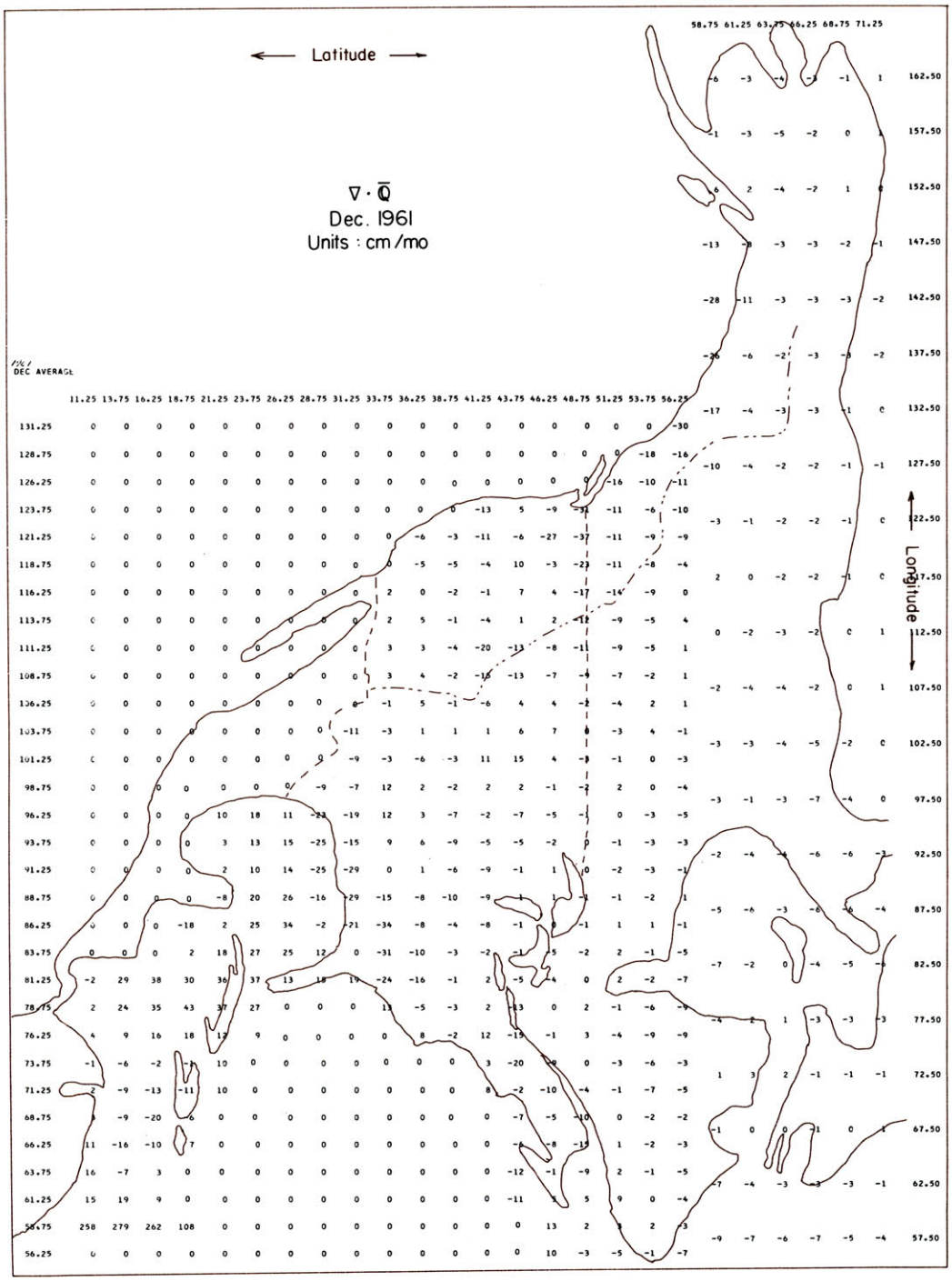


Figure 53. Mean monthly divergence of the vertically integrated water vapor flux. December, 1961. Units: gm $(cm^2\ mo)^{-1}$.

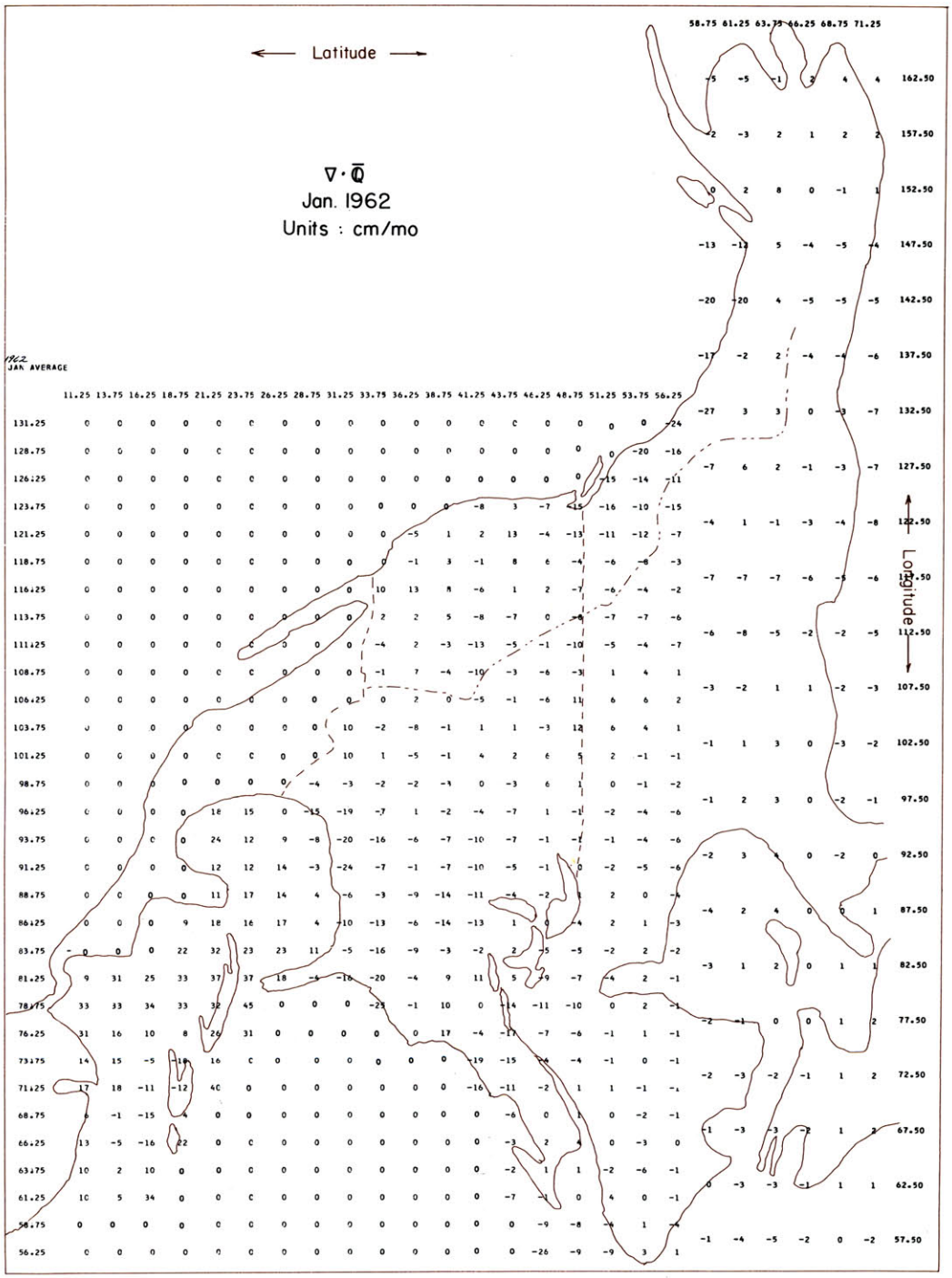


Figure 54. Mean monthly divergence of the vertically integrated water vapor flux. January, 1962. Units: gm $(cm^2\ mo)^{-1}$.

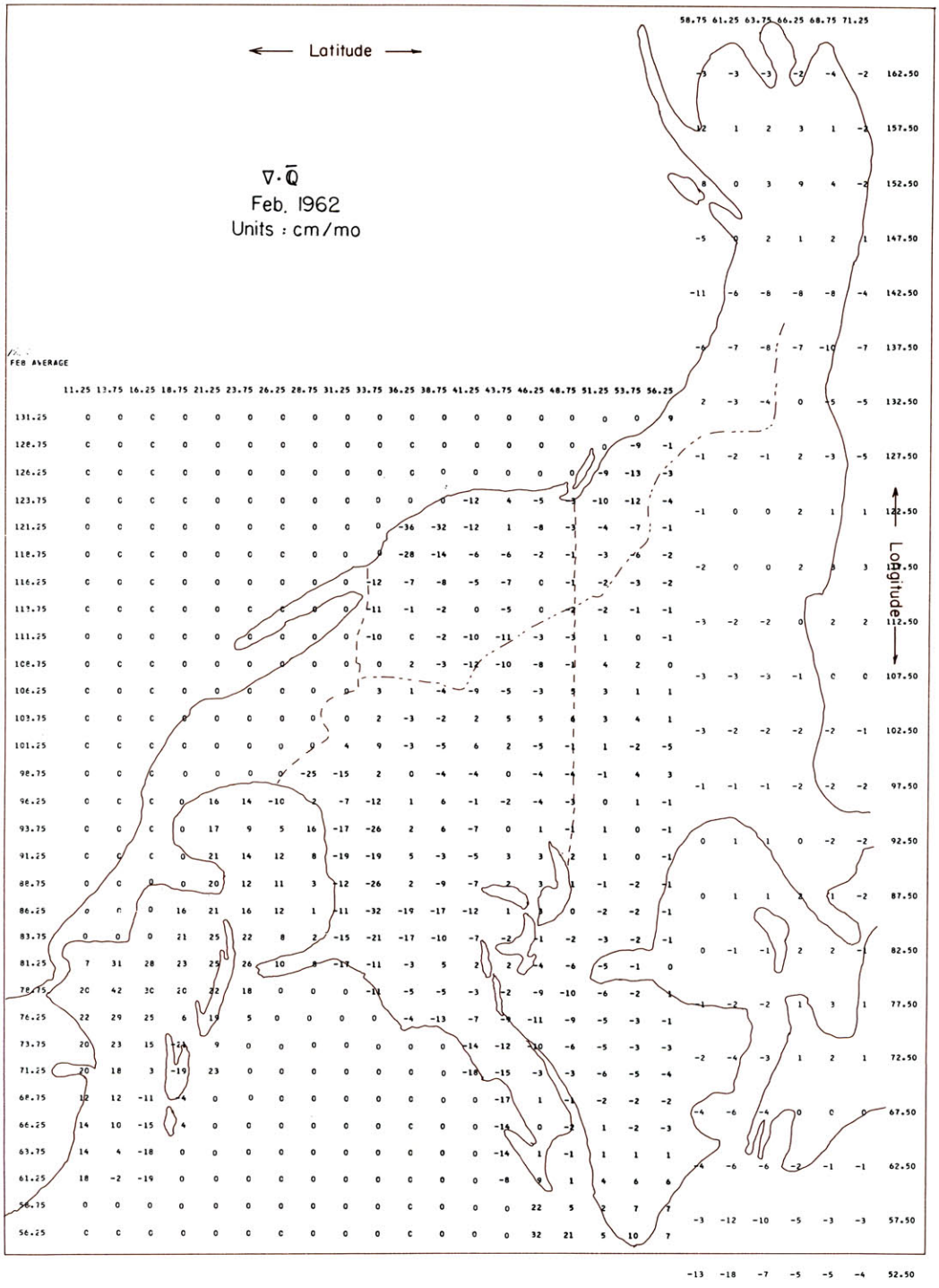


Figure 55. Mean monthly divergence of the vertically integrated water vapor flux. February, 1962. Units: gm $(cm^2\ mo)^{-1}$.

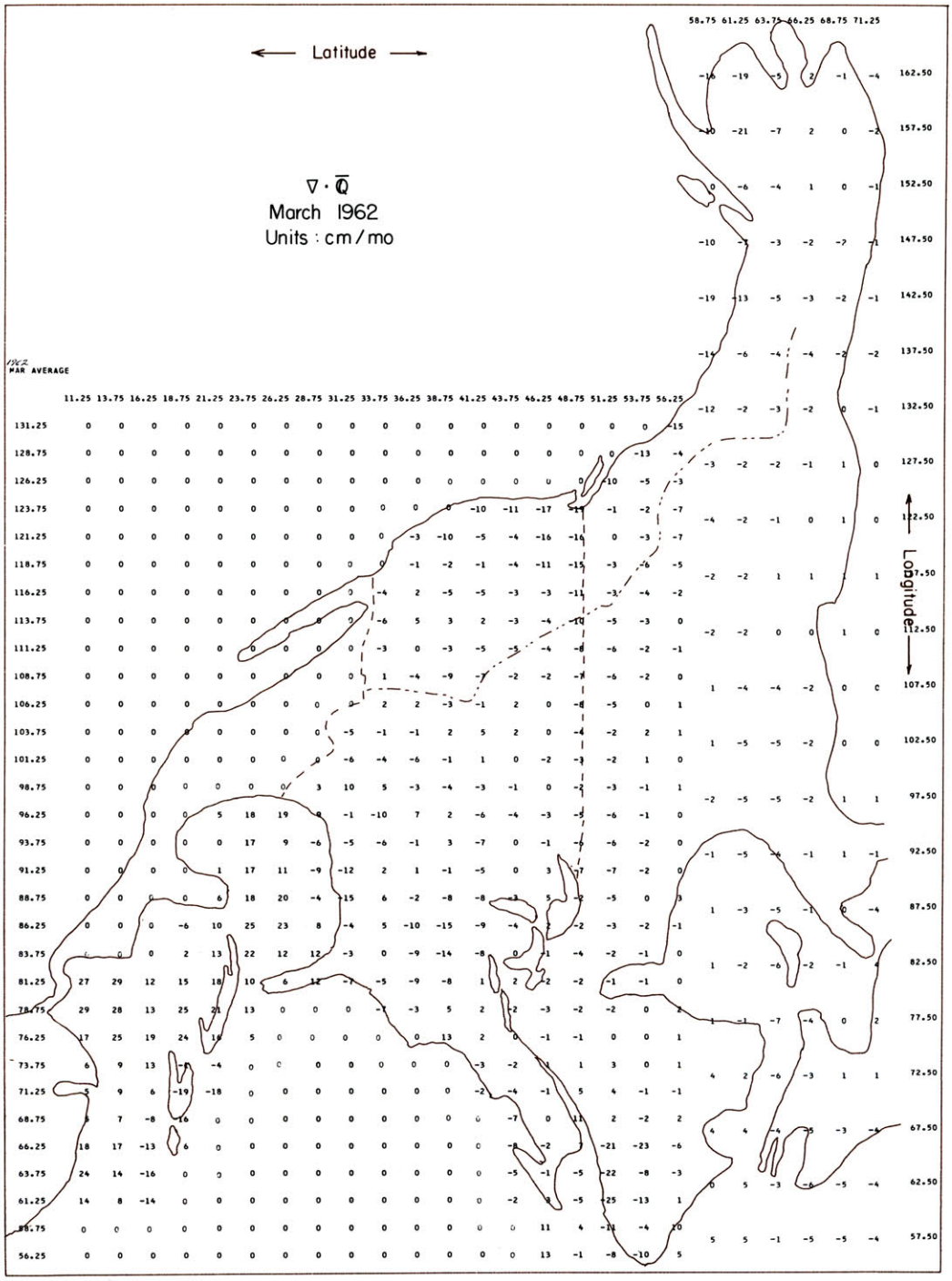


Figure 56. Mean monthly divergence of the vertically integrated water vapor flux. March, 1962. Units: gm $(cm^2\ mo)^{-1}$.

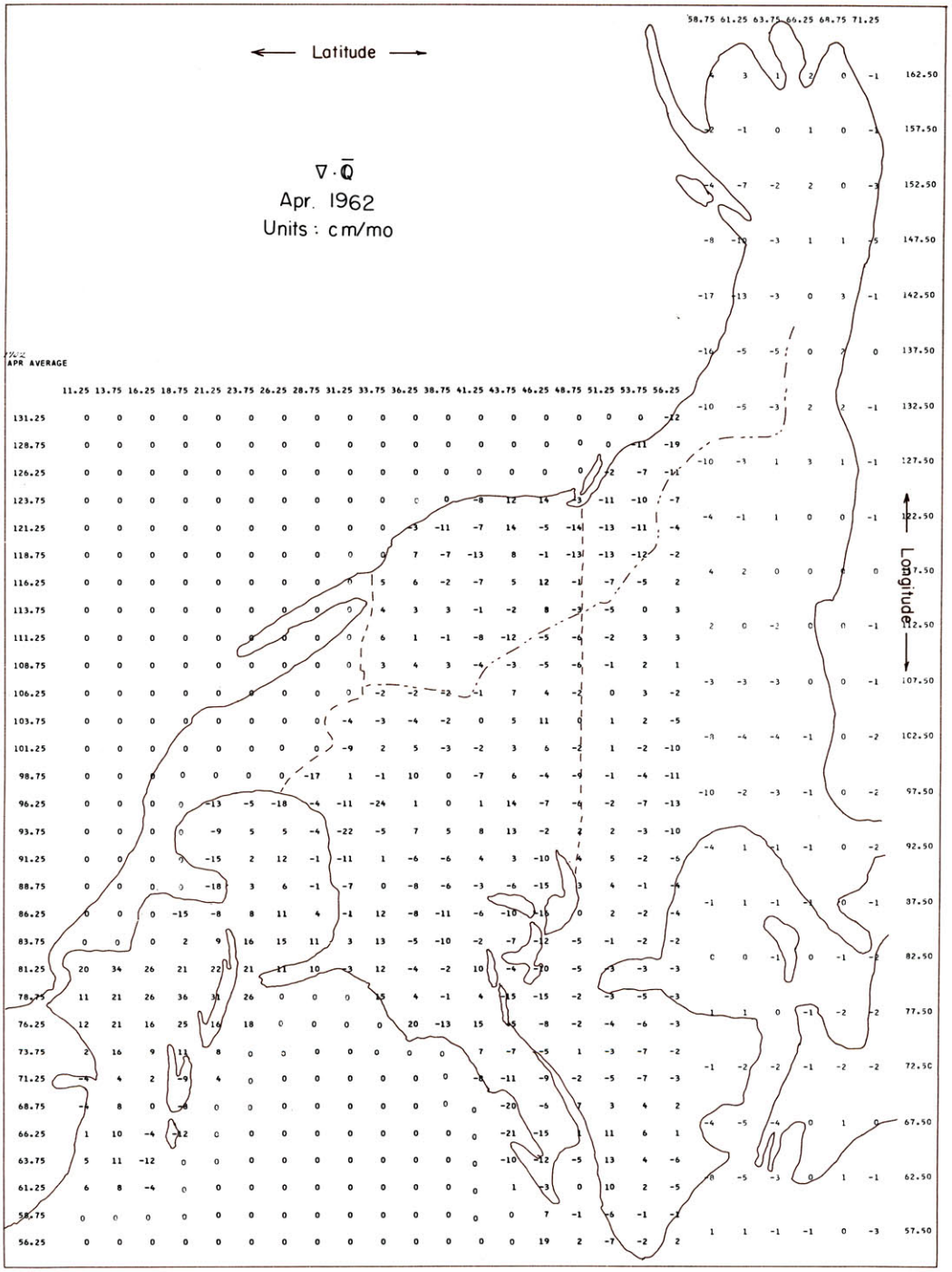


Figure 57. Mean monthly divergence of the vertically integrated water vapor flux. April, 1962. Units: gm $(cm^2\ mo)^{-1}$.

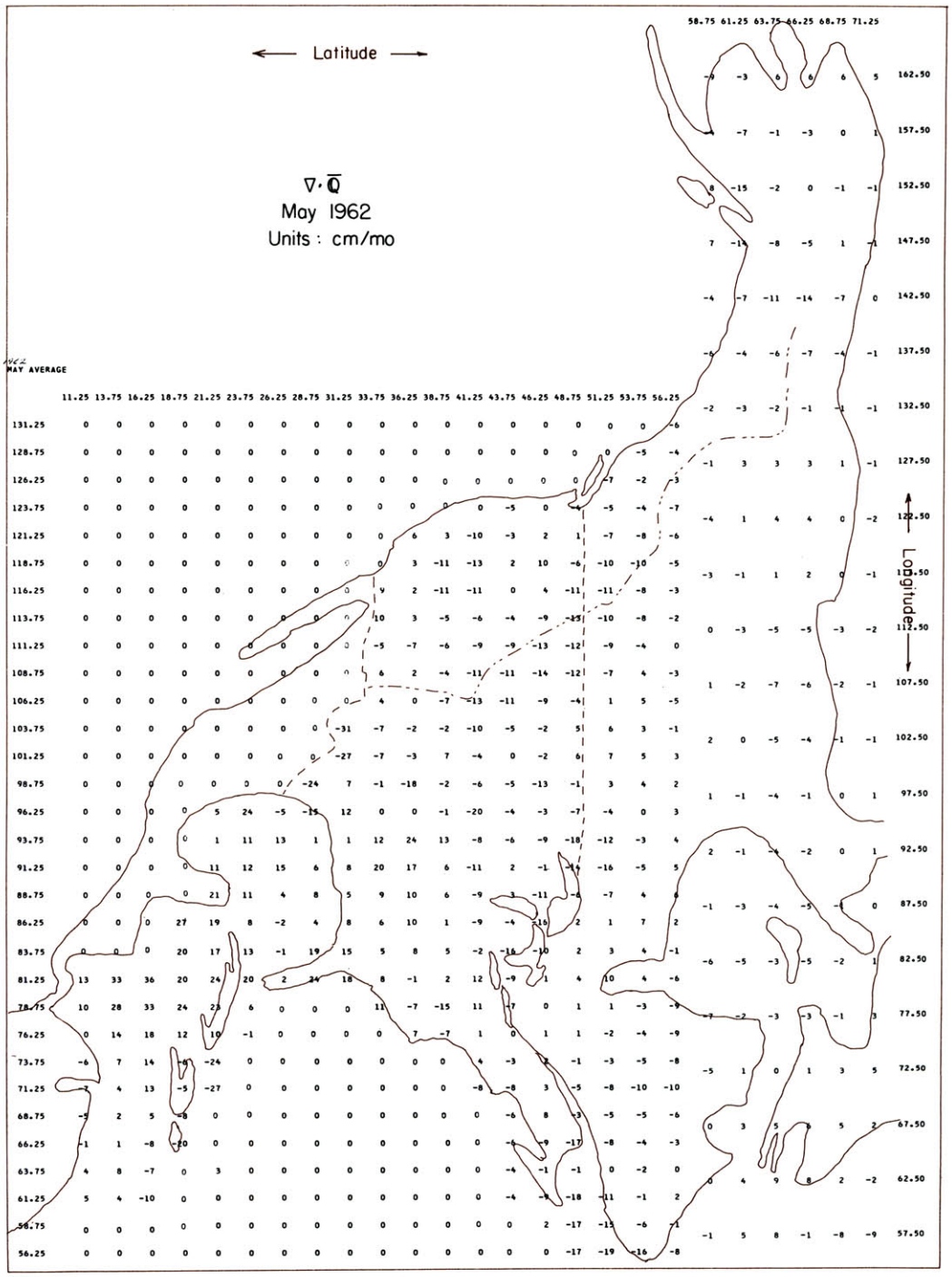


Figure 58. Mean monthly divergence of the vertically integrated water vapor flux. May, 1962. Units: gm $(cm^2\ mo)^{-1}$.

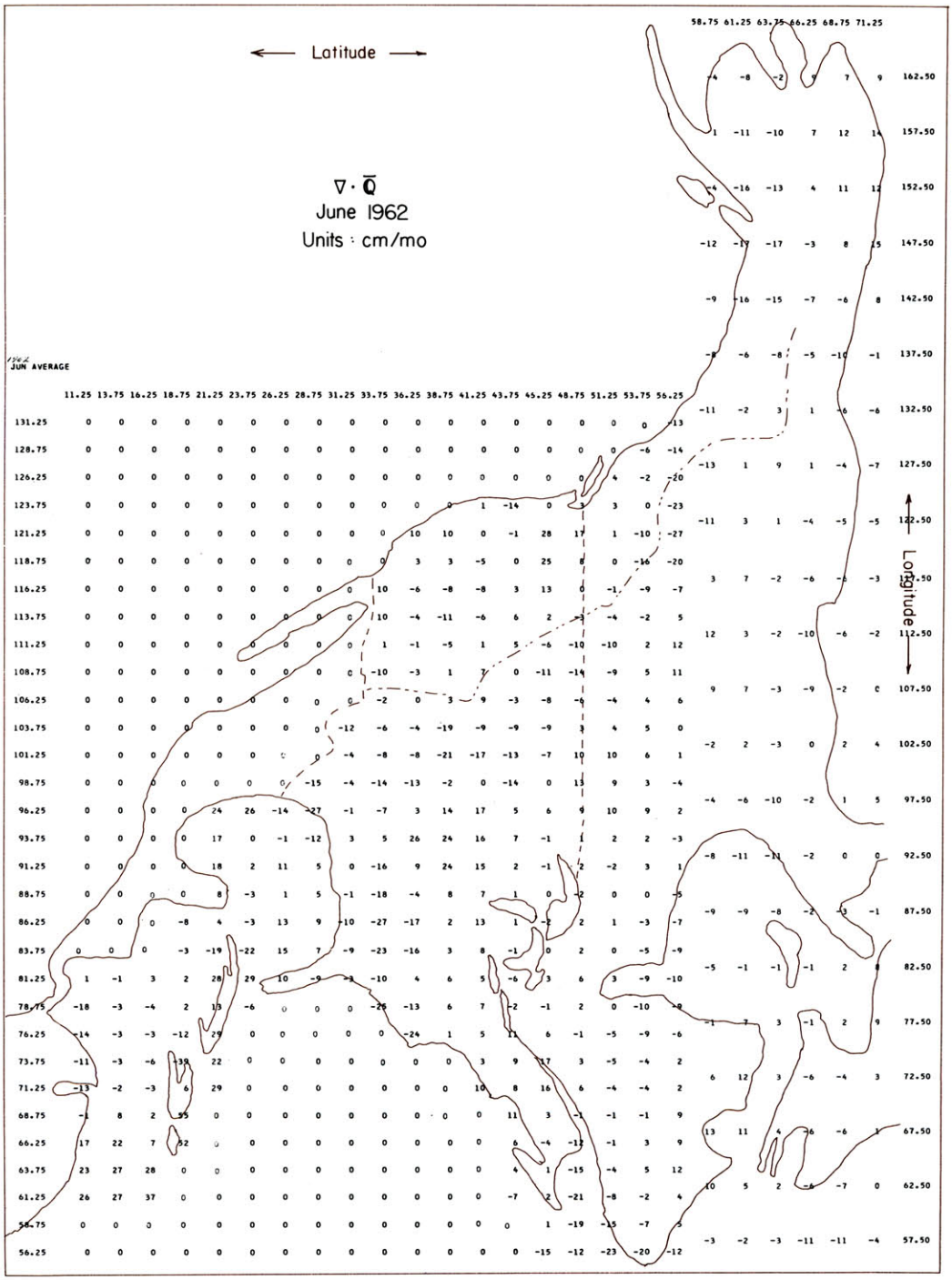


Figure 59. Mean monthly divergence of the vertically integrated water vapor flux. June, 1962. Units: gm $(cm^2\ mo)^{-1}$.

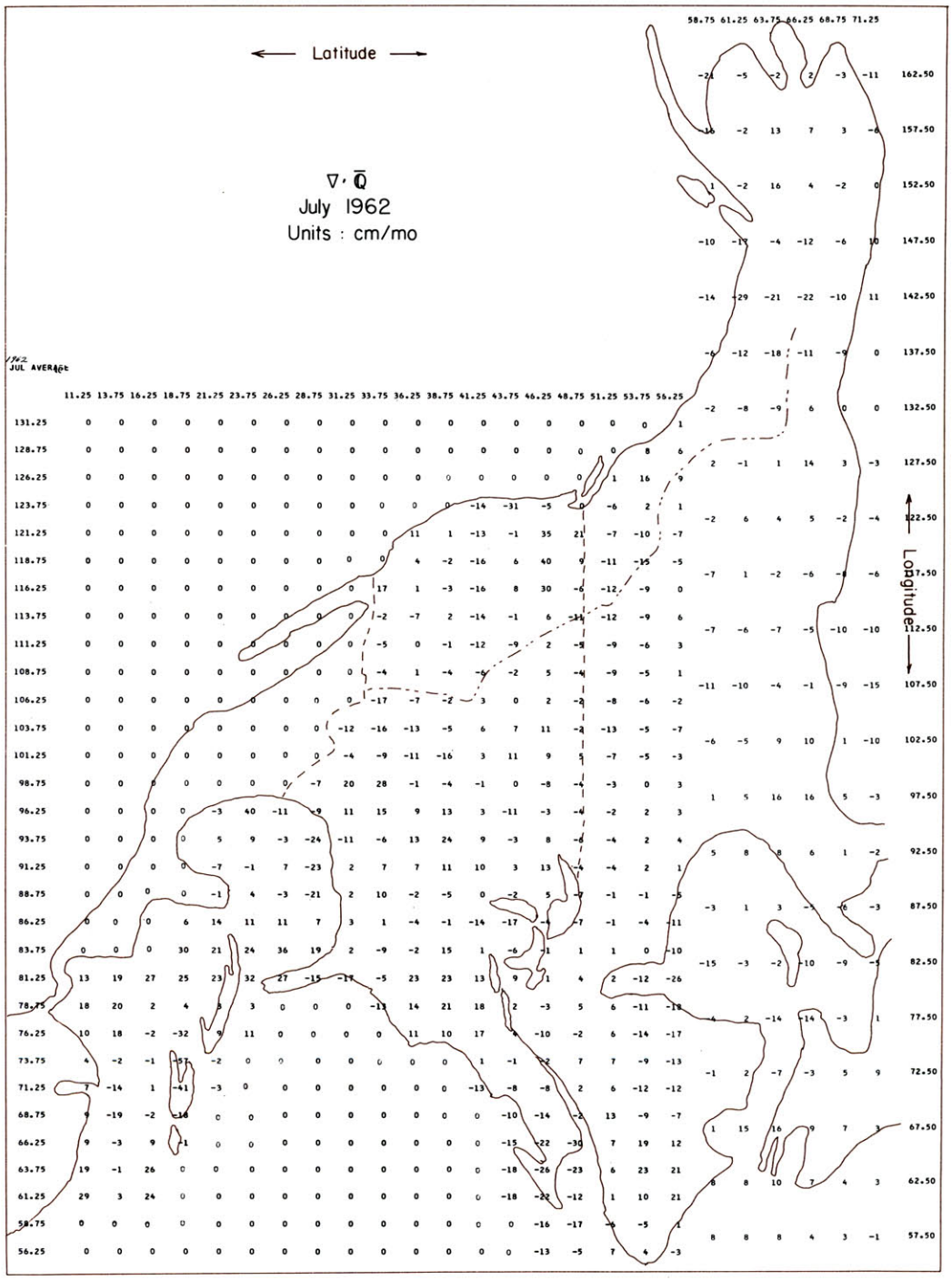


Figure 60. Mean monthly divergence of the vertically integrated water vapor flux. July, 1962. Units: gm $(cm^2\ mo)^{-1}$.

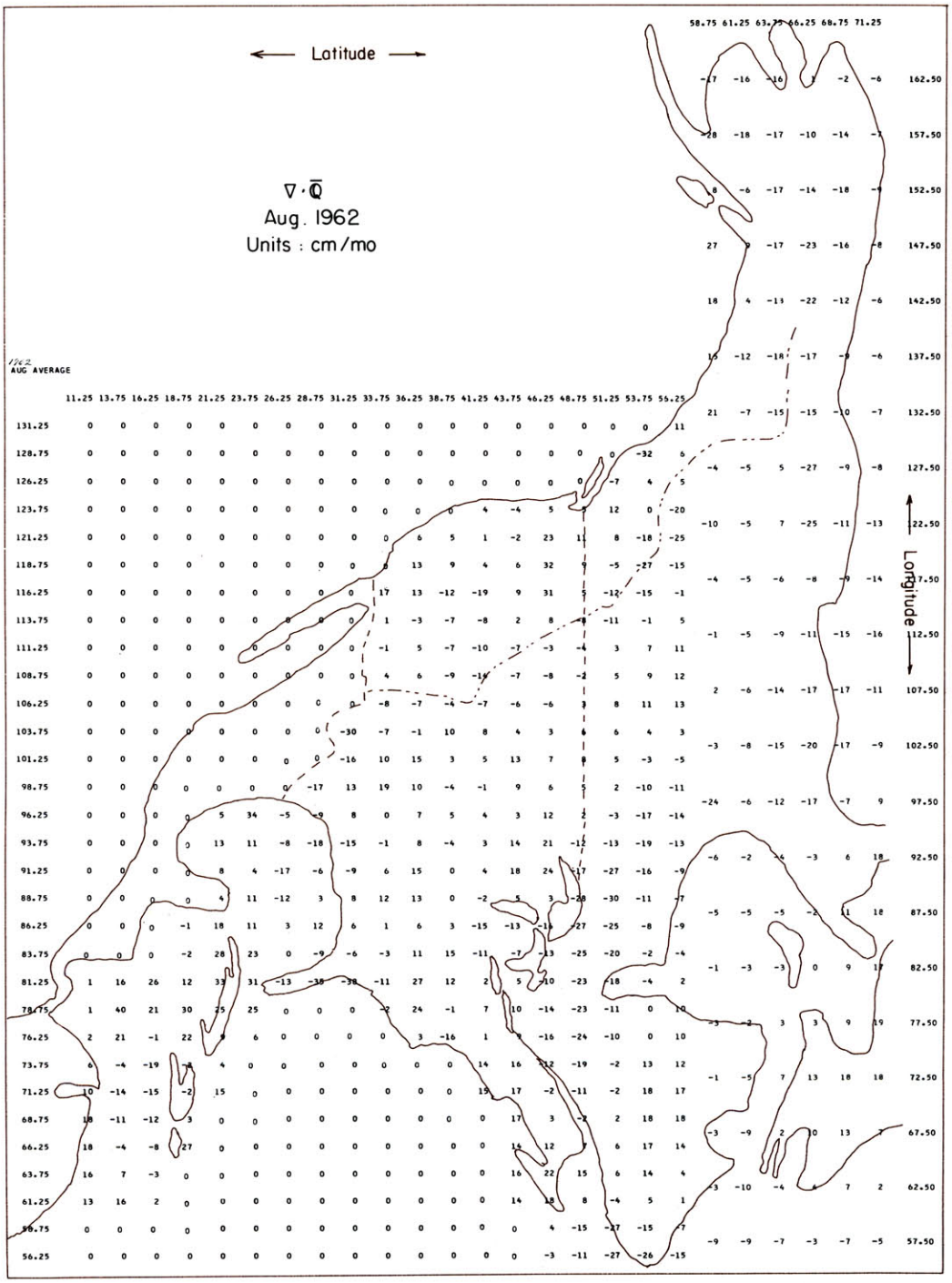


Figure 61. Mean monthly divergence of the vertically integrated water vapor flux. August, 1962. Units: gm $(cm^2\ mo)^{-1}$.

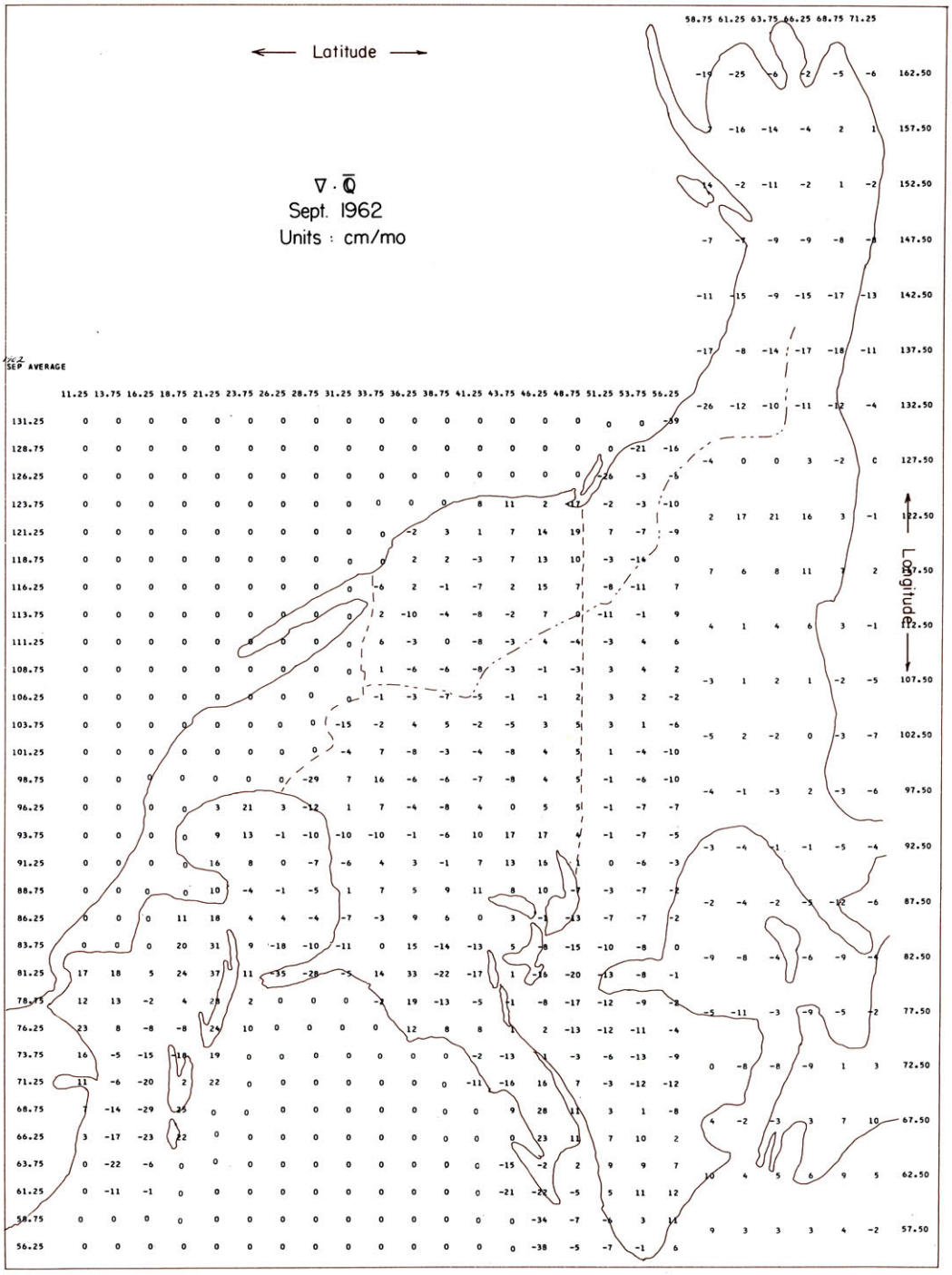


Figure 62. Mean monthly divergence of the vertically integrated water vapor flux. September, 1962. Units: gm $(cm^2\ mo)^{-1}$.

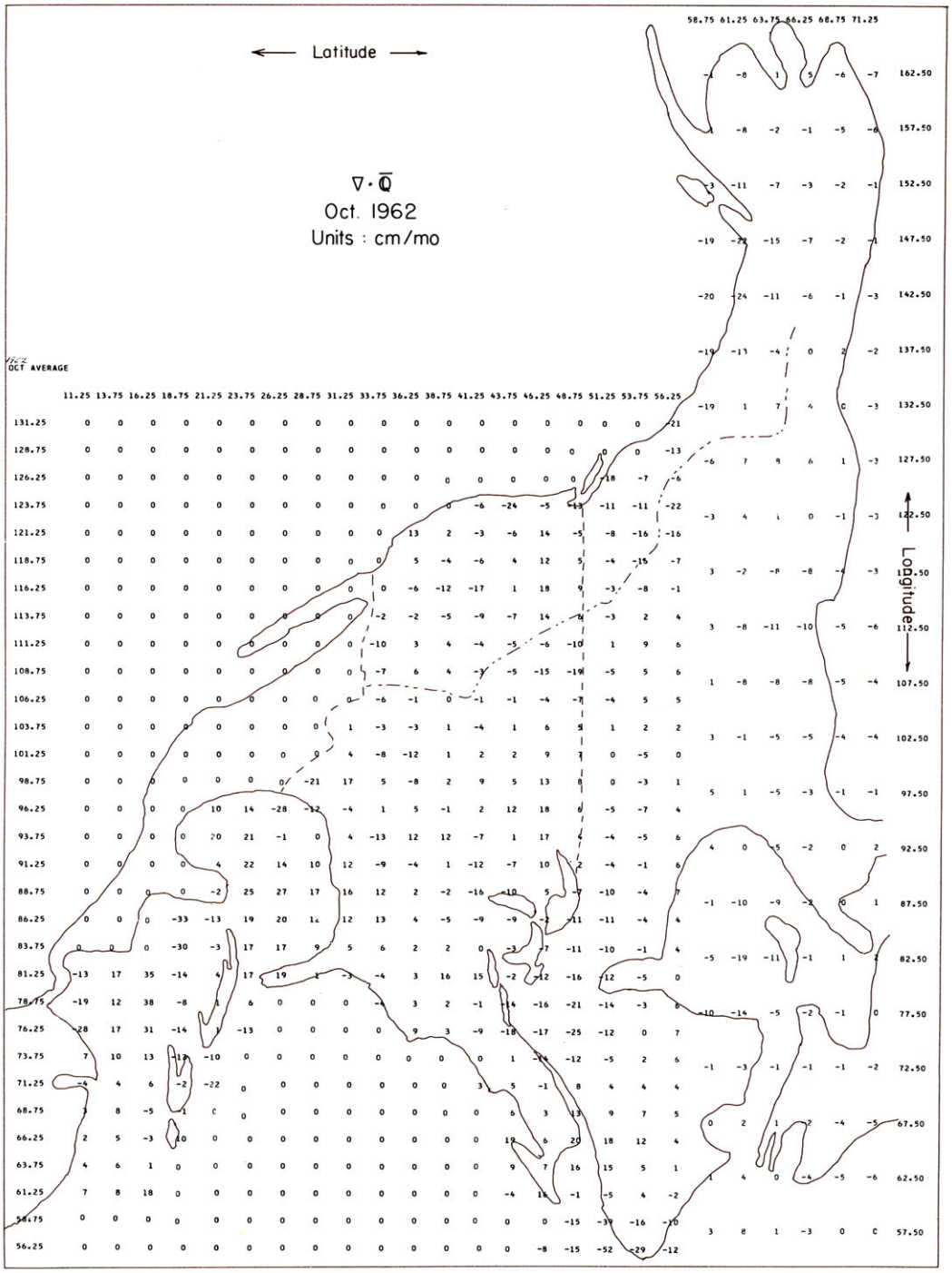


Figure 63. Mean monthly divergence of the vertically integrated water vapor flux. October, 1962. Units: gm $(cm^2\ mo)^{-1}$.

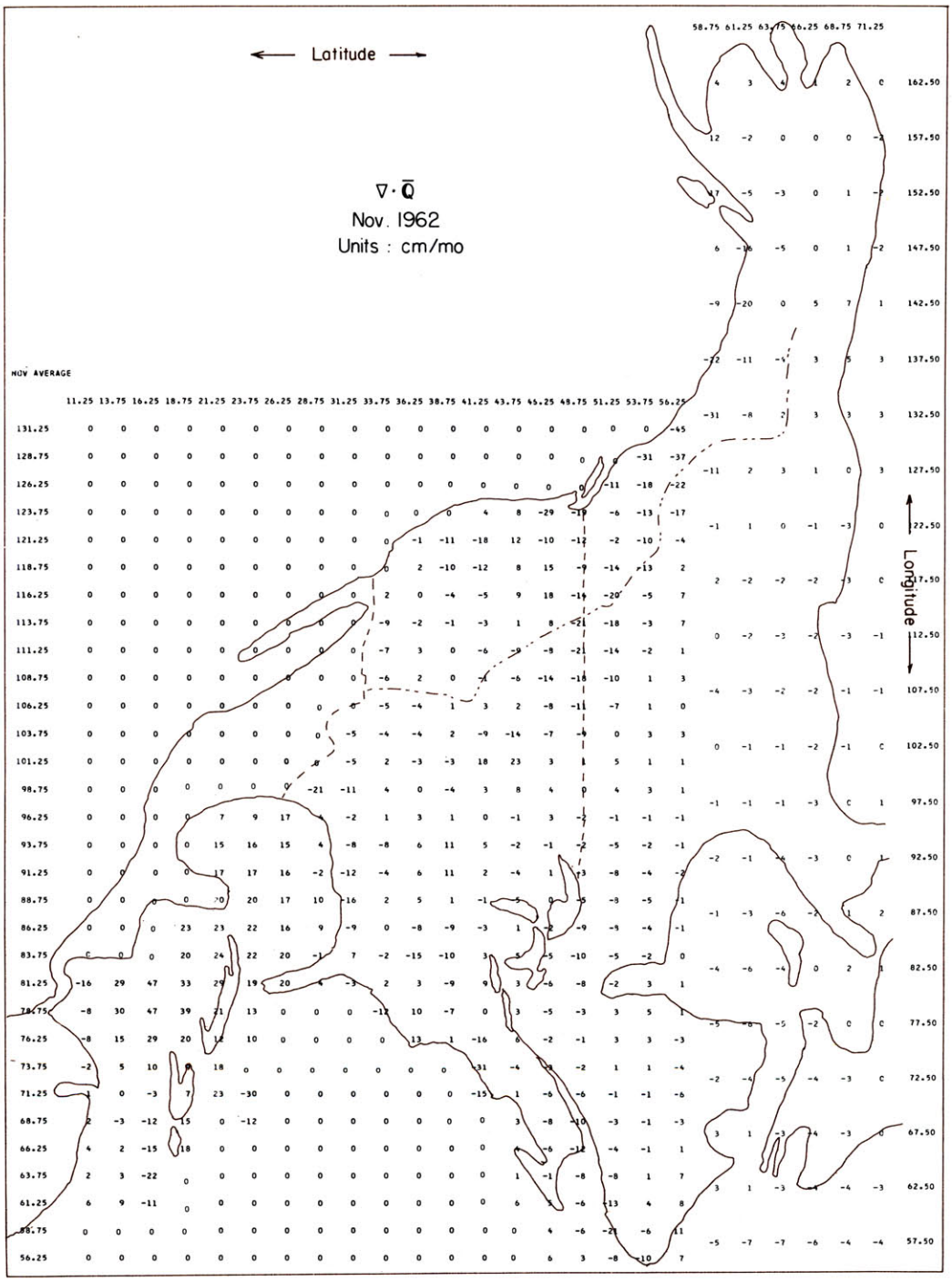


Figure 64. Mean monthly divergence of the vertically integrated water vapor flux. November, 1962. Units: gm $(cm^2\ mo)^{-1}$.

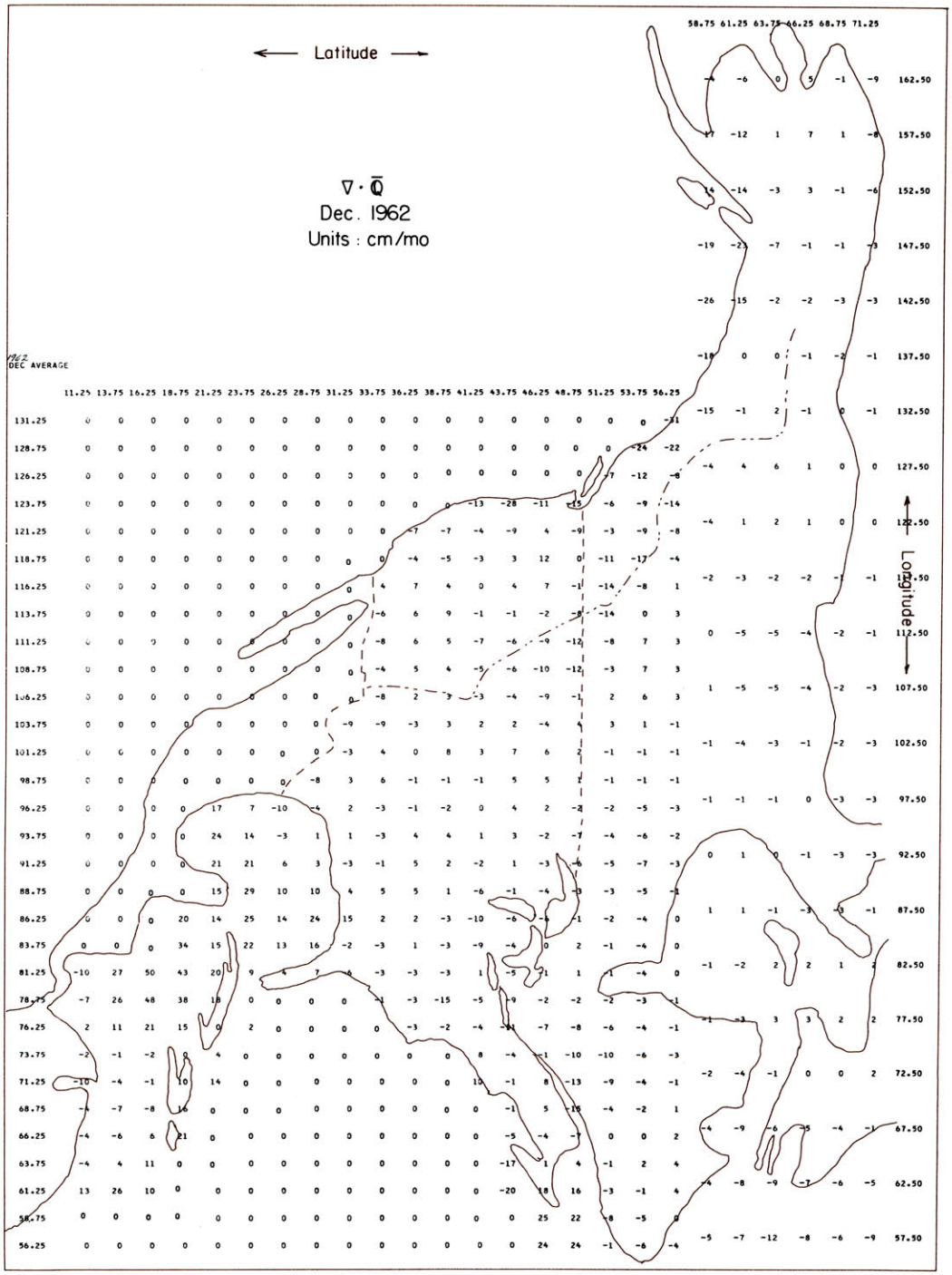


Figure 65. Mean monthly divergence of the vertically integrated water vapor flux. December, 1962. Units: gm $(cm^2\ mo)^{-1}$.

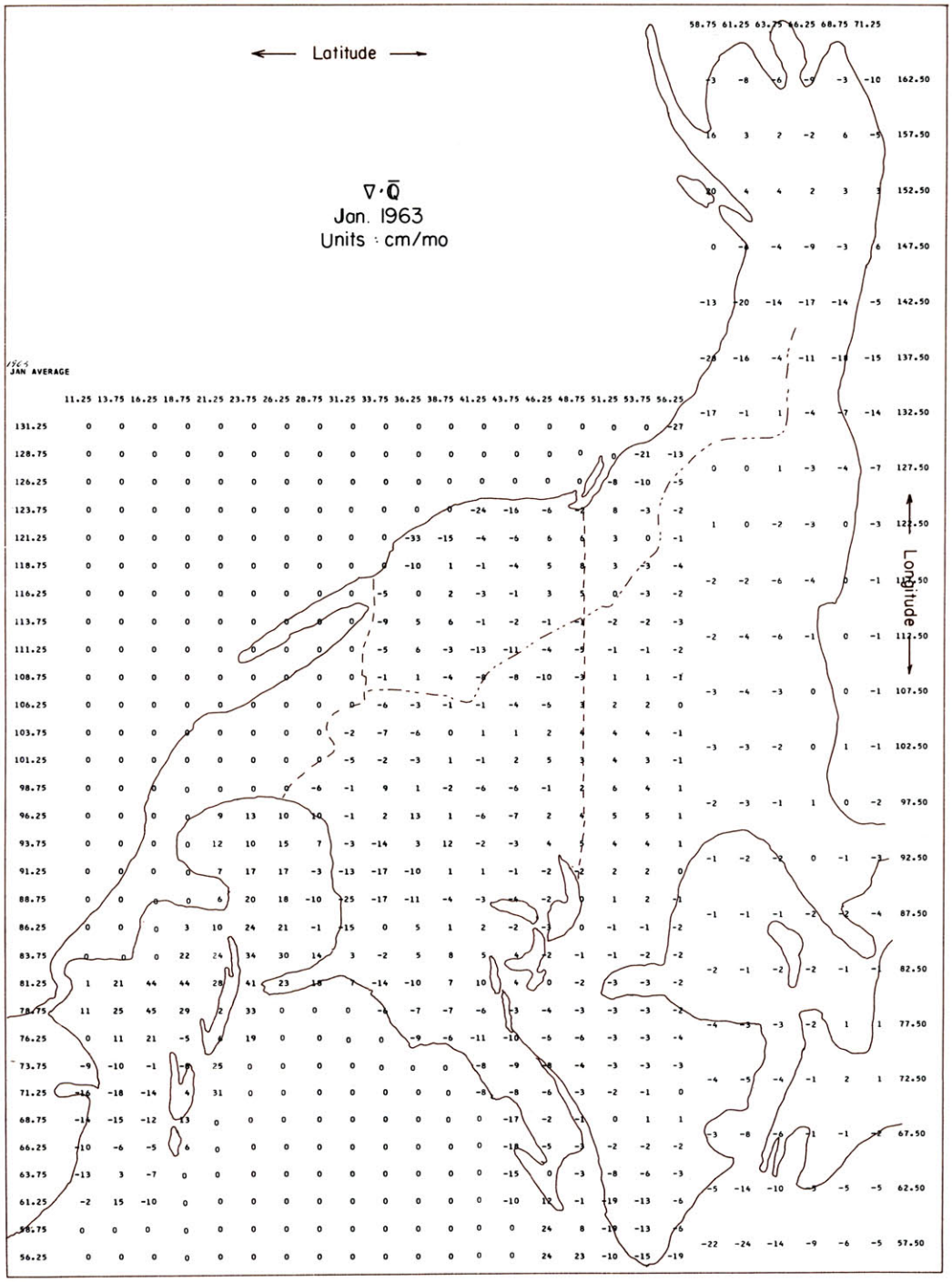


Figure 66. Mean monthly divergence of the vertically integrated water vapor flux. January, 1963. Units: gm $(cm^2\ mo)^{-1}$.

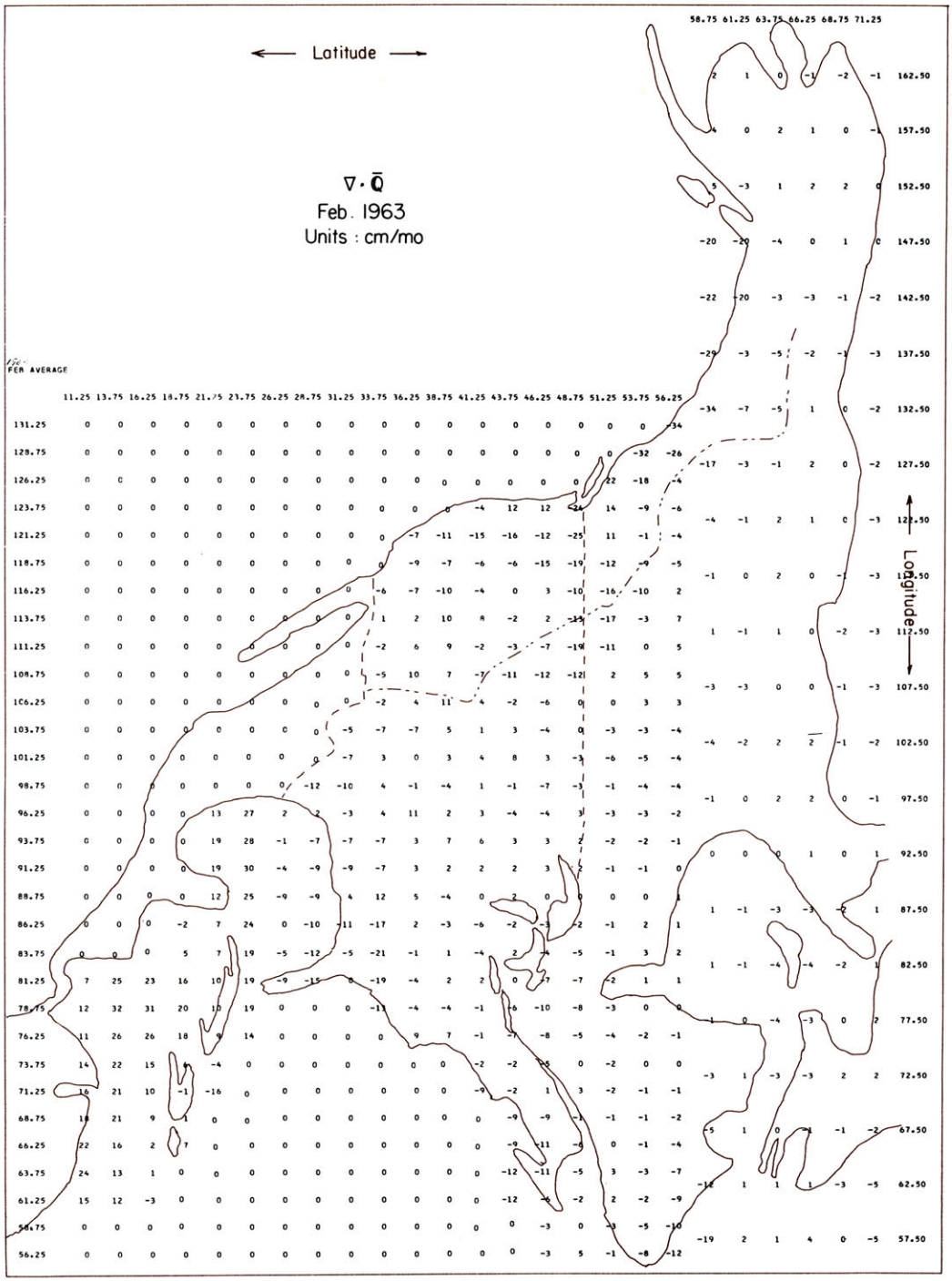


Figure 67. Mean monthly divergence of the vertically integrated water vapor flux. February, 1963. Units: gm $(cm^2\ mo)^{-1}$.

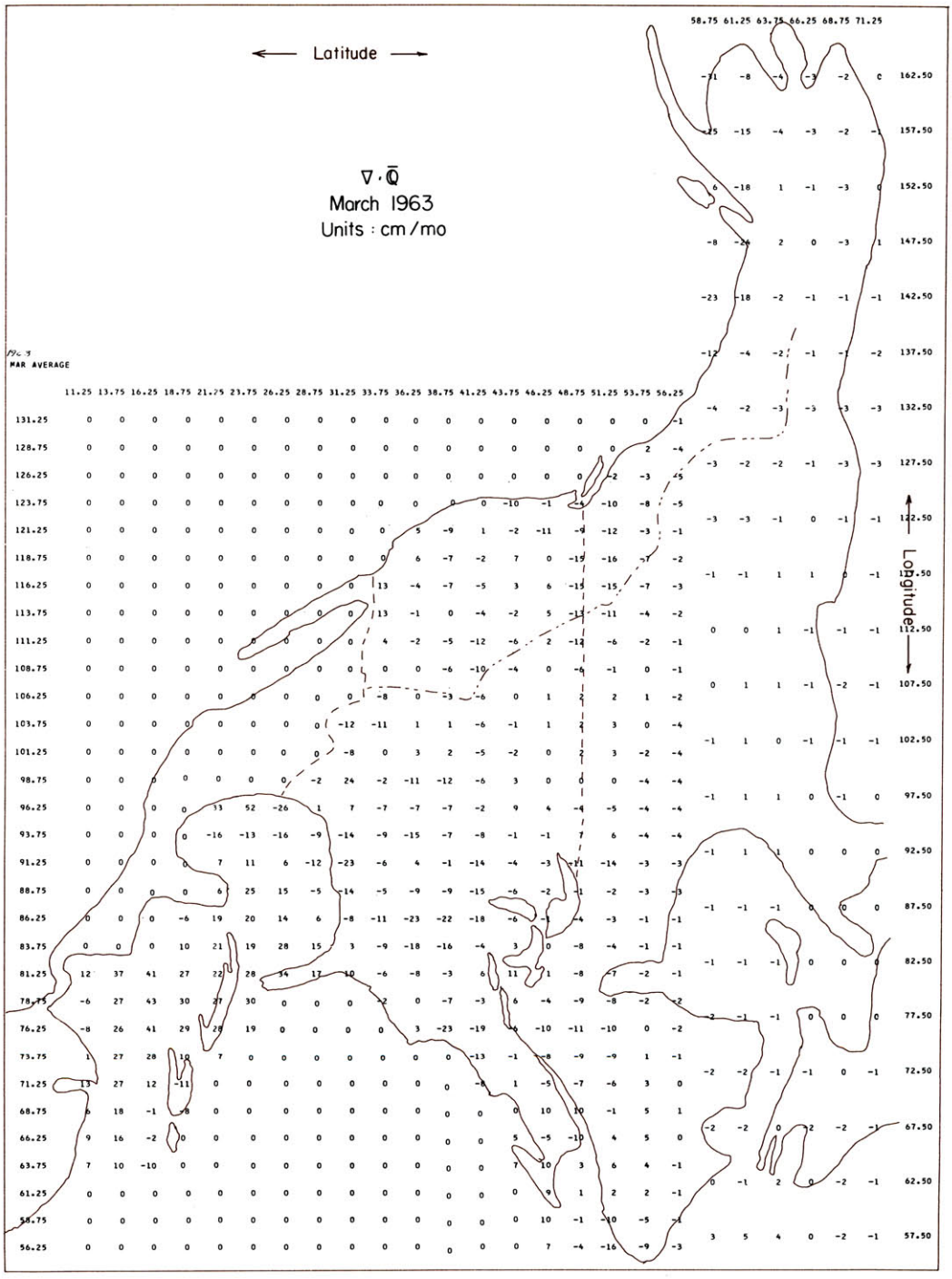


Figure 68. Mean monthly divergence of the vertically integrated water vapor flux. March, 1963. Units: gm $(cm^2\ mo)^{-1}$.

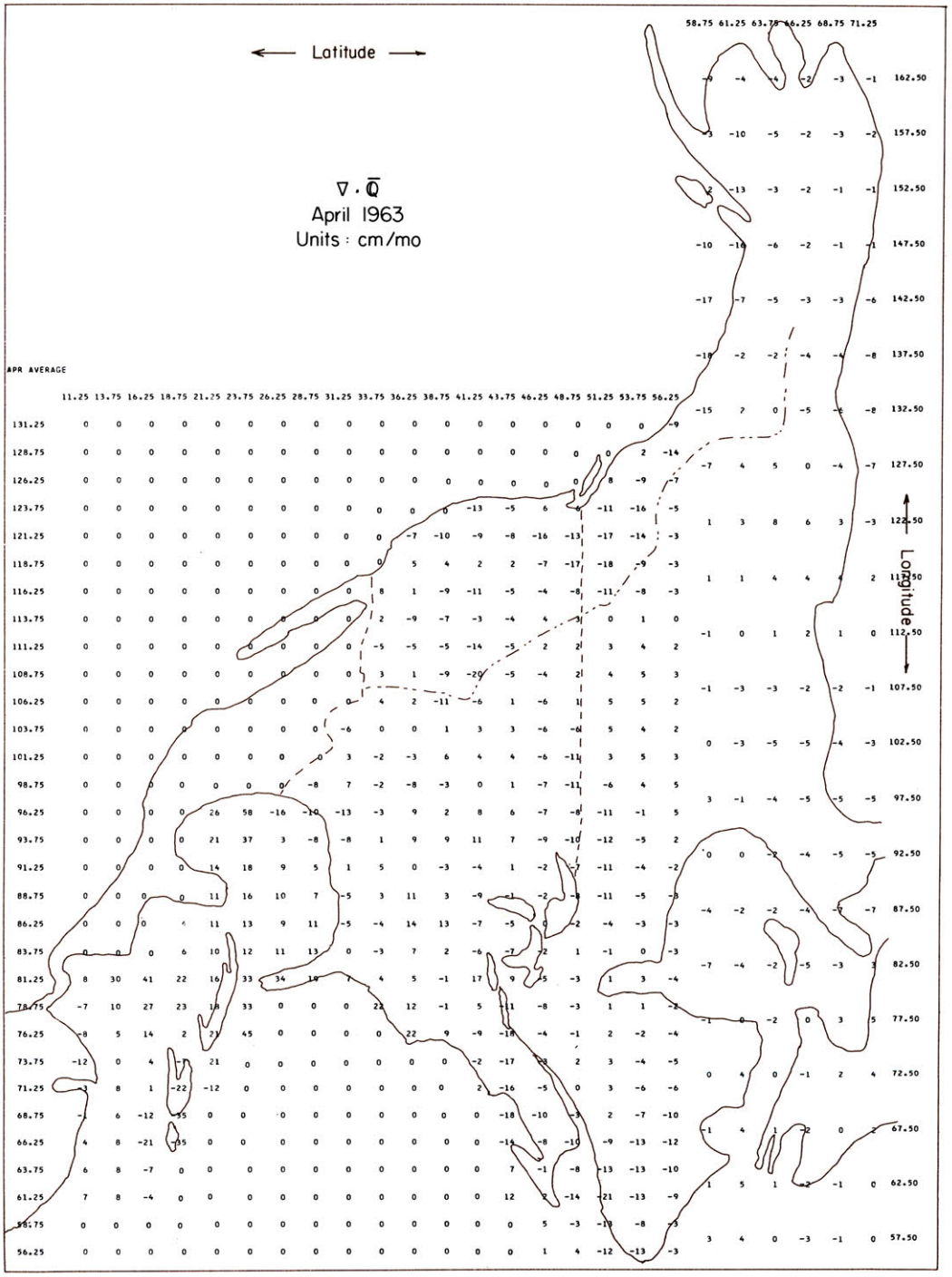


Figure 69. Mean monthly divergence of the vertically integrated water vapor flux. April, 1963. Units: gm $(cm^2\ mo)^{-1}$.

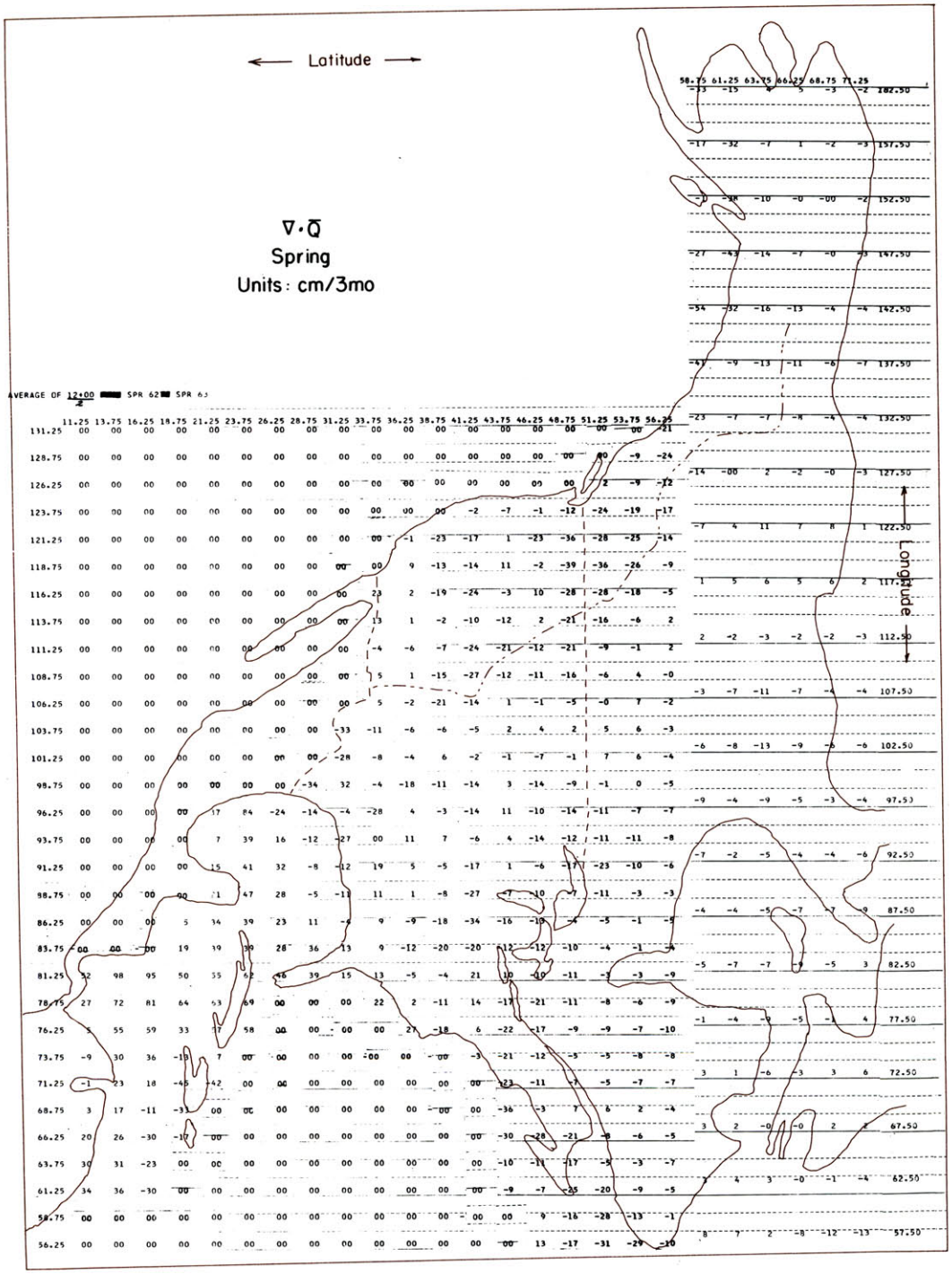


Figure 70. Mean seasonal divergence of the vertically integrated water vapor flux. Spring (March-May). Units: gm $(cm^2\ 3\ mo)^{-1}$.

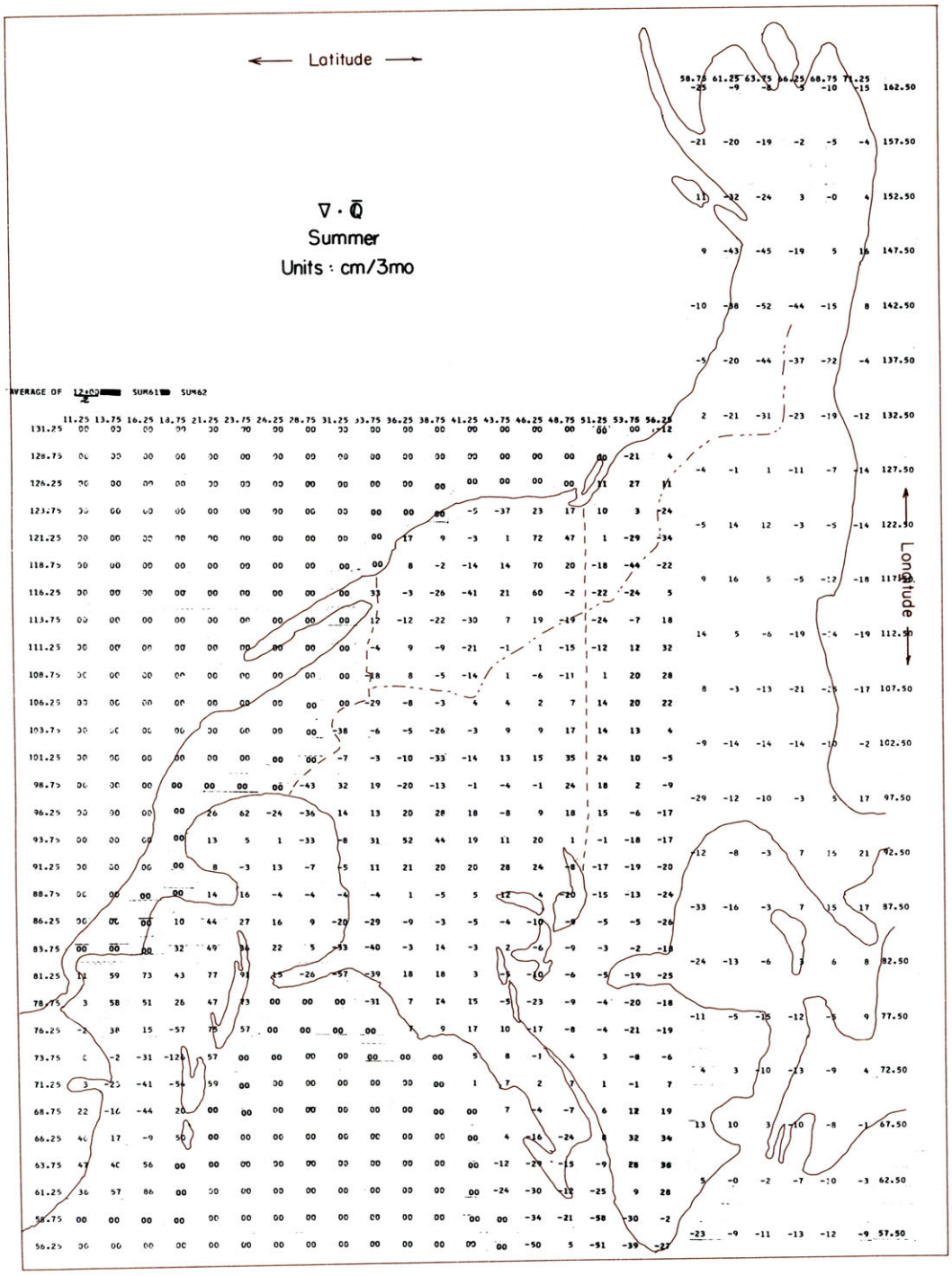


Figure 71. Mean seasonal divergence of the vertically integrated water vapor flux. Summer (June-August). Units: gm $(cm^2\ 3\ mo)^{-1}$.

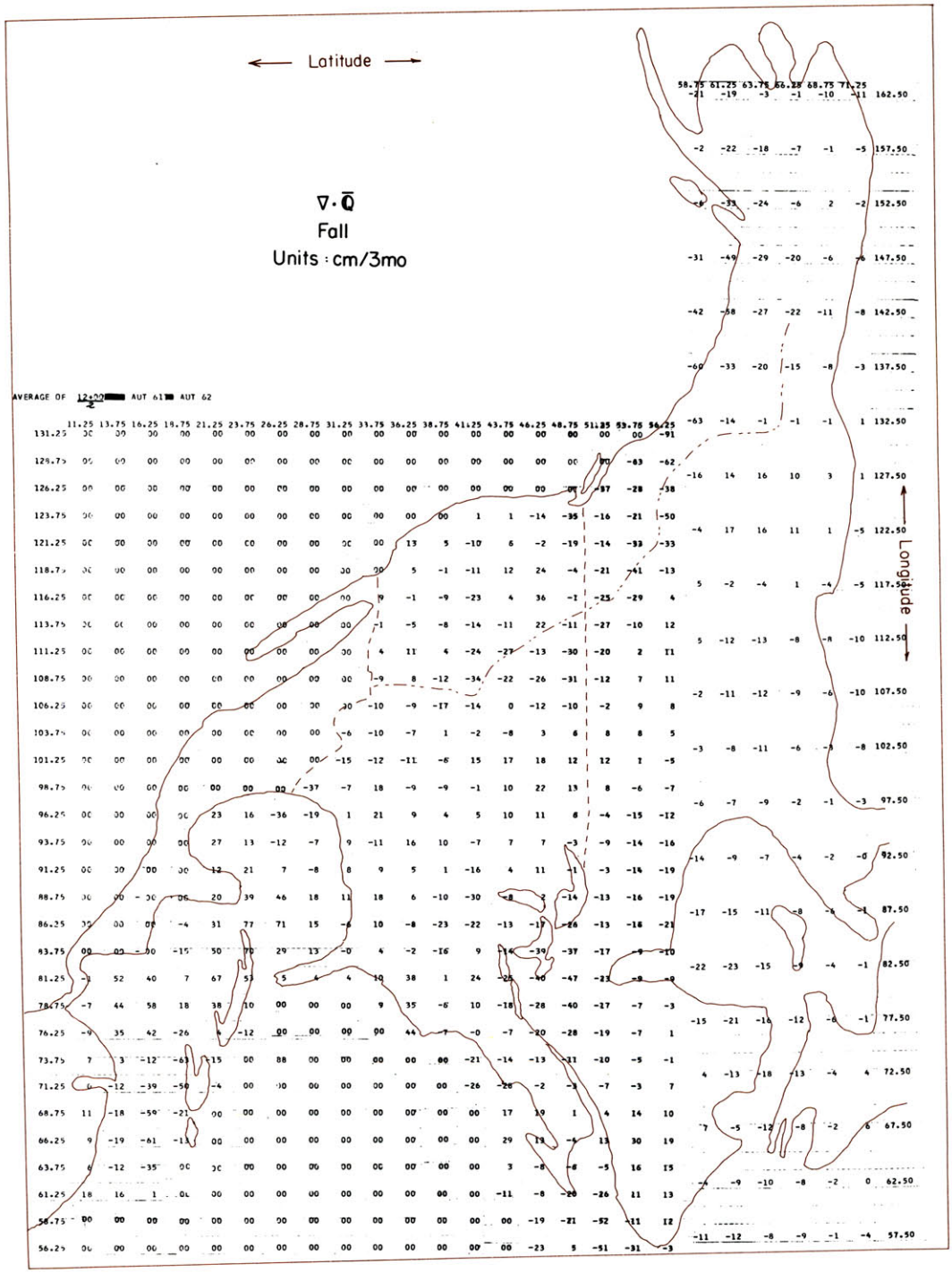


Figure 72. Mean seasonal divergence of the vertically integrated water vapor flux. Fall (September-November). Units: gm $(cm^2\ 3\ mo)^{-1}$.

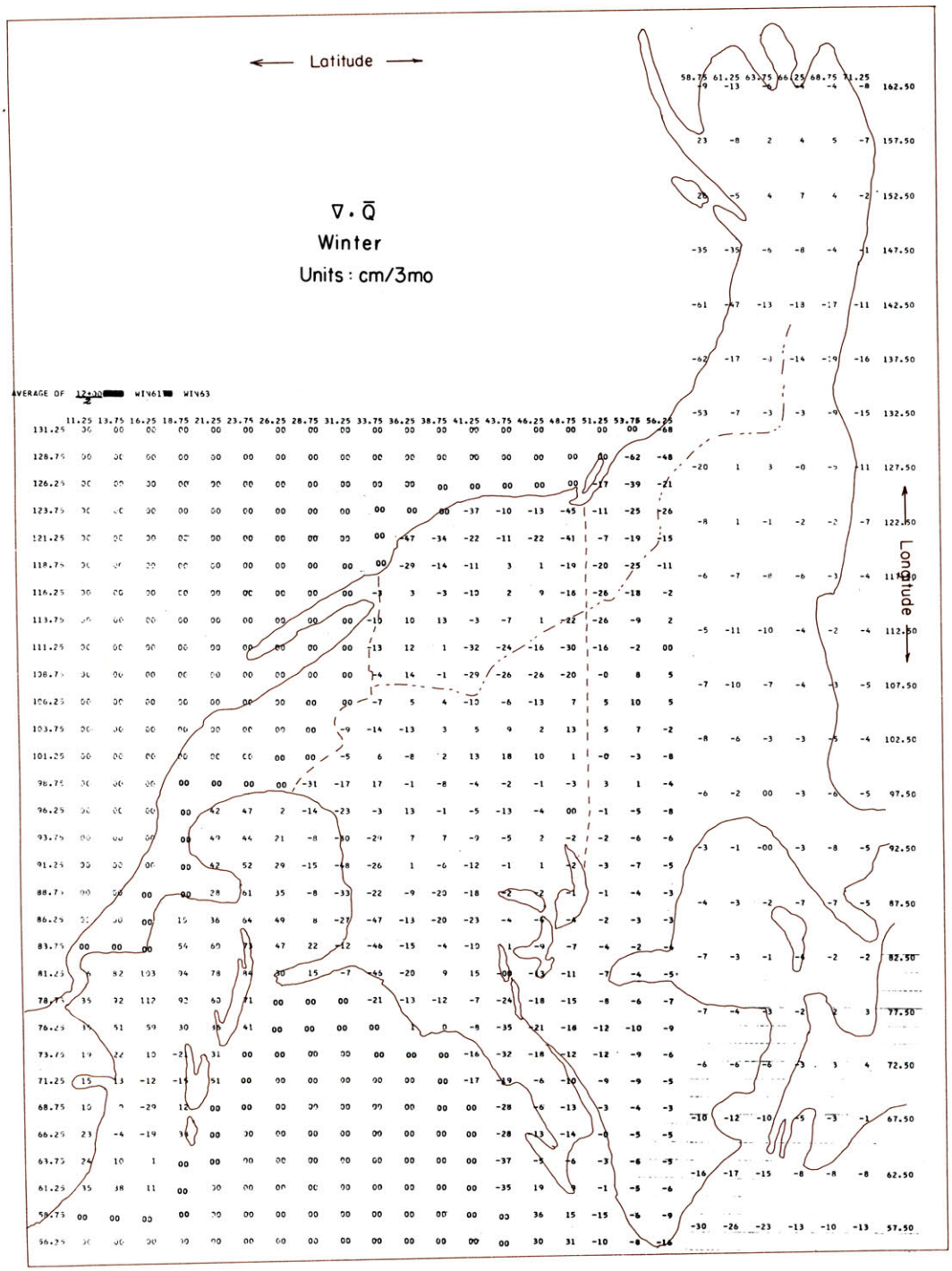


Figure 73. Mean seasonal divergence of the vertically integrated water vapor flux. Winter (December-February). Units: gm $(cm^2\ 3\ mo)^{-1}$.

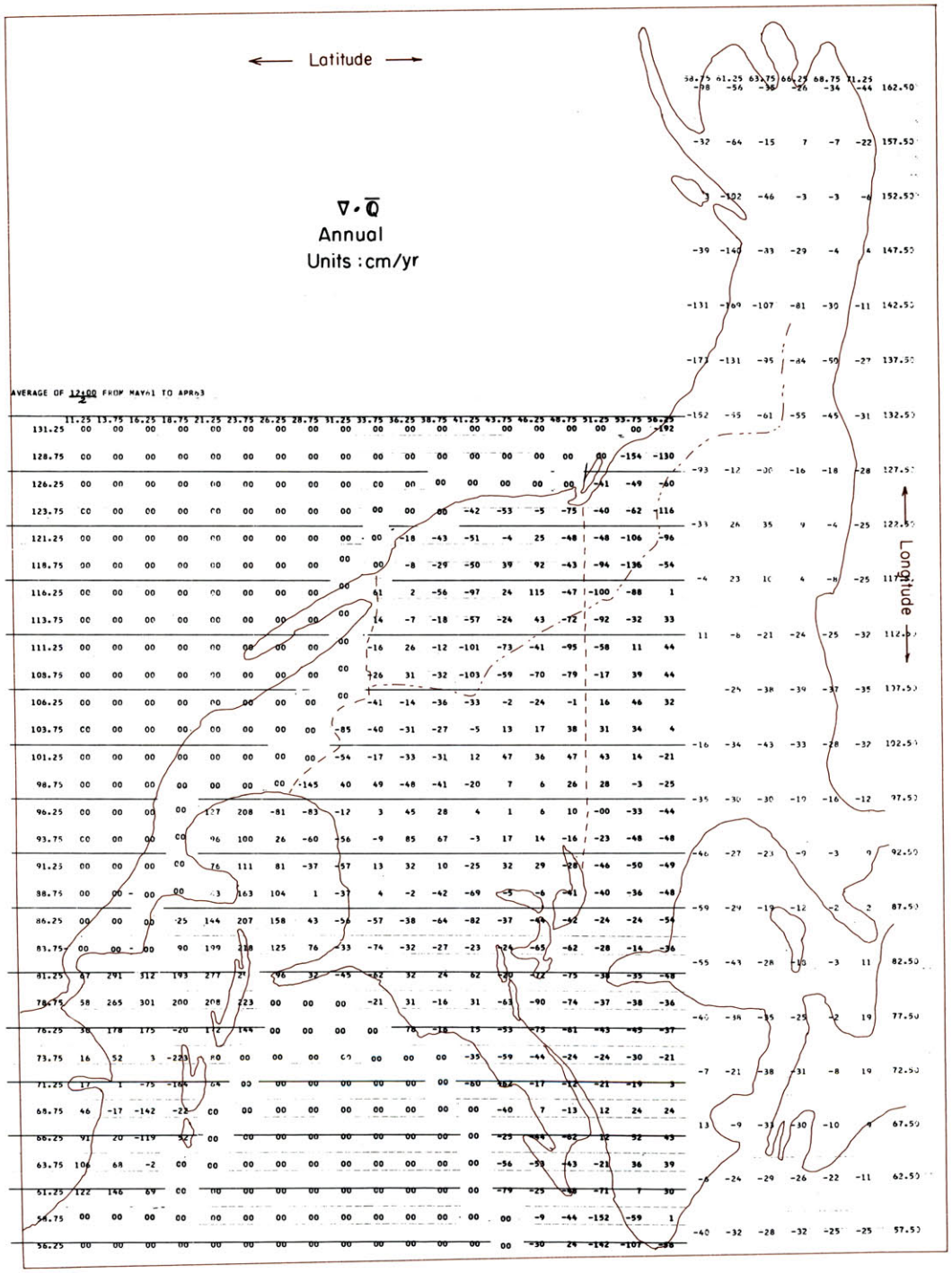


Figure 74. Mean annual divergence of the vertically integrated water vapor flux. May 1961-April 1963. Units: gm $(cm^2\ yr)^{-1}$.

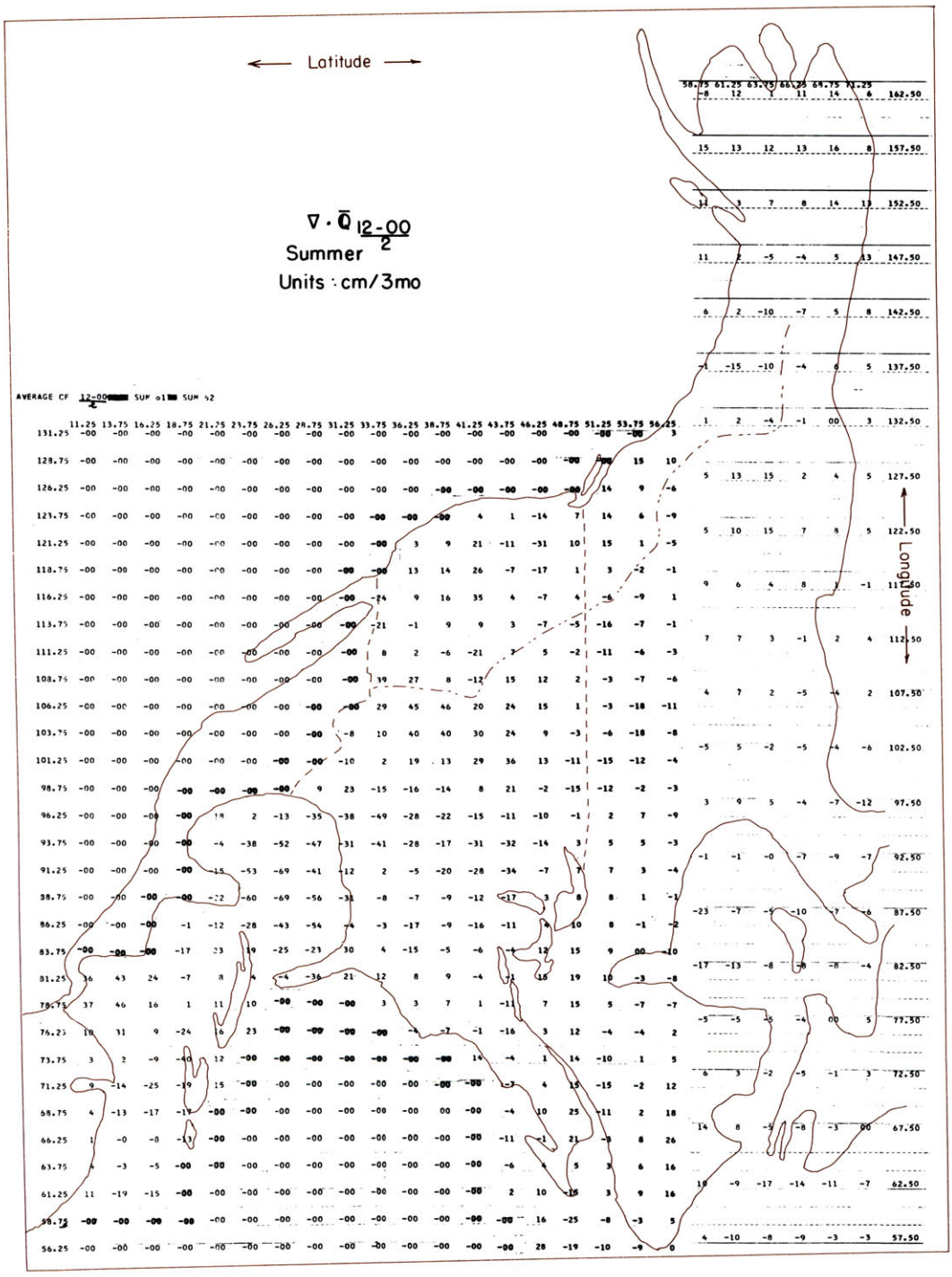


Figure 75. Mean seasonal difference, (12 GMT-00 GMT)/2 of the divergence of the vertically integrated water vapor flux. Summer (June-August). Units: gm $(cm^2\ 3\ mo)^{-1}$.

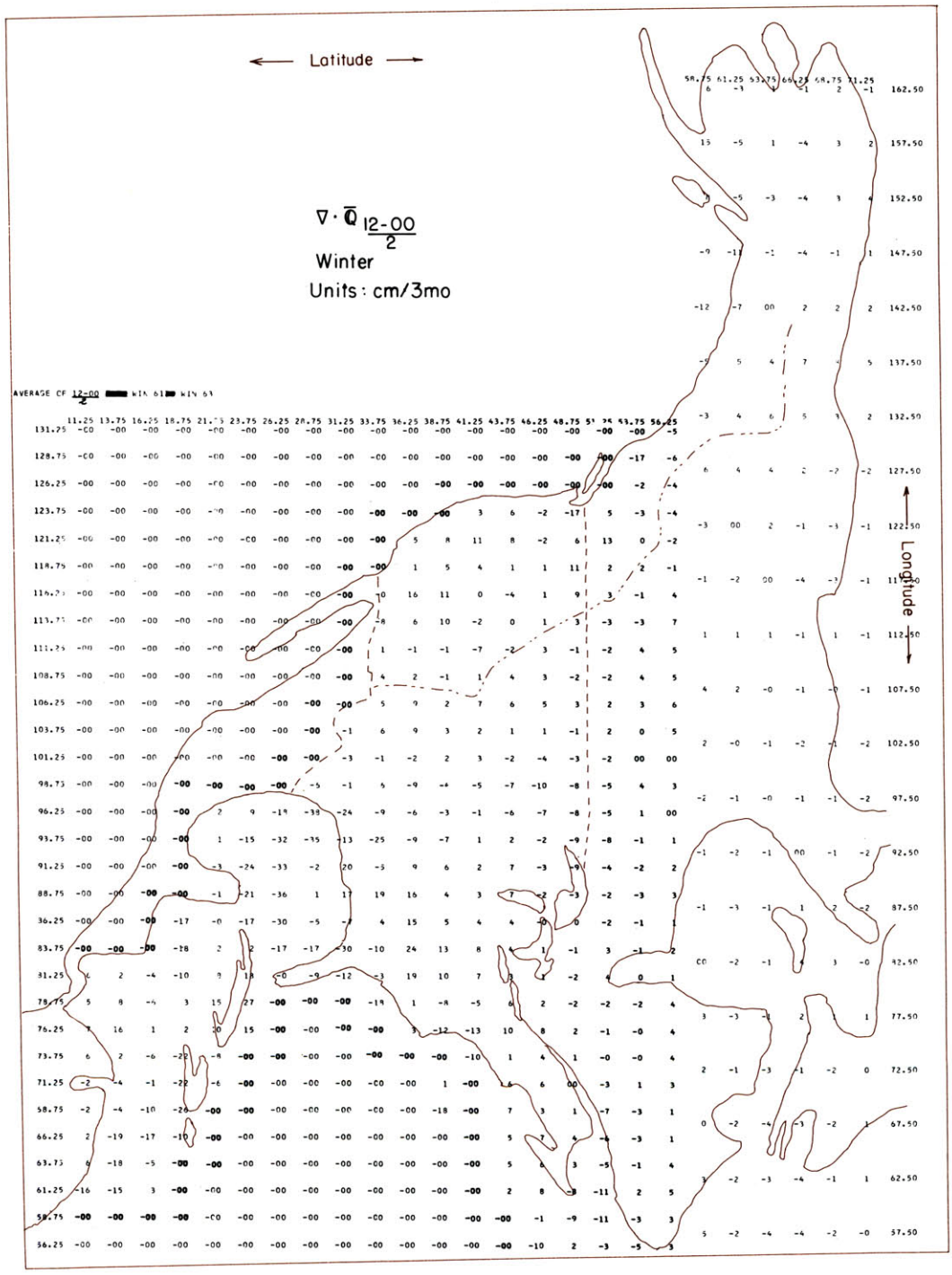


Figure 76. Mean seasonal difference, (12 GMT-00 GMT)/2 of the divergence of the vertically integrated water vapor flux. Winter (December-February). Units: gm $(cm^2\ 3\ mo)^{-1}$.

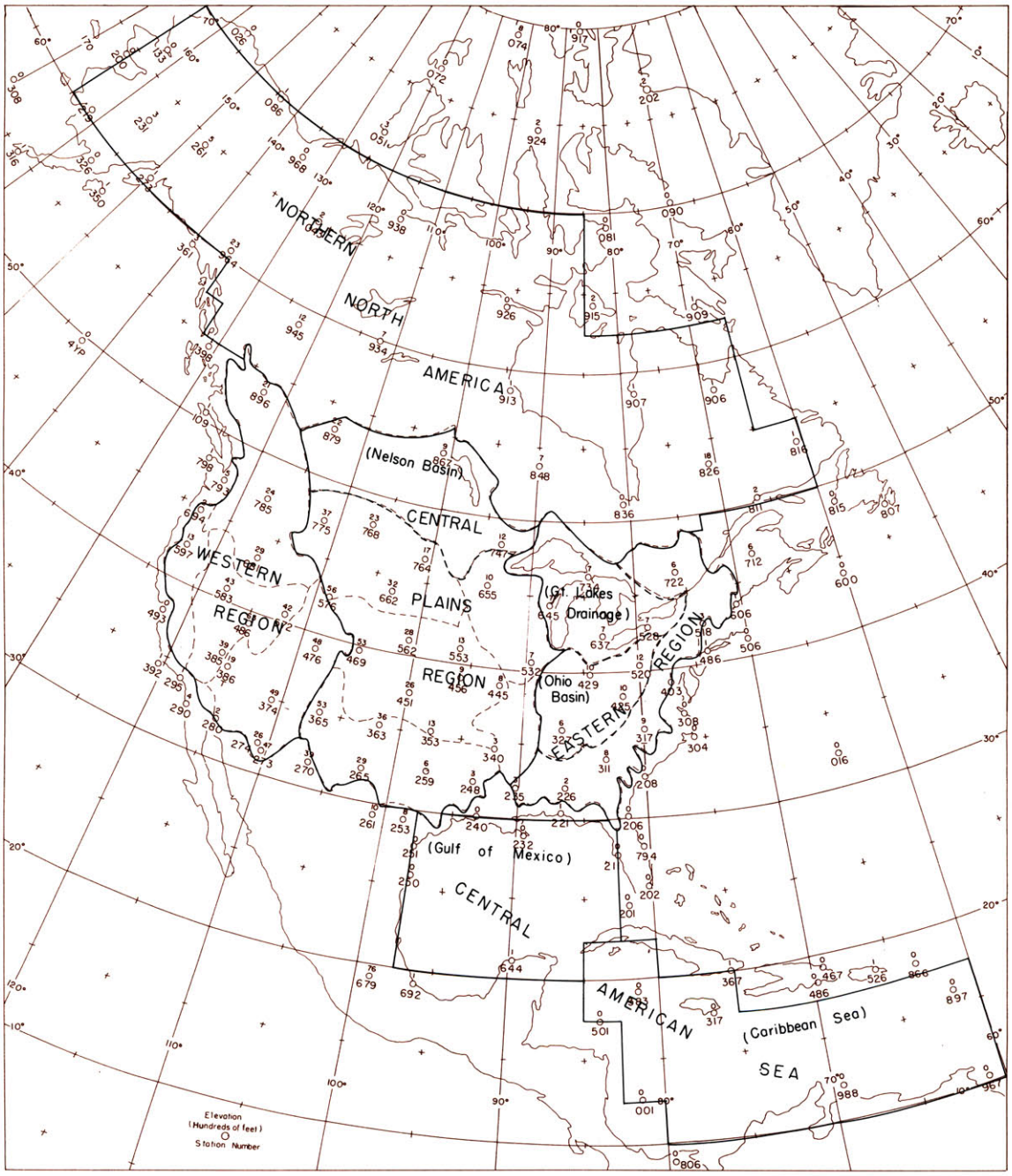


Figure 77. Regions of water balance computations.

Figure 78. Total net annual flux across selected boundaries. Upper figure is total for May, 1961-April, 1962; lower figure for May, 1962-April, 1963. Flux is positive in the direction of the arrow. Total annual flux divergence is shown for each enclosed area. Units: $10^{13}$ kg/yr.

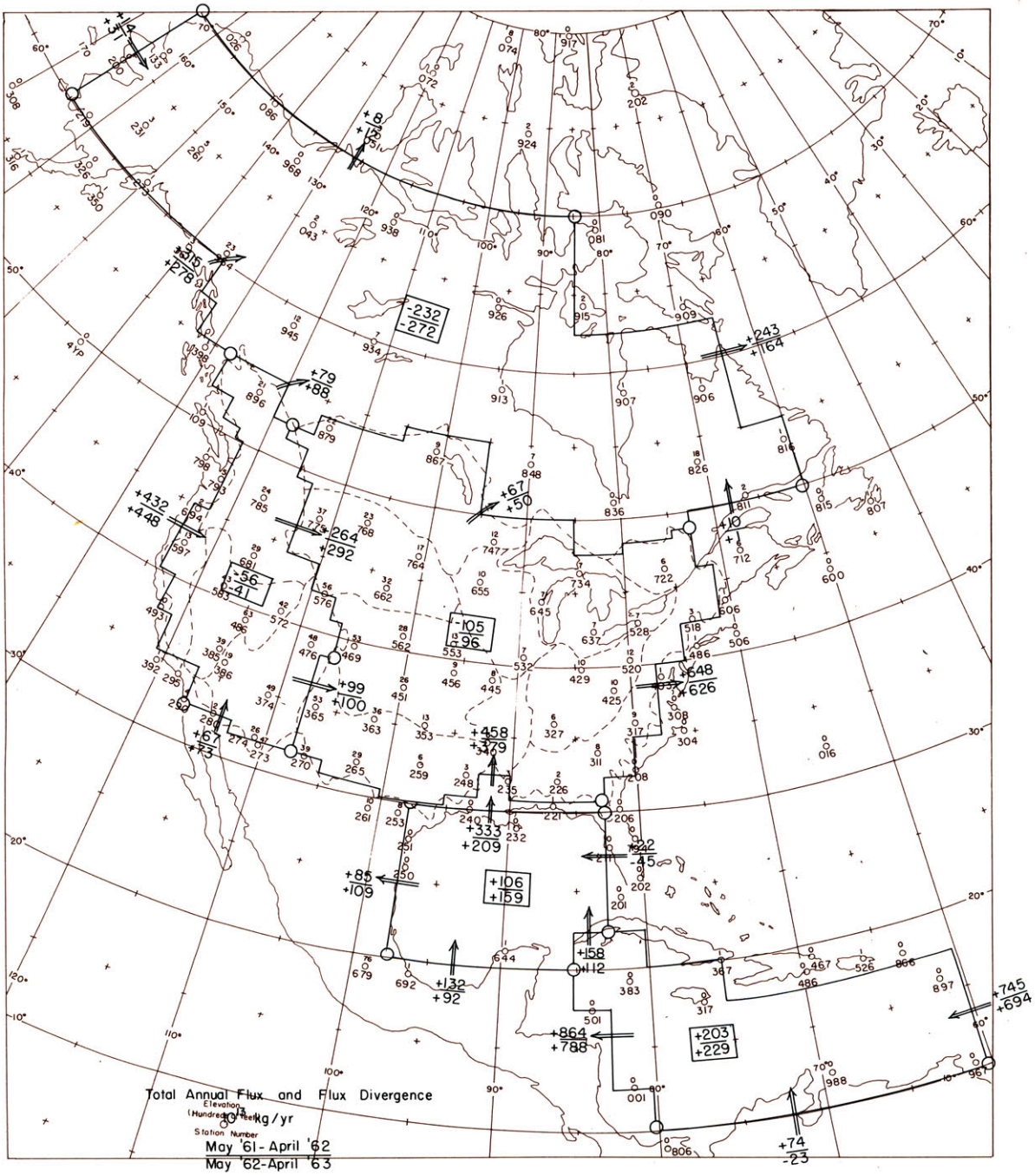
Total Annual Flux and Flux Divergence
Elevation
(Hundreds of Feet)
Station Number
kg/yr
May '61 - April '62
May '62 - April '63

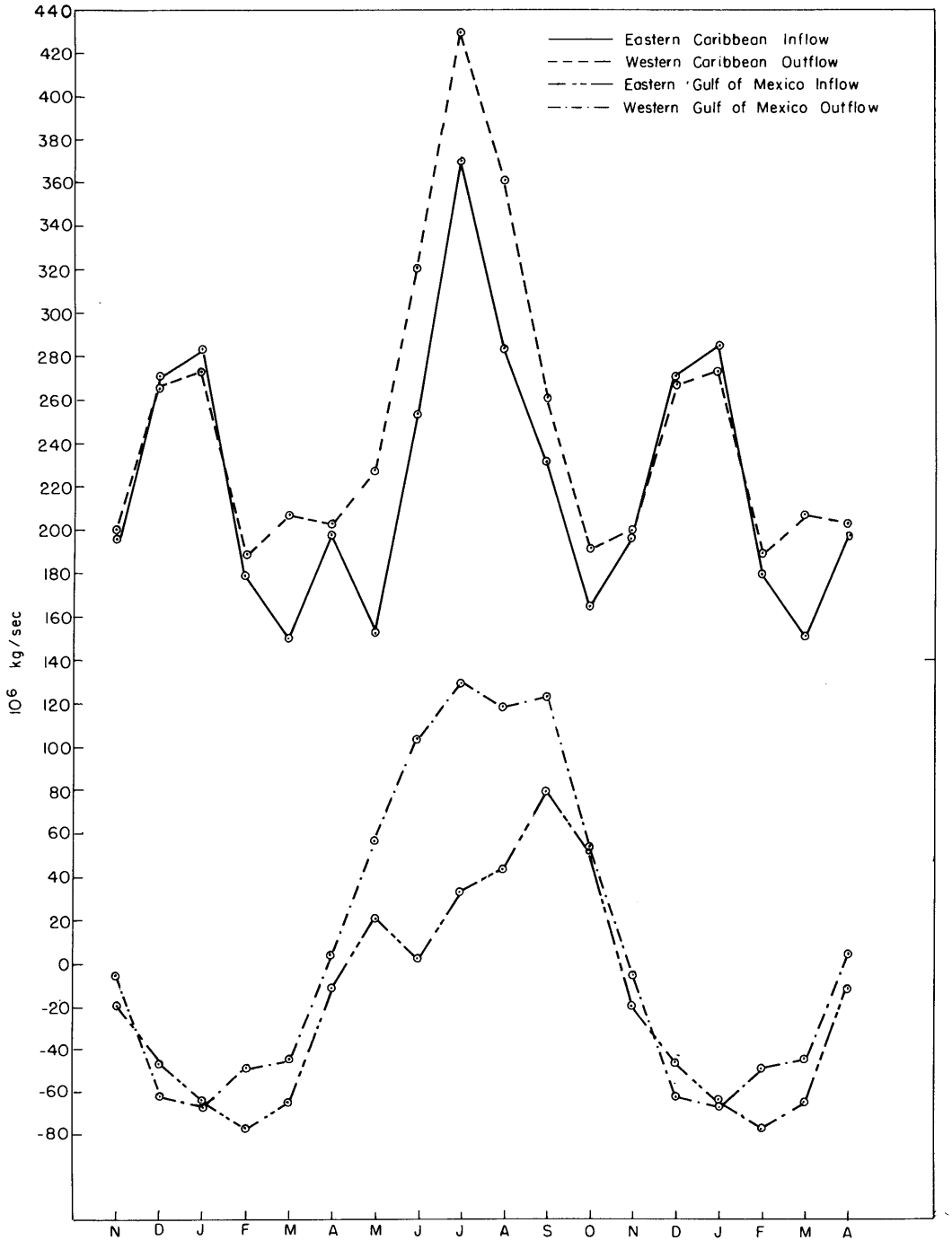


Figure 79. Mean monthly vertically integrated water vapor flux across various sections of the boundary around the Gulf of Mexico and Caribbean Sea, May 1961-April 1963. Units: $10^6$ kg $sec^{-1}$.

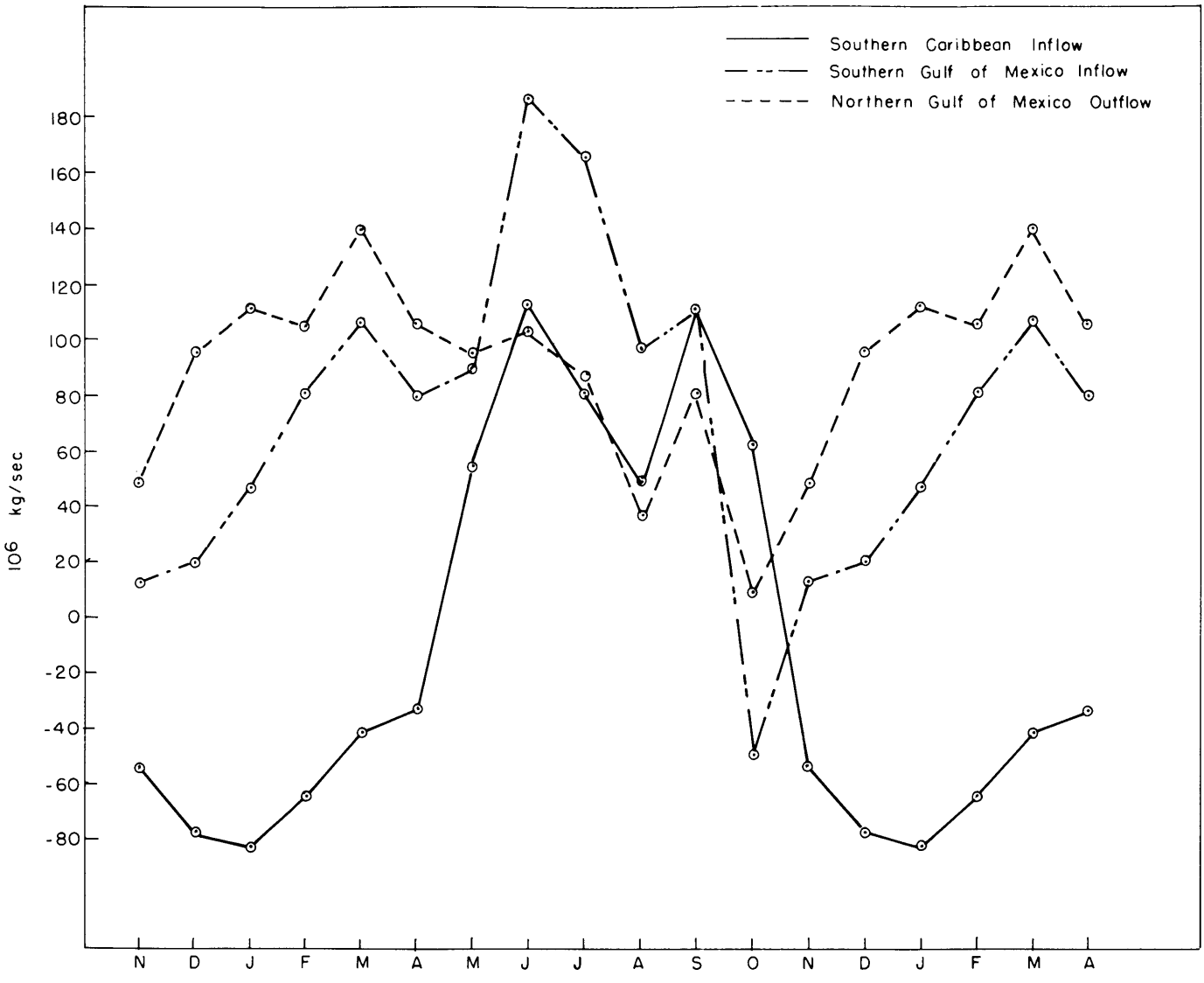


Figure 80. Mean monthly vertically integrated water vapor flux across various sections of the boundary around the Gulf of Mexico and Caribbean Sea, May 1961-April 1963. Units: $10^6$ kg $sec^{-1}$.

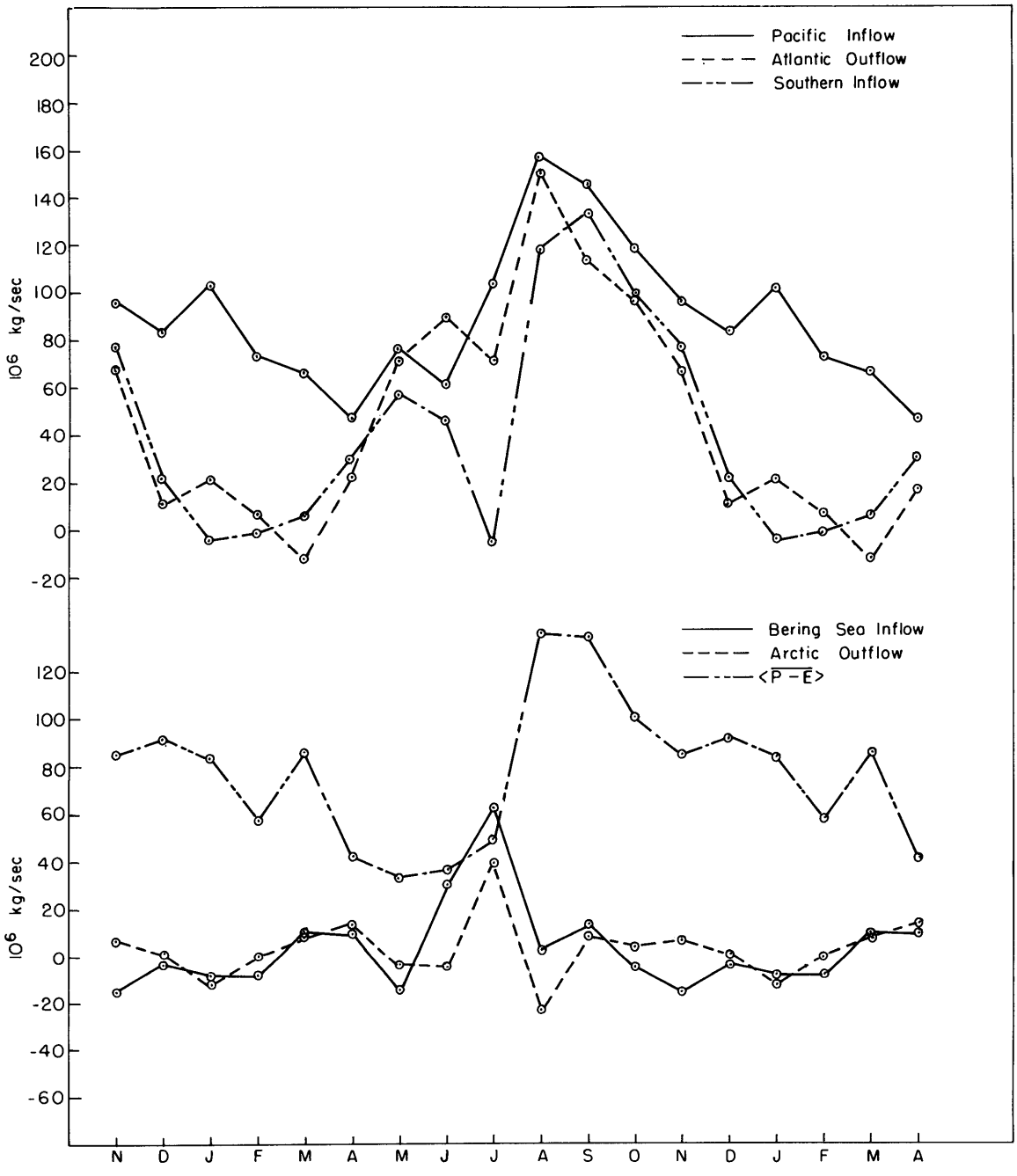


Figure 81. Mean monthly vertically integrated water vapor flux across various sections of the boundary of Northern North America, May 1961-April 1963. Units: $10^6$ kg $sec^{-1}$.

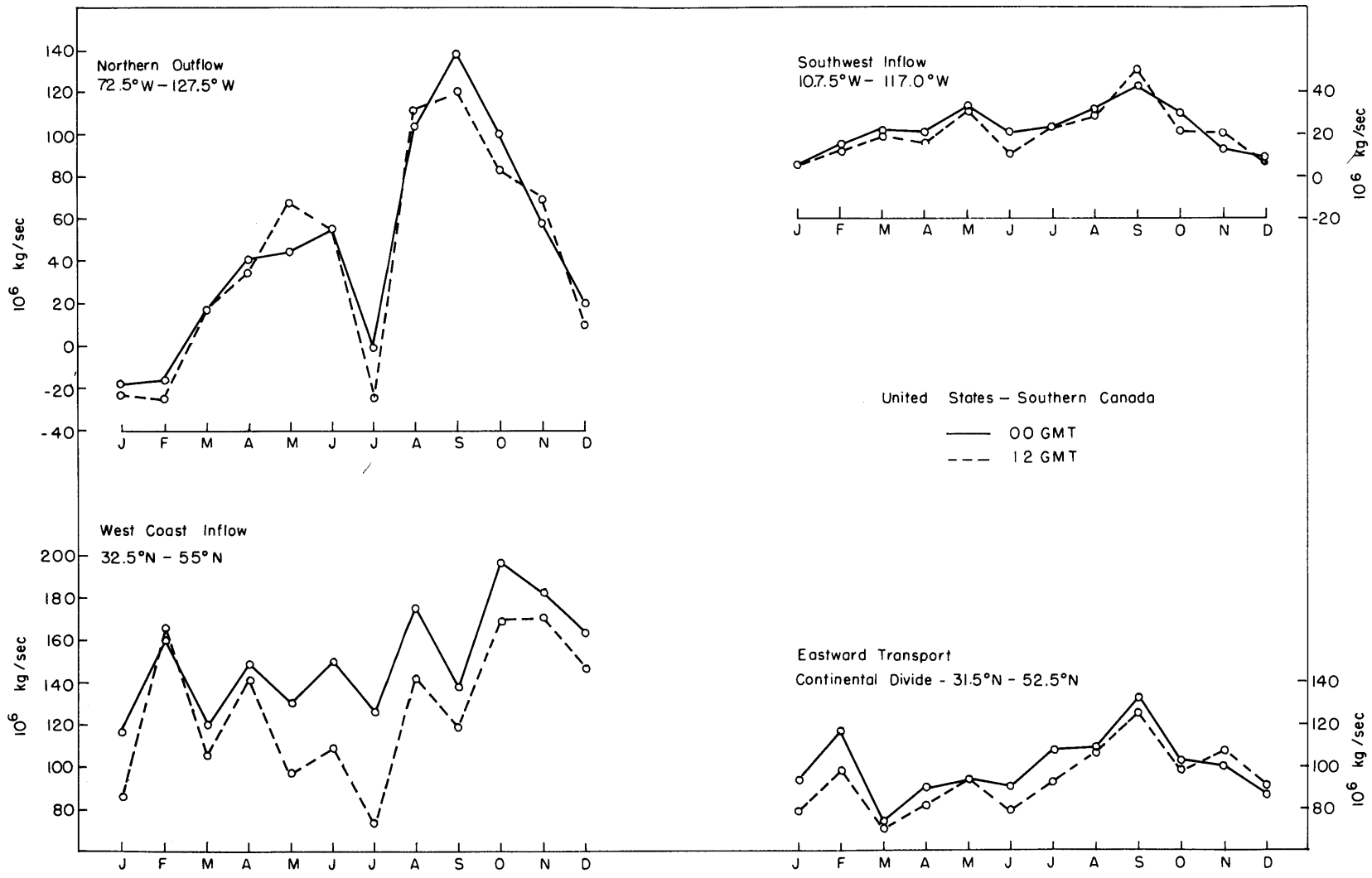


Figure 82. Mean monthly vertically integrated water vapor flux across various sections of the boundary of the United States and Southern Canada, May 1961-April 1963. Also shown is the estimated transport across the Continental Divide. Units: $10^6$ kg $sec^{-1}$.

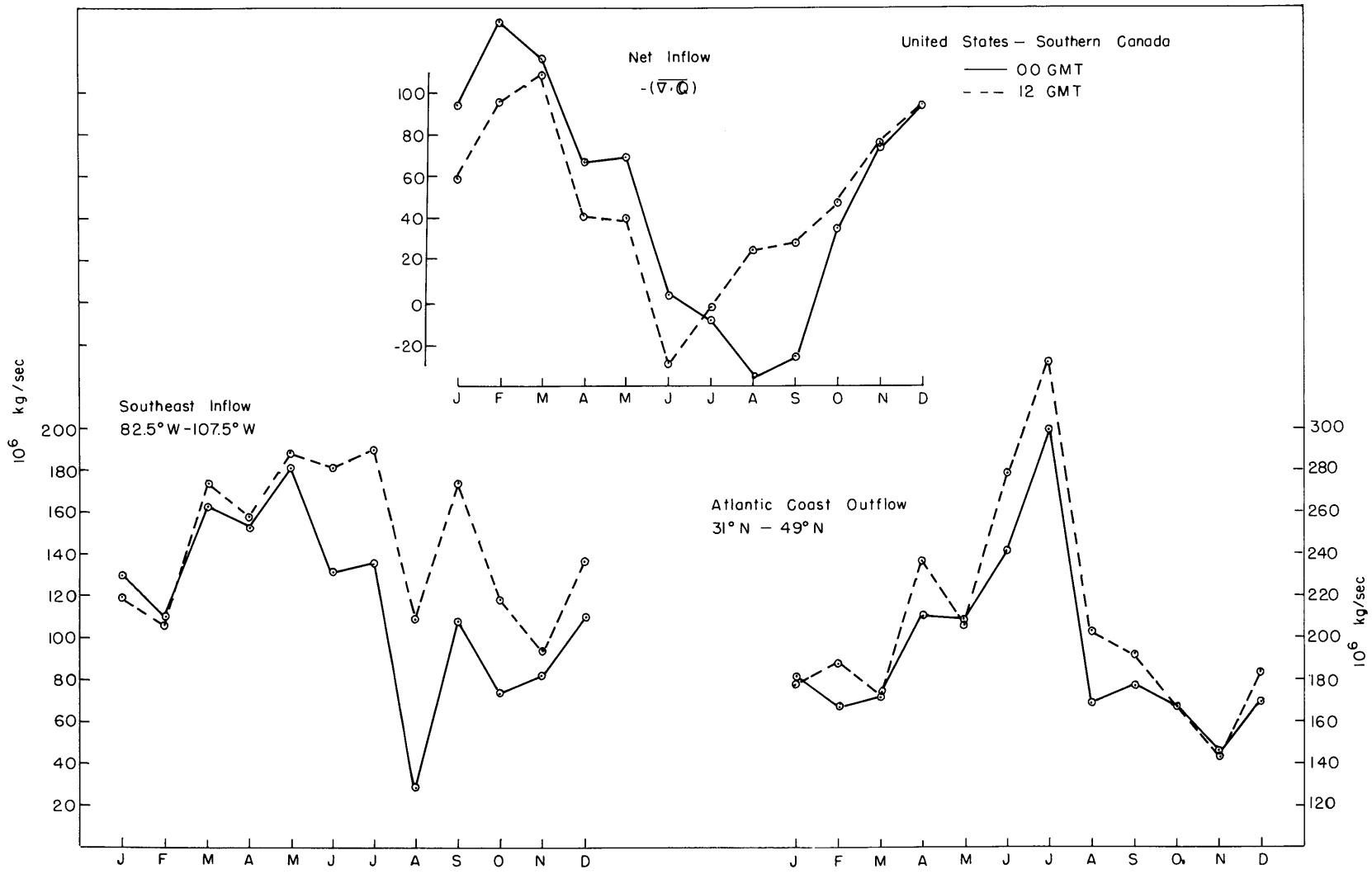


Figure 83. Mean monthly vertically integrated water vapor flux across various sections of the boundary of the United States and Southern Canada, May 1961-April 1963. Also shown is the net mean monthly inflow to the area. Units: $10^6$ kg $sec^{-1}$.

Figure 84. Water balance of the Caribbean Sea, May 1961-Arpil 1963. Upper: Difference between mean monthly evaporation and precipitation, $\langle \overline{E-P} \rangle$ , evaluated by means of the water vapor balance equation. Also shown are mean monthly climatological estimates of evaporation, $\langle \overline{E} \rangle$ , by Budyko (1963) and Colón (1963).
Lower: Values for mean monthly precipitation which result when $\langle \overline{E-P} \rangle$ is subtracted from the evaporation estimates of Budyko and Colón.

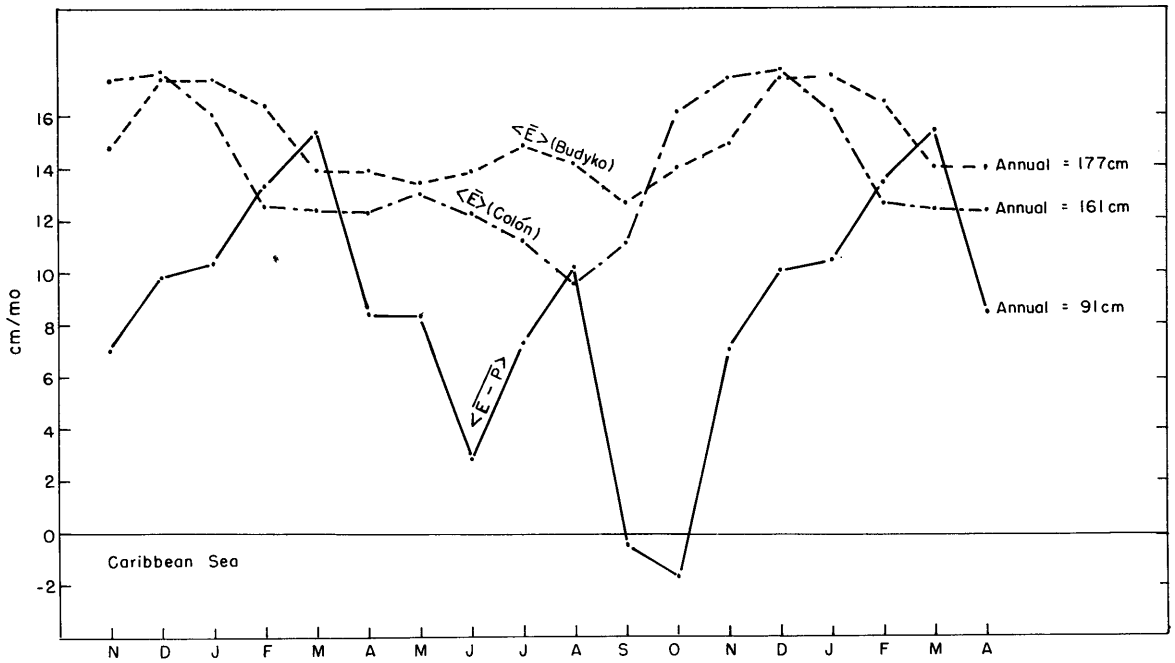
cm/mo
16
14
12
10
8
6
4
2
0
-2
$\overline{E}$>(Budyko)
$\overline{E}$>(Colón)
$\overline{E}$ - $\overline{P}$>
Annual = 177cm
Annual = 161cm
Annual = 91cm
Caribbean Sea
N D J F M A M J J A S O N D J F M A

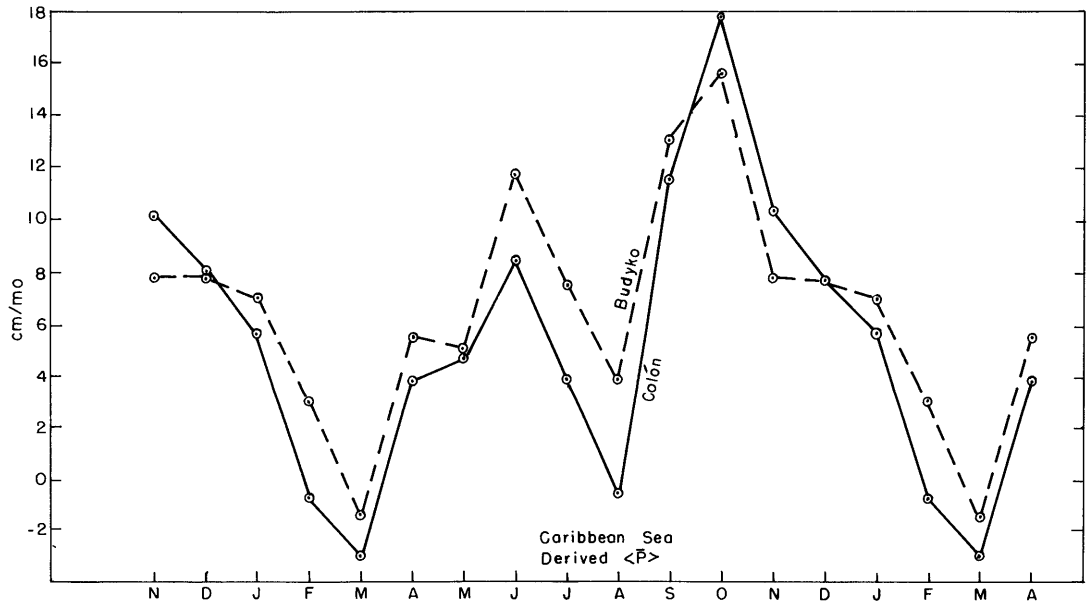
cm/mo
18
16
14
12
10
8
6
4
2
0
-2
Budyko
Colón
Caribbean Sea
Derived <$\overline{P}$>
N D J F M A M J J A S O N D J F M A

Figure 85. Water balance - Gulf of Mexico (upper) and Central American Sea (lower), May 1961-April 1963. The difference between mean monthly evaporation and precipitation, $\langle\overline{E-P}\rangle$, is evaluated by means of the water vapor balance equation. Mean monthly climatological estimates of evaporation, $\langle\overline{E}\rangle$ are from Budyko (1963). The derived values of precipitation are obtained by subtracting $\langle\overline{E-P}\rangle$ from $\langle\overline{E}\rangle$.

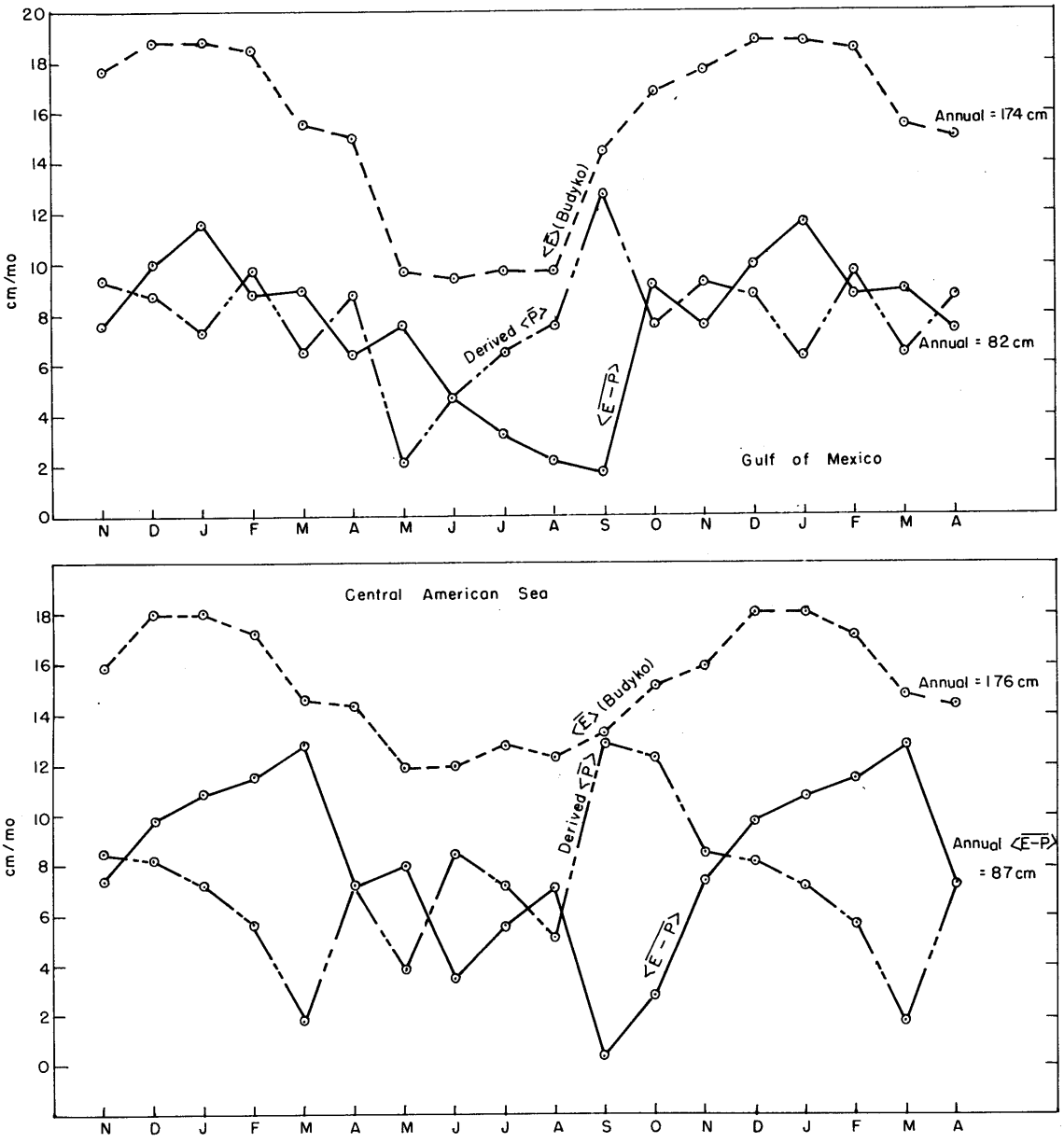
cm/mo
Annual = 174 cm
Annual = 82 cm
Gulf of Mexico
Derived ⟨P⟩
⟨E⟩ (Budyko)
⟨E - P⟩
Central American Sea
Annual = 176 cm
Annual ⟨E-P⟩ = 87 cm
N D J F M A M J J A S O N D J F M A

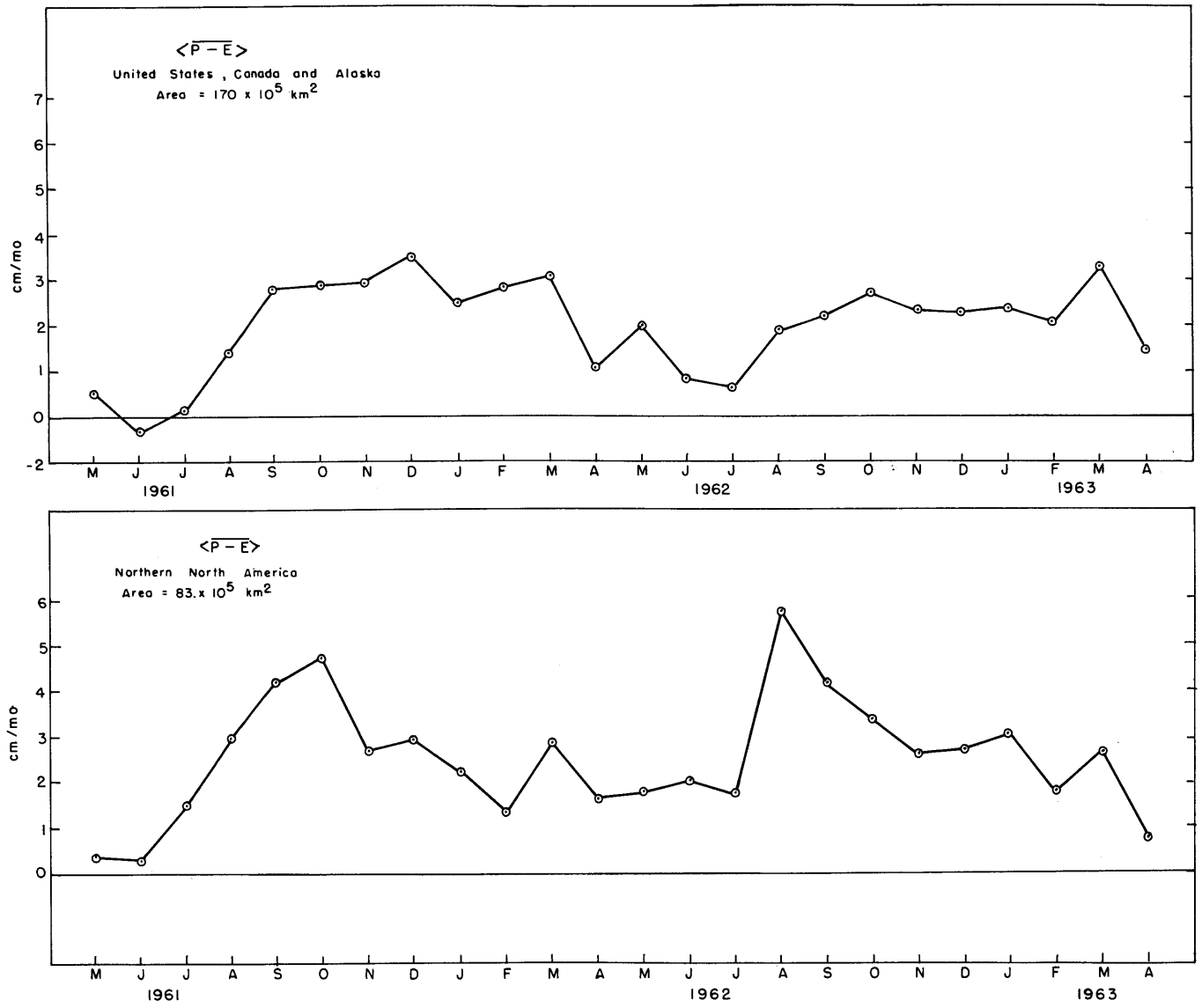


Figure 86. Mean monthly difference between precipitation and evapotranspiration, $\langle \overline{P-E} \rangle$ . Upper: United States, Canada and Alaska. Lower: Northern North America. $\langle \overline{P-E} \rangle$ is evaluated from the water vapor balance equation.

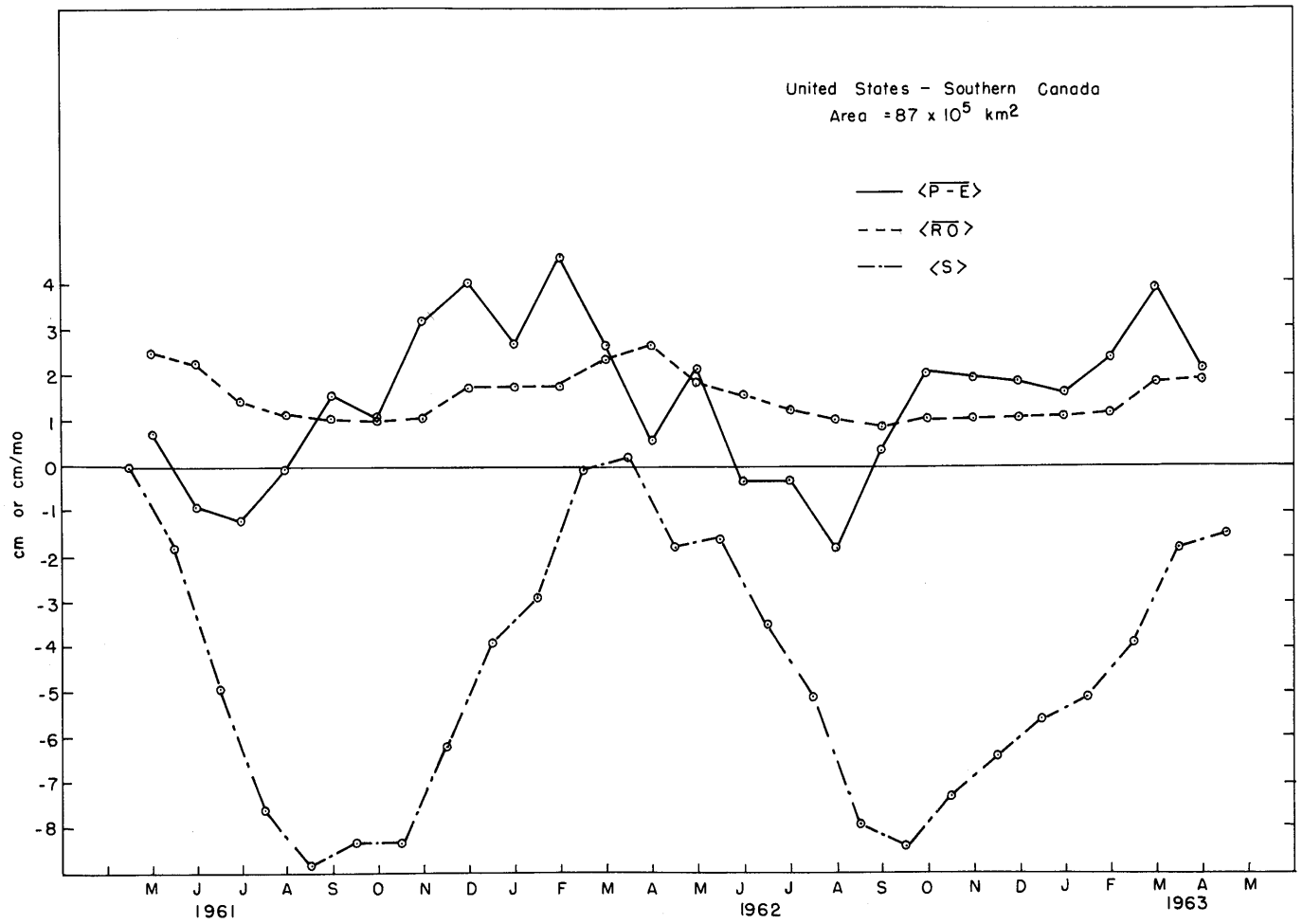


Figure 87. Water balance of the United States-Southern Canada. Surface and subsurface storage, $\langle S \rangle$, represents the change from conditions on May 1, 1961. Runoff, $\langle \overline{RO} \rangle$, is the total streamflow from the area. The difference between precipitation and evapotranspiration, $\langle \overline{P-E} \rangle$, is evaluated by means of the water vapor balance equation.

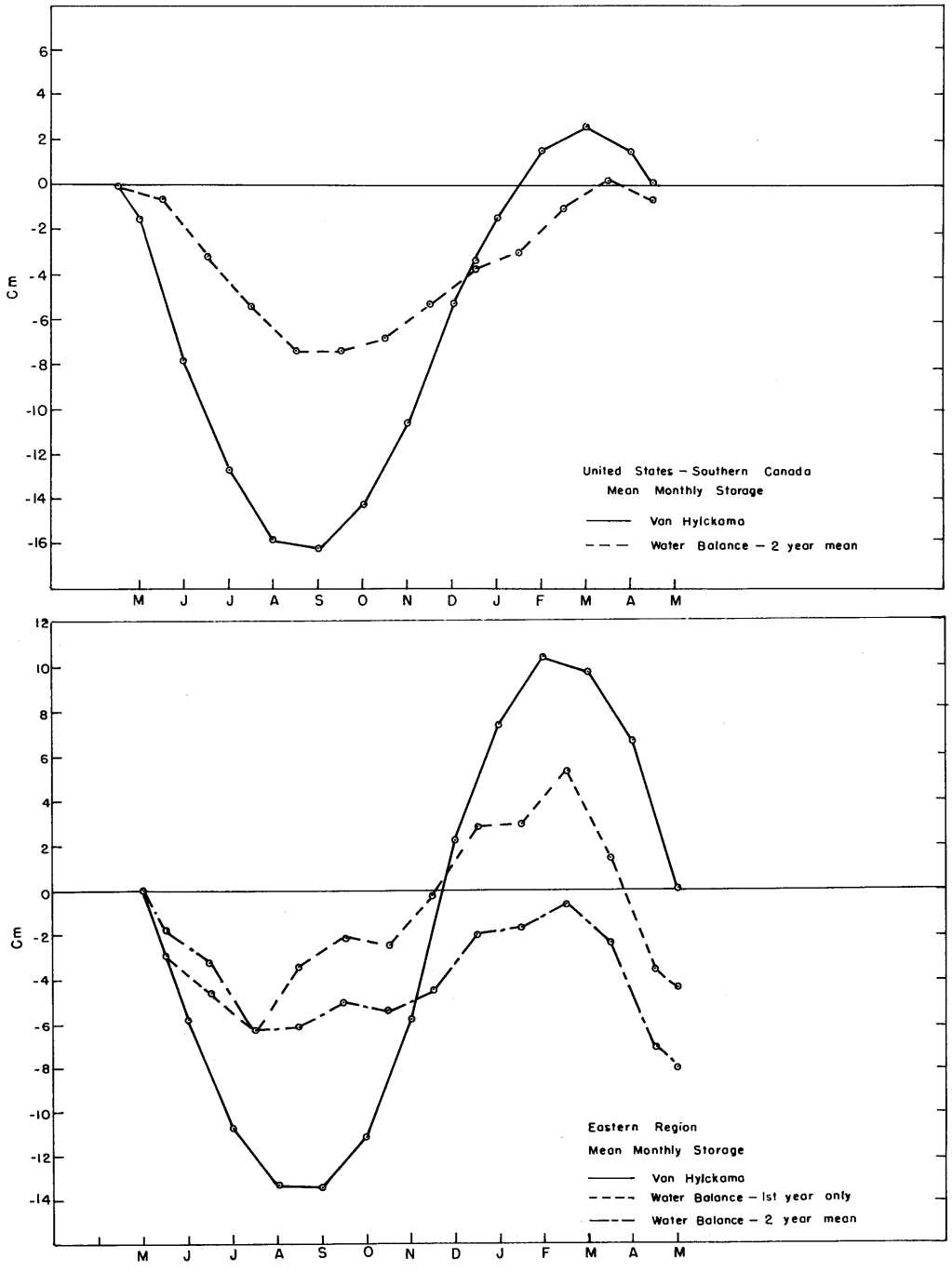


Figure 88. Mean monthly surface and subsurface storage changes computed for May 1961-April 1963 by means of the water vapor balance equation, and changes computed by Van Hylckama (1956). Upper: United States-Southern Canada. Lower: Eastern Region.

Figure 89. Upper left: Estimated precipitation, $\langle \overline{P} \rangle$ , United States and Southern Canada (except Nelson Basin), for the period May 1961-December 1962, based on data from LaRue and Younkin (1963). Evapotranspiration, $\langle \overline{E} \rangle$ , computed by means of the water vapor balance equation. ⊗ indicates the mean precipitation, and evapotranspiration obtained for February, 1962, using precipitation reports from climatological summaries.
Lower left: Mean monthly evapotranspiration for the Eastern Region, and the Western and Central Plains Region (except Nelson Basin), computed by means of the water vapor balance equation. Precipitation for the Eastern Region is estimated from climatological summaries. Data is from the period May 1961-December 1962.
Upper right: Percentage of total monthly storage loss due to streamflow; United States and Southern Canada.
Lower right: Percentage of total monthly storage loss due to streamflow; Eastern Region.

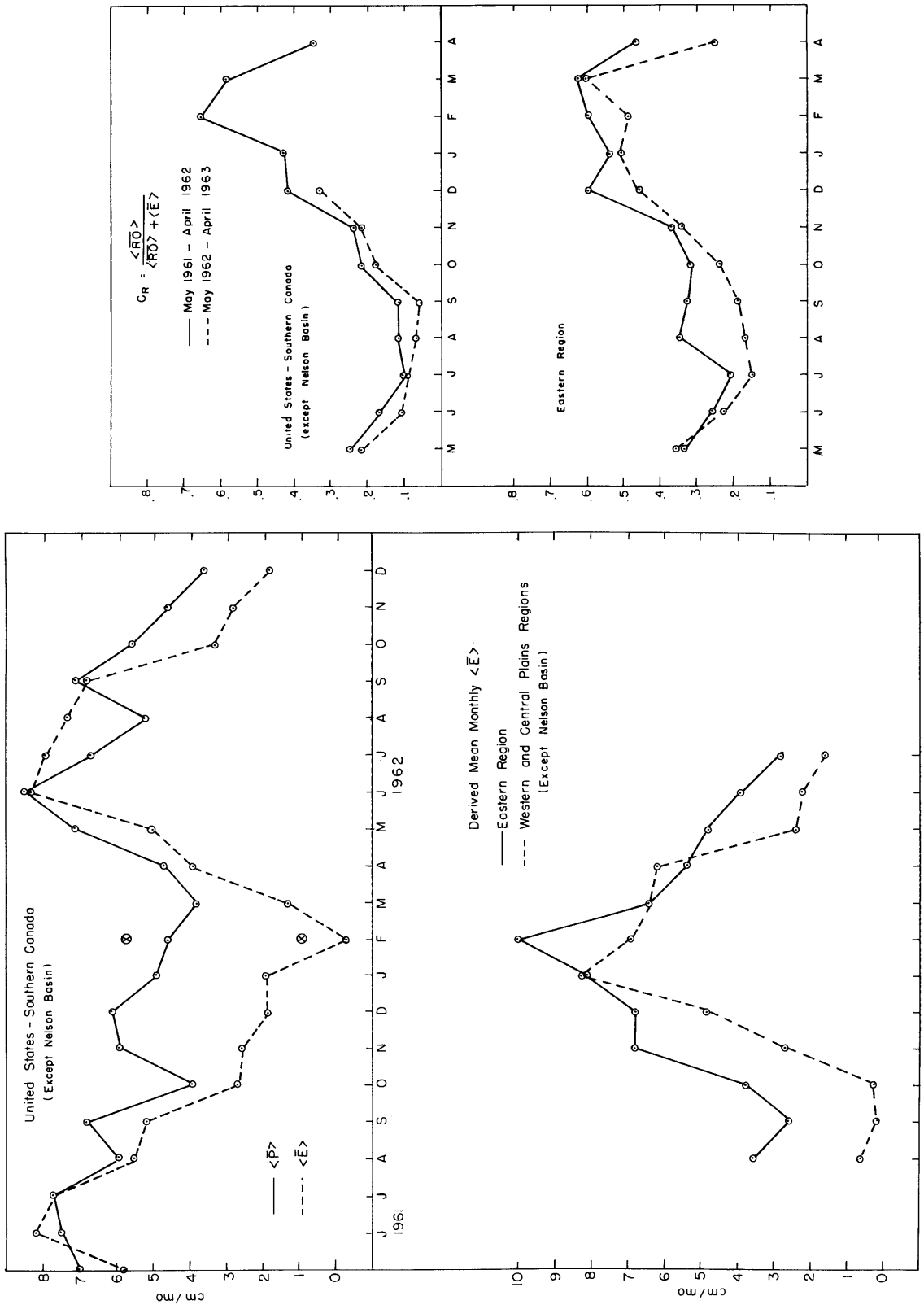
United States - Southern Canada
(Except Nelson Basin)
cm/mo
<P̄>
<Ē>
1961
1962
J F M A M J J A S O N D J F M A M J J A S O N D
Derived Mean Monthly <Ē>
Eastern Region
Western and Central Plains Regions
(Except Nelson Basin)
$C_R = \frac{\langle \overline{RO} \rangle}{\langle \overline{RO} \rangle + \langle \overline{E} \rangle}$
May 1961 - April 1962
May 1962 - April 1963
United States - Southern Canada
(except Nelson Basin)
Eastern Region
M J J A S O N D J F M A M J J A S O N D J F M A

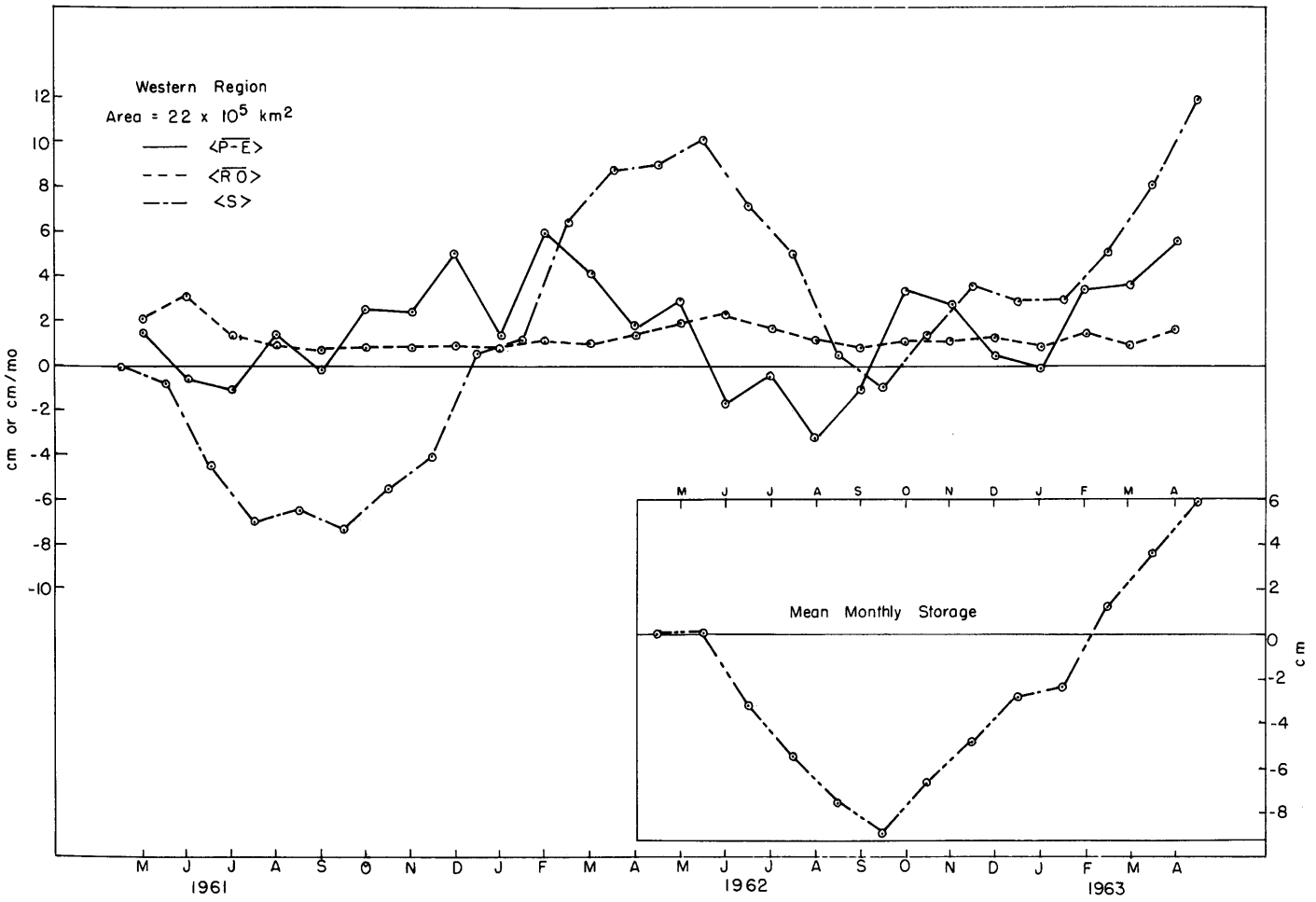


Figure 90. Water balance-Western Region. Storage $\langle S \rangle$ represents the change from conditions on May 1, 1961. Runoff, $\langle \overline{RO} \rangle$, is the total streamflow from the area. The difference between precipitation and evapotransporation, $\langle \overline{P-E} \rangle$, is evaluated by means of the water vapor balance equation.

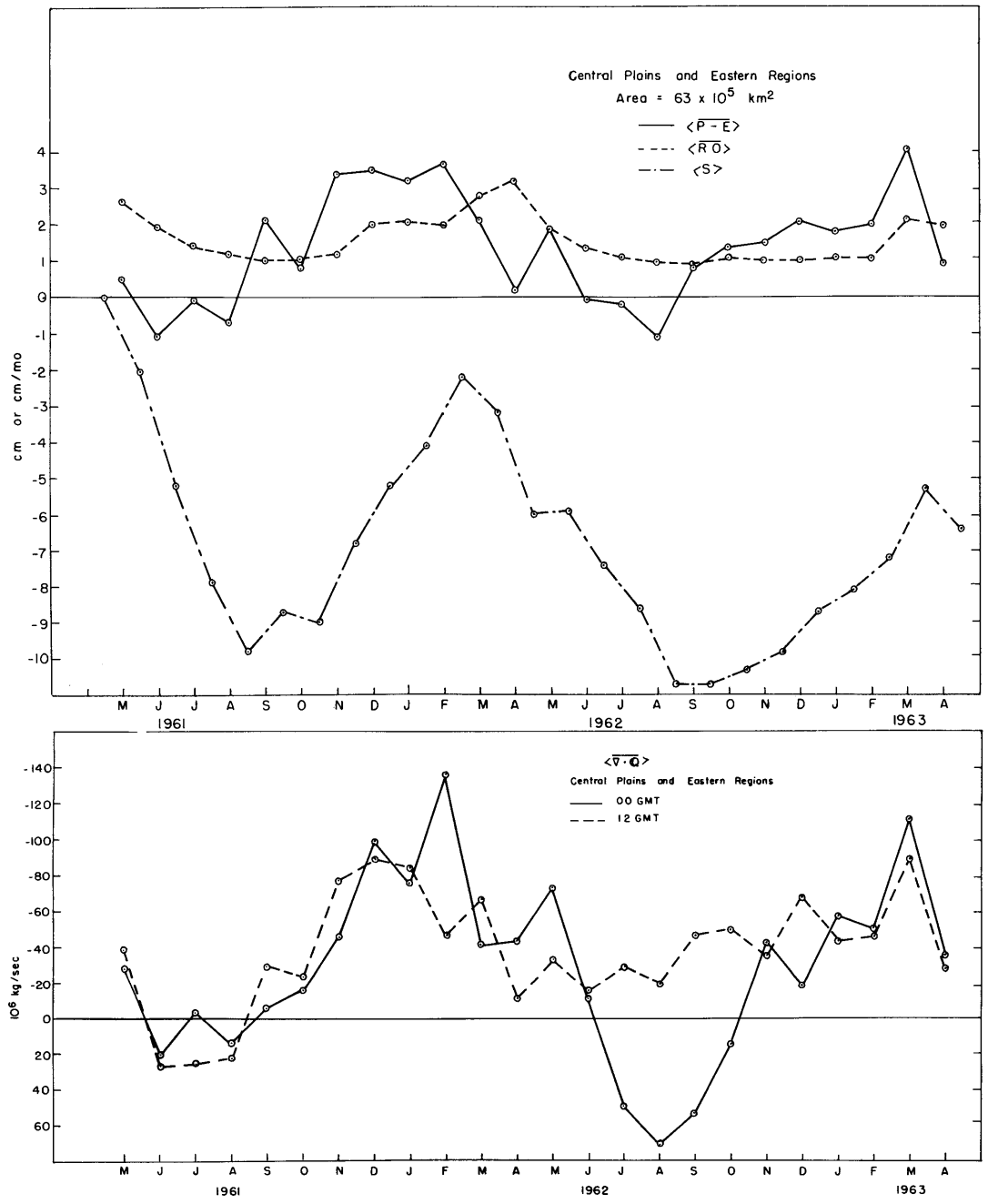


Figure 91. Water balance-Central Plains and Eastern Region. Upper: Water balance components. Storage, $\langle S \rangle$, represents the change from conditions on May 1, 1961. Runoff, $\langle \overline{RO} \rangle$, is the total streamflow from the area. The difference between precipitation and evaporation, $\langle \overline{P-E} \rangle$, is evaluated by means of the water vapor balance equation. Lower: Mean monthly instantaneous outflow from the region, $\langle \overline{\nabla \cdot Q} \rangle$, 00 GMT and 12 GMT.

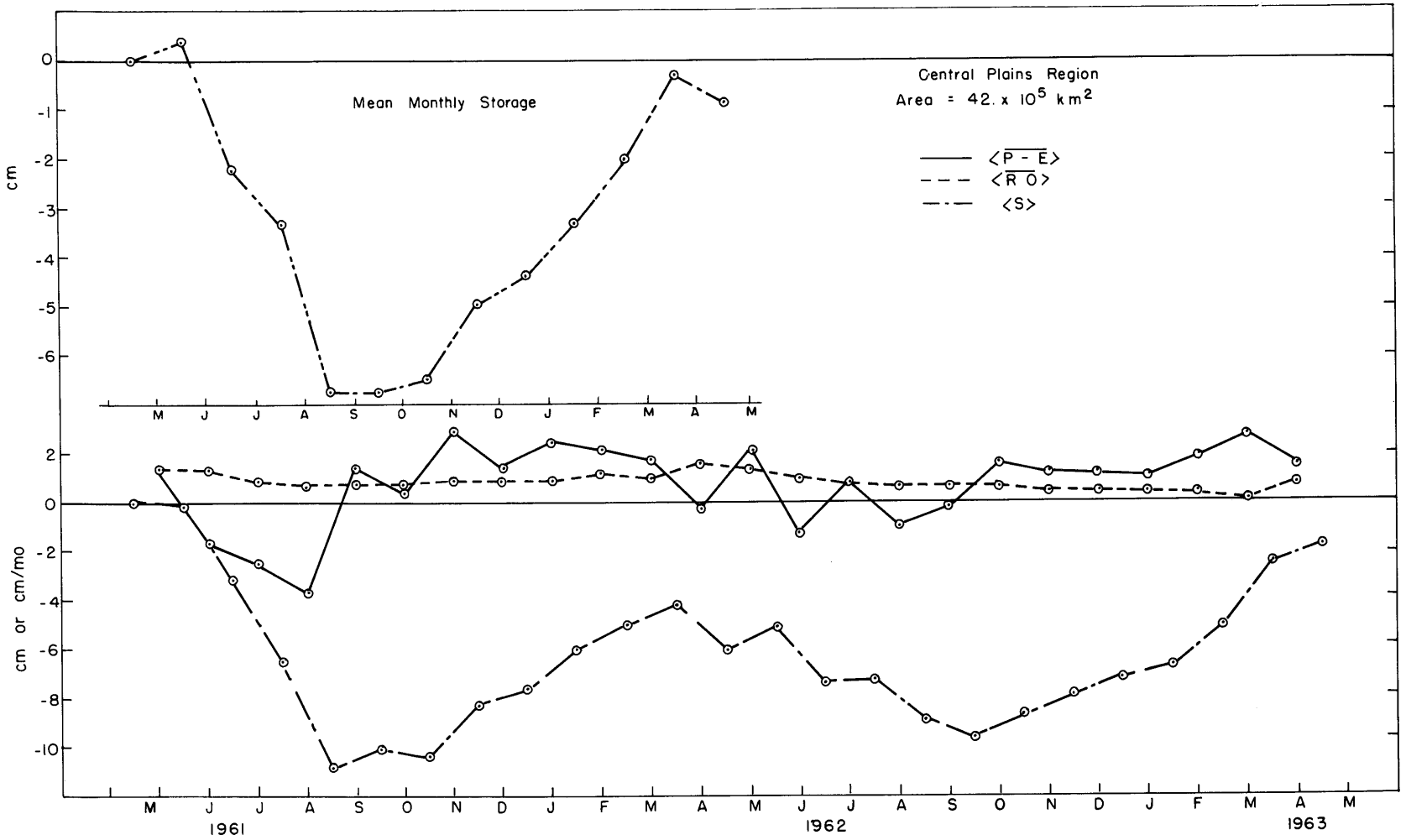


Figure 92. Water balance-Central Plains Region. Storage, $\langle S \rangle$, represents the change from conditions on May 1, 1961. Runoff, $\langle \overline{RO} \rangle$, is the total streamflow from the area. The difference between precipitation and evapotranspiration, $\langle \overline{P-E} \rangle$, is evaluated by means of the water vapor balance equation.

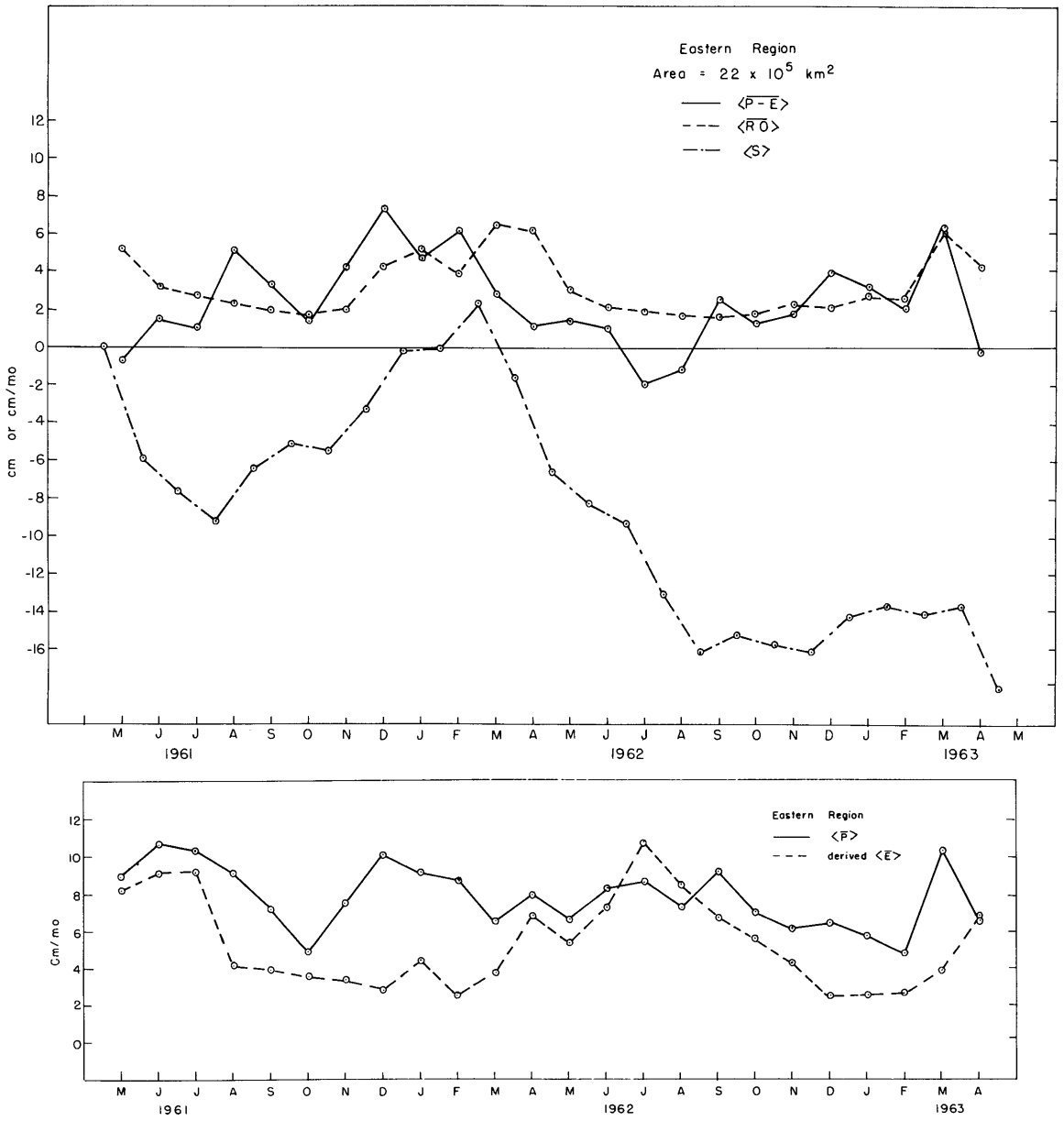


Figure 93. Water balance-Eastern Region. Upper: Water balance components. Storage, $\langle S \rangle$, represents the change from conditions on May 1, 1961. Runoff, $\langle \overline{RO} \rangle$ is the total streamflow from the area. The difference between precipitation and evapotranspiration, $\langle \overline{P-E} \rangle$ is evaluated by means of the water vapor balance equation. Lower: Mean monthly precipitation obtained from climatological summaries. Mean monthly evapotranspiration is obtained by means of the water vapor balance equation.

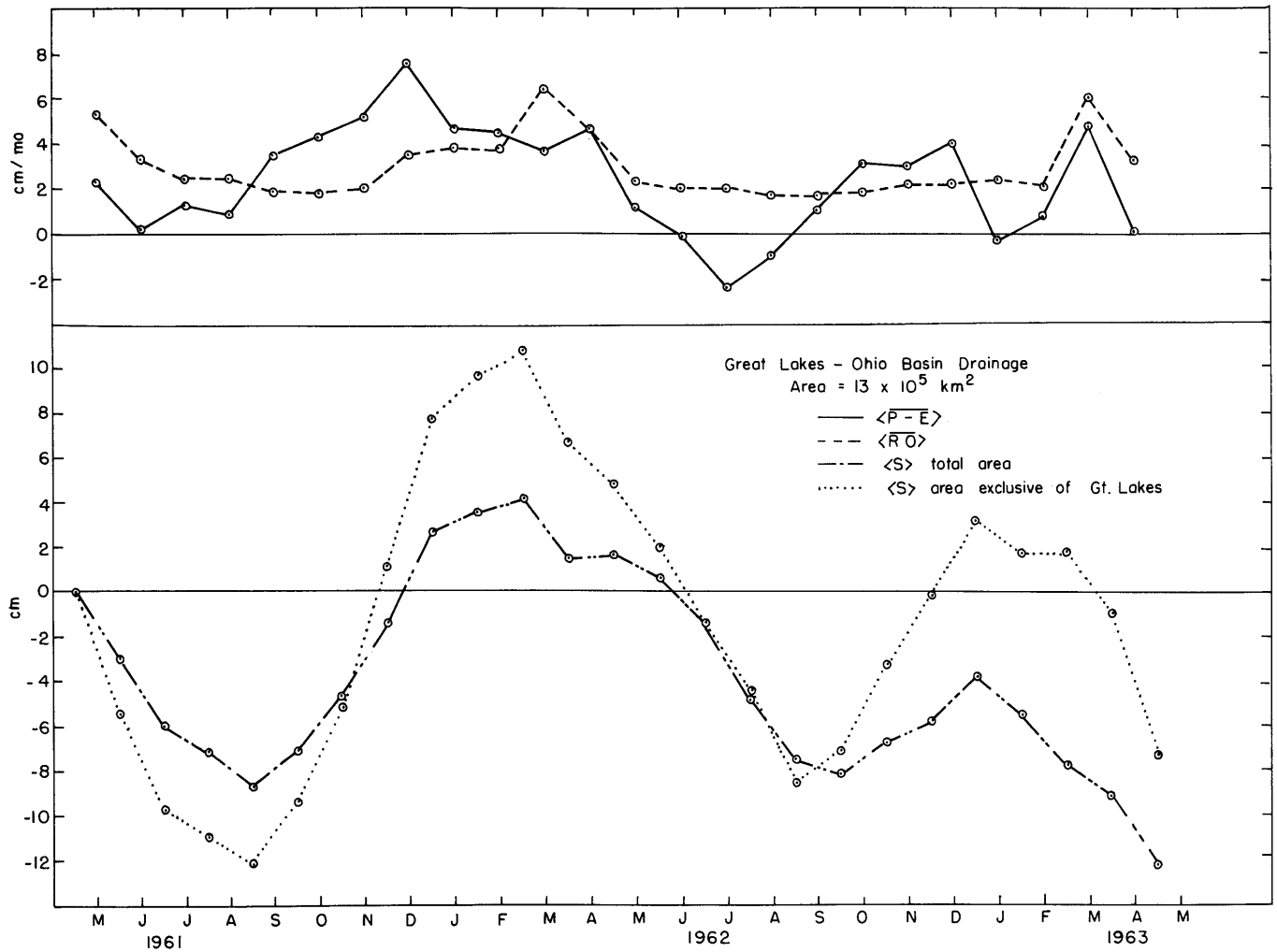


Figure 94. Water balance-Great Lakes-Ohio Basin Drainage. Storage, $\langle S \rangle$, represents the change from conditions on May 1, 1961. Runoff, $\langle \overline{RO} \rangle$, is the total streamflow from the area. The difference between precipitation and evapotranspiration, $\langle \overline{P-E} \rangle$, is evaluated by means of the water vapor balance equation.

Figure 95. Water balance-Great Lakes Drainage (left) and Ohio Basin (right); May 1961-April 1963. Upper left: Mean monthly values of the difference between precipitation and evapotranspiration, $\langle \overline{P-E} \rangle$, evaluated by means of the water vapor balance equation. $\langle \overline{RO} \rangle$ is the total streamflow from the area.
Lower left: Mean monthly surface and subsurface storage changes computed by means of the water vapor balance equation, and changes computed from Van Hylckama (1956).
Upper right: Mean monthly values of $\langle \overline{P-E} \rangle$, $\langle \overline{RO} \rangle$, and storage, $\langle S \rangle$. $\langle \overline{P-E} \rangle$ and $\langle S \rangle$ are obtained through use of the water vapor balance equation.
Lower right: Mean monthly precipitation, $\langle \overline{P} \rangle$, obtained from climatological summaries. Mean monthly evapotranspiration, $\langle \overline{E} \rangle$, obtained by means of the water vapor balance equation.

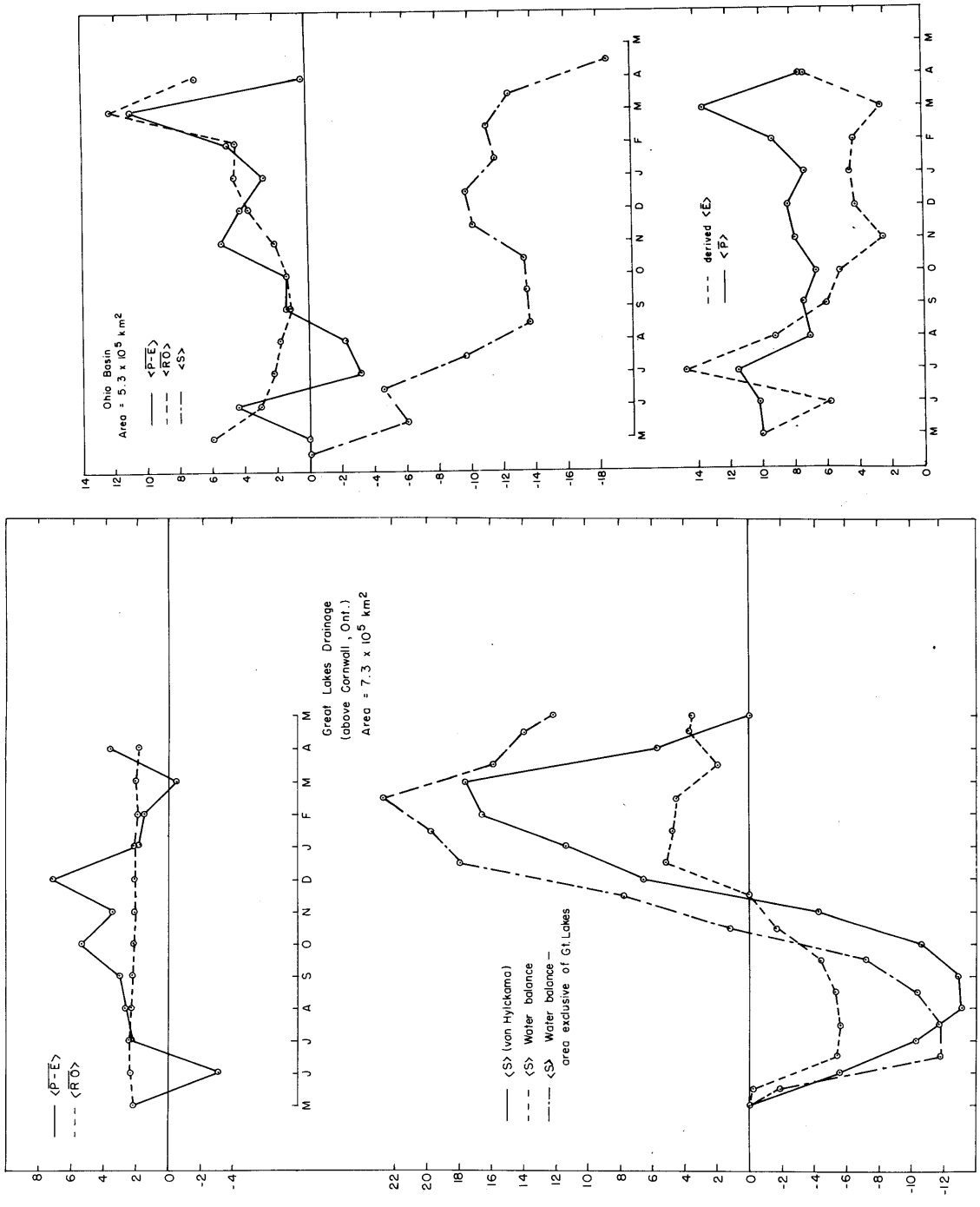
Ohio Basin
Area = 5.3 x 10^5 km^2
<P-E>
<RO>
<S>
derived <E>
<P>
Great Lakes Drainage
(above Cornwall, Ont.)
Area = 7.3 x 10^5 km^2
<S> (van Hylckama)
<S> Water balance
<S> Water balance — area exclusive of Gt Lakes
M J J A S O N D J F M A M

Figure 96. Vertical distribution of net water vapor outflow, $\langle \nabla \cdot \overline{qv} \rangle$, January, 1962, 1963 and July, 1961, 1962. The western area is bounded on the south by 30°N (100°W-105°W) and 32.5°N (105°W-Pacific Coast); on the north by 47.5°N, and extends from 100°W to the Pacific Coast. The eastern area is bounded by latitudes 30°N and 47.5°N, and longitudes, 80°W and 100°W. $\langle \nabla \cdot \overline{qv} \rangle$ is an average over the total enclosed area.

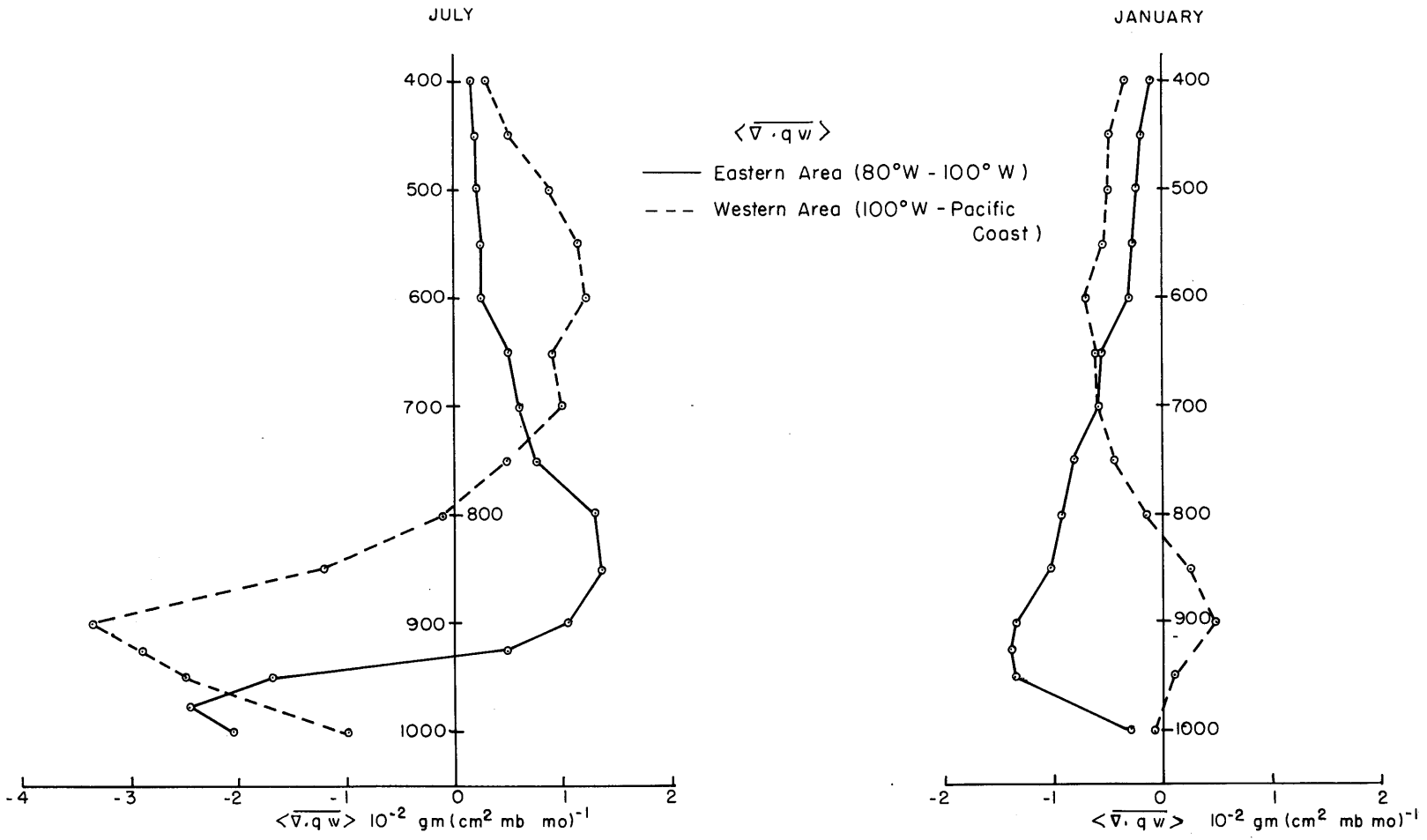
JULY
JANUARY
$\langle \overline{\nabla \cdot q w} \rangle$
Eastern Area (80°W - 100° W)
Western Area (100°W - Pacific Coast)
400
500
600
700
800
900
1000
-4
-3
-2
-1
0
1
2
$\langle \overline{\nabla \cdot q w} \rangle$ $10^{-2}$ gm (cm$^2$ mb mo)$^{-1}$

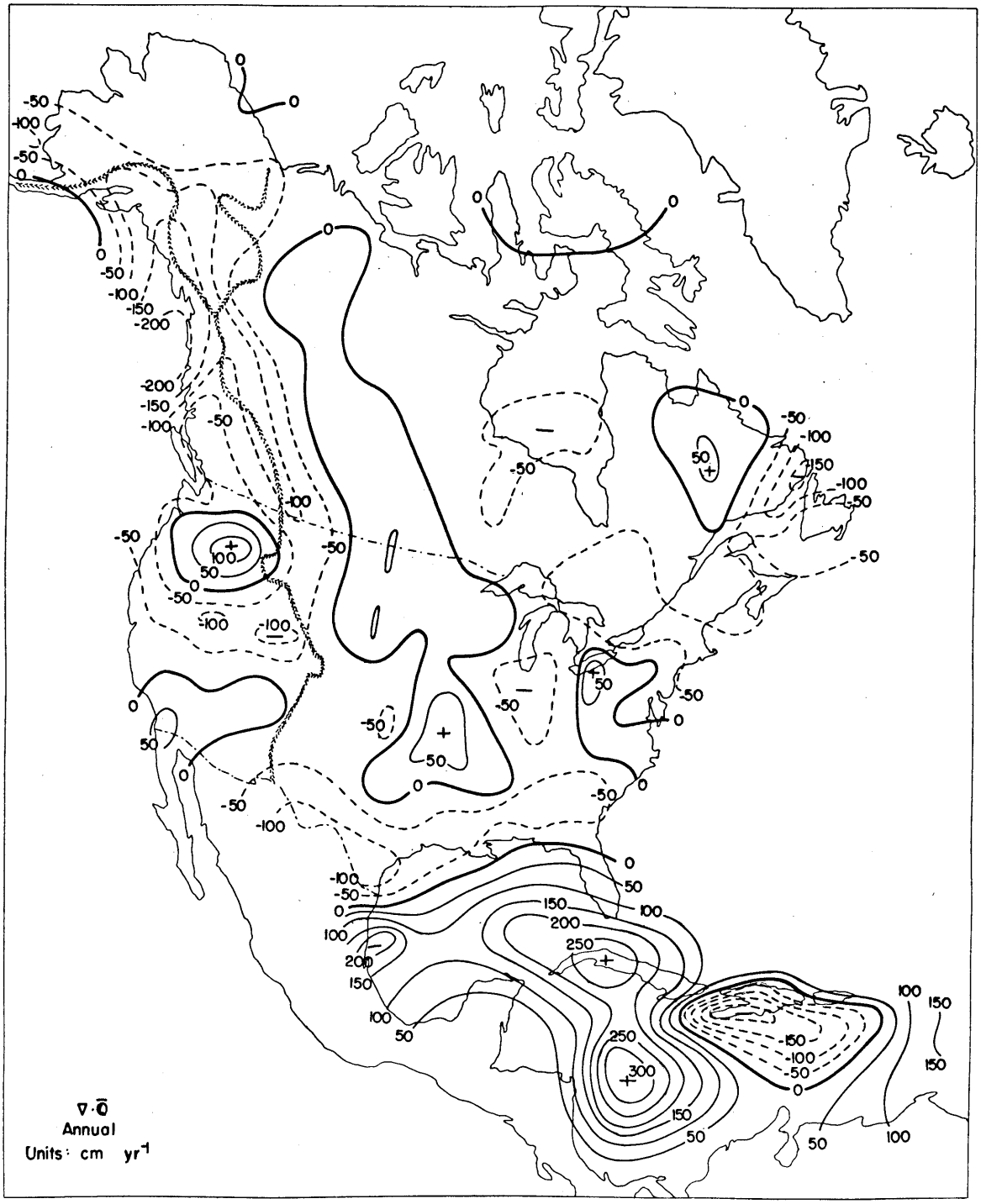


Figure 97. Mean annual divergence of the vertically integrated water vapor flux. May 1961 - April 1963. Units: cm $yr^{-1}$.

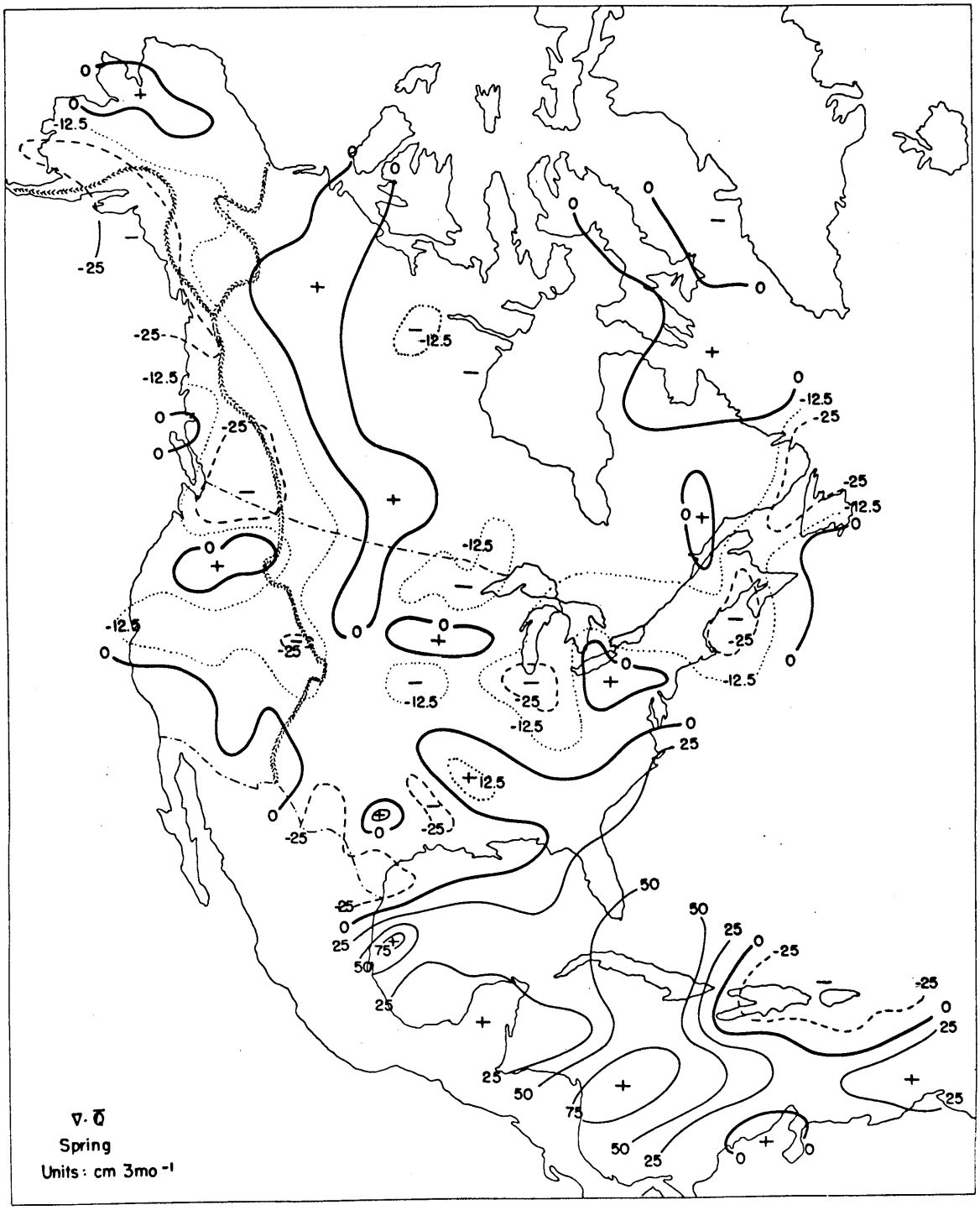


Figure 98. Mean seasonal divergence of the vertically integrated water vapor flux. Spring (March-May). Units: cm 3 $mo^{-1}$.

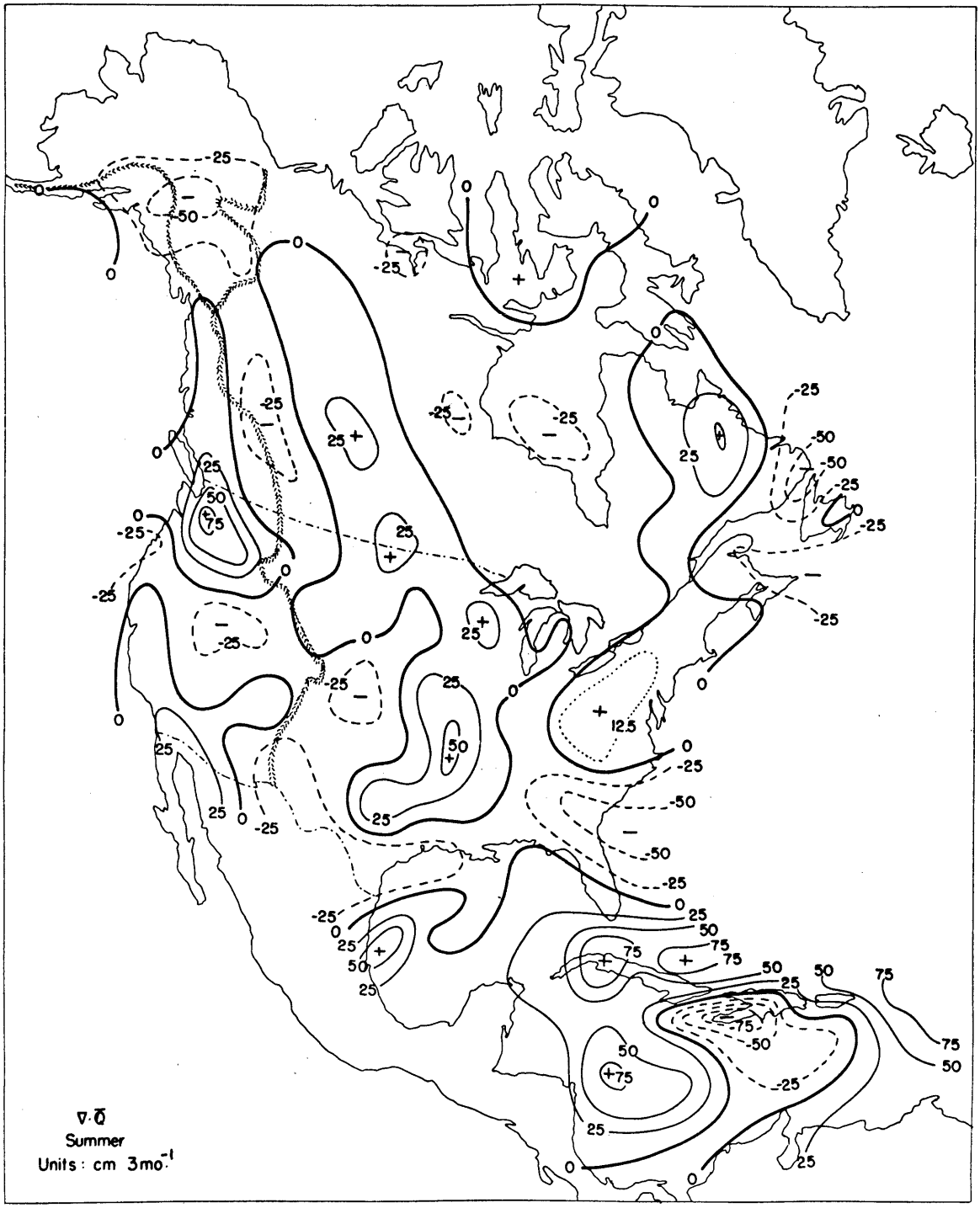


Figure 99. Mean seasonal divergence of the vertically integrated water vapor flux. Summer (June-August). Units: cm 3 $mo^{-1}$.

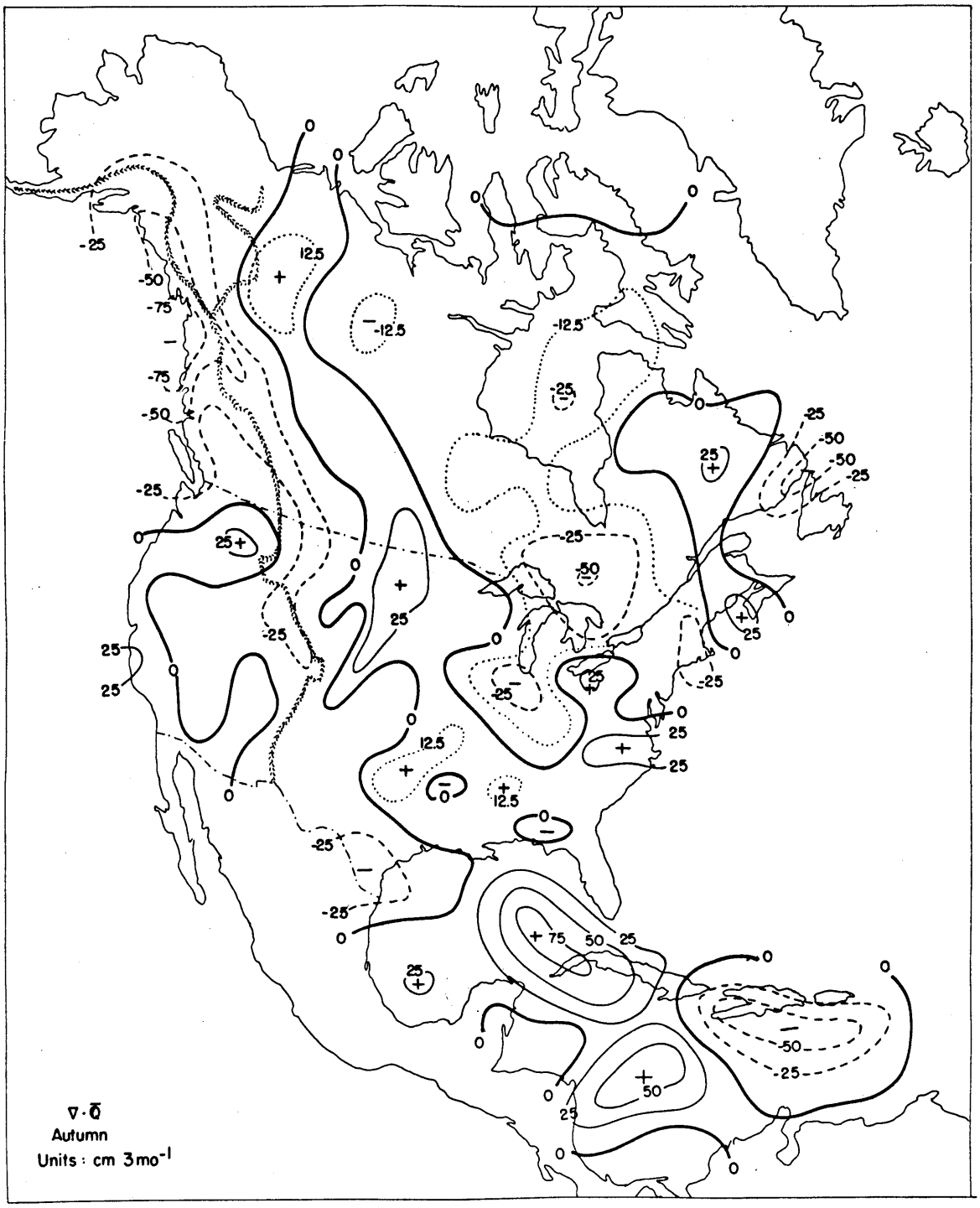


Figure 100. Mean seasonal divergence of the vertically integrated water vapor flux. Fall (September-November). Units: cm 3 $mo^{-1}$.

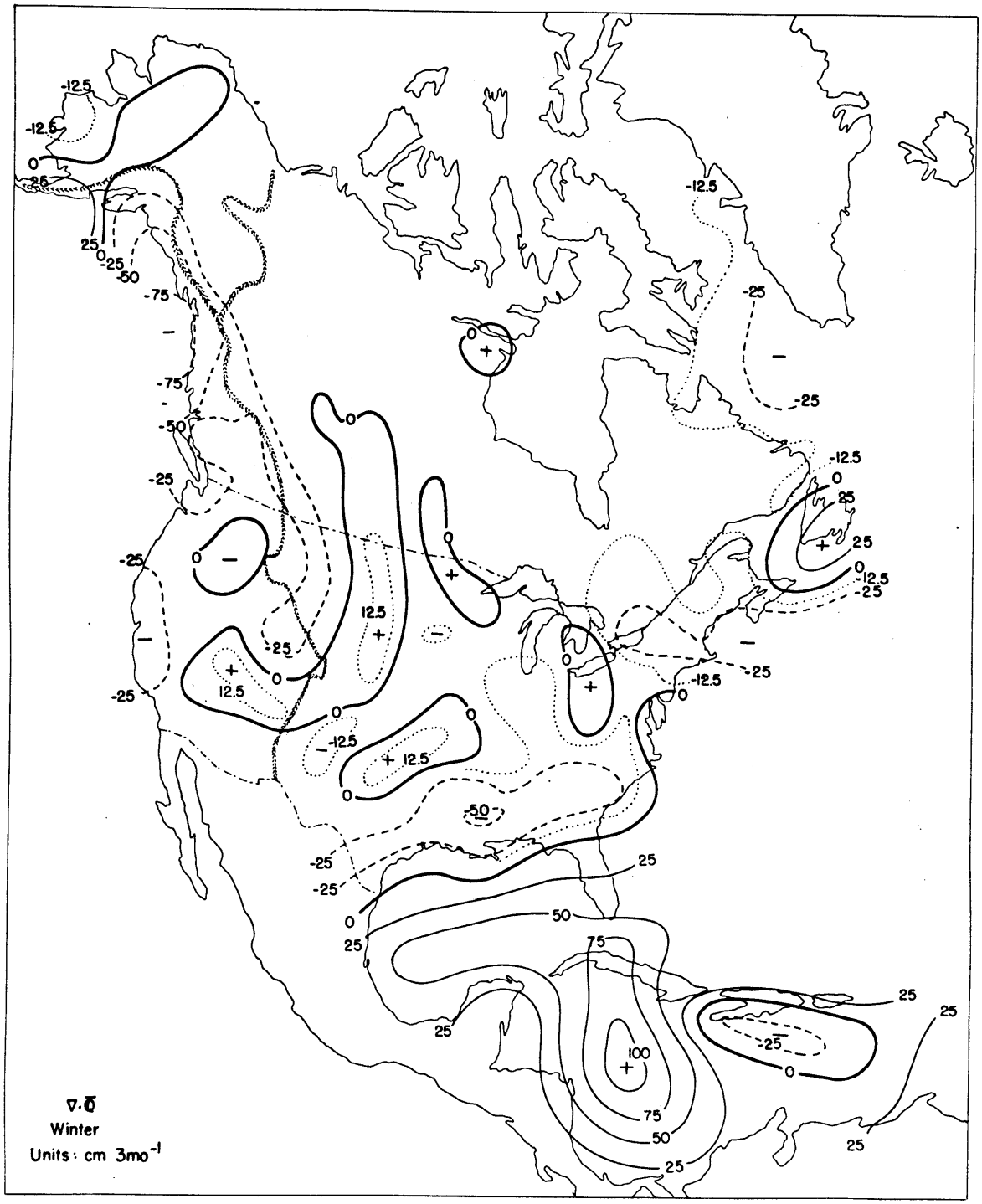


Figure 101. Mean seasonal divergence of the vertically integrated water vapor flux. Winter (December-February). Units: cm 3 $mo^{-1}$.

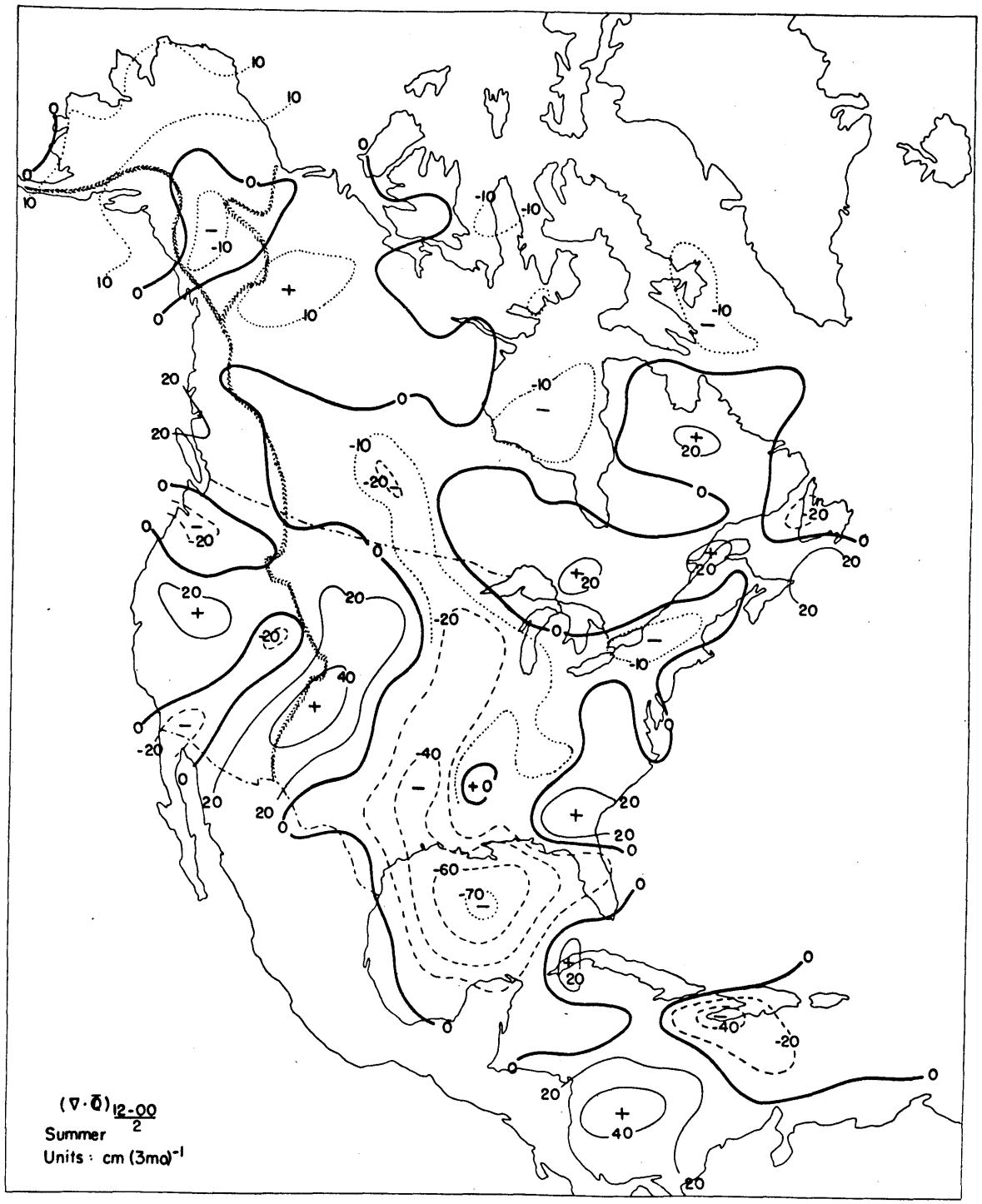


Figure 102. Mean seasonal difference, (12 GMT-00 GMT)/2, of the divergence of the vertically integrated water vapor flux. Summer (June-August). Units: cm $3mo^{-1}$.

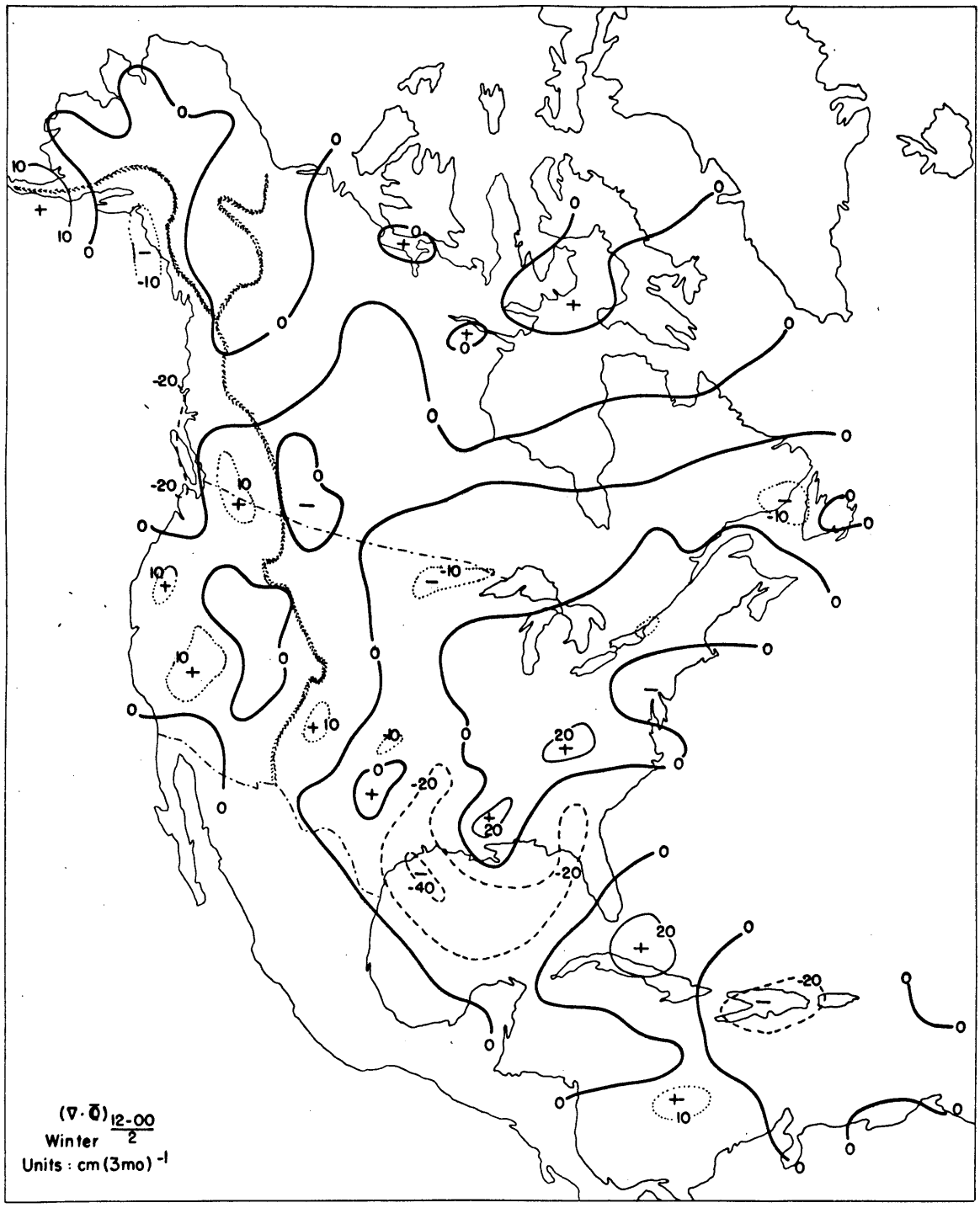


Figure 103. Mean seasonal difference, (12 GMT-00 GMT)/2, of the divergence of the vertically integrated water vapor flux. Winter (December-February). Units: cm $3mo^{-1}$.

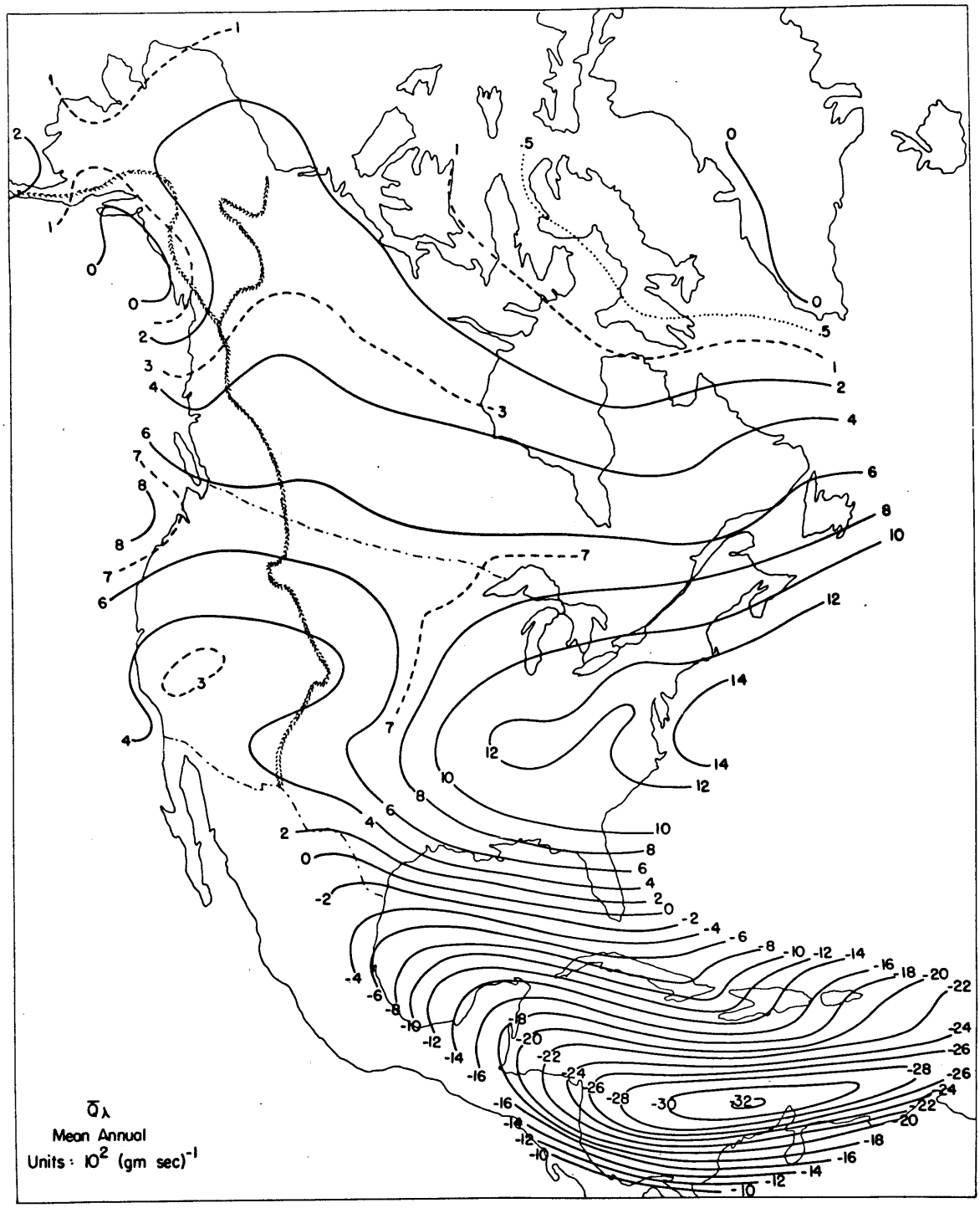


Figure 104. Mean annual vertically integrated total zonal water vapor flux. May 1961 - April 1963. Units: $10^2$ gm (cm sec)$^{-1}$.

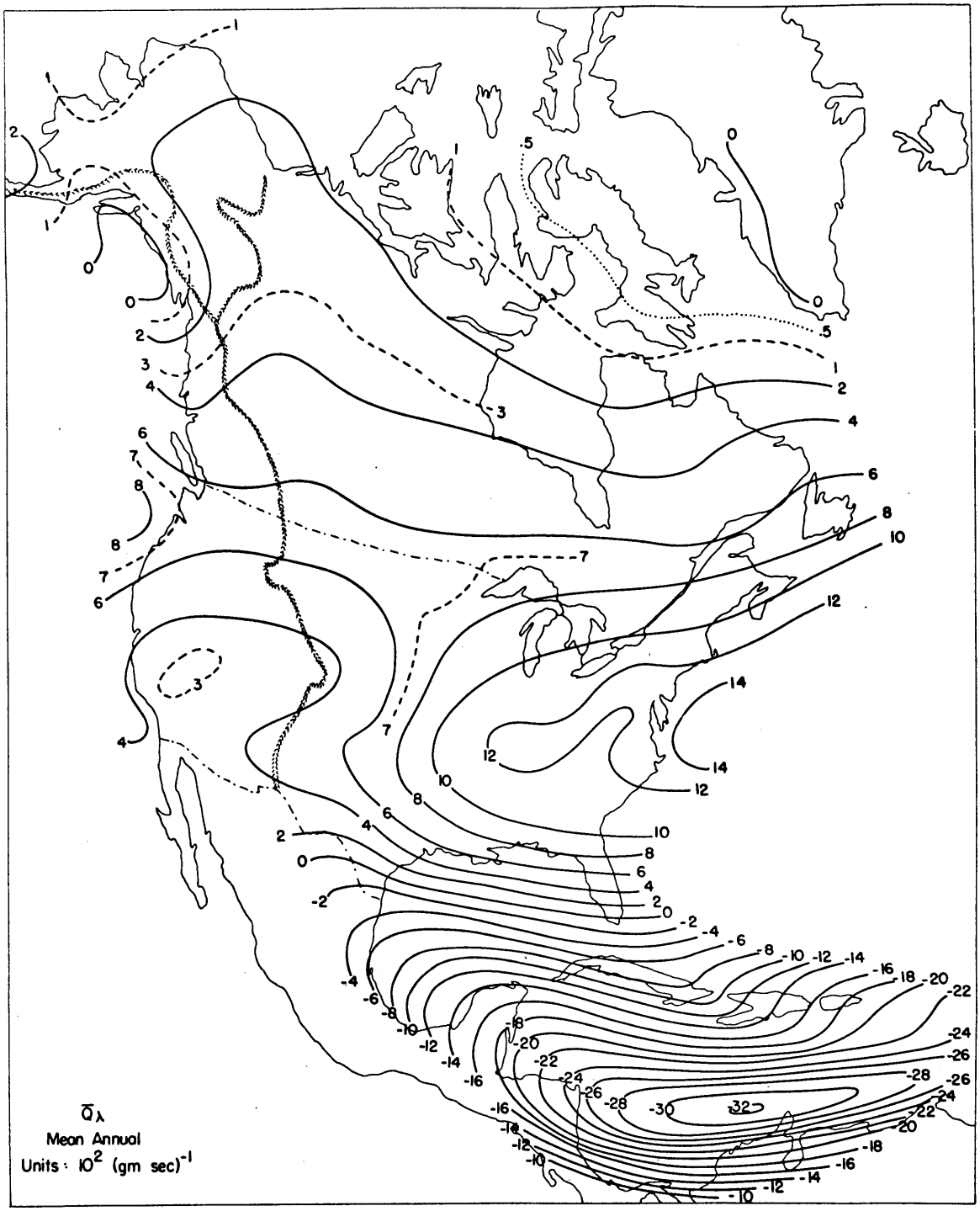


Figure 104. Mean annual vertically integrated total zonal water vapor flux. May 1961 - April 1963. Units: $10^2$ gm (cm sec)$^{-1}$.

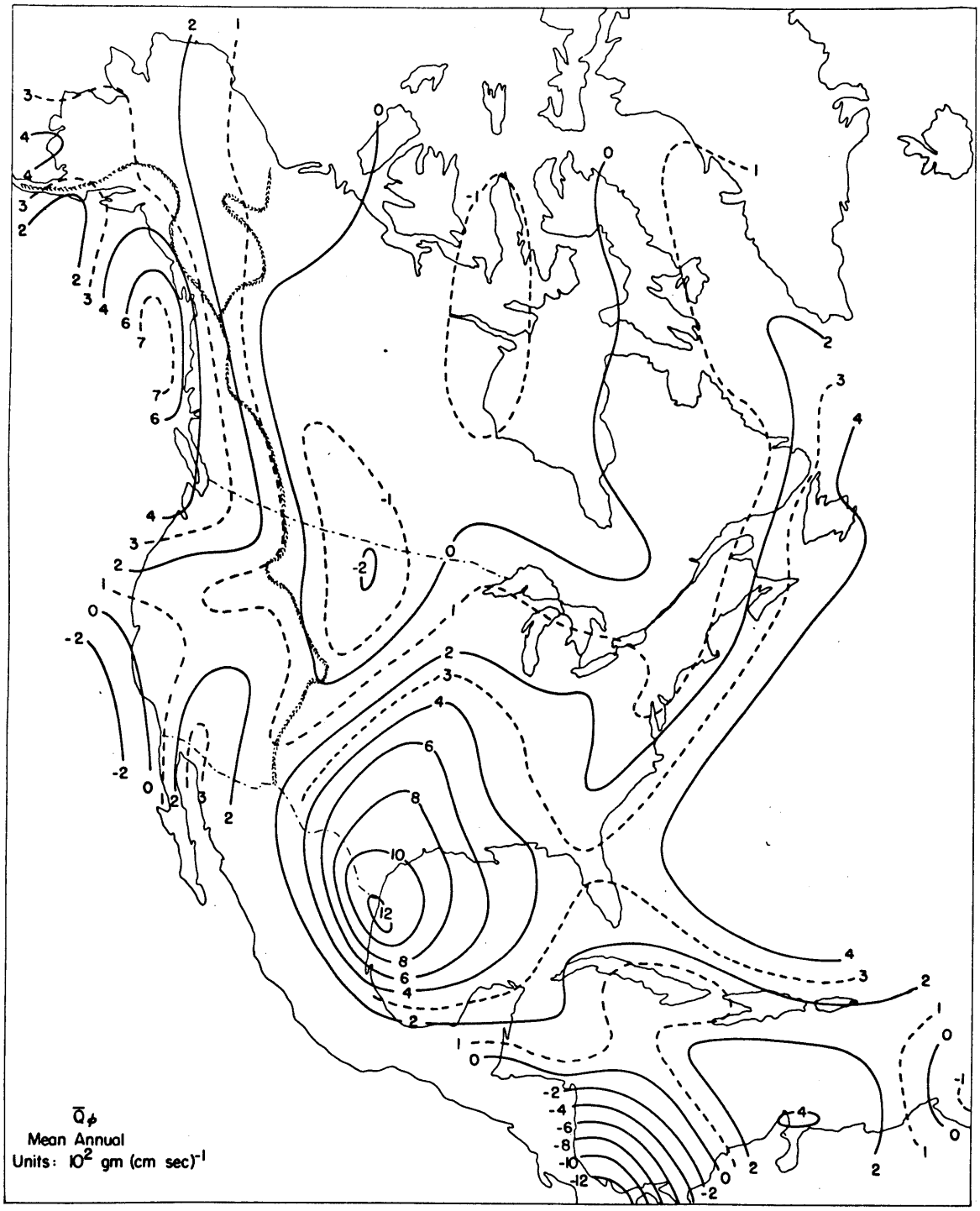


Figure 105. Mean annual vertically integrated total meridional water vapor flux. May 1961 - April 1963. Units: $10^2$ gm (cm sec)$^{-1}$.

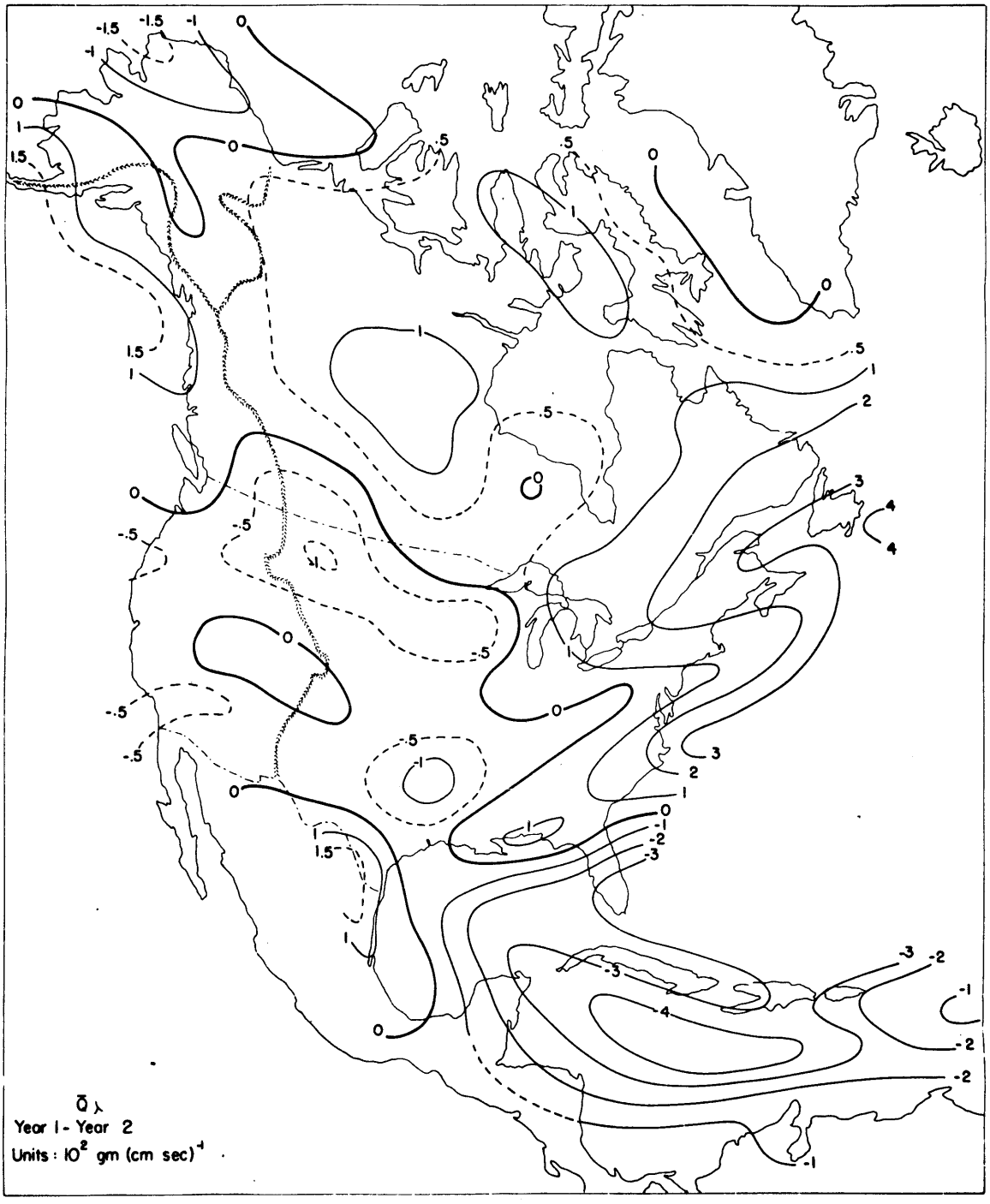


Figure 106. Year to year difference in the mean annual vertically integrated total zonal water vapor flux. (May 1961 - April 1962) - (May 1962 - April 1963). Units: $10^2$ gm (cm sec)$^{-1}$.

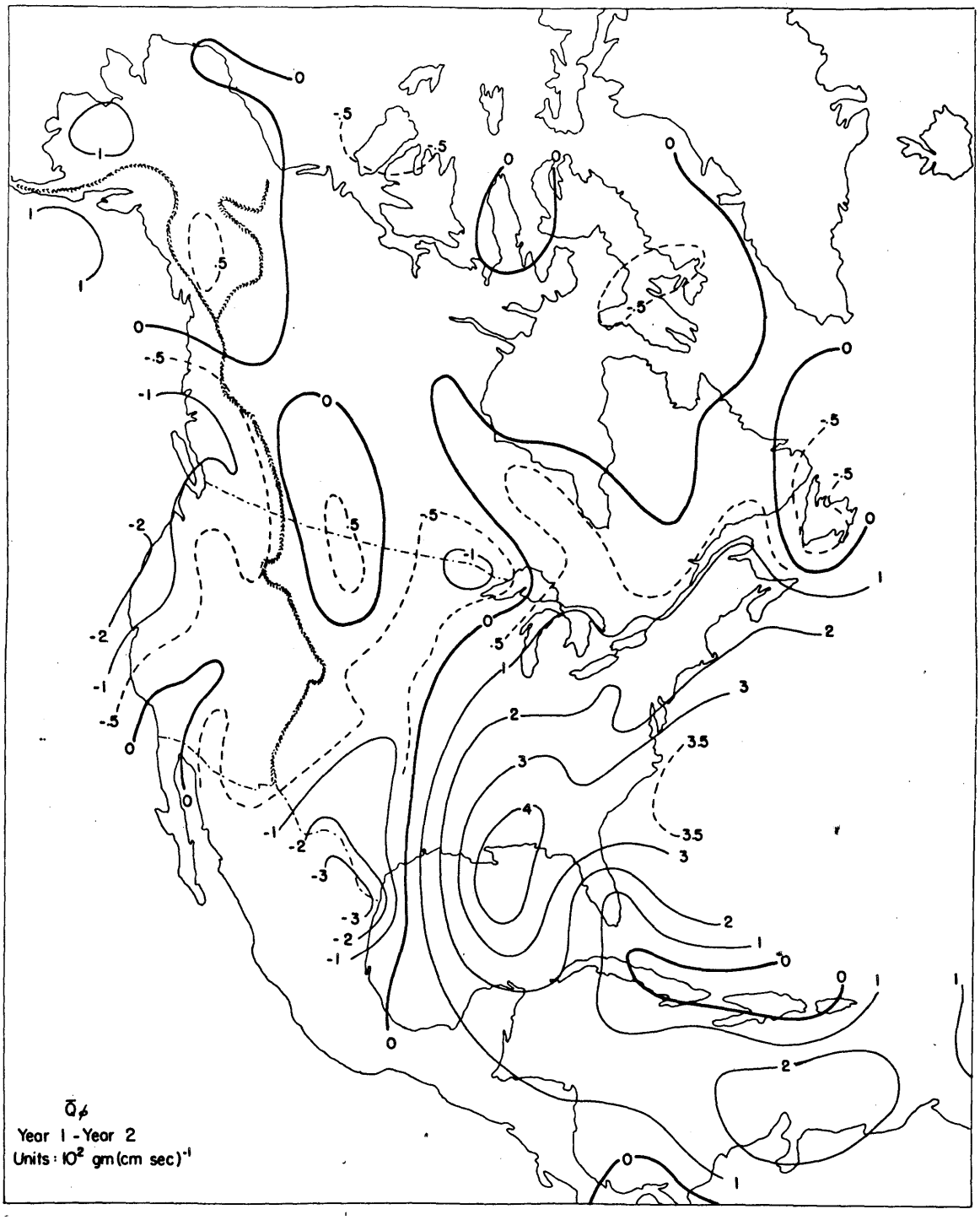


Figure 107. Year to year difference in the mean annual vertically integrated total meridional water vapor flux. (May 1961 - April 1962) - (May 1962 - April 1963). Units: $10^2$ gm (cm sec)$^{-1}$.